Translational development of MyD88 as a biomarker for selecting patients with lymphoma responsive to histone deacetylase inhibitors

Semira Sheikh

St John's College

Department of Oncology, University of Oxford

Thesis submitted for degree of DPhil

Trinity Term 2017

Translational development of MyD88 as a biomarker for selecting patients with lymphoma responsive to histone deacetylase inhibitors

Semira Sheikh, St John's College

Submitted for degree of DPhil

Trinity Term 2017

ABSTRACT

Histone deacetylase inhibitors (HDIs) are promising new agents for the treatment of haematological malignancy including lymphoma. HDIs have potent anti-proliferative effects in cell-based studies; in the clinical setting, however, the outcome of HDI therapy is complex and difficult to predict. The adapter protein MyD88 (Myeloid Differentiation Primary Response Gene 88) is expressed in haematopoietic tissues and has recently been found to be the target for somatic mutation in lymphoid malignancies. MyD88 was also identified as a candidate biomarker in a loss-of-function screen and may mediate sensitivity to HDIs. In this project I investigated the roles of MyD88 and the recurrent MyD88 mutation, L265P, in lymphoma. Immunohistochemical analysis of tumour tissue microarrays from patients with DLBCL showed higher expression of MyD88 compared to patients with prostate or colorectal carcinoma. In DLBCL lymphoma cell lines of the ABC subtype, those cells expressing endogenous wild-type MyD88 (RIVA) were found to be less sensitive to HDI treatment compared to those cells carrying a heterozygous MyD88 L265P mutation (HBL-1). MyD88-mutated cells also showed higher levels of IL-6 expression on cytokine analysis. Disruption of the TLR/MyD88/NF-κB signalling pathway by blocking either the TLR receptor, MyD88 aggregation or IL-6 secretion resulted in decreased HDI sensitivity. Finally, a CADOR array identified potential interacting bromodomain (BRD) proteins of the acetylated MyD88 protein.

Collectively my findings suggest that MyD88 expression and secretion of pro-inflammatory cytokines may contribute to the sensitization of cancer cells to HDI. Moreover, MyD88 may be a direct target for HDAC- and BRD- inhibitors. Therefore, both expression level of MyD88 and MyD88 mutation status could serve as potential biomarkers for HDI sensitivity in patient selection.

DECLARATION

I confirm that the contents of this thesis are all my own work and that the work of others is appropriately referenced. No part of my thesis has been accepted or is currently being submitted for any other degree or diploma in this university or elsewhere. My research was carried out under the supervision of Professor Nicholas La Thangue, Laboratory of Cancer Biology, Department of Oncology, University of Oxford.

Semira Sheikh

July 2017

PUBLICATIONS DURING DPHIL

(1) New M, **Sheikh S**, Bekheet ME et al (2016). TLR Adaptor Protein MYD88 Mediates Sensitivity to HDAC Inhibitors via a Cytokine-Dependent Mechanism. Cancer Res 2016; 76(23):6975.

(2) **Sheikh S**, Coutts A and La Thangue NB (2016). Transfection (book chapter). In: Basic Science Methods for Clinical Researchers. Elsevier.

(3) Olzscha H, Bekheet ME, **Sheikh S** and La Thangue NB (2015). HDAC inhibitors. Invited chapter for the edition "HDACs" in Methods in Molecular Biology, Springer.

(4) **Sheikh S**, Bekheet ME, Olzscha H and La Thangue NB (2015). Predicting and monitoring responses to epigenetic drugs. In: Drug Discovery in Cancer Epigenetics. Translational Epigenetics Series (Editors G Egger and P Arimondo). Elsevier.

(5) Olzscha H, **Sheikh S** and La Thangue NB. Deacetylation of chromatin and gene expression regulation. Critical Reviews in Oncogenesis DOI 10.1615/CritRevOncog.2014012463.

(6) **Sheikh S**, Olzscha H, and La Thangue NB. Oncology Biomarkers in clinical practice – a new horizon. Drug Target Review 2014; 1(1).

ACKNOWLEDGEMENTS

I would like to thank my supervisor Professor Nicholas La Thangue for accepting me as a student in his laboratory, and for his scientific guidance, advice and support. I would also like to thank Dr Graham Collins for agreeing to be my second supervisor on this project.

I am very grateful to all the members, past and present, of the La Thangue group who made life in the lab a friendly and worthwhile experience for me. In particular, I am indebted to Dr Maria New who got me started on the MyD88 project, Dr Heidi Olzscha who was a patient and helpful source of advice and collaborator on publications, Dr Shonagh Munro who always lent a helping hand when the science let me down, and Dr Amanda Coutts for sharing scientific insights and discussions. Further, I would like to thank Leticia Campo (GCP lab), Dr Liz Soilleux and Professor Kevin Gatter (OUH Histopathology) who provided a lot of help and advice on the immunohistochemistry part of this project.

Finally, to my family: none of this would have been possible without your love and support. Thank you.

LIST OF ABBREVIATIONS

ABC	Activated B cell
Apaf-1	Apoptosis pathway activating factor
APC	Adenomatous polyposis coli
APML	Acute promyelocytic leukaemia
BCR	B cell receptor
BET	Bromodomain and extra-terminal
BRD	Bromodomain
BTK	Bruton's tyrosine kinase
CBP	CREB-binding protein
CCC	Consensus clustering classification
CDK	cyclin-dependent kinases
CLL	Chronic lymphocytic leukaemia
CML	Chronic myeloid leukaemia
COO	Cell of origin
CR	Complete remission
DLBCL	Diffuse large B cell lymphoma
ERK	Extracellular signal-related kinase
FasL	Fas ligand
FISH	fluorescence *in situ* hybridization
GCB	Germinal center B cell
GvHD	Graft versus host disease
HAT	Histone acetyltransferase
HDAC	Histone deacetylase
HDI	HDAC inhibitor
HIFα	Hypoxia inducible factor alpha
HR23B	Human ultraviolet excision repair protein RAD23 homologue B
HSP90	Heat shock protein 90
IHC	Immunohistochemistry
IL-6 R	IL-6 receptor
IP	Immunoprecipitation
IRAK	Interleukin-1 receptor-associated kinase
ITAM	Immunoreceptor tyrosine-based activation motif
KMT2D	Histone-lysine N-methyltransferase 2D
LC3	microtubule-associated protein 1A/1B-light chain 3
LPL	Lymphoplasmacytic lymphoma
LPS	Lipopolysaccharide
MALT	Mucosa-associated lymphoid tissue
MAPK	Mitogen-activated protein kinase
MOZ	Monocytic zinc finger protein
MST1	mammalian STE20-like kinase 1
MyD88	Myeloid Differentiation Primary Response Gene 88
NGS	Next generation sequencing
NHL	Non-Hodgkin’s lymphoma
NUT	Nuclear protein in testis
OS	Overall survival
PBMC	Peripheral blood mononuclear cell
PBML	Primary mediastinal B cell lymphoma
PCNSL	Primary central nervous system lymphoma
PFS	Progression-free survival

PI3K	Phosphoinositide 3-kinase
PML	Promyelocytic leukaemia
PR	Partial response
PRC2	Polycomb repressive complex 2
RAR	Retinoic acid receptor
SEB	*Staphylococcal* enterotoxin B
SMZL	Splenic marginal zone lymphoma
STAT	Signal transducer and activator of transcription
TLR	Toll-like receptor
TMA	Tissue microarray
TNF	Tumour necrosis factor
TRAF6	TNF receptor associated factor 6
TRAIL	TNF-related apoptosis-inducing ligand
UPS	Ubiquitin proteasome system
VEGF	Vascular endothelial growth factor
vHL	von-Hippel Lindau
WM	Waldenstrom's macroglobulinaemia
WRN	Werner Syndrome ATP-dependent helicase
WT	wild-type

TABLE OF CONTENTS

CHAPTER 1. INTRODUCTION 12
1.1 Diffuse large B cell lymphoma (DLBCL) biology and classification 12
1.2 Biological heterogeneity and functional classifications of DLBCL 13
1.2.1 Cell of origin (COO) 13
1.2.2 Consensus Clustering Classification (CCC) 15
1.2.3 Stromal signatures 15
1.3 Determining cell of origin 16
1.4 Mutational landscape in DLBCL 17
1.5 MyD88 as an emerging target in lymphoma 20
1.5.1 Physiology and structure of MyD88 20
1.5.2 The role of MyD88 in TLR signalling 21
1.5.3 The role of MyD88 in cellular transformation 25
1.5.4 The MyD88 L265P mutation in DLBCL 27
1.5.5 Other MyD88 mutations in DLBCL 29
1.5.6 The MyD88 L265P mutation in other lymphomas 31
1.5.7 The MyD88 L265P mutation as a gain-of-function mutation and oncogenic driver 33
1.5.8 MyD88 mutation as a prognostic indicator 33
1.6 Epigenetic control of gene expression and the role of histone acetylation in cancer 36
1.6.1 Chromatin control and the role of epigenetic readers, writers and erasers 36
1.6.2 Histone acetylation and cancer 37
1.6.3 Non-histone proteins as targets of acetylation 39
1.6.4 HDAC classes and function 41
1.6.5 HDACs as therapeutic targets 44
1.6.6 Cellular outcomes of HDI treatment 46
1.6.7 Clinical outcomes of HDI treatment 52
1.6.8 The effect of HDIs in DLBCL 56
1.6.9 HDI summary 57
1.7 Bromodomains: structure and function 58
1.7.1 Bromodomains as therapeutic targets in cancer 59
1.7.2 The role of bromodomain inhibition in DLBCL 60
1.8 Biomarkers and personalized medicine 62
1.8.1 Definition and classification of biomarkers 62
1.8.2 Examples of existing biomarkers 63

1.8.3 Personalized medicine for lymphoma patients 66
1.9 Work that has led up to this project 70
1.9.1 Genome-wide loss-of-function screen 70
1.9.2 MyD88 as a sensitivity determinant for HDI treatment 72
1.9.3 MyD88 as a candidate companion diagnostic biomarker for lymphoma 72
1.10 Aims of project 73
CHAPTER 2. MATERIALS AND METHODS 74
2.1 Antibodies 74
2.2 Cells and cell culture 75
2.3 Drug and antibody treatments 76
2.4 Immunoblotting and immunoprecipitation 77
2.5 FACS (Fluorescence-activated cell sorting) analysis 78
2.6 Tetrazolium MTT (3-(4,5-dimethylthiazolyl-2)-2,5-diphenyltetrazolium bromide) cell proliferation assay 79
2.7 RNA extraction and cDNA synthesis 79
2.8 qRT-PCR 79
2.9 Nuclear extraction 80
2.10 Cytokine analysis 80
2.11 Transfection 81
2.12 Electroporation 82
2.13 Nucleofection 82
2.14 Lentiviral transduction 83
2.15 Patient samples 83
2.16 Immunohistochemistry and pathology examination 84
2.17 CADOR array 85
2.18 Immunoprecipitation of His-tagged proteins 85
CHAPTER 3. MYD88 EXPRESSION AND RESPONSE TO HDI TREATMENT 87
3.1 Introduction 87
3.2 MyD88 expression in clinical disease 89
3.3 MyD88 expression in a panel of cell lines 98
3.4 Lymphoid cell lines show sensitivity to HDI treatment 102
3.5 Strategies for depleting MyD88 in non-adherent cells: transient transfection, electroporation, nucleofection and generation of shRNA cell lines 109
3.6 Chemical inhibition of MyD88 114
3.7 Conclusions 118

CHAPTER 4. CYTOKINE EXPRESSION IN LYMPHOMA CELL LINES AND EFFECT OF CYTOKINE SIGNALLING PATHWAYS ON HDI SENSITIVITY 119
4.1 Introduction 119
4.2 Cytokine expression profiles of RIVA and HBL-1 cell lines 121
4.3 Effect of IL-6 inhibition on HDI sensitivity 129
4.4 Effect of LPS and recombinant IL-6 on lymphoid cell lines and HDI sensitivity 136
4.5 Intersection of IL-6 signalling and the JAK-STAT pathway 142
4.6 TLR4 receptor blockade affects HDI sensitivity in RIVA but not HBL-1 cells 146
4.7 Conclusion 151
CHAPTER 5. MYD88 ACETYLATION AND RESPONSE OF CANCER CELL LINES TO BROMODOMAIN INHIBITION 153
5.1 Introduction 153
5.2 Acetylation of MyD88 in lymphoma cells 155
5.3 CADOR array and potential bromodomain readers of MyD88 158
5.4 Recognition of MyD88 acetylation by bromodomain readers 164
5.5 Investigation of potential nuclear localization of MyD88 167
5.6 Effect of bromodomain inhibition on HDI response in lymphoid cell lines 172
5.7 Conclusion 177
CHAPTER 6. DISCUSSION 178
6.1 Outcomes of project and conclusions 178
6.1.1 MyD88 is highly expressed in tissue samples from patients with lymphoma 178
6.1.2 The MyD88-mutated cell line HBL-1 secretes IL-6, and neutralization of IL-6 can reduce the sensitivity of HBL-1 cells to HDI treatment 180
6.1.3 MyD88 may be acetylated and several potential interacting bromodomain readers can be identified using a CADOR array 184
6.2 Project limitations 190
6.2.1 Manipulation of MyD88 levels in suspension cells 190
6.2.2 HDAC and BRD specificities 190
6.2.3 Cell fate measurements 191
6.2.4 Cell lines 192
6.2.5 Use of small-molecular agents 193
6.2.6 IHC staining consistency 194
6.3 Future work 195
6.3.1 MyD88 acetylation status, and implicated bromodomains (readers) and histone acetyltransferases (writers) 195
6.3.2 Introducing targeted mutations in MyD88 with the CRISPR-Cas9 system 197

6.3.3 Identifying potential drug combinations 198
6.3.4 Correlating MyD88 protein expression and MyD88 mutation status with patient outcome 199
6.3.5 Measuring circulating free DNA from patients with DLBCL 199
6.4 Project Summary 201
APPENDIX A 202
APPENDIX B 202
APPENDIX C 204
APPENDIX D 205
APPENDIX E 206
REFERENCES 207

CHAPTER 1. INTRODUCTION

1.1 Diffuse large B cell lymphoma (DLBCL) biology and classification

Diffuse large B cell lymphoma (DLBCL) represents the most frequent non-Hodgkin's lymphoma (NHL) in adulthood, accounting for 30% to 40% of all new NHL diagnoses (WHO 2014). It is an aggressive lymphoma, arising de novo in the majority of cases, or, less frequently, from indolent B cell malignancies, and is rapidly fatal if left untreated.

Although the outcome from DLBCL has improved over time with the advent of immunotherapy, epidemiologic data from the Surveillance, Epidemiology, and End Results (SEER) database in the United States suggest that recent decades have seen a steady increase in DLBCL incidence, particularly in the elderly population (Tilly*, et al* 2012); (https://seer.cancer.gov/). Moreover, up to 30% of patients with newly diagnosed disease will be resistant or refractory to conventional chemotherapy regimens and, having failed first-line therapy, salvage options are limited, with most relapsed/refractory patients ultimately succumbing to their disease (Sehn and Gascoyne 2015, Tilly*, et al* 2012).

Two developments have significantly influenced our understanding and management of DLBCL over recent years: firstly, the addition of the chimeric monoclonal antibody rituximab to the most commonly used initial chemotherapy regimen comprising cyclophosphamide, doxorubicin, vincristine, and prednisolone (CHOP), has been shown to increase the rates of complete remission (CR), progression-free and overall survival significantly (Coiffier*, et al* 2002, Feugier*, et al* 2005, Habermann*, et al* 2006, Pfreundschuh*, et al* 2006, Sehn*, et al* 2005). Although newly diagnosed DLBCL can therefore be treated to CR in about 75% of cases (Coiffier*, et al* 2010), a 10-year progression-free survival (PFS) of 36.4% and a 10-year overall survival (OS) of 43.5% suggest that the optimization of frontline therapy and the availability of effective salvage treatments remain the two key objectives. In addition, delivering standard-

dose chemotherapy to elderly patients can be challenging given an increased prevalence of co-morbidities in this patient population.

Secondly, although it has been well recognized that DLBCL is a heterogeneous disease with respect to clinical presentation and disease course, only through recent advances in molecular biology and genetics has it been possible to understand these characteristics at a molecular level and elucidate some of the oncogenic pathways involved in DLBCL lymphomagenesis. The use of gene expression profiling (GEP) techniques in DLBCL suggests that this (up until now) histologically defined disease entity displays significant heterogeneity at a molecular level.

Therefore, the classification of DLBCL into molecular sub-types should in the future allow a more personalized approach to therapy in patients who present with DLBCL that is histologically otherwise indistinguishable (Intlekofer and Younes 2014, Nogai*, et al* 2011, Scott 2015a, Sehn*, et al* 2005).

1.2 Biological heterogeneity and functional classifications of DLBCL

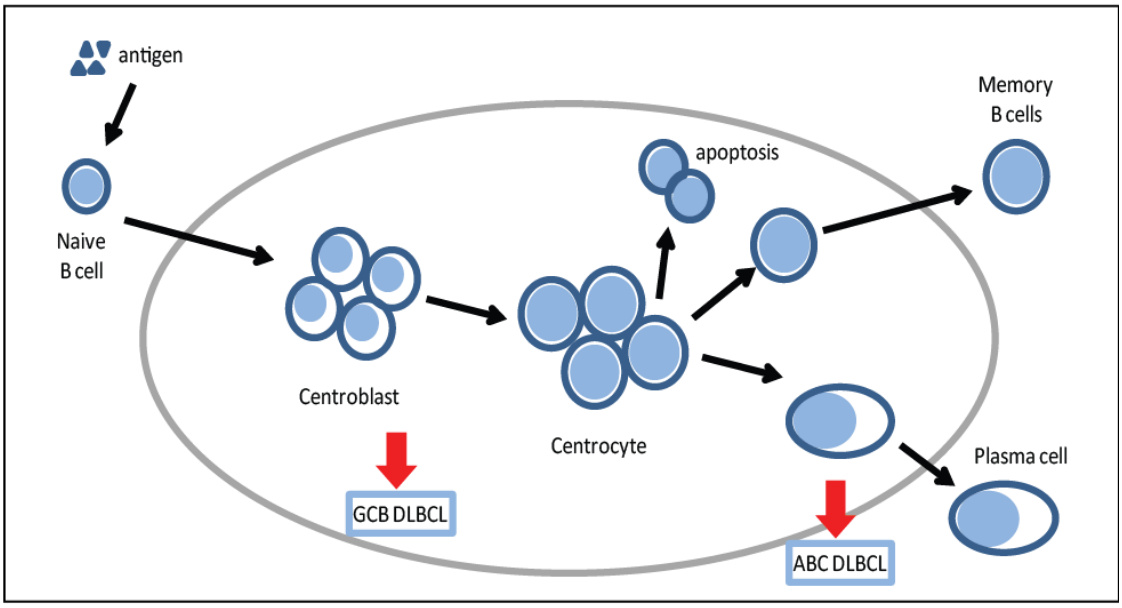
Three functional classifications have emerged as a result of GEP in DLBCL: two classifications, referred to as the cell of origin (COO) and the consensus clustering classification (CCC), are based on transcriptional disease profiling, whereas the stromal signature classification relates to the tumour microenvironment.

1.2.1 Cell of origin (COO)

The COO classification distinguishes three major molecular subtypes of DLBCL which are thought to arise from B cells at different stages of differentiation: these are referred to as activated B cell (ABC), germinal center B cell (GCB), and primary mediastinal B cell lymphoma (PMBL) and account for approximately 30%, 48%, and 22% of DLBCL diagnoses, respectively (Alizadeh*, et al* 2000, Rosenwald*, et al* 2002). ABC DLBCLs appear to derive from B cells at the plasmablastic stage and characteristically show constitutive activation of the NF-kB pathway, whilst GCB DLBCLs originate from germinal center B cells, with a large proportion of this

subtype displaying a deregulated BCL2 pathway (Figure 1.1). PMBL, finally, is thought to originate from a population of thymic B cells and shows a high prevalence of amplification of 9p24 (Alizadeh*, et al* 2000, Joos*, et al* 1996, Lenz*, et al* 2008b). Histologically indistinguishable, all three subtypes differ in the expression of hundreds of genes.

Figure 1.1



The origin of ABC and GCB DLBCL subtypes. The two major DLBCL subtypes are thought to arise from B cells in the germinal centre. Antigen is encountered and processed by naive B cells that then circulate to a lymph node. In the germinal centre, activated B cells proliferate as centroblasts, before undergoing selection as centrocytes. Selected B cells then either mature into plasma cells or memory B cells before exit from the lymph node into the circulation. The GCB subtype of DLBCL is thought to originate from centroblasts, whereas the ABC subtype arises from plasmablastic cells just prior to germinal centre exit.

Adapted from: (Pasqualucci*, et al* 2011b, Sehn and Gascoyne 2015)

1.2.2 Consensus Clustering Classification (CCC)

The CCC classification also identifies three DLBCL subtypes which are based on the transcriptional heterogeneity found solely within tumours. These DLBCL subtypes are categorized by their reliance on B cell receptor (BCR) signalling, oxidative phosphorylation (OxPhos), or the presence of an increased inflammatory and immune cell infiltrate (host response, HR-type) (Abedin*, et al* 2016, Chapuy*, et al* 2016, Chapuy*, et al* 2013, Monti*, et al* 2005). The BCR-type DLBCLs have been found to highly express some of the proximal mediators of the BCR pathway such as spleen tyrosine kinase (SYK), and rely heavily on proximal BCR signalling (Chen*, et al* 2013). Both BCR-dependent ABC DLBCLs with high baseline NF-kB activity as well as BCR-dependent GCB DLBCLs with low baseline NF-kB activity have been included in this group, with different consequences observed after inhibition of proximal BCR pathway inhibition (Chapuy*, et al* 2016, Chen*, et al* 2013). By contrast, BCR-independent OxPhos-type DLBCL has been shown to display enhanced mitochondrial energy transduction, greater incorporation of nutrient-derived carbons into the tricarboxylic acid cycle, and increased glutathione levels. Whilst these tumours are relatively insensitive to BCR survival signalling, disruption of the fatty acid oxidation programme and glutathione synthesis were proven to be selectively toxic to this tumour subset (Caro*, et al* 2012). HR-type DLBCLs, finally, are characterized by an increased expression of T/natural killer cell receptor and activation pathway components, complement cascade members, macrophage/dendritic cell markers, and inflammatory mediators (Monti*, et al* 2005). This DLBCL subtype is thought to share features of histologically defined T cell/histiocyte-rich B cell lymphoma.

1.2.3 Stromal signatures

To add to the complexity of DLBCL as a disease category, the discovery of gene signatures termed “stromal-1” and “stromal-2” which relate to the composition of the tumour microenvironment, have been correlated with outcome but appear to be independent from COO and CCC (Lenz*, et al* 2008a): the prognostically more favourable "stromal-1" signature is

characterized by extracellular matrix deposition and macrophage infiltration of the tumour, whereas tumours identified as "stromal-2" display a high level of angiogenesis and density of blood vessels.

All three classifications described above provide some insights into different aspects of disease pathogenesis and suggest different tumour cell dependencies that may be exploited for targeted therapy.

1.3 Determining cell of origin

Differentiating patient subgroups by cell of origin has been found to have prognostic implications, with the majority of patients diagnosed with the DLBCL GCB subtype exhibiting a superior outcome compared to patients with the ABC subtype. Thus, 5-year OS rates amongst patients with GCB DLBCL were reportedly 60% compared to 30% in patients with ABC DLBCL in retrospective analyses carried out prior to the introduction of rituximab (Wright*, et al* 2003). In patients treated with an anthracycline-containing regimen plus rituximab, however, the impact of GCB/ABC subtyping remains more controversial (Hans*, et al* 2004, Nyman*, et al* 2009, Ott*, et al* 2010).

In view of its prognostic significance and the emergence of novel therapies that aim to selectively target distinct biological pathways, a reliable method of determining the cell of origin in the diagnosis of DLBCL is required; GEP is not routinely available in the clinic due to the need for fresh-frozen tissue and a lack of commercially available standardized tests (Sehn and Gascoyne 2015). Accordingly, immunohistochemistry (IHC)-based algorithms have been developed, with the Hans algorithm, which designates patients as GCB versus non-GCB on the basis of three IHC markers (i.e. the presence of CD10, BCL6, and IRF4/MUM1), being the most commonly used (Hans*, et al* 2004, Sehn and Gascoyne 2015). However, any such IHC-based disease stratification can only be seen as an imperfect substitute for GEP, as they are limited

by the number of markers examined and the reproducibility of IHC itself (de Jong*, et al* 2007). Alternative techniques, such as the Lymph2Cx, a 20-gene NanoString based assay that can be carried out using formalin-fixed paraffin-embedded tissue (FFPET) may improve COO assignment in the future (Scott 2015b).

1.4 Mutational landscape in DLBCL

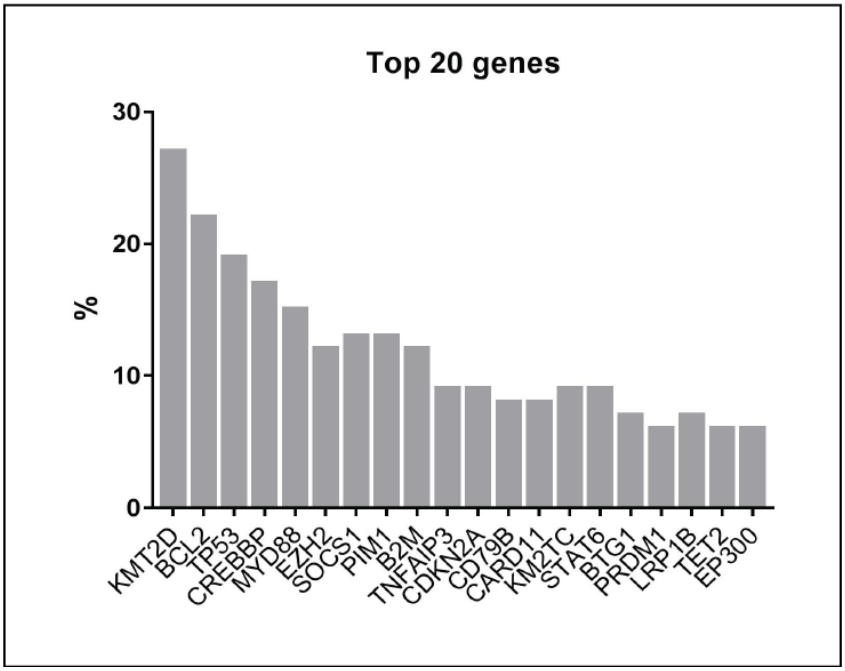
The identification of targetable mutations in DLBCL has been of particular interest, with the use of distinct treatment regimens for molecularly defined subtypes being a primary goal of novel drug development strategies.

The use of next generation sequencing (NGS) technology in several recent studies has helped to provide insight into the significant molecular heterogeneity and complexity of DLBCL at the single nucleotide level (Bohers*, et al* 2015, Lohr*, et al* 2012, Morin*, et al* 2011, Pasqualucci*, et al* 2011b, Zhang*, et al* 2013). The number of genetic lesions has been reported to range widely between cases, sometimes exceeding 100 lesions per case (Pasqualucci*, et al* 2011b); these include point mutations, copy number aberrations, and chromosomal translocations, with some alterations found to be shared across subtypes, whereas others are found predominantly to be subtype-associated (Pon and Marra 2016, Sehn and Gascoyne 2015, Testoni*, et al* 2015).

Figure 1.2 shows the top 20 mutated genes in DLBCL; Table 1.1 summarizes some of the most frequently found somatic mutations and pathways affected in ABC and GCB DLBCL. Much interest has centered on the finding that a high frequency of genetic alterations across both the GCB and ABC subtypes of DLBCL can be found to affect histone and chromatin modifying enzymes such as CBP (*CREBBP*), p300 (*EP300*), and KMT2D (*MLL2*). This suggests that tumour development may be influenced by the reprogramming of the epigenome, which in turn has therapeutic implications given the potential of histone deacetylase inhibitors, for instance, to restore physiological acetylation levels (Pasqualucci*, et al* 2011b, Sehn and Gascoyne 2015).

Increased expression of MYC, which promotes cellular growth and differentiation, has been linked with poorer outcome in patients with DLBCL, and also appears to be strongly influenced by deregulation of BCL2 which is most commonly seen in GCB-type DLBCL (Pon and Marra 2016, Sehn and Gascoyne 2015, Testoni*, et al* 2015). By contrast, many of the known genetic mutations leading to aberrant intracellular signalling circuits in ABC DLBCL have been found to converge on the NF-kB pathway, resulting in its constitutive activation (Knittel*, et al* 2016, Wang*, et al* 2013). Gain-of-function mutations in elements of the BCR (*CD79A*, *CD79B*, *CARD11*), or TLR (*MyD88*) signaling pathways have been reported and are thought to be mostly due to somatic mutations: thus, in approximately 10% of patients with ABC DLBCL, gain-of-function mutations in the *CARD11* gene have been reported, whereas in about 20% of patients NF-kB activation has been linked to mutations in *CD79A* or *CD79B*. Loss-of-function mutations of the negative regulator of NF-kB signalling, *TNFAIP3/A20*, through somatic mutation or deletion have been described in up to 25% of patients with ABC DLBCL (Knittel*, et al* 2016, Pasqualucci*, et al* 2011b, Testoni*, et al* 2015, Wang*, et al* 2013).

Figure 1.2

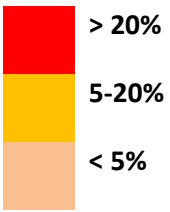


The top 20 most mutated genes in DLBCL. (Source: http://cancer.sanger.ac.uk/cosmic; April 2017)

Table 1.1 Distribution of selected somatic mutations identified by NGS in ABC and GCB DLBCL.

Pathway	Gene	GCB DLBCL Frequency (%)	ABC DLBCL Frequency (%)
BCR/ NF-kB pathways	*MyD88*	< 5	30-37
	CD79A/B	< 5	5-20
	CARD11	5-20	10
	TBL1XR1	unknown	5-20
Immune response	*TNFRSF14*	13	unknown
Apoptosis	*BCL2*	34-45	13
PI3K/mTOR/AKT pathway	*GNA13*	11	unknown
	SGK1	13	unknown
	FOXO1	5-20	5-20
Epigenetic regulation	*MLL2*	32-38	32-38
	EZH2	22	unknown
	MEF2B	11	11
	CREBBP/EP300	32	5-20

Sources: (Bohers, *et al* 2014, Pasqualucci, *et al* 2011b)



1.5 MyD88 as an emerging target in lymphoma

1.5.1 Physiology and structure of MyD88

MyD88 (Myeloid Differentiation Primary Response Gene 88) was originally discovered as a gene that is up-regulated during IL-6 induced myeloid differentiation (Lord*, et al* 1990). It has since been found to act predominantly as an essential adapter protein in mediating downstream signaling through the TLR (Toll-like receptor)- and interleukin-1 (IL-1) receptor pathways which are implicated in innate immunity (Wang*, et al* 2014, Wang JQ 2013).

In mammals, loss of MyD88 leads to deficient innate immune responses: for example, MyD88-deficient mice have decreased resistance to a variety of bacterial and parasitic infections, and inactivating mutations in MyD88 in humans result in an increased susceptibility to pyogenic infections in affected individuals (Scanga*, et al* 2002, Takeuchi*, et al* 2000, von Bernuth*, et al* 2008).

Experimental models show that MyD88 knockout mice will have decreased macrophage activation after stimulation with lipopolysaccharide (LPS), significantly reduced levels of pro-inflammatory cytokine production and impaired T helper cell responses (Adachi*, et al* 1998). Moreover, B cells deficient in MyD88 have been observed to be less capable of efficient antigen presentation via MHC class II, and to have impaired proliferation and antibody responses following LPS stimulation (Kawai*, et al* 1999, Wang*, et al* 2013).

Interestingly, loss of Tube, the homologue of MyD88 in Drosophila, leads to a plethora of fungal and microbial infections in Drosophila (Horng and Medzhitov 2001). MyD88, and its functional equivalents, therefore can be seen to play a crucial role in many different organisms, which may serve as an explanation as to why it is an evolutionarily highly conserved molecule (Wang*, et al* 2013).

The MyD88 protein usually contains 296 amino acids and is composed of three main domains: an N-terminal death domain (DD), an intermediary domain (INT), and a Toll/IL-1 receptor

homology domain (TIR) at the C-terminus (Figure 1.3a) (Into*, et al* 2010, Ngo*, et al* 2011). The TIR domain mediates interaction of MyD88 with other TIR domain-containing proteins (receptors or adapters), whereas the DD domain associates with interleukin-1 receptor-associated kinases (IRAK) to facilitate downstream signalling (Deguine and Barton 2014). The INT domain is thought to play a role in IRAK4 activation, and a splice variant of MyD88, MyD88s, which lacks the INT domain, has been shown to inhibit LPS-induced downstream NF-kB activation (Burns*, et al* 2003, Janssens*, et al* 2003). Despite its sequence similarity to TLR TIR domains, structural differences in the BB loop of the MyD88 TIR domain are thought to prevent spontaneous TIR dimerization of MyD88 molecules in the absence of TLR ligation. Thus, conformational changes that occur on TLR ligand recognition could bring the TIR domains into close proximity, allowing for a change in avidity and initiation of MyD88 signalling (Deguine and Barton 2014, Khan*, et al* 2004).

1.5.2 The role of MyD88 in TLR signalling

To date, ten TLRs have been described in humans, and these are summarized in Table 1.2. Despite their ability to recognize a vast range of differing pathogen associated molecular patterns (PAMPs), all TLRs have strikingly similar intracellular signalling pathways (Takeda and Akira 2004). With the exception of TLR3, a MyD88-dependent signalling pathway downstream of the TLR TIR domain is common to all TLRs. Following receptor ligation, the MyD88 protein is recruited to the TIR domains of the activated TLR via TIR-TIR interaction. TLRs 2 and 4 have been shown to require an additional adapter molecule, TIRAP (also known as Mal), which directly mediates the TLR/TIR-MyD88/TIR interaction and is thought to aid more efficient MyD88 recruitment and TLR signal amplification (Ohnishi*, et al* 2009).

The clustering of TIR domains allows the oligomerization of MyD88 DDs with DDs of IRAKs to take place. This leads to the formation of a signalling platform which is also referred to as the

Myddosome (Figure 1.3b) (Motshwene*, et al* 2009). The Myddosome has been described as assembling in a sequential and hierarchical fashion, consisting of between six to eight MyD88 DDs forming a ring which is further stabilized by the binding of four IRAK4 DDs, followed by four IRAK2 DDs (or four of the related IRAK1 DDs), with the eventual oligomer resembling a helical structure (Lin*, et al* 2010, Motshwene*, et al* 2009). Consistent with this role of the MyD88 DD, experiments in which a MyD88 DD-INT domain construct was over-expressed showed this to result in spontaneous downstream NF-kB signalling events (Medzhitov*, et al* 1998). IRAK4 is responsible for the phosphorylation of IRAK1 and IRAK2, a process facilitated by the Myddosome complex which is thought to bring the kinase domains of the different IRAK family members into close proximity to allow phosphorylation-mediated activation to take place. Using shRNA knockdown and a small-molecule selective IRAK4 inhibitor, Ngo *et al* showed that IRAK4 kinase activity in particular was important for the transduction of signals downstream from MyD88 to promote survival of ABC DLBCL cell lines (Ngo*, et al* 2011).

Table 1.2 TLRs, their ligands and sub-cellular localization.

TLR	Cellular localization	Ligand	Adaptor proteins
1	Plasma membrane	Triacetylated peptides	MyD88, TIRAP
2	Plasma membrane	Triacetylated peptides	MyD88, TIRAP
3	Endosome	Double-stranded DNA	TRIF
4	Plasma membrane	Lipopolysaccharide	MyD88, TIRAP, TRIF, TRAM
5	Plasma membrane	Flagellin	MyD88
6	Plasma membrane	Diacetylated peptides	MyD88, TIRAP
7	Endosome	Single-stranded RNA	MyD88
8	Endosome	Single-stranded RNA	MyD88
9	Endosome	CpG DNA	MyD88
10	Plasma membrane	Unknown	MyD88 (presumed)

NB. Most TLRs form homodimers upon activation, but TLR2 is capable of forming heterodimers with TLR1 or TLR6 which help to distinguish tri-acetylated and di-acetylated peptides, respectively. The ligand-specificity and biological function of TLR10 is as yet unknown. *TIRAP*, TIR Domain Containing Adapter Protein; *TRIF*, TIR-Domain-Containing Adapter-Inducing Interferon-β; *TRAM*, Translocating Chain-Associating Membrane Protein.

Sources: (Takeda and Akira 2004, Wang*, et al* 2014)

Following the activation of IRAK1/2, the E3 ubiquitin ligase, TRAF6 (TNF receptor associated factor 6) is recruited to the complex via the TRAF-binding domain. Subsequently, TRAF6 is thought to form a cytoplasmic complex with another protein kinase, TAK1, activating TAK1 through ubiquitylation. TAK1 then regulates the activation of both the NF-kB and mitogen-activated protein kinase (MAPK) pathways (Knittel*, et al* 2016, Takeda and Akira 2004, Wang*, et al* 2014) (Figure 1.3c). In resting cells, the members of the NF-kB transcription factor family are kept inactive in the cytoplasm by binding to inhibitory IkB proteins. On stimulation, TAK1 activates IkB kinase β through phosphorylation. As a consequence, IkB is phosphorylated and targeted for proteasomal degradation. NF-kB proteins are therefore released from IkB and translocate to the nucleus where they activate their target genes (Nogai*, et al* 2013, Solt and May 2008).

Figure 1.3 MyD88 structure and its role in TLR-signalling and NF-κB activation.

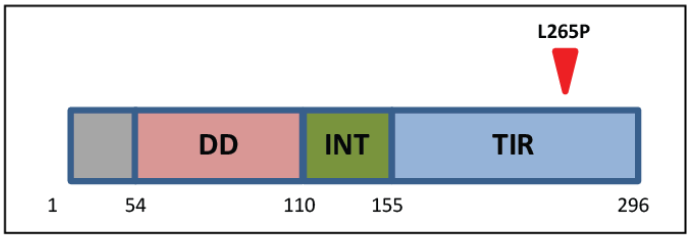
a. The MyD88 protein is composed of three domains: a C-terminal TIR (Toll IL-1R) domain, an N-terminal death domain (DD) and an intermediate (INT) domain which links the two and is necessary for IRAK4 activation.

b. The MyD88 protein can associate directly with TLR receptors through TIR-TIR interactions which in turn leads to MyD88 clustering and oligomerization. MyD88 DDs can interact with IRAK DDs, forming a structure which has also been termed the "Myddosome" (Motshwene*, et al* 2009).

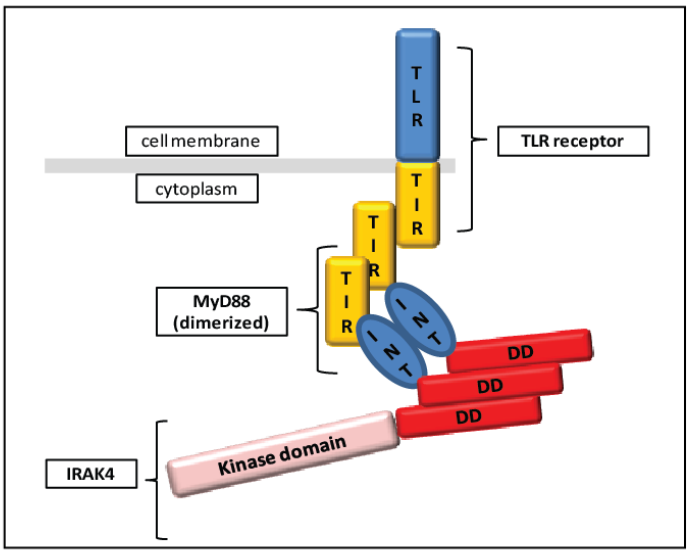
c. Once signalling is activated through the TLR receptor, MyD88 is recruited to the TLR-TIR domain through TIR-TIR interactions. Subsequently, the interaction of the MyD88 DD with IRAK4 establishes a platform for downstream signalling, leading to activation of the NF-κB and MAPK pathways. The eventual outcome is the transcription of genes for pro-inflammatory cytokines (IL), such as for example IL-6.

Figure 1.3

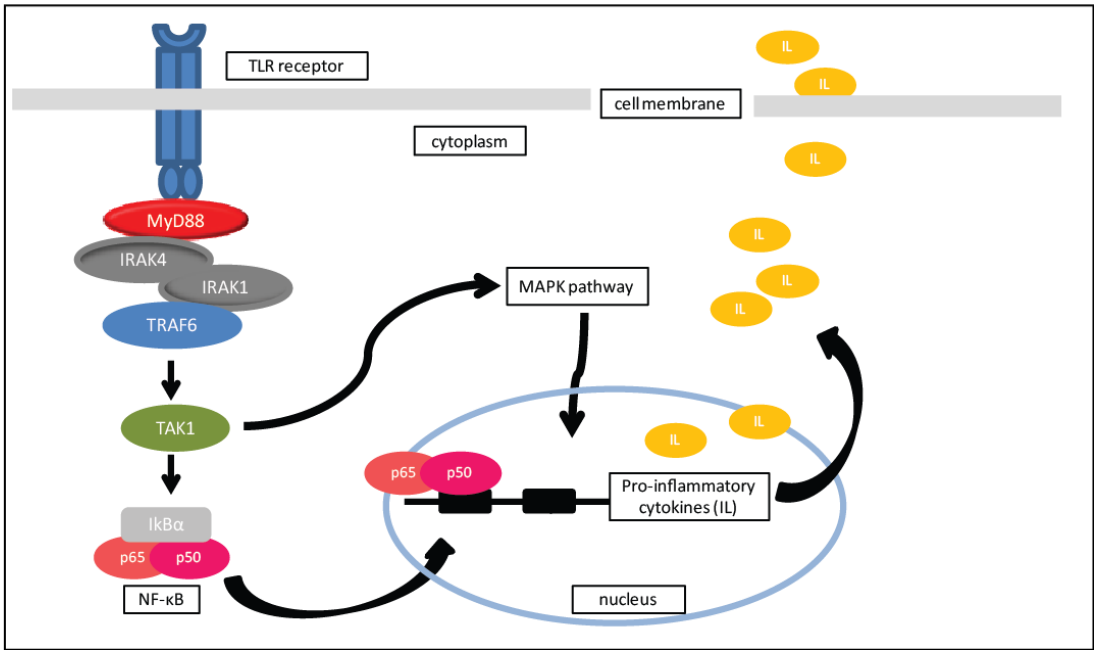
a.



b.



c.



MyD88 signalling may be further regulated by other interacting proteins: Into *et al* showed that endogenous MyD88 in RAW264.7 mouse macrophages may be present as dimers that can be visualized as small speckle-like structures by immunofluorescence. Following TLR activation, oligomerized MyD88 could recruit sequestosome 1 (SQSTM1) and histone deacetylase 6 (HDAC6), both implicated in the accumulation of polyubiquitinated proteins, to the complex. As a result, a down regulation of the MyD88-TRAF6 complex and TLR-induced IL-6 was observed (Into*, et al* 2010).

Although its role in TLR signalling suggests that MyD88 should primarily be a cytoplasmic protein, there are also reports of the localization of MyD88 in the cell nucleus (Aguirre and Hermoso 2005, Jaunin*, et al* 1998, Rebl*, et al* 2017). Therefore, the sub-cellular localization of MyD88 still requires further clarification. Interestingly, one group has also identified a conserved region spanning the N-terminal domain of MyD88 and involving the death domain (aa28-67), that appears to regulate c-MYC activity in monocyte/macrophage RAW264.7 cells; deletion or mutation of just one residue (F36D) significantly promoted c-MYC expression, and its activity could be abrogated by a phosphoinositide 3-kinase (PI3K) inhibitor (Zhang*, et al* 2009). The mechanism by which this interaction may take place, however, has so far not been elucidated.

1.5.3 The role of MyD88 in cellular transformation

Given its role in TLR signalling and the induction of a pro-inflammatory cytokine response, wild-type (WT) MyD88 has been implicated in promoting tumour cell growth in some cancer models: APC^{min} mice, which due to a truncating mutation of the APC tumour suppressor gene develop multiple intestinal tumours, were found to have significantly smaller and less frequent adenocarcinomas when bred into a MyD88 deficient ($MyD88^{-/-}$) background (Rakoff-Nahoum and Medzhitov 2007). In a murine mammary cancer model, inhibition of MyD88 homodimerization using a small-peptide inhibitor was shown to lead to both decreased

tumour volume and expression of pro-inflammatory chemokines CCL2 and CCL5. These effects could be replicated in the human breast cancer cell line MDA-MB-231 (Egunsola*, et al* 2012).

Furthermore, exposure of mice to a combination of DMBA/TPA (7,12-dimethylbenz[*a*]anthracene /12-*O*-tetradecanoylphorbol 13-acetate) is known to cause skin papilloma due to a pro-inflammatory process. MyD88$^{-/-}$ mice were less likely to develop skin tumours compared to their MyD88^{WT} counterparts (Swann*, et al* 2008). Surprisingly, when the authors examined the effects of the 3′-methylcholanthrene (MCA) model of chemical carcinogenesis (a model where MCA induces fibrosarcomas in treated animals and examines the effects of innate and adaptive immune surveillance mechanisms on the development of cancer), MyD88$^{-/-}$ mice again were found to form fewer tumours compared to the MyD88^{WT} controls that were treated in a similar manner. MyD88-deficient mice, however, did not show a defective ability to reject highly immunogenic transplanted tumors, including MCA sarcomas.

Taken together, the authors concluded that MyD88 promotes tumour development through inflammation-driven mechanisms, but that its role in immunosurveillance may be more complicated (Swann*, et al* 2008).

The role of MyD88 in cell transformation is not entirely clear however: on the one hand, constitutive activation of the NF-kB pathway may lead to the production of pro-inflammatory cytokines such as IL-6 and IL-10, and chronic inflammatory states have been implicated in carcinogenesis (Kfoury*, et al* 2014). On the other hand, MyD88 may also exert a pro-tumourigenic effect through its involvement in other signalling pathways. For example, MyD88$^{-/-}$ cells displayed reduced activation of Ras-MAPK signalling, and inhibition of WT MyD88 in cells reduced phosphorylation of ERK (extracellular signal-related kinase), a key MAP kinase. Mechanistically, MyD88 was shown to bind directly to ERK and thereby prevent or decrease its de-phosphorylation and inactivation, a process which was thought to facilitate Ras-pathway mediated cell transformation (Coste*, et al* 2010). Interestingly, MyD88 was also

found to be over-expressed in tumour sections from patients with solid cancers, including lung and colon cancer, and shown to interact with phosphorylated ERK by proximity ligation assay.

Collectively, these results suggest that MyD88 signalling can lead to distinct outputs and may be influenced by the cell type, microenvironment and its own expression within the cell. Depending on a combination of these variables, MyD88 may act at the intersection between inflammation and transformation and promote carcinogenesis by various mechanisms.

1.5.4 The MyD88 L265P mutation in DLBCL

Using high-throughput re-sequencing of mRNA to search for sequence variants in ABC DLBCL cell lines, Ngo *et al* discovered a recurrent, missense single-nucleotide mutation of the MyD88 coding region in four different ABC DLBCL cell lines (Ngo*, et al* 2011). To extend this finding, the group then re-sequenced the MyD88 coding region in 382 lymphoma biopsy samples. Somatic mutations in the MyD88 gene on chromosome 3 were demonstrated to occur in 39% of ABC DLBCL in this series, thereby constituting the most frequently recognized recurrent mutation in this DLBCL subtype (Bohers*, et al* 2014, Ngo*, et al* 2011). Strikingly, 29% of ABC DLBCL in the study by Ngo *et al* were shown to harbour the same mutation in *MyD88*, resulting in the substitution of the amino acid leucine to proline at position 265 (L265P mutation). By contrast, this mutation occurred very rarely in the GCB and PBML subtypes of DLBCL. The majority of the MyD88 L265P mutations were heterozygous, with only six biopsy samples found to be homozygous (Ngo*, et al* 2011).

These findings were corroborated by another research group in France who analyzed MyD88 mutational status in 161 patients with de novo DLBCL (Bohers*, et al* 2014). Thirty patients (19%) were found to have MyD88 mutations, with a significantly higher proportion of these occurring in ABC DLBCL (31%) compared to GCB DLBCL (9.7%). As before, the most common mutation was MyD88 L265P (18/30 patients); one patient was found to carry a homozygous MyD88 L265P mutation.

How the MyD88 L265P mutation contributes to lymphomagenesis is at present only incompletely understood: the mutation occurs at an evolutionarily invariant residue in a β-sheet at the hydrophobic core of the MyD88 TIR domain, and another mutation (M232T) has been found at a structurally adjacent methionine residue (Ngo*, et al* 2011, Shaffer*, et al* 2012). These mutations are thought to therefore disrupt the tertiary structure of the TIR domain. Moreover, many of the other known MyD88 mutations (Figure 1.4) cluster in the BB loop of the TIR domain which interacts with the TIR domains of engaging TLRs (Knittel*, et al* 2016, Shaffer*, et al* 2012), suggesting that TLRs may influence MyD88 signalling in lymphoma. Some evidence favouring this hypothesis has been generated through experiments in chronic lymphocytic leukaemia (CLL), where TLR stimulation of MyD88-mutated CLL cells induced much higher levels of certain cytokines (including IL-6) and chemokines as compared to MyD88-unmutated CLL cells. When the MyD88-inactivating mutation E52DEL was present, by contrast, TLR stimulation did not result in an increased secretion of cytokines (Puente*, et al* 2011). Presumably, the enhanced cytokine production in response to TLR ligation may aid the recruitment of macrophages and T lymphocytes by CLL cells, creating a favourable niche for their survival. In addition, activation of TLRs in CLL cells promotes the proliferation of tumour cells and protects them from spontaneous apoptosis (Muzio*, et al* 2009).

The biochemical and functional relationship between known MyD88 mutants and specific TLRs in DLBCL, however, remains to be elucidated.

Another mechanism that may come into play in this context is the fact that mutated TIR domains have been observed to spontaneously oligomerize and form cytosolic Myddosome complexes in lymphoma cell lines; moreover, lymphoma-associated TIR domain mutants were able to interact with wild-type MyD88 to initiate downstream NF-kB signalling (Avbelj*, et al* 2014). This finding might also provide an explanation for how a heterozygous MyD88 mutation status may suffice as an oncogenic driver.

1.5.5 Other MyD88 mutations in DLBCL

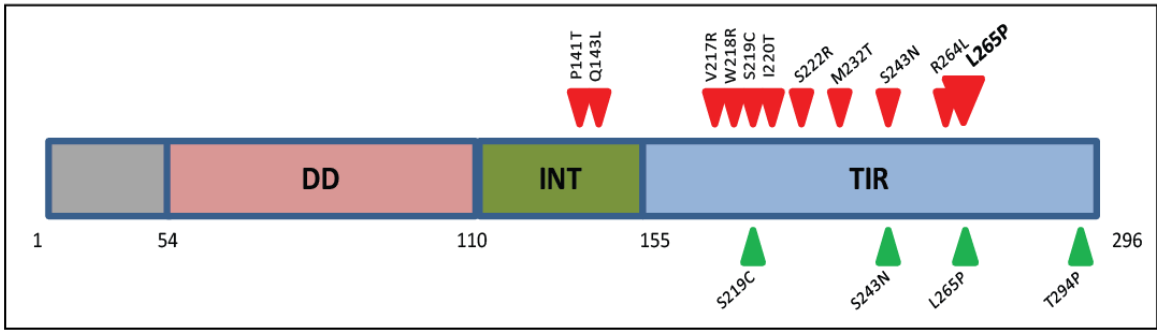
MyD88 mutations other than MyD88 L265P have been described in DLBCL (Bohers*, et al* 2015, Bohers*, et al* 2014, Ngo*, et al* 2011); (http://www.uniprot.org/uniprot/Q99836). The main sequence variants are illustrated in Table 1.3 and Figure 1.4. However, many of these have been found to occur relatively rarely and as yet lack functional characterization, and their putative contribution to lymphomagenesis remains largely unknown.

Table 1.3 Reported MyD88 sequence variants in DLBCL.

Position	Sequence variant	Description	Reference
141	P→T	Unknown pathological significance. Found in ABC DLBCL	(Bohers*, et al* 2014)
143	Q→L	Unknown pathological significance. Found in ABC DLBCL	(Bohers*, et al* 2014)
217	V→F	Unknown pathological significance. Found in ABC DLBCL	(Ngo*, et al* 2011)
218	W→R	Unknown pathological significance. Found in ABC DLBCL	(Ngo*, et al* 2011)
219	S→C	Unknown pathological significance. Found in ABC and GCB DLBCL, and Burkitt's Lymphoma	(Ngo*, et al* 2011)
220	I→T	Unknown pathological significance. Found in ABC DLBCL	(Ngo*, et al* 2011)
222	S→R	Unknown pathological significance. Found in ABC DLBCL	(Ngo*, et al* 2011)
232	M→T	Constitutive NF-κB activation. Found in ABC DLBCL	(Ngo*, et al* 2011)
243	S→N	Unknown pathological significance. Found in ABC and GCB DLBCL	(Ngo*, et al* 2011)
264	R→L	Unknown pathological significance. Found in ABC DLBCL	(Bohers*, et al* 2014)
265	L→P	Gain of function oncogenic driver. Found in various lymphoid malignancies	(Ngo*, et al* 2011)
294	T→P	Unknown pathological significance. Found in GCB DLBCL	(Ngo*, et al* 2011)

Adapted from: www.uniprot.org; (Bohers*, et al* 2014, Ngo*, et al* 2011)

Figure 1.4



Reported MyD88 sequence variants in DLBCL. Schematic representing the localization of reported sequence variants. Sequence variants depicted by red arrowheads represent those occurring in the ABC DLBCL subtype, whereas the green arrowheads show those variants observed in GCB DLBCL. Note that some sequence variants can be observed in either ABC or GCB DLBCL. See also Table 1.3.

Adapted from: (Bohers*, et al* 2014, Ngo*, et al* 2011)

1.5.6 The MyD88 L265P mutation in other lymphomas

The MyD88 L265P mutant has also been found to be present in a number of other, usually indolent, lymphoid malignancies, most notably in Waldenstrom's macroglobulinaemia (WM), a disease entity also known as lymphoplasmacytic lymphoma (LPL) (Table 1.4). The original patient series (Treon*, et al* 2012) reported that 91% of biopsy samples (49/54) from WM patients analyzed by whole genome sequencing were shown to carry the MyD88 L265P mutation, and other, or subsequent, WM cohorts have found similar frequencies of this particular mutation (Morin*, et al* 2011, Poulain*, et al* 2013, Treon*, et al* 2014, Varettoni*, et al* 2013). As in DLBCL, most cases are heterozygously mutated for MyD88 L265P, and no distinguishing clinical or laboratory features were identified in those patients who were homozygous compared to those who were heterozygous (Poulain*, et al* 2013, Treon*, et al* 2014).

Other low-grade lymphomas found to have a notable increase in MyD88 L265P mutations are gastric mucosa-associated lymphoid tissue (MALT) lymphoma, and splenic marginal zone lymphoma (SMZL); nine percent of patients with MALT lymphoma were shown to carry the mutation in one study, and other series have detected MyD88 L265P in six to 15% of SMZL (Martinez-Lopez*, et al* 2015, Ngo*, et al* 2011, Varettoni*, et al* 2013).

Primary central nervous system lymphoma (PCNSL), which is predominantly classified as being of the ABC DLBCL phenotype, has also been demonstrated to have a high rate of MyD88 L265P mutations (Braggio*, et al* 2015, Gonzalez-Aguilar*, et al* 2012). Interestingly, MyD88 L265P mutations are also found at a high frequency in other immune-privileged extra-nodal sites such as for example primary testicular lymphoma (Braggio*, et al* 2015, Gonzalez-Aguilar*, et al* 2012, Kraan*, et al* 2013, Kraan*, et al* 2014).

Mostly, however, the patient numbers in many of these cohorts are relatively small, and the clinical and pathologic features in these patients are only beginning to be collated and

characterized to gain a better understanding of the functional significance and contribution of MyD88 to the disease process.

Table 1.4 summarizes the frequency of MyD88 L265P in some of the B cell neoplasms described above.

Table 1.4 Frequency of the MyD88 L285P mutation in B cell neoplasms.

Disease	Reported frequency of L265P mutation	Total number of cases	Reference
ABC DLBCL	29%	155	(Ngo, *et al* 2011)
ABC DLBCL	6.5%	124	(Choi, *et al* 2013b)
ABC DLBCL	31%	77	(Bohers, *et al* 2014)
CBCL	69%	16	(Pham-Ledard, *et al* 2012)
PCNSL	79%	19	(Braggio, *et al* 2015)
PCNSL	36%	14	(Montesinos-Rongen, *et al* 2011)
PCNSL	38%	29	(Gonzalez-Aguilar, *et al* 2012)
Testicular DLBCL	71%	14	(Kraan, *et al* 2014)
CLL	2.9%	310	(Puente, *et al* 2011)
CLL	6.6%	91	(Wang, *et al* 2011)
LPL	91%	54	(Treon, *et al* 2014)
LPL	79%	67	(Poulain, *et al* 2013)
LPL	100%	58	(Varettoni, *et al* 2013)
LPL	84%	32	(Patkar, *et al* 2015)
MALT	9%	56	(Ngo, *et al* 2011)
MALT	3.8%	53	(Li, *et al* 2012)
SMZL	15%	86	(Martinez-Lopez, *et al* 2015)
SMZL	13%	46	(Yan, *et al* 2012)
SMZL	5.1%	117	(Rossi, *et al* 2012)
SMZL	6%	84	(Varettoni, *et al* 2013)

CBCL, cutaneous DLBCL (leg-type); *PCNSL*, primary central nervous system lymphoma; *CLL*, chronic lymphocytic leukaemia; *LPL*, lymphoplasmacytic lymphoma (also known as Waldenstrom's macroglobulinaemia); *MALT*, gastric mucosa-associated lymphoid tissue lymphoma; *SMZL*, splenic marginal zone lymphoma.

Adapted from (Wang, *et al* 2013).

1.5.7 The MyD88 L265P mutation as a gain-of-function mutation and oncogenic driver

Using an RNA interference screen, Ngo *et al* showed that ABC DLBCL relied on the expression of MyD88 and its associated kinases, IRAK1 and IRAK 4, for their survival, whilst GCB DLBCL, Burkitt's lymphoma, mantle cell lymphoma and myeloma cell lines did not. Co-expression of MyD88 (or IRAK1) coding region cDNA was able to rescue shRNA-silenced cells.

Furthermore, in complementation experiments in DLBCL cell lines harbouring the MyD88 L265P mutation, knockdown of MyD88 followed by rescue with the MyD88 L265P mutant form was able to promote cell survival by leading to spontaneous assembly of Myddosome complexes. This, in turn, initiated persistent downstream NF-kB activation, suggesting that MyD88 L265P is a gain-of-function driver mutation in ABC DLBCL. MyD88 knockdown in ABC DLBCL cells confirmed that the most significantly enriched signature was related to NF-kB signaling, and also showed overlap with a JAK kinase signalling signature, implicating a role for MyD88 at the intersection of these two pathways (Ngo*, et al* 2011). Moreover, this finding may also highlight the importance of the stromal response and the niche microenvironment for tumour survival (Wang*, et al* 2013).

1.5.8 MyD88 mutation as a prognostic indicator

Several studies have analyzed the clinical outcomes in lymphoma patients found to have MyD88 mutations: in WM, somatic mutations in MyD88 were found to be important determinants of clinical presentation and may, in addition, be associated with overall survival. In the absence of MyD88 L265P, patients with WM were more likely to be female, have splenomegaly and express CD27, a member of the tumour necrosis factor (TNF) receptor family which may be involved in B cell activation and memory (Mori*, et al* 2013, Poulain*, et al* 2013). Patients who are MyD88 wild-type ($MyD88^{WT}$) have also been shown to be older (Treon*, et al* 2014), but the impact of MyD88 mutation status on survival remains controversial. Independent studies from Italy (Varettoni*, et al* 2013) and India (Patkar*, et al* 2015) have suggested that patients with the MyD88 L265P mutation were more likely to have a greater

disease burden and a higher risk of disease progression, as well as being more likely to develop progressive disease post-treatment. By contrast, one study from the US reported that MyD88^{WT} patients had a significantly higher mortality from progressive disease during follow-up (Treon*, et al* 2014).

In DLBCL, patients with MyD88 mutations have been reported to be significantly older than those patients without mutations in MyD88, which is consistent with the observation that the proportion of DLBCL cases of the ABC subtype increase with advancing age (Bohers*, et al* 2014, Mareschal*, et al* 2011). The association of MyD88 L265P and prognosis in DLBCL is not clear, however: one retrospective study of 175 newly diagnosed DLBCL cases identified the presence of MyD88 L265P as an independent prognostic factor for outcome in this cohort. Cell of origin in this study was assessed by Hans algorithm and MyD88 mutations were predominantly observed in the ABC DLBCL subgroup as would be expected. On multivariate analysis, only MyD88 mutation status but not ABC subtype predicted for inferior OS after 40 months of follow-up (Fernandez-Rodriguez*, et al* 2014). A similar trend to poorer outcome with MyD88 L265P has been found in two subsequent studies, although these differences did not reach statistical significance (Cao*, et al* 2016, Juskevicius*, et al* 2017).

Interestingly, another patient cohort found MyD88 protein expression regardless of mutation status to be significantly associated with tumour recurrence and shortened disease-free survival (Choi*, et al* 2013b). In this patient series, MyD88, as detected by IHC, was found to be over-expressed in approximately 40% of DLBCL cases and mostly in the ABC subtype, but did not correlate with MyD88 mutation status. Carried out in an exclusively Korean cohort, a much lower incidence of the MyD88 L265P mutation was detected (6.5%), and presence of the mutation was not shown to have a prognostic impact.

In summary, MyD88 has been shown to play an important role in canonical NF-kB signalling, and mutations in MyD88, in particular the MyD88 L265P mutation, may act as an oncogenic

driver in a subgroup of ABC DLBCL. MyD88 may therefore be a target for pharmacologic inhibition in lymphoma but further investigation into the contribution of MyD88 to lymphoma pathophysiology and its usefulness as a prognostic marker of disease and a predictive marker for the development of a targeted treatment approach are clearly needed.

The following sections will now describe how acetylation of histone- and non-histone proteins may play an important role in carcinogenesis and how histone deacetylases (HDACs) and bromodomain-containing proteins have been identified as possible targets in DLBCL.

1.6 Epigenetic control of gene expression and the role of histone acetylation in cancer

Epigenetics is commonly defined as the genetic information that is inherited without any change in the nucleotide sequence of DNA. Recently, techniques such as whole genome sequencing have improved our understanding of the human epigenome and led to the discovery of a complex network of epigenetic modifications which often are found to be disrupted in cancer cells (Esteller 2008, Hatzimichael and Crook 2013). The study of characteristic epigenetic patterns associated with certain cancers therefore holds great promise for unravelling important mechanisms involved in carcinogenesis as well as the discovery of targeted cancer therapies and the development of biomarkers that could allow for a more personalized treatment approach to patients (Ellis*, et al* 2009, Esteller 2008, La Thangue and Kerr 2011).

1.6.1 Chromatin control and the role of epigenetic readers, writers and erasers

Chromatin is the physiological scaffold of DNA. It is a highly complex yet dynamic structure, which is made up of DNA, histone- and non-histone proteins, and exists in two functional conformational states: a densely compacted and therefore transcriptionally inert state termed heterochromatin, and an open, transcriptionally active state termed euchromatin (Ellis*, et al* 2009). The dynamic remodelling of chromatin is thought to underlie most, if not all, DNA-mediated processes, and in particular gene transcription, DNA replication and repair, and apoptosis (Ellis*, et al* 2009, Esteller 2008, Inche and La Thangue 2006). The functional unit of chromatin is the nucleosome which consists of approximately 147 DNA base pairs wrapped around an octamer of core histone proteins H2A, H2B, H3 and H4. Histone proteins are small, highly evolutionarily conserved basic proteins which are found in the nuclei of most eukaryotic cells (Bannister and Kouzarides 2011, Marino-Ramirez*, et al* 2006). The four core histones each contain a globular domain which enables dimerization, and a flexible charged N-terminus, also referred to as the histone tail, which may be modified by a wide range of reversible post-translational modifications (PTMs). The most common PTMs include acetylation of lysine,

methylation of lysine or arginine, phosphorylation of serine or threonine, lysine ubiquitination, lysine sumoylation, and arginine deamination, where each modification is mediated by a specific enzyme (Bannister and Kouzarides 2011, Ellis*, et al* 2009, Inche and La Thangue 2006).

Epigenetic modifications can alter the accessibility of chromatin due to both direct structural effects and their ability to facilitate protein interactions, for example the recruitment and assembly of other multi-component protein complexes or the cross-talk between different epigenetic marks. This has led to the concept of "epigenetic writers, erasers and readers", a precise system that serves to fine-tune gene expression, and which is also sometimes referred to as the "histone code" (Bannister and Kouzarides 2011, Ellis*, et al* 2009, New*, et al* 2012). Thus, epigenetic writers (e.g. DNA methyltransferases and histone acetyltransferases) lay down epigenetic marks which can be modified or abolished by epigenetic erasers (e.g. histone demethylases or histone deacetylases), whereas epigenetic readers (e.g. bromodomains) contain specific protein-protein interaction modules which allow them to recognize different covalent modifications on chromatin and to dock at specific regions within the genome (Dawson*, et al* 2012).

1.6.2 Histone acetylation and cancer

Histone acetylation, and in particular the acetylation status of histones H3 and H4, appears to play a key role in chromatin assembly, transcriptional regulation and gene expression (Ellis*, et al* 2009, Nebbioso*, et al* 2012). Unlike N^{α}-terminal acetylation, ε-amino lysine acetylation of proteins is much more readily reversible (Glozak*, et al* 2005). Histone acetyltransferases (HATs) acetylate proteins on their N-ε lysine residues, whereas histone deacetylases (HDACs) provide the deacetylation event and maintain the equilibrium of lysine acetylation on histones (Glozak*, et al* 2005).

In general, histone acetylation has been associated with an open chromatin structure and an active transcriptional state, whereas the removal of acetyl groups by HDACs has been shown

to lead to compaction of nucleosomes and a closed chromatin structure, and consequently the repression of gene transcription (Esteller 2008, Mummaneni and Shord 2014).

Both HATs and HDACs have become implicated in the de-regulation of epigenetic events during carcinogenesis in solid as well as haematological malignancies (Inche and La Thangue 2006, New*, et al* 2012). Aberrant histone acetylation is thought to occur through a variety of mechanisms, including chromosomal translocations, specific somatic gene mutations and the abnormal recruitment and localization of epigenetic modifiers that mediate particular acetylation events (Bannister and Kouzarides 2011, Esteller 2008). For instance, p300/CREB-binding protein (CBP), a HAT- and bromodomain-containing protein that acts as a co-activator of transcription and regulates chromatin remodelling, can be targeted by the adenovirus E1A and SV40 T antigen proteins. As a result, p300/CBP becomes aberrantly recruited to the promoter regions of genes involved in cell division and proliferation, a process that has been shown to result in cellular transformation (Ellis*, et al* 2009).

Another example is the chromosomal translocation t(8;16) which has been identified in some types of acute leukaemia; this results in the fusion of monocytic zinc finger protein (MOZ) and CBP and enhances the intrinsic ability of MOZ to up-regulate the transcription of NF-kB target genes (Katsumoto*, et al* 2008). The tat-interacting protein Tip60 is a HAT which has been implicated in mediating an important acetylation-dependent switch from cell cycle arrest to apoptosis by means of regulating the acetylation status of p53. Thus, the acetylation of lysine 120 (K120) of the DNA-binding domain of p53 can be catalyzed by Tip60, an event that occurs rapidly after DNA damage. Mutations in K120, from lysine to arginine (K120R), as well as decreased expression of Tip60 through mono-allelic loss have both been described in human cancer; in cell-based studies, a K120R mutant was shown to induce a state of defective apoptosis with reduced transcription of pro-apoptotic target genes (Ellis*, et al* 2009, Inche and La Thangue 2006, Sykes*, et al* 2006).

By contrast, HDACs are not usually somatically mutated in cancer, but rather over-expressed or aberrantly localized (Inche and La Thangue 2006). In a number of solid tumours, including colorectal, prostate, cervical and breast cancers, over-expression of HDAC1 and HDAC2 has been described. In colorectal cancer, this finding was linked with a more aggressive clinical picture. Interestingly, both shRNA knockdown of HDAC1 and HDAC2 in colorectal cancer cell lines as well as pharmacological HDAC inhibition were shown to be effective at suppressing cell growth (Weichert*, et al* 2008). De-regulated HDAC activity has also been demonstrated in acute promyelocytic leukaemia (APML), in which the retinoic acid receptor (RAR) gene on chromosome 15 is fused with the promyelocytic leukaemia (PML) gene on chromosome 17, leading to the characteristic t(15;17). This results in a PML-RARA fusion protein which, through aberrant high-affinity binding of HDACs leads to transcriptional silencing of retinoid target genes, a block in terminal myeloid differentiation and excess proliferation of the leukaemic cells (Chen*, et al* 1996, Horlein*, et al* 1995, Huang*, et al* 2000, Inche and La Thangue 2006).

1.6.3 Non-histone proteins as targets of acetylation

It is increasingly being recognized that in addition to histones, many HATs and HDACs have a wide range of non-histone protein substrates, including transcription factors, cytoskeletal proteins, molecular chaperones and nuclear import factors, many of which may also play prominent roles in oncogenesis (Ellis*, et al* 2009, Glozak*, et al* 2005). A study in cancer cell lines, for instance, identified 3600 acetylation sites on 1750 proteins associated with many different intracellular functions (Choudhary*, et al* 2009).

p53 is perhaps one of the most well-known examples of how non-histone protein acetylation can influence cell growth and differentiation: p53 was shown to interact with p300/CBP in a p53-HAT complex, and p300/CBP can acetylate p53 at multiple lysine residues, thereby activating its sequence-specific DNA binding activity. Further work which showed that p53 can be deacetylated by two different HDACs, HDAC1 and SIRT1, led to the suggestion that acetylation of p53 affects its stability, with the acetylated form being more stable than the de-

acetylated form. Thus, deacetylation of p53 by SIRT1 targets it for more rapid destruction, and thereby for example decreases its ability to transcriptionally activate the cell cycle inhibitor p21, which causes cells to re-enter the cell cycle following DNA repair (Glozak*, et al* 2005).

HDAC6, a cytoplasmic HDAC, is thought to regulate the chaperone activity of the ubiquitous heat shock protein 90 (HSP90) through deactylation: for example, the balance of acetylation and deacetylation will influence how HSP90 will bind to its client proteins and impact on their transport to the proteasome for degradation (Olzscha*, et al* 2015).

Furthermore, the function of tumour suppressor proteins, oncoproteins and cytoskeletal proteins can be affected by changes in their acetylation status, and therefore affect their roles in cancer progression (Khan and La Thangue 2008). Some important examples are summarized in Table 1.5.

Table 1.5 Examples of non-histone proteins that are known substrates for HATs and HDACs.

Functional class	Protein example	Consequences of acetylation
Cytoskeletal	α-tubulin	Acetylation disrupts protein-protein interaction
Chaperone	HSP90	Acetylation disrupts protein-protein interaction
Cell cycle regulation	E2F1	Acetylation increases transcriptional activation and protein stability
	pRb	Acetylation disrupts protein-protein interaction
Transcription	c-MYC	Acetylation increases protein stability
	YY1	Acetylation decreases DNA binding affinity
	p53	Acetylation increases DNA binding affinity, transcriptional activation and protein stability
Cell signalling	STAT3	Acetylation increases DNA binding affinity, transcriptional activation and promotes protein-protein interactions

HSP, heat shock protein; *pRb*, retinoblastoma protein; *YY1*, yin and yang 1; *STAT3*, signal transducer and activator 3. Sources: (Glozak*, et al* 2005, Khan and La Thangue 2008)

1.6.4 HDAC classes and function

To date, 18 HDAC enzymes have been described in humans. These are grouped into four different classes, based on their homology to yeast proteins and are outlined in Figure 1.5 and Table 1.6. Furthermore, HDACs can be divided into Zn^{2+} -dependent (Classes I, II, IV) and Zn^{2+} -independent (Class III only) enzymes, depending on their active site. Class III HDACs are also known as sirtuins and are NAD-dependent enzymes. The Zn^{2+}-dependency, particularly of HDAC classes I and II, is the target for most approaches to HDAC inhibition, and the majority of HDAC inhibitors developed to date will target class I and/or class II enzymes. Class III sirtuins are generally not affected by current HDAC inhibitors that target the Zn^{2+} -dependent HDACs but interest has recently focused on the inhibition of sirtuins as a potential anti-cancer strategy (although this will not be discussed further here) (Hu*, et al* 2014).

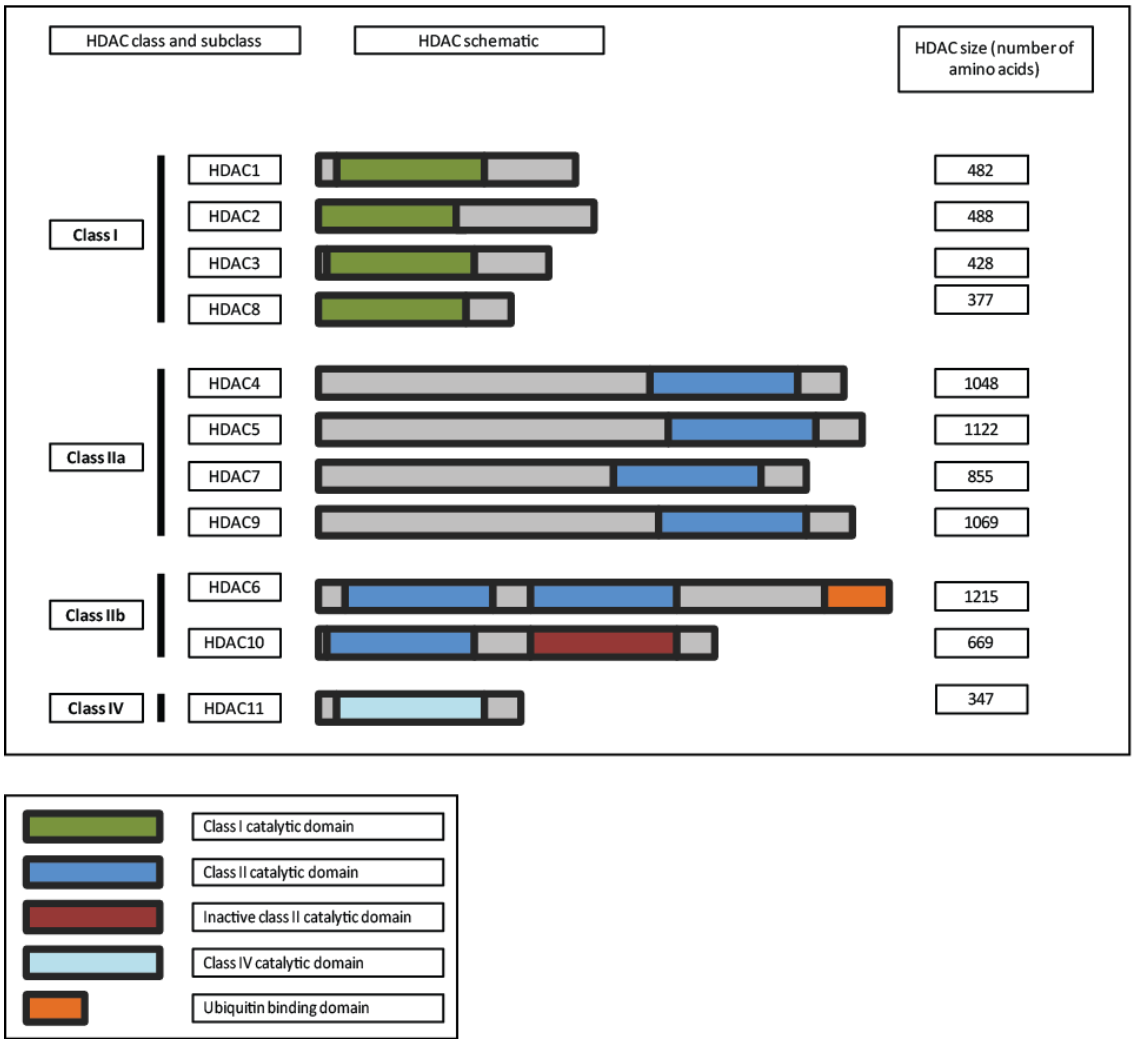
HDAC6 is unique compared to other members of the HDAC family in that it possesses two catalytic domains and is cytoplasmic in its subcellular location. HDAC10 also has been shown to have two putative catalytic domains, although one of these is not thought to be functional (Guardiola and Yao 2002).

The tissue and subcellular expression of HDACs varies: class I HDACs have been found to be ubiquitously expressed in all tissues and are mainly localized in the nucleus, although HDAC3 has been shown to shuttle between the nucleus and the cytoplasm (Haberland*, et al* 2009). Class II and class IV HDACs have more tissue-specific expression patterns (for example, HDAC5 and HDAC9 are highly expressed in muscle, heart and brain), and members of both classes can also move between the nucleus and the cytoplasm (Yang and Seto 2008). In addition, some redundancy has been observed between different HDACs: for example, HDAC1 and HDAC2 have been shown to have approximately 86% sequence homology and often occur together in transcriptionally repressive complexes (Haberland*, et al* 2009). Conditional knock-out studies in mice showed that the presence of at least one of these enzymes is required for B cell development, whereas the elimination of HDAC1 and HDAC2 in mature resting B cells had no

negative impact. Whilst their function may be partially overlapping, however, both HDAC1 and HDAC2 appear to have specific functions and target specificities as well, as loss of one of these HDACs cannot be fully compensated by the presence of the other and vice versa (Yamaguchi*, et al* 2010).

The promising activity of HDAC inhibition in certain types of lymphoma has led to the investigation of HDAC expression in lymphoma cell lines and patient samples: in one study, 73 samples from patients with cutaneous T cell lymphoma (CTCL) were analyzed by IHC for the expression of HDAC1, HDAC2, HDAC6, and acetylated histone H4. HDAC1 was found to be abundantly expressed; HDAC2 and acetylation of histone H4 were significantly more common in aggressive subtypes of CTCL, but only high expression of HDAC6 was associated with overall survival independent of CTCL subtype (Marquard*, et al* 2008). In other types of lymphoma, variable HDAC expression has also been reported; for example, class I HDAC enzymes were highly expressed in a panel of lymphoma cell lines and tissue sections from primary lymphoid tumours, whereas there was significant variability of class II enzyme expression. HDAC6 was most frequently altered, and it was found to be very weakly expressed or absent in 9/14 lymphoid cell lines and in 83/89 primary lymphoma tissue specimens (96% of DLBCL cases and 82% of Hodgkin lymphoma cases) (Gloghini*, et al* 2009). Although a consistent pattern of HDAC expression in lymphoma is yet to emerge, this data suggests that significant variability of HDAC expression exists in different tissue and tumour types, and therefore may influence the response to HDAC inhibition (Gloghini*, et al* 2009).

Figure 1.5



Schematic representing the human Zn^{2+}-dependent HDAC superfamily. Eighteen HDACs have so far been described in humans and are subdivided into four classes. Only classes I, II and IV HDACs are shown here; class III HDACs (sirtuins) are not represented. The HDAC name and designated class are shown on the left. The domain organization of each subclass is represented in the depiction, and the size of each HDAC (number of amino acids) is given on the right.

Adapted from: (d'Ydewalle*, et al* 2012, New*, et al* 2012)

Table 1.6 Characteristics of HDAC enzymes in HDAC classes I, II and IV.

HDAC	Class	Size (kDa)	Subcellular localisation	Putative involvement in cancer
1	I	22-55	Nuclear	Upregulated in gastric, colorectal and pancreatic cancer
2	I	22-55	Nuclear	Upregulated in gastric, colorectal and cervical cancer
3	I	22-55	Nuclear and cytoplasmic	Upregulated in lung, colorectal and prostate cancer
4	IIA	120-135	Nuclear and cytoplasmic	Upregulated in breast cancer
5	IIA	120-135	Nuclear and cytoplasmic	Downregulated in colorectal cancer and acute myeloid leukaemia
6	IIB	120-135	Cytoplasmic	Upregulated in oral squamous cell carcinoma
7	IIA	120-135	Nuclear and cytoplasmic	Upregulated in colorectal cancer
8	I	22-55	Nuclear	Upregulated in neuroblastoma
9	IIA	120-135	Nuclear and cytoplasmic	Upregulated in medulloblastoma/astrocytoma
10	IIB	120-135	Nuclear and cytoplasmic	Upregulated in lung cancer and hepatocellular carcinoma
11	IV	30-50	Nuclear	Upregulated in breast cancer

Source: (Khan and La Thangue 2008, New*, et al* 2012)

1.6.5 HDACs as therapeutic targets

The growing recognition that aberrant acetylation events on histone and non-histone proteins are involved in the initiation and progression of cancer makes the possibility of reversing these changes an appealing target for developing specific and mechanism-based drugs that can redress this imbalance in acetylation status and re-instate a normal acetylation equilibrium (Esteller 2008, Khan and La Thangue 2008). The development of HDAC inhibitors (HDIs) in this context has generated much interest, and HDIs have rapidly emerged as a promising class of small-molecule agents with potent anti-proliferative effects in cell-based studies. HDIs have been shown to cause apoptosis in many different tumour cell lines (Inche and La Thangue 2006), whilst other outcomes such as cell cycle arrest, autophagy, induction of differentiation, generation of reactive oxygen species and anti-angiogenic effects have also been demonstrated (Bezecny 2014, Mai and Altucci 2009). Moreover, HDIs represent an attractive

modality for cancer treatment because their growth-inhibitory and apoptotic activity appears to be predominantly restricted to malignant cells.

HDIs can be divided into pan-HDAC inhibitors and HDAC-specific inhibitors; for example, vorinostat/SAHA and trichostatin A/TSA are general inhibitors, depsipeptide/romidepsin specifically inhibits class I HDACs, LBH589/panobinostat inhibits enzymes of classes I and II (Marks 2010), and tubastatin predominantly inhibits HDAC6 (Butler*, et al* 2010). Alternatively, HDIs can also be classified according to their chemical structure, and therefore into hydroxamates, cyclic peptides, benzamides and aliphatic fatty acids (Table 1.7) (Khan and La Thangue 2008, Marks 2010).

Table 1.7 Classification of HDIs by chemical structure.

HDI class	**Examples of compounds**	**Pharmacologic profile/ potency in vitro (IC_{50})**
Short chain fatty acids	valproic acid phenylbutyrate	Short plasma $T_{1/2}$, rapid metabolism IC_{50} - millimolar
Hydroxamic acids	trichostatin A SAHA (vorinostat) PXD101 (belinostat) LBH589 (panobinostat)	Pan-HDAC inhibitors IC_{50} - nanomolar
Benzamides	MS-275 (entinostat) CI-994 (tacedinaline) MGCD0103 (mocetinostat)	IC_{50} - micromolar
Cyclic peptides	Romidepsin (depsipeptide)	IC_{50} - low nanomolar

Sources: (New*, et al* 2012, Zain and O'Connor 2010)

1.6.6 Cellular outcomes of HDI treatment

Whilst HDIs were initially developed as epigenetic agents that affect transcriptional activation and gene expression through modulation of chromatin, it is now clear, as is also outlined above, that the effects of HDIs go beyond chromatin control and also affect multiple non-histone proteins, thereby modifying gene expression and cellular function via multiple pathways (Zain and O'Connor 2010). The most important outcomes of HDI treatment are summarized in Figure 1.6 and briefly described below.

Cell cycle control and proliferation. The most commonly described effect of HDIs on cancer cells from both haematological and solid tumours is the ability to block proliferation due to cell cycle arrest in G1 or G2/M phase, thought to be due to the down-regulation of cyclin and cyclin-dependent kinases (CDK) which are involved in growth control (Zain and O'Connor 2010). For example, HDI treatment has been shown to cause enhanced acetylation of the NF-kB subunit p52 which then, through increased interaction with p65 prevents the latter from binding to the cyclin D1 promoter (Hu and Colburn 2005). Several HDACs (e.g. HDACs 1,2,3,4) have been associated with a decrease in p21, a cyclin-dependent kinase inhibitor, and therefore promote cell cycle progression. Conversely, HDIs consistently cause up-regulation of p21, leading to G1/S arrest (Richon*, et al* 2000, Wilson*, et al* 2008, Wilson*, et al* 2006, Yamaguchi*, et al* 2010).

Another mechanism of action of HDIs which leads to cell cycle arrest is the transcriptional down-regulation of enzymes that are important for nucleotide synthesis, for example of CTP synthetase and thymidylate synthetase after treatment with SAHA or trichostatin A (TSA) (Glaser*, et al* 2003).

Finally, other pathways that can influence cell proliferation and differentiation in lymphoid cells, such as the JAK-STAT pathway, can be influenced by HDIs. De-regulated STAT (signal transducer and activator of transcription) signalling is implicated in lymphomagenesis, and

STAT3 in particular is found to be constitutively activated in several lymphomas (Zain and O'Connor 2010). In a persistently phosphorylated state, pSTAT3 is able to interact with the NF-kB family member p65, causing it to remain in the nucleus and leading to enhanced production of pro-inflammatory cytokines such as Interleukin-6 (IL-6), and a pro-carcinogenic microenvironment (Yu*, et al* 2009). Interestingly, after treatment with SAHA, pSTAT3 could be seen to localize to the cytoplasm in stained patient tissue sections (Duvic*, et al* 2007). Thus, as nuclear localization of pSTAT3 is important for its function as a transcription factor, this shift in location may correlate with its inactivation and an anti-proliferative effect of SAHA.

Apoptosis. Cell death by apoptosis is a preferred outcome in the treatment of cancers. Preclinical studies have shown a direct correlation between apoptotic tumour cell death and therapeutic efficacy of HDIs (Zain and O'Connor 2010), and GEP of HDI-treated cells suggest an increased expression of pro-apoptotic over anti-apoptotic proteins (Inoue*, et al* 2007, Zhang*, et al* 2006).

HDIs have been shown to induce apoptosis via either the extrinsic or intrinsic pathways in cancer cells both in vitro and in vivo (Bolden*, et al* 2006). The extrinsic apoptotic pathway is initiated in response to extracellular stimuli via binding of cell surface receptors to ligands such as for example TNF-related apoptosis-inducing ligand (TRAIL), TNF-α, and Fas ligand (FasL), resulting in activation of caspase 8 and leading to apoptosis via the final common pathway (Ashkenazi 2002, Bolden*, et al* 2006). HDIs have been shown to increase the expression of death receptors and their ligands, such as TRAIL, Fas and FasL, on leukemic cells following treatment with valproic acid, and of TNF-α after treatment with romidepsin (Insinga*, et al* 2005).

By contrast, the intrinsic mitochondrial pathway is activated in response to intracellular stimuli such as for example oxidative stress, hypoxia or DNA damage, which increase mitochondrial permeability. This causes the release of proteins including cytochrome c and Smac into the

cytosol, which leads to the induction of Apaf-1 (apoptosis pathway activating factor) followed by the activation of caspases 9 and 3, and ultimately, the final common pathway of apoptosis (Ashkenazi 2002, Burz*, et al* 2009). Of note, different HDIs may differ with respect to their effects on the balance of pro-apoptotic and anti-apoptotic proteins in cancer cells: for example, SAHA and romidepsin are both HDIs which have been licensed for clinical use in lymphoid malignancies; they differ in their structure and their potency, but have both been shown to induce caspase-dependent apoptosis in lymphoma cell lines and tumour regression in xenograft mouse models. SAHA causes apoptosis by a p53-independent mechanism, but cells that over-express BCL2 (which is commonly seen in human lymphoma) and BCL-X_L were resistant to SAHA-induced apoptosis. By contrast, romidepsin induced apoptosis in cells that over-expressed BCL2, but not those that over-expressed BCL- X_L, indicating important differences in how HDIs mediate cell death (Zain and O'Connor 2010).

Additional mechanisms by which HDIs can induce apoptosis include the generation of reactive oxygen species (ROS) that lead to increased mitochondrial permeability, or a direct effect on the acetylation status of non-histone proteins such as Bid or p53 (Butler*, et al* 2002, Ruefli*, et al* 2002).

Non-apoptosis cell death. Several HDIs, including SAHA and butyrate, have also been shown to be able to induce caspase-independent cell death in a panel of cancer cell lines. In HeLa cells, Apaf-1 knockout, over-expression of BCL- X_L, and pharmacological inhibition of caspase activity did not prevent HDI-mediated cell death, and morphological features of autophagy were seen (Shao*, et al* 2004). This observation may also help to reconcile some discrepancies in the literature; for instance, caspase activation has been reported to be necessary for HDI-induced cell death, whereas other studies have found that caspase inhibition did not abrogate cell death after HDI treatment (Henderson*, et al* 2003, Mitsiades*, et al* 2004). Therefore, HDIs may be able to induce both modes of cell death, and better methods for measuring this specifically and accurately will need to be developed (Shao*, et al* 2004). Moreover, this finding may also

impact the treatment of different malignancies, as many chemotherapy-resistant cancers have been found to have apoptotic defects (Hanahan and Weinberg 2000).

Angiogenesis. HDIs can influence angiogenesis directly by up-regulating angiogenesis inhibitors such as thrombospondin and von-Hippel Lindau (vHL) factor, as well as down-regulating factors that promote angiogenesis, e.g. vascular endothelial growth factor (VEGF) and hypoxia inducible factor alpha (HIF-α) (Jeong*, et al* 2002, Zain and O'Connor 2010). In addition, HDIs have also been shown to negatively regulate the expression of survivin, an anti-apoptotic protein which is expressed by endothelial cells, thereby inhibiting the growth of vascular endothelium. In tissue biopsies from patients with CTCL, treatment with SAHA for four weeks was shown to reduce microvessel density, and in a CTCL cell line, HH, thrombospondin was increased eight-fold (Duvic*, et al* 2007). Similarly, in another cohort of CTCL patients treated with the HDI panobinostat, GEP of patient samples has shown the consistent down-regulation of the pro-angiogenic genes guanylate cyclase 1A3 (GUCY1A3) and ANGPT1 (Ellis*, et al* 2008).

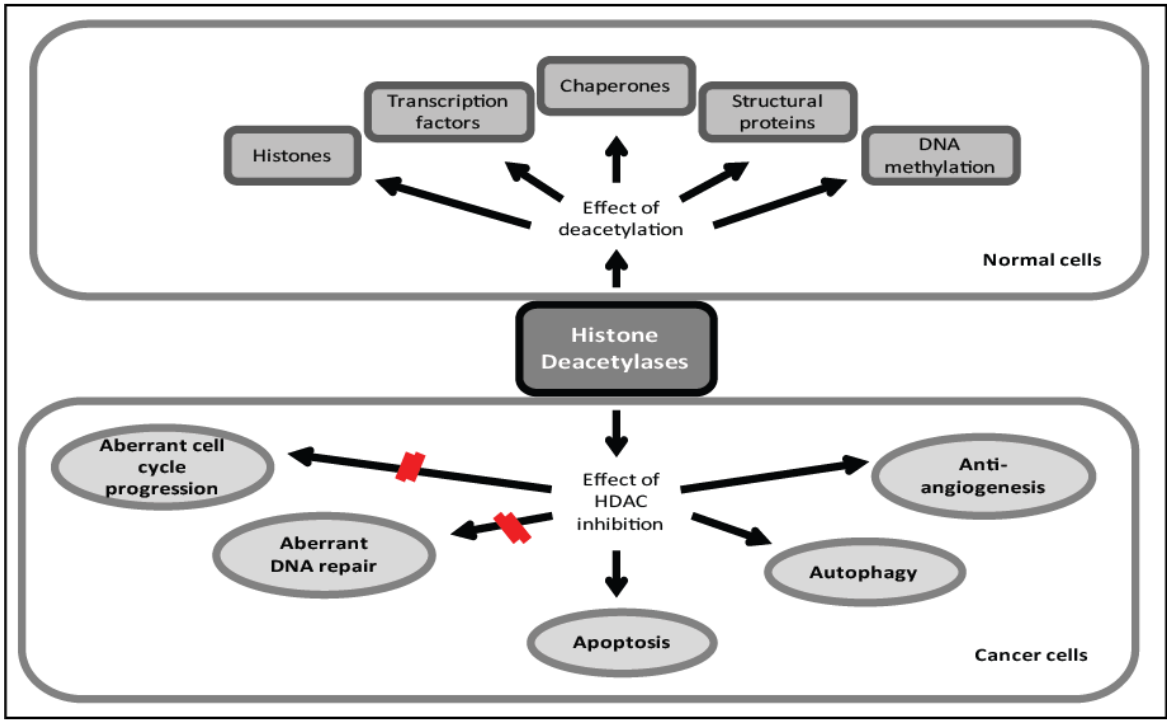
Protein quality control. Protein quality control mechanisms are important to maintain the integrity of the proteome and allow cells to respond to internal and external stimuli. Protein translation, protein folding mediated by molecular chaperones, post-translational modifications, and protein degradation by autophagy or the ubiquitin proteasome system (UPS) are all thought to play a role in this process (Hartl*, et al* 2011, Olzscha*, et al* 2015). Several ways in which HDIs may affect these mechanisms have been described. For example, HDAC6 is able to bind misfolded polyubiquitinated proteins and, through association with dynein motors, aid with their transport to aggresomes where they are processed. Inhibition of HDAC6 leads to a failure of misfolded protein clearance from the cytoplasm, and as a result cells become hypersensitive to the aggregates that these misfolded proteins then form (Kawaguchi*, et al* 2003, Lee*, et al* 2010). As outlined above (Section 1.6.3), HDAC6 also interacts and deacetylates the chaperone protein HSP90. HDI-mediated inhibition of HDAC6 leads to hyper-acetylation of HSP90 and the release of some of its client proteins, including c-

Raf and AKT which are pro-growth and pro-survival. These then undergo poly-ubiquitination and are targeted to the proteasome for degradation (Bali*, et al* 2005, Olzscha*, et al* 2015). Interestingly, HDAC6 has also been shown to directly down-regulate the proteasomal shuttling factor HR23B via its BUZ domain, an event that is independent of its deacetylase activity. Low HR23B levels are thought to lead to a reduction of the levels of ubiquitinated proteins transported to the proteasome and ultimately desensitize cells to apoptosis (Khan*, et al* 2010, New*, et al* 2013).

Immune Function. HDIs also have a range of different effects on the immune system. In a mouse model of allogeneic bone marrow transplantation, SAHA mitigated the severity of acute graft versus host disease (GvHD) by suppressing the secretion of pro-inflammatory cytokines TNF-α, IL-1 and IFN-γ (Khan and La Thangue 2008). In patients receiving SAHA as GvHD prophylaxis after allogeneic bone marrow transplantation, reduced levels of pro-inflammatory cytokines were measured in patient plasma, decreased ex vivo responses of peripheral blood mononuclear cells to pro-inflammatory TLR4 stimuli occurred and, in addition, an increase in the number to regulatory T cells was observed (Choi*, et al* 2015). Furthermore, HDIs may modulate innate and adaptive immune responses by influencing the activation and function of antigen presenting cells: GEP carried out after treatment of cells with the HDI dacinostat/LAQ824 was shown to selectively inhibit dendritic cell-controlled T helper 1 (Th1) effector but not Th2 effector cell activation and migration, and only neutrophil but not monocyte chemotaxis was impaired (Brogdon*, et al* 2007).

HDIs appear to have anti-inflammatory properties which can be recognized at doses that are lower than those used in the treatment of cancer, and the relevance of these immune effects on cancer cells are as yet not fully understood.

Figure 1.6



The multiple roles of HDACs in cells and the effects of HDAC inhibition. Acetylation regulates both histone and non-histone proteins, thereby influencing many physiological pathways (upper panel). Many of these pathways are abnormal in cancer cells and can promote tumour cell survival, proliferation and metastasis. HDAC inhibition can inhibit some of these abnormal pathways (red bars) and promote various cellular outcomes, depicted in the lower panel.

Sources: (Khan and La Thangue 2008, New*, et al* 2012)

1.6.7 Clinical outcomes of HDI treatment

In the clinical setting, the outcomes of HDI-based therapy remain complex and difficult to predict. Strikingly, as HDIs have entered clinical studies, it has become clear that haematological malignancies, and in particular lymphoproliferative diseases, seem to be especially sensitive to HDAC inhibition.

Three of the four HDIs that have been FDA-approved to date (at the time of writing, May 2017), are licensed for the treatment of lymphoma (Table 1.8) (Heerboth*, et al* 2014). Several other drugs with inhibitory activity against HDACs are currently undergoing pre-clinical and clinical investigation, both in solid and haematological malignancies (Table 1.9A). Many of these compounds are also tested in combination with a variety of other anticancer agents and modalities such as radiation, and some examples are provided in Table 1.9B.

Table 1.8 HDIs currently FDA-approved as anticancer agents.

Name	Trade name	Chemical structure	Indication	HDAC specificity
Vorinostat (SAHA)	Zolinza	Hydroxamate	Relapsed Cutaneous T cell lymphoma (CTCL)	Pan-inhibitor
Romidepsin (Depsipeptide/FK228)	Istodax	Cyclic peptide	Relapsed CTCL; Relapsed peripheral T-cell lymphoma (PTCL)	Class I
Belinostat (PXD101)	Beleodaq	Hydroxamate	Relapsed PTCL	Pan-inhibitor
Panobinostat (LBH509)	Farydaq	Hydroxamate	Relapsed multiple myeloma	Classes I and II

CTCL, cutaneous T cell lymphoma; *PTCL*, peripheral T cell lymphoma.

Adapted from: (New*, et al* 2012)

Table 1.9A Examples of HDIs currently in clinical trials.

Trial phase	Drug examples and HDI class/HDAC specificity	Description	ClinicalTrials.gov identifier
Phase I	**Entinostat** Benzamide/Class I	Paediatric patients with recurrent or refractory tumours	NCT02780804
	CHR-3996 Benzamide/Class I	Patients with advanced solid tumours	NCT00697879
	Panobinostat Hydroxamic acid/Pan-HDI	Patients with myelofibrosis	NCT01298934
	CHR-2845 (Tefinostat) Hydroxamic acid/Pan-HDI	Patients with advanced or refractory haematological malignancy	NCT00820508
Phase II	**ITF-2357 (Givinostat)** Benzamide derivative/Class I and II	Patients with relapsed/refractory CLL	NCT00792831
	Panobinostat Hydroxamic acid/Pan-HDI	Patients with advanced small cell lung cancer	NCT01222936
	Entinostat Benzamide/Class I	Patients with metastatic melanoma	NCT00185302
	MK-0683 (Vorinostat) Hydroxamic acid/Pan-HDI	Patients with Polycythemia Vera and Essential Thrombocythaemia	NCT00866762
Phase III	**Vorinostat** Hydroxamic acid/Pan-HDI	Patients with advanced/refractory malignant pleural mesothelioma	NCT00128102
	Valproic Acid Short chain fatty acid/Class I	Patients with metastatic cervical cancer	NCT00532818
	Panobinostat Hydroxamic acid/Pan-HDI	Patients with CTCL	NCT00490776
	Vorinostat Hydroxamic acid/Pan-HDI	Patients with relapsed/refractory CTCL	NCT01728805

Source: www.clinicaltrials.gov

Table 1.9B Examples of HDIs in trials with other therapeutic agents or modalities.

Combination therapy	Example of trial/Phase	Type of malignancy	ClinicalTrials.gov identifier
HDAC inhibitor **+ conventional chemotherapy**	**vorinostat** + CHOP chemotherapy Phase I/II	Haematological (untreated PTCL)	NCT00787527
HDAC inhibitor **+ radiation**	**vorinostat** + radiotherapy Phase I	Brain metastases	NCT00838929
HDAC inhibitor **+ proteasome inhibitor**	**belinostat** + bortezomib Phase II	Haematological (multiple myeloma)	NCT00431340
HDAC inhibitor **+ "IMiD"**	**panobinostat** + lenalidomide Phase II	Haematological (Hodgkin lymphoma)	NCT01460940

IMiD, immunomodulatory imide drugs.

Source: www.clinicaltrials.gov

SAHA, romidepsin and belinostat are currently the only HDIs approved for the treatment of lymphoma. In 2006, SAHA was approved for the treatment of patients with relapsed or refractory CTCL after the publication of two pivotal Phase II studies: in the first study, of 33 patients with heavily pre-treated disease, eight achieved a partial response, with an overall clinical benefit rate of 58%. In the second study, 74 patients with previously treated CTCL received escalating doses of SAHA with an overall response rate of around 30%, and symptomatic relief from pruritus in 32% of patients (Duvic*, et al* 2007, Olsen*, et al* 2007).

Romidepsin is a pro-drug which releases a zinc-binding thiol once it has undergone reduction within cells, and, as a result, it is able to reversibly inhibit the zinc-containing catalytic domains of HDAC1 and HDAC2. Romidepsin was approved for the treatment of CTCL in 2009 after a Phase II multi-centre trial in 71 patients who had had multiple prior lines of therapy

demonstrated an overall response rate of 34% with significant durable responses in some of these patients (Piekarz*, et al* 2009). In 2011, romidepsin also received regulatory approval for peripheral T-cell lymphoma (PTCL) after it was shown in two Phase II trials to induce complete and durable responses in pre-treated, relapsed patients (Coiffier*, et al* 2012).

Belinostat has been approved for the treatment of PTCL since July 2014. This was based on results from a single-arm, multi-centre Phase II study of 120 patients with PTCL which showed an overall response rate of 25.8% and a CR rate of 10.8% with good tolerability of the drug (McDermott and Jimeno 2014, Poole 2014).

By contrast, single-agent HDI studies in patients with relapsed solid tumours, including non-small cell lung, colorectal, breast and renal cell cancers, have only shown limited clinical benefit and have failed to replicate the efficacy of HDIs shown in lymphoid malignacies. Several of these studies had high discontinuation rates due to unacceptable side effects, with nausea, diarrhoea and thrombocytopenia being reported most frequently (Dhanak and Jackson 2014a, Slingerland*, et al* 2014).

These results highlight the fact that a clearer understanding of the biological activity of these agents is needed which will help to determine their optimal clinical application and the most useful combination therapies. Likewise, better methods for monitoring the effects of HDI treatment are needed. Most studies use histone acetylation as a surrogate measure for HDI activity, but histone acetylation is ubiquitous, occurs at multiple residues after HDAC inhibition and can be seen regardless of whether cell death is a consequence of treatment or not. Therefore, histone acetylation is not a reflection of drug sensitivity (Luchenko*, et al* 2014). Some of the effects of HDAC inhibition also appear to be model- or cell type-dependent, such as the role of caspases in mediating apoptosis and the phase of the cell cycle during which arrest occurs (Bates*, et al* 2015, Mitsiades*, et al* 2003). GEP studies in cell lines, xenograft models and patient samples have found that only a relatively small number of genes (between

2% and 5%) are influenced by HDAC inhibition (Bates*, et al* 2015, Khan and La Thangue 2008, Mitsiades*, et al* 2004). In addition, some studies have shown that the levels of most genes induced or repressed by HDI treatment return to baseline within 24 hours, and that across the patient population, few genes are regulated in common (Bates*, et al* 2015, Duvic*, et al* 2007). These observations seem to suggest that the mechanism of action of HDAC inhibition may not solely rely on the regulation of transcription and a sustained gene expression programme, but that other biological pathways and the acetylation status of non-histone proteins play important roles.

1.6.8 The effect of HDIs in DLBCL

The clinical role of HDIs in B cell malignancies remains to be defined. HDIs have been shown to have significant preclinical activity across a range of DLBCL cell lines (Cai*, et al* 2013, Thompson*, et al* 2013). Variable expression of different HDACs has been reported, but cells with the highest HDAC expression levels on HDAC profiling appear to display increased sensitivity to HDI treatment (Cai*, et al* 2013). Resistance to HDIs, however, has also been raised as a problem and may be mediated by increased JAK-STAT activation (McKinney, submitted), or through the expression of anti-apoptotic proteins of the BCL2 family (Thompson*, et al* 2013).

Not much trial data on the response of DLBCL to HDIs is currently available and some reports of HDI efficacy in DLBCL are anecdotal (Zain*, et al* 2007). Most patients with relapsed or refractory DLBCL are recruited into HDI studies that allow patients with other B cell malignancies or advanced cancer in general to be included. In one Phase II study of 18 patients with relapsed DLBCL, treatment with oral SAHA led to a complete response in one patient while another patient developed stable disease. The other 16 patients, however, all had progressive disease (Crump*, et al* 2008). Therefore, the numbers of patients to evaluate in any given trial are small and it is difficult to draw meaningful conclusions. It does appear that some

select patients with DLBCL are able to respond to HDI monotherapy but that the biological pathways underlying response and resistance require further elucidation.

1.6.9 HDI summary

As outlined above, HDIs show promising anticancer activity in both preclinical and clinical trials, with relatively little effect on normal tissues and a favourable toxicity profile. The exact mechanisms by which their activity is mediated, and the pathways affected, however, remain to be fully elucidated. It is also not well understood whether classes of HDIs or certain individual HDIs are more therapeutically effective against specific cancer types. HDIs have consistently shown clinical activity in some haematological, especially T cell-mediated, malignancies, but the clinical outcomes with HDI monotherapy in solid tumours are less encouraging. Therefore, combination therapies of HDIs with chemotherapeutic and biological agents are now being explored in many disease settings.

1.7 Bromodomains: structure and function

Bromodomains (BRDs) are protein recognition and interaction modules that act as (mainly) epigenetic readers by specifically recognizing ε-N-lysine acetylation motifs. BRDs are approximately 110 amino acids long and are highly evolutionarily conserved structures. The BRD sequence motif was first discovered in, and is therefore named after, the *brahma* gene in Drosophila. Sixty-one BRDs, contained in 46 proteins, are present in the human genome and are classed into eight families, based on structure and sequence similarity (Barbieri*, et al* 2013, Filippakopoulos*, et al* 2012, Filippakopoulos*, et al* 2010, Muller*, et al* 2011). BRDs have been identified in a number of nuclear proteins, including HATs (e.g. PCAF), ATP-dependent chromatin remodelling complexes (e.g. BAZ1B), helicases (e.g. SMARCA), methyltransferases (e.g. MLL), transcriptional co-activators (e.g. TRIM/TIF1), transcriptional mediators (e.g. TAF1), and the BET (bromodomain and extra-terminal; contain tandem BRDs) family (e.g. BRD4) (Filippakopoulos*, et al* 2012, Filippakopoulos*, et al* 2010, Muller*, et al* 2011). This clearly implicates BRDs in the recognition of histone modifications and chromatin function, and BRDs are thought to have an important role in targeting chromatin-modifying enzymes to specific sites (Muller*, et al* 2011). However, non-histone proteins also can bind to BRDs: for example, acetylated p53 can bind to CBP via its BRD, and BRD4 can bind acetylated lysines on the NF-kB subunit p65 (Barbieri*, et al* 2013, Brand*, et al* 2015).

All BRD molecules share a conserved fold that consists of four α helices that are linked by two loop regions of variable length (ZA and BC loops); these line the site that binds to the acetylated lysine residue and determine its binding specificity (Barbieri*, et al* 2013, Filippakopoulos*, et al* 2012). Differences in the acetyl-binding pockets of BRD are not just important for the characterization of BRD proteins but also for the design of selective BRD inhibitors (Chaidos*, et al* 2015).

Co-crystal structures of BRDs bound to acetylated peptides have demonstrated that acetylated lysine residues are recognized by a central deep hydrophobic pocket; an asparagine residue

present in most BRDs then anchors the acetylated lysine via a hydrogen bond (Filippakopoulos*, et al* 2012, Muller*, et al* 2011); in some BRDs this interaction is mediated by a residue other than asparagine, for example a tyrosine or threonine (Filippakopoulos*, et al* 2012).

To date, only a small number of BRD substrates have been reported and mapped to specific sites. The dissociation constants (KD) for these interactions range from nano-to milli-molar concentrations, and it is not quite clear which affinity window determines specificity of BRD-protein binding (Filippakopoulos*, et al* 2012, Muller*, et al* 2011). Interestingly, however, it has been suggested that a combination of modifications, or the presence of several acetylation sites can influence substrate recognition and the affinity of the binding interaction (Filippakopoulos*, et al* 2012, Moriniere*, et al* 2009, Muller*, et al* 2011).

1.7.1 Bromodomains as therapeutic targets in cancer

Given their role in mediating gene expression by determining target specificity of chromatin modifying complexes, BRDs have been implicated in the development of cancer. Several BRDs have been found to be aberrantly expressed in different types of cancer, and a number of oncogenic rearrangements have been reported (Barbieri*, et al* 2013, Muller*, et al* 2011). For example, the expression of SMARCA2 has been found to be down-regulated in hepatocellular carcinoma, whereas BRPF1 has been reported to be up-regulated in lung cancer (Barbieri*, et al* 2013). The recurrent t(15;19) chromosomal translocation leads to a fusion protein of BRD4 (or BRD3) and NUT (nuclear protein in testis) which promotes an aggressive form of human squamous carcinoma by blocking cellular differentiation (Barbieri*, et al* 2013, Filippakopoulos*, et al* 2012). The BRD4-NUT protein has been shown to be able to recruit CBP/p300, thereby stimulating HAT activity, ultimately leading to inactive hyperacetylated chromatin domains (Filippakopoulos*, et al* 2010, French*, et al* 2001, Reynoird*, et al* 2010). Depletion of BRD-NUT by RNA interference results in squamous differentiation and cell cycle arrest, and selective inhibition of BRD-NUT with a small-molecule inhibitor was demonstrated to lead to tumour shrinkage and survival of mice xenografted with BRD4-NUT tumours (French*, et al* 2003,

French*, et al* 2008). Therefore, BRDs are attractive targets for the design of pharmacologically active molecules that are directed to the acetyl-lysine binding pocket and compete with the lysine acetylation-BRD interaction (Muller*, et al* 2011). Selective inhibitors for BET BRDs have been published; these have been based on a triazolodiazepine scaffold that mimics the interactions observed in BET peptide complexes. The specific BET inhibitors I-BET762, JQ1 and I-BET151 have been shown to displace BET proteins from acetylated histones, to block cancer cell proliferation and to induce apoptosis in a wide range of cancer cell lines (Barbieri*, et al* 2013, Chaidos*, et al* 2015, Filippakopoulos*, et al* 2010). In addition, ligands for non-BET BRDs and pan-BRD inhibitors are under development (Brand*, et al* 2015).

1.7.2 The role of bromodomain inhibition in DLBCL

Mutations in *CREBBP/EP300* have been described in DLBCL (Table 1.1). In addition, *c-MYC* translocations are reported to occur in up to 11% of patients, and c-MYC protein over-expression in up to 30% of patients (Trabucco*, et al* 2015). Inhibition of BRD-target genes, therefore, may be beneficial in patients with DLBCL. The BET inhibitor JQ1 has high affinity for BRD4, a scaffolding factor that aids the selective targeting of chromatin-modifying complexes and thus facilitates transcription. JQ1 is a competitive inhibitor of BRD4 and prevents it from binding to chromatin (Filippakopoulos*, et al* 2010). In cancer cells, BRD4 has been shown to preferentially occupy enhancers and super-enhancers, and its loss leads to a decrease in transcription of these genes (Loven*, et al* 2013). In particular, in DLBCL cell lines and primary patient samples, asymmetric loading of BRD4 at super-enhancers has been described; thus, BET BRDs were found to support the growth programme in DLBCL and the transcription of known DLBCL oncogenes *c-MYC* and *BCL2*, regardless of COO subclass (Chapuy*, et al* 2013).

In preclinical studies, JQ1 has been reported to induce both G1 cell cycle arrest and apoptosis or senescence in a panel of DLBCL cell lines, and to delay tumour progression in DLBCL xenograft models; the suppression of *c-MYC* has been observed in this context and proposed as a possible underlying mechanism for its activity (Chapuy*, et al* 2013, Trabucco*, et al* 2015).

In ABC DLBCL cell lines specifically, JQ1 has also been shown to reduce NF-kB activity and viability of cells, in part by inducing apoptosis. Interestingly, the mechanism is thought to involve reduced phosphorylation and therefore inhibition of IkB kinase (Ceribelli*, et al* 2014).

Other BET BRD inhibitors, for example OTX015, have also shown promising preclinical activity in DLBCL: its anti-proliferative activity was demonstrated in both in vitro and in vivo systems, whereby OTX015 was found to be mainly cytostatic and induced apoptosis only in a subset of cell lines. Moreover, OTX015 inhibited a number of different signalling pathways, including the MYC, NF-kB, TLR and JAK-STAT pathways. Finally, synergistic effects were observed with several anticancer agents such as the HDI SAHA, the PI3K-delta inhibitor idelalisib and the hypomethylating agent decitabine (Boi*, et al* 2015).

In this context, it is also of note that BET BRD inhibitors have been found to induce genes similar to those induced by HDIs in *MYC*-induced murine lymphoma. These genes were primarily linked to the apoptotic pathway and included *Egr1*, *Trp53inp1*, *Gadd45a* and *Bbc3*. Therefore, opportunities for combination therapy with HDIs may become tractable (Bhadury*, et al* 2014).

Several BRD inhibitors have now also advanced into clinical trials, and patients with relapsed DLBCL are being recruited into Phase I studies, with response data currently awaited (www.clinicaltrials.gov). In an open-label dose escalation Phase I study of OTX015, 33 patients with lymphoma were treated with the study drug. Two patients with DLBCL achieved a CR and one patient with DLBCL achieved a partial response; two further patients with DLBCL had evidence of clinical activity, albeit not meeting objective response criteria (Amorim*, et al* 2016). An interim report on another BET BRD inhibitor, CPI-0610, shows that 24 patients with DLBCL were recruited onto an ongoing Phase I study, and after 6 cycles of treatment two of these patients had achieved a CR (Abramson*, et al* 2015).

Taken together, these early results support the further clinical development of BRD inhibitors in patients with lymphoma.

1.8 Biomarkers and personalized medicine

Advances in genomic analysis have helped to accumulate a large body of knowledge with regards to the underlying molecular pathogenesis of DLBCL and the cellular pathways involved. Targeted therapies can be developed based on this information. Therefore, the next step in harnessing this improved understanding of lymphoma biology is to identify and validate biomarkers related to these deregulated pathways and disease phenotypes. The concept of precision, or personalized, medicine, aims to individualize cancer treatment and match the right patient with the right drug.

1.8.1 Definition and classification of biomarkers

A biomarker can generally be defined as an objective and measurable characteristic of a biological or pathogenic process (Strimbu and Tavel 2010). A biomarker for a given disease does not necessarily have to be directly related to an endpoint, but can be affected in parallel with the condition. Similarly, as high throughput analyses make it possible to measure several different disease characteristics or molecular changes that occur with the treatment of a disease at the same time, a set of biomolecules that determine a particular disease state can be used as a biomarker, or molecular, signature which may be able to give more information on a disease state than a single biomarker on its own (Sheikh*, et al* 2015).

Three different types of cancer biomarkers have been described: prognostic, pharmacodynamic, and predictive (La Thangue and Kerr 2011). According to this classification, a prognostic biomarker is used to evaluate the overall outcome of a patient and can aid with selecting patients for treatment. Prognostic biomarkers however do not directly predict the response to a given treatment or therapy. Pharmacodynamic biomarkers are used to assess

the impact of a drug on a disease; they provide a post-treatment measure of whether, and to what degree, a pharmacological response has been obtained in the tissue of interest, or, more globally, the patient. As a result, pharmacodynamic biomarkers can help to optimize drug dosing and select rational drug or treatment combinations.

By contrast, predictive biomarkers, which are sometimes also referred to as companion diagnostic biomarkers, can identify those patients who are most likely to benefit from a therapeutic intervention. In addition, some predictive biomarkers can also help to identify patients who are likely to be at an increased risk for serious adverse reactions as the result of treatment with a drug, or allow monitoring response to a drug with the aim of adjusting treatment (e.g. schedule, dose, or discontinuation) to achieve improved safety or efficacy. Therefore, predictive biomarkers are useful in allowing patient stratification and personalisation to be introduced into a treatment schedule (La Thangue and Kerr 2011, Sheikh*, et al* 2015).

1.8.2 Examples of existing biomarkers

Prognostic. As outlined above, DLBCL has become recognized as a heterogeneous disease, and GEP can be used to distinguish the two major subgroups, ABC and GCB DLBCL. Patients with ABC DLBCL have been shown to relapse more frequently and are proving much more challenging to cure with conventional chemotherapy regimens. Therefore, DLBCL subgroup classification carries a prognostic impact for patients. In addition, both the ABC and GCB subtypes can be found to harbour specific genetic mutations that can be linked with treatment outcome. Some examples are listed in Table 1.10. GEP in conjunction with mutational analysis may therefore be useful for prognostic purposes and have important implications in tailoring therapeutic strategies in patients with DLBCL (Carbone*, et al* 2014, Intlekofer and Younes 2014).

Pharmacodynamic. The measuring of the acetylation status of specific marker proteins is an example of a pharmacodynamic biomarker and may be used to guide treatment with HDIs: in preclinical mouse models, a marked increase in acetylated histone H4 was demonstrated in the blood and tumour after treatment with the HDI PXD101 (Plumb*, et al* 2003). Similarly, SAHA treatment of a cohort of patients with pelvic adenocarcinoma led to increased histone acetylation in peripheral blood mononuclear cells in all patients (Ree*, et al* 2014). Another example is the HDAC6-specific HDI ACY-1215 which was shown to cause an increase in acetyl-tubulin, a specific substrate of HDAC6, following treatment of patients, and was used to determine therapeutic drug plasma levels and guide dose escalation in a Phase I trial (Yee*, et al* 2016).

Predictive. The hallmark of chronic myeloid leukaemia (CML) is the recurrent t(9;22) translocation resulting in the bcr-abl oncoprotein, a constitutively active tyrosine kinase. Imatinib, a selective inhibitor of bcr-abl, has arguably been one of the most successful targeted therapies developed to date, and is now established as first-line therapy in CML. An important example of a predictive biomarker, therefore, is the detection of a mutation (Y315I) in the catalytic site of bcr-abl which correlates with resistance to therapy with a conventional tyrosine kinase inhibitor, therefore allowing the selection of more appropriate treatments for affected patients (La Thangue and Kerr 2011).

A biomarker that determines tumour sensitivity to HDIs is the dual function protein HR23B (human ultraviolet excision repair protein RAD23 homologue B), which is involved in DNA repair as well as shuttling proteins to the proteasome (Fotheringham*, et al* 2009). HR23B was identified using a genome-wide loss-of-function screen, and initial studies revealed that HR23B governs the sensitivity of CTCL cells to treatment with SAHA. Subsequently, the analysis of pre- and post-treatment tumour samples from patients with CTCL confirmed HR23B as a predictive biomarker in CTCL (Khan*, et al* 2010). These findings are supported by two recent clinical studies: a correlation between the level of HR23B expression and clinical response was

reported in patients with unresectable hepatocellular carcinoma who were treated with the HDI belinostat; high expression levels of HR23B in tumours correlated with disease stabilization upon treatment (Yeo*, et al* 2012). Similarly, in a series of patients with mesenchymal tumours, HR23B protein levels as determined by IHC could predict for treatment response to SAHA (Angelika Ihle*, et al* 2016).

Table 1.10 Examples of current and emerging biomarkers in DLBCL.

Biomarker	Biological function/ Pathway	Oncogenic alteration	DLBCL subtype	Assay	Potential therapeutic agent
Gene mutations					
CREBBP/ EP300	HAT	Mutation or deletion	ABC and GCB	Sequencing	HDI
EZH2	H3K27 methyltransferase	Mutation	GCB	Sequencing	EZH2 inhibitor
CD79A/CD79B	BCR signalling component	Mutation in proximal ITAM	ABC	Sequencing	BTK inhibitor; SYK inhibitor; PKC inhibitor
CARD11	BCR and NF-kB signalling	Mutation in coiled coil domain	ABC	Sequencing	MALT inhibitor
MyD88	TLR and NF-kB signalling	L265P and other mutations	Mostly ABC	Sequencing	IRAK inhibitor; ?MyD88 inhibitor
TNFAIP3 (A20)	Inhibitor of NF-kB activation	Mutation or deletion	ABC	Sequencing	Proteasome inhibitor
Oncogenic proteins					
c-MYC	Transcription factor	Translocation, amplification, over-expression	ABC and GCB	IHC FISH	BET BRD inhibitor
BCL2	Apoptosis	Translocation, amplification, over-expression	ABC and GCB	IHC FISH	BH3 mimetic
BCL6	Transcription factor	Translocation, over-expression	GCB	IHC FISH Sequencing	BCL6 inhibitor
Biological pathways					
PI3K/AKT/mTOR	Growth factor signalling	Mutations	GCB	IHC for pAKT, sequencing	PI3K inhibitor; AKT inhibitor; mTOR inhibitor
JAK-STAT	Cytokine signalling	Amplification, mutations	ABC	IHC for pSTATs, sequencing	JAK inhibitor; STAT inhibitor

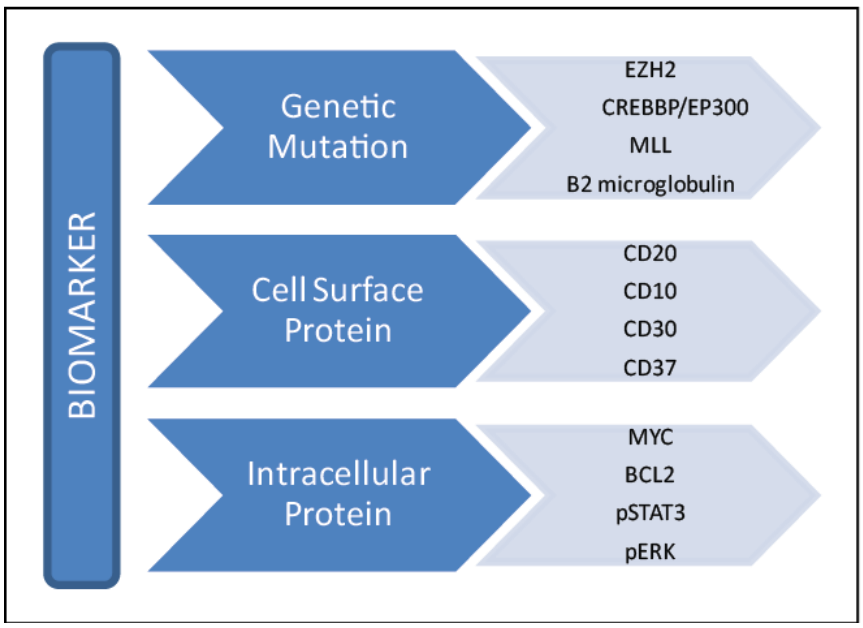
BTK, Bruton's tyrosine kinase; *FISH*, fluorescence *in situ* hybridization; *ITAM*, immunoreceptor tyrosine-based activation motif; *p*, phosphorylated

Source: (Carbone*, et al* 2014, Intlekofer and Younes 2014, Testoni*, et al* 2015)

1.8.3 Personalized medicine for lymphoma patients

Most response-specific biomarkers that are currently in clinical use have been identified through retrospective analysis of clinical data (La Thangue and Kerr 2011). The recent advent of omics technology, including NGS and proteomics, will make it more feasible to analyze a large array of candidate biomarkers simultaneously and in a timely manner, as well as allow a more systematic and prospective approach to biomarker discovery and validation (Figure 1.7).

Figure 1.7



Potential biomarkers in DLBCL. The schematic shows a set of potential biomarkers including genetic mutations, cell surface proteins and intracellular proteins that could be analyzed in patient biopsies in order to stratify patients for new treatment strategies.

Adapted from: (Carbone*, et al* 2014)

By seeking to match the genetic and molecular profile of each individual cancer with a specific targeted therapy, personalized medicine aims to transition from treatment with broadly acting cytotoxic drugs to more effective and less toxic treatments, with a net increase in clinical benefit (Intlekofer and Younes 2014, La Thangue and Kerr 2011). It is envisaged that biomarkers will be used to guide selection of those patients likely to respond to a specific therapy (positive selection strategy), or, conversely, to identify those patients who are likely to be resistant (negative selection strategy). For instance, in GCB DLBCL, recurrent somatic mutations in the histone lysine N-methyltransferase EZH2 have been observed that confer a gain-of-function. EZH2 forms the functional enzymatic component of the polycomb repressive complex 2 (PRC2) and catalyses the trimethylation of histone 3 lysine 27 (H3K27), a histone mark that causes repression of PRC2 target genes (Cao*, et al* 2002). Under normal conditions, EZH2 plays a role in the germinal centre B cell reaction by transiently suppressing genes that regulate proliferation and terminal plasmacytic differentiation, a process which is thought to be mainly mediated through the repressive H3K27 histone methylation mark. Excessive trimethylation of H3K27 caused by mutations in EZH2 (the most common lymphoma-associated mutation being Y641N) results in excessive repression of PRC2 target genes and promotes lymphoid transformation of cells (Beguelin*, et al* 2013). The mutant forms of EZH2 can be specifically inhibited by targeted drugs which can reactivate silenced PRC2 target genes by decreasing the methylation of H3K27 (Intlekofer and Younes 2014). A positive selection approach for therapy, therefore, will aim to identify those patients with GCB DLBCL who have EZH2 mutations and may benefit from therapy with a specific EZH2 inhibitor.

Conversely, being able to predict which patients will likely be resistant to a particular drug and not benefit from treatment, forms the basis of most negative selection approaches. For example, ibrutinib, a Bruton's tyrosine kinase (BTK) inhibitor, was found to have an overall response rate (ORR) of 38% in relapsed or refractory patients with ABC DLBCL but only 5% ORR in patients with GCB, suggesting that ibrutinib primarily has efficacy in ABC DLBCL. However,

within the ABC DLBCL subgroup, the response rate differed according to the underlying genetic lesion: thus, patients with mutations in *CARD11*, or in *MyD88* (but with WT *CD79A/B*) were shown to be completely ibrutinib-resistant (Dunleavy, *et al* 2013, Wilson, *et al* 2015, Zhang, *et al* 2015). Patients with these mutations are therefore unlikely to respond to ibrutinib and should be considered for an alternative agent.

Figure 1.8 depicts a possible algorithm for the selection of a targeted agent.

Figure 1.8

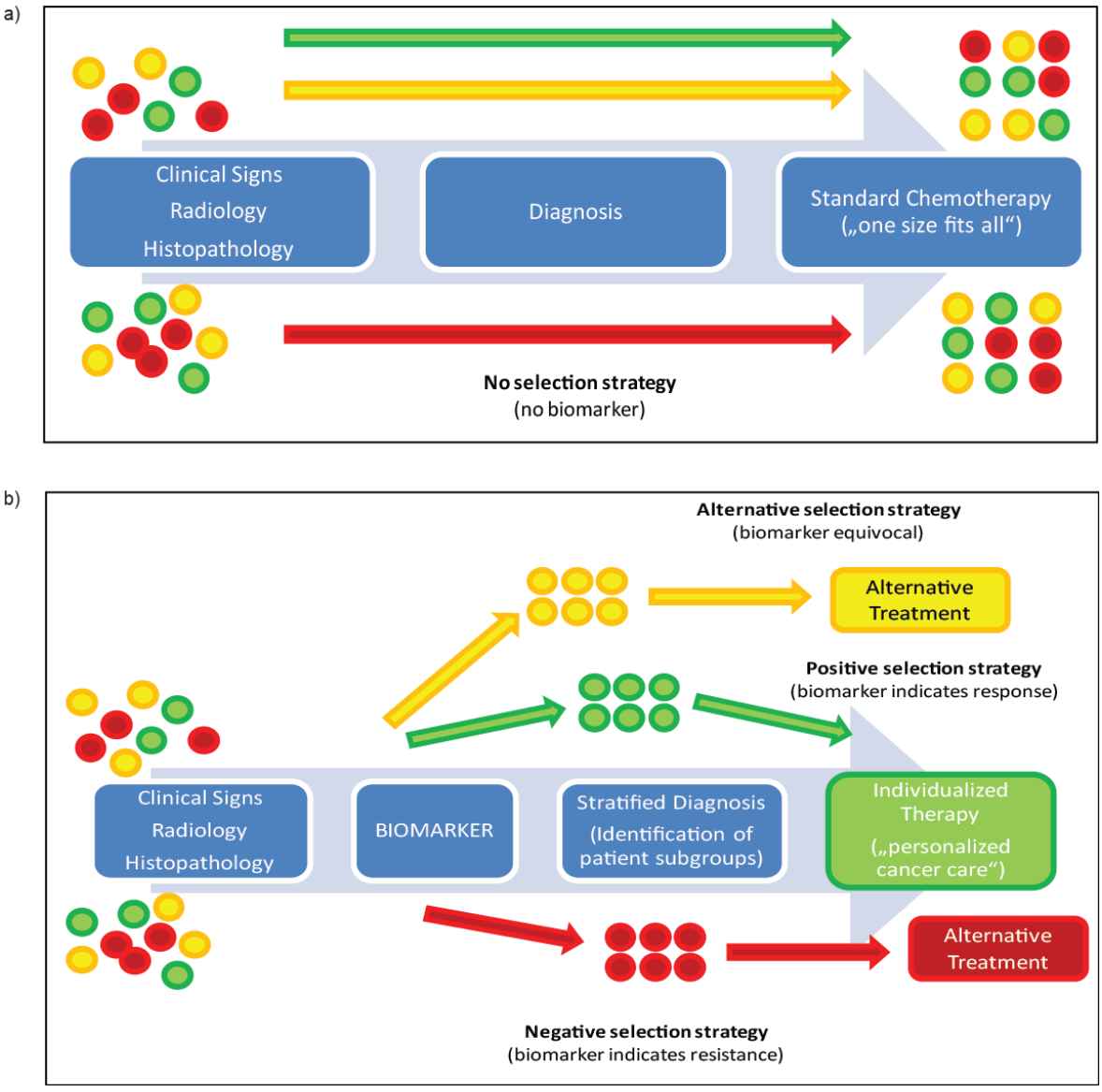


Figure 1.8 Personalized medicine selection strategies.

How the use of biomarkers may aid in early patient selection and treatment stratification in a personalized approach to cancer medicine: the upper panel depicts the current practice of assigning patients with DLBCL to therapy. In the absence of predictive biomarkers (i.e. no selection strategy), a heterogeneous group of patients will be assigned to receive the same treatment.

The lower panel shows how the availability of predictive biomarkers and targeted treatments could change current practice. Upon diagnosis, patients who are found to have a biomarker that predicts for response to a specific targeted therapy (green group) can be assigned to this particular treatment (positive selection strategy). By contrast, a biomarker that can predict that a patient is unlikely to respond to a given therapy (red group), will allow these patients to be considered for alternative treatments (negative selection strategy). Similarly, if testing for a particular biomarker happens to be equivocal or not interpretable (yellow group), affected patients can be considered for alternative treatments (alternative selection strategy).

Sources: (Intlekofer and Younes 2014, Khan and La Thangue 2008)

Despite the promise of personalized medicine, however, several significant challenges remain: a clear mechanistic understanding of biomarkers informing on response or outcome of a disease process is desirable. The analysis of patient samples for the detection of a biomarker should be standardized and reproducible. In this context, tumour heterogeneity and the presence of sub-clones, as well as the potential absence of any actionable mutations in patient samples present potential limitations to this approach, or at least require alternative selection strategies for therapy to be put in place. Finally, clinical trials demonstrating a clear benefit to patients treated with a biomarker-driven, targeted treatment strategy, will need to be conducted to provide the evidence base for this approach (Intlekofer and Younes 2014, La Thangue and Kerr 2011, Prasad*, et al* 2016).

1.9 Work that has led up to this project

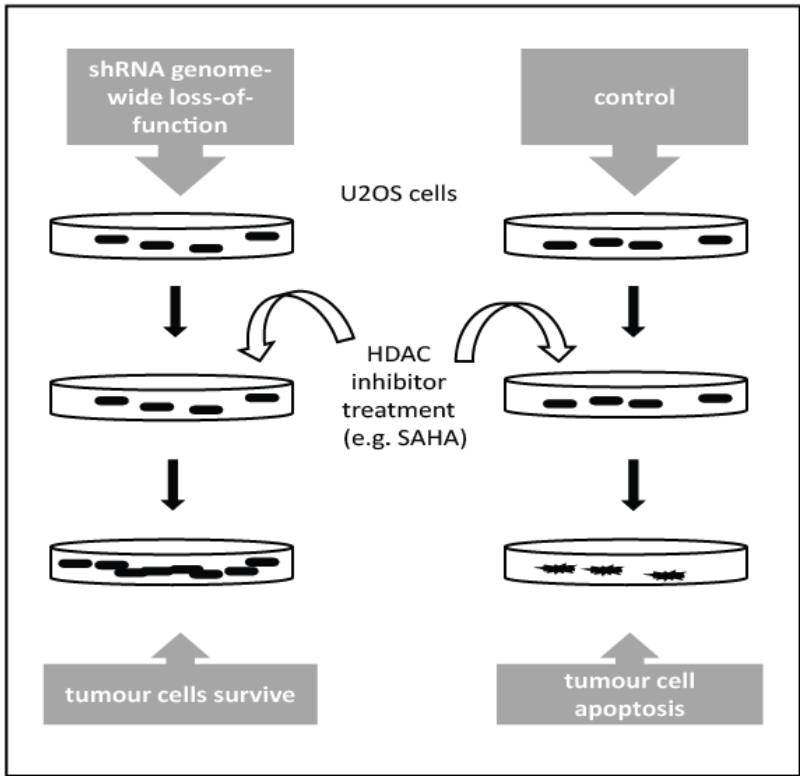
1.9.1 Genome-wide loss-of-function screen

Although the molecular pathways through which HDIs mediate their anti-proliferative effects on cancer cells remain to be fully elucidated (Section 1.6.6), haematological malignancies appear to be particularly responsive to HDI therapy (Khan and La Thangue 2008, Zain and O'Connor 2010). The identification and development of a biomarker which predicts for tumour sensitivity to an HDI, therefore, would be a useful adjunct for the management of cancer patients eligible for HDI therapy.

Susan Fotheringham and others in Professor La Thangue's research group employed an unbiased, screen-driven approach to identify a number of genes implicated in the modulation of HDI activity as candidate biomarkers (Fotheringham*, et al* 2009, New*, et al* 2016). The principle of the genome-wide loss-of-function screen that they carried out in U2OS osteosarcoma cells is outlined in Figure 1.9: a shRNA library targeting approximately 8000 genes thought to be involved in human cancer was used to silence these genes before

exposing cells to SAHA treatment for a prolonged period of time (25 days) and monitoring for the emergence of cell colonies resistant to drug treatment. The assumption was that those cells that evaded SAHA-induced apoptosis had undergone silencing of genes important for HDI-mediated cell death. Consequently, surviving cell colonies were harvested and sequenced to identify these genes (Fotheringham*, et al* 2009). In this way, the group identified and validated HR23B as a biomarker for patients with CTCL undergoing HDI-based treatment (Khan*, et al* 2010) (Section 1.8.2).

Figure 1.9



Genome-wide loss-of-function screen. Fotheringham *et al* employed a genome-wide loss-of-function screen using a shRNA library targeting approximately 8000 genes. Under conditions of lethal drug treatment with an HDI, U2OS osteosarcoma cells survive only if a shRNA targets a key gene required for the killing effect of the drug. Such genes are therefore necessary for the drug to kill cells, i.e. they are dominant and positive regulators of drug response.

1.9.2 MyD88 as a sensitivity determinant for HDI treatment

Another potential biomarker identified in the screen was MyD88. To determine the role of MyD88 as a sensitivity determinant for HDI treatment, Maria New used U2OS osteosarcoma cells and showed that over-expression of MyD88 or transfection of U2OS cells with the MyD88 L265P mutant resulted in enhanced apoptosis after SAHA treatment. In addition, the identification of a lysine acetylation site on the MyD88 protein led to the hypothesis that HDIs may exert a direct effect on the acetylated protein (New*, et al* 2016).

1.9.3 MyD88 as a candidate companion diagnostic biomarker for lymphoma

The finding that MyD88 and its mutant form could influence HDI sensitivity, together with the fact that MyD88 frequently appears to be mutated in lymphoma, and that HDIs have been shown to have increased efficacy in lymphoma, made further investigation of MyD88 in lymphoma a plausible next step in an attempt to validate it as a biomarker.

1.10 Aims of project

The aims of my project were therefore twofold: firstly, I wanted to gain a mechanistic understanding of the role of MyD88 in lymphoma cell lines and its role in the context of HDAC inhibition. In particular, and carrying on from the work done in U2OS cells, I wanted to find out whether MyD88 acts as a sensitivity determinant for HDI treatment in lymphoma cells, and how it may regulate cell fate in this system. To this effect, I aimed to assess the susceptibility of different DLBCL lymphoma cell lines to treatment with an HDI and assess changes in HDI-mediated sensitivity on manipulation of MyD88 levels by siRNA or small-molecule-mediated inhibition of MyD88. I also wanted to investigate the influence of the MyD88 L265P mutation on HDI sensitivity and determine the contribution of the different components of the TLR-MyD88-NF-kB signalling pathway in this process.

The second aim of this thesis was to find out whether MyD88 expression in patient tissue samples could be used as a biomarker to determine a response to HDI treatment and therefore investigate the clinical relevance of MyD88 expression. Specifically, I aimed to develop an IHC staining protocol for tissue samples taken from patients with lymphoma and other malignancies, and to design a tissue staining score with which to stratify MyD88 expression in tumour tissue and which could be used in a clinical trial setting.

CHAPTER 2. MATERIALS AND METHODS

2.1 Antibodies

The following commercially available primary antibodies were used for immunoblotting (IB), immunohistochemistry (IHC), or immunoprecipitation (IP):

Antibody	Indication	Dilution	Species/Secondary	Source
Actin	IB	1/1000	M	Sigma
Acetylated histone H3	IB	1/500	R	Millipore 06-599
Acetyl-lysine	IB IP	1/1000 1µg	R	Cell signaling 9441
Cleaved Caspase 3 (D175)	IB	1/500	R	Cell signalling 9664
Cleaved PARP (D214)	IB	1/1000	R	Cell signalling 9541
Histone H3	IB	1/500		Millipore 06-755
HDAC6 (D2E5)	IB	1/1000	R	Cell signalling 7558
MyD88 (D80F5)	IB IP	1/1000 1µg	R	Cell signalling 4283
MyD88	IHC	1/2000	M	Abcam 133739
STAT3 (79D7)	IB IP	1/1000 1µg	R	Cell signalling 4904
pSTAT3 (Y705)	IB	1/1000	R	Cell signalling 9131
p65	IB IP	1/1000 1µg	R	Santa Cruz Sc-109
IgG	IP IHC	1µg 1/800-1/2000	R/M	Merck
IL-6	IB	1/500	R	Abcam 6672
TLR4	IB	1/1000	R	Abgent AP9685c
TLR4 (functional)	IB	2µg	R	Abcam ab30667
His	IB	1/10,000	n/a	Thermo Scientific
HR23B	IHC	1/400	M	BD Biosciences
BRWD3	IP, IB	1/500	R	ThermoFisher

M, mouse*; R*, rabbit

The following commercially available secondary antibodies were used; blots were incubated with secondary antibody for 60-90 minutes.

Antibody	Indication	Dilution	Source
Mouse	Secondary	1/10,000	Sigma
Rabbit	Secondary	1/10,000	Sigma

2.2 Cells and cell culture

The cancer cell lines used and their respective MyD88 mutation status are summarized in the tables below. RIVA, HBL-1, SUDHL-4 and Mieu cell lines were a kind gift from Professor Alison Banham (Nuffield Department of Clinical Laboratory Sciences, Oxford University). All cell lines were grown at 37^{o}C with 5% CO_2 in a humidified incubator. Cells were maintained in the recommended culture medium supplemented with 5-10% foetal calf serum (FCS) and 1% Pen/Strep antibiotic.

Cell line	Adherent (A)/ Suspension (S)	Cell type	Medium/% FCS	Source
RIVA	S	DLBCL, ABC sub-type	RPMI 5-10%	Alison Banham lab
HBL-1	S	DLBCL, ABC sub-type	RPMI 5-10%	Alison Banham lab
SUDHL-4	S	DLBCL, GCB sub-type	RPMI 10%	Alison Banham lab
Mieu	S	DLBCL, GCB subtype	RPMI 10%	Alison Banham lab
U2OS	A	Osteosarcoma	DMEM 5%	NLT lab
MCF7	A	Breast cancer	DMEM 5%	NLT lab
RCK8	S	DLBCL, ABC subtype	RPMI 5%	ATCC
HL-60	S	Myeloid	RPMI 5%	NLT lab
U937	S	Myeloid	RPMI 5%	NLT lab
U2932	S	DLBCL, ABC subtype	RPMI 5%	ATCC
L428	S	Hodgkin lymphoma	RPMI 5%	NLT lab

DLBCL, Diffuse Large B cell Lymphoma; *GCB*, germinal centre B cell; *ABC*, activated B cell; *ATCC*, American Type Culture Collection; *FCS*, foetal calf serum (Labtech); *RPMI1640*, Roswell Park Memorial Institute medium (Gibco®); *DMEM*, Dulbecco's Modified Eagle's Medium (Gibco®)

Cell line	MyD88 mutation status	Consequence of MyD88 mutation	Source/References
RIVA	no MyD88 mutation found		Own sequencing, Susan Fotheringham (personal communication) (Ezell*, et al* 2016)
HBL-1	L265P	Oncogenic driver	Own Sequencing, Susan Fotheringham (personal communication) (Ezell*, et al* 2016, Mondello*, et al* 2017, Ngo*, et al* 2011)
SUDHL-4	none reported		Cell line encyclopaedia (Ezell*, et al* 2016)
Mieu	unknown		(Brown*, et al* 2008)
U2OS	none reported		ATCC Cell line encyclopaedia
MCF7	none reported		ATCC Cosmic database
RCK8	none reported		Cosmic database DSMZ (Ezell*, et al* 2016)
HL-60	none reported		ATCC Cell line encyclopaedia Cosmic database
U937	none reported		ATCC Cell line encyclopaedia
U2932	none reported		(Amini*, et al* 2002, Ezell*, et al* 2016)
L428	MyD88 D228N	Shortened but fully functional protein	Cosmic database

Sources: Cell line encyclopedia (https://portals.broadinstitute.org/ccle/); ATCC (https://www.lgcstandards-atcc.org/); Cosmic database (http://cancer.sanger.ac.uk/cell_lines); DSMZ (https://www.dsmz.de/)

2.3 Drug and antibody treatments

For drug and antibody treatments, cells were counted either manually with a haemocytometer or by FACS, and a fixed number of cells (usually 1-2x10^6 unless otherwise specified) was plated (see below for specific experimental conditions and set-up). Time points for sequential treatments were based on reports in the literature or time points ascertained by viability assays.

Antibody treatments: Cells were treated with anti-IL-6 or anti-TLR4 antibody for at least 60 minutes prior to any drug treatments.

LPS treatments: LPS (Sigma) was added 2 hours prior to drug treatment, or, in the case of MyD88 inhibitor treatment, LPS was added 2 hours before the addition of the MyD88 inhibitor.

Human recombinant IL-6 (Gibco®) was added to plated cells 3 hours prior to drug treatment.

Drug treatments: Suberoylanilide hydroxamic acid (SAHA; Sigma), tubastatin (Chemietek), etoposide (Sigma), doxorubicin (Sigma), or T6167923 (Aobious Inc) were added at the indicated concentrations and for the indicated times before harvesting. All compounds were solubilised in dimethylsulfoxide (DMSO, Sigma) and added to media at a 1:1000 dilution to minimise vehicle effects. DMSO was also used to mock-treat control cells.

2.4 Immunoblotting and immunoprecipitation

Cells were harvested by centrifuging at 1,500 rpm for 5 minutes and then washed in ice-cold Phosphate Buffered Saline (PBS) for 5 minutes.

For immunoblotting, cells were lysed in RIPA buffer (Tris 50mM, NaCl 150mM, SDS 0.1%, Na Deoxycholate 0.5%, Triton X100, NP401%, with added protease inhibitors) for 45 minutes at 4^{o}C. Cell extracts were then centrifuged at 13,200 rpm for 10 minutes to remove cell debris.

For immunoprecipitation (IP), cells were harvested as above, lysed in TNN (50mM Tris pH=7.4, 5mM EDTA, 0.5% NP40, 120mM NaCl, with protease and phosphatase inhibitors) buffer and then incubated with 1µg of the appropriate primary antibody overnight, at 4^{o}C on a rotating wheel. After that, 30µL of Trublot IgG beads (Rockland Inc) were added for 2 hours at 4^{o}C and then washed four times with TNN buffer before boiling with 90µL 4x sodium dodecyl sulfate (SDS) sample buffer containing 2-beta-mercaptoethanol, prior to immunoblotting.

Protein concentration in lysates was determined by Bradford assay (Sigma) and calculated from a calibration curve.

Lysates for IB were boiled with SDS sample buffer, separated on 12%, 10% or 8% SDS-PAGE gels (depending on molecular weight of proteins of interest) at 200 V for 60 minutes before transfer at 400 mA (2 hours) to Immobilon PVDF membrane (Millipore).

Gels were loaded as per Bradford assay or with a fixed volume of lysate (nuclear extracts); for IP samples, 2% of the lysate was loaded as the input.

Membranes were blocked with 5% skimmed milk and then incubated with the primary antibody overnight at 4^{o}C. The appropriate secondary antibody was added the next day for 60-90 minutes before 3x PBST washes. Detection of immunoreactive bands was carried out by developing with ECL Western Blot reagent. The blots shown are representative of at least three independent experiments, unless otherwise indicated.

Densitometric analysis on individual blots was carried out where indicated using ImageJ software *(*https://imagej.net).

2.5 FACS (Fluorescence-activated cell sorting) analysis

FACS analysis was carried out as described elsewhere (Kalac*, et al* 2011): briefly, cells were cultured and treated as above (Section 2.3), and then harvested into 0.3mL cold PBS. After harvesting, cells were fixed in 70% ethanol/PBS for one hour at 4^{o}C and washed twice with ice-cold PBS before being incubated for one hour with 1x RNAseA (Sigma) and 20ng/mL propidium iodide (Sigma) at 37^{o}C. Samples then were run on an Accuri6 C6 Flow cytometer, and a minimum of 10,000 events were acquired, analyzed and quantified using CFlow Plus software. Initial cell population gating was carried out using FSC vs SSC, and subsequently, cells were gated to exclude aggregates on a FL2-A vs FL2-H plot. A PI histogram of the gated cells was used to distinguish the cell cycle phases (sub-G1, G1, S, G2).

All FACS experiments were carried out in triplicate and, unless otherwise indicated, the results shown are representative of at least three biological replicates.

2.6 Tetrazolium MTT (3-(4,5-dimethylthiazolyl-2)-2,5-diphenyltetrazolium bromide) cell proliferation assay

The protocol for this assay was obtained from Dr Heidi Olzscha (NLT lab). Cells were plated at a density of 40,000 cells per well, in triplicate for each treatment condition per cell line, in 96-well plates. Plates were then incubated for 24 hours at 37^{o}C in a cell culture incubator and treated with the appropriate drug at pre-defined concentrations (range 1mM to 100pM) and returned to the incubator. After 24, 48 and 72 hours, MTT reagent (10µL) was added to each well and incubated at 37^{o}C for 3 hours. After this, 100µL detergent reagent (20% SDS/50% DMF) was added before recording absorbance at 570 nm on a Tecan microplate reader. The experiments were performed at least in biological triplicate, unless indicated otherwise.

2.7 RNA extraction and cDNA synthesis

RNA was extracted from treated and untreated RIVA and HBL-1 cell line pellets using the Trizole RNA extraction protocol (Invitrogen). cDNA synthesis was carried out using the SuperScript III reagent kit (Invitrogen), and the PCR product was purified with Quiaquick PCR Purification kit (Quiagen) before sending it for sequencing.

Sequencing primer for MyD88: CTG ATG ATT ACC TGC AG

2.8 qRT-PCR

For qRT-PCR analysis, RNA was extracted using the Trizole method, and cDNA was generated using the SuperScript III protocol, as described above (Section 2.7). The gene expression analysis was performed by quantitative real-time PCR (Stratagene Mx3005P^{TM}) with standard SYBR-Green PCR kits (SYBR® green qPCR Mastermix, Agilent). Reactions were set to an initial incubation at 95^{o}C for 180 seconds, followed by 60 cycles at 95^{o}C for 30 seconds and 57^{o}C for 30 seconds. The relative expression of each target gene normalized to actin was calculated using the $2^{-\Delta\Delta ct}$ method. Primers (KiCqStart®SYBR®Green Primers, Sigma) were as follows:

Primer name		Sequence
MyD88	**Forward**	**GTTGTCTCTGATGATTACCTG**
	Reverse	**GGGGAACTCTTTCTTCATTG**
IL-6	**Forward**	**GCAGAAAAAGGCAAAGAATC**
	Reverse	**CTACATTTGCCGAAGAGC**
IL-6R	**Forward**	**CTGGAAACTATTCATGCTACC**
	Reverse	**GACTGTTCTGAAACTTCCTC**

2.9 Nuclear extraction

The protocol for nuclear extraction was modified from Dianov *et al* (personal communication). Briefly, cells were harvested from cell culture, and washed once in ice-cold PBS. After this, Buffer I (20mM Tris pH=7.4, 2.5mM $MgCl_2$, 0.5% NP40 with added protease inhibitors) at an amount twice that of the cell pellet was added to the cell pellet, and the pellet was then re-suspended by vortexing, and subsequently incubated on ice for 10 minutes. Following this, the sample was spun at 13,200 rpm for 2 minutes and the supernatant collected as the cytoplasmic extract (CE). The remaining pellet was re-suspended in Buffer II (20mM PO_4 buffer pH=8.0, 0.5M NaCl, 1mM EDTA, 0.75% Triton-X 100, 10% glycerol, 5mM $MgCl_2$ with added protease inhibitors) and then left on ice for 15 minutes. After this, the suspension was centrifuged once again at 13,200 rpm for 2 minutes and the supernatant collected as the nuclear extract (NE). Nuclear and cytoplasmic fractions were frozen at -20^{o}C before running on an SDS-PAGE gel.

2.10 Cytokine analysis

Cytokine release was determined using a BD^{TM} cytometric bead array (CBA) Human Inflammatory Cytokine kit (BD Biosciences UK) which determines six cytokines: IL-1β, IL-10, IL-6, IL-8, TNF-α and IL-12p. The kit provides six antibodies that are specific for each of the six inflammatory cytokines that are measured; each antibody is conjugated to a capture bead with a distinct fluorescence intensity. The six bead populations are mixed together and incubated

with the fluid to be analyzed (in this case, cell culture supernatant). During the incubation, complexes form between the capture bead, the analyte (inflammatory cytokine) and the detection reagent, and the resultant fluorescent signal can then be measured using flow cytometry.

For each experiment, the same starting number of cells ($1x10^6$) was plated for the indicated time, and the supernatant analyzed for cytokine content. Normal medium (RPMI with 5% FCS; all cell lines analyzed were grown in this medium), with or without DMSO (mock), served as the baseline (negative) control, and to ensure that cytokine expression was indeed unique to the cell line under investigation and not already present in the medium (e.g. due to the addition of foetal calf serum).

Cells were treated for 24 hours as indicated and centrifuged prior to harvesting. 50µL of the cell supernatant was used for cytokine analysis. The unique fluorescence intensities of each of the six different beads permits cytokine levels to be simultaneously assessed, and absolute cytokine levels (pg/mL) were determined by constructing a standard curve using known standards.

2.11 Transfection

Cells were seeded to be 60-80% confluent at transfection. Lipofectamine®2000 (Thermo Fisher Scientific), Lipofectamine® RNAiMAX (Invitrogen), or Oligofectamine™ (Invitrogen) was diluted in Opti-MEM (Gibco®) medium according to the manufacturer's instructions, before mixing with siRNA which had also been diluted in Opti-MEM. Different MyD88 siRNAs used were as follows: smart-pool (Dharmacon); ESIRNA MyD88 (Sigma (EHU029771)), or custom MyD88 siRNA (5'-CGACUGAAGUUGUGUGUGUUU-3'). Non-targeting NT2 siRNA (Dharmacon) was used as the negative control. The mix was incubated for 5-15 minutes before adding to cells, to achieve a final concentration of siRNA of 25-50nM.Post-transfection, cells were harvested after 48-72 hours.

2.12 Electroporation

Cells were centrifuged at 1,200 rpm for 5 minutes at room temperature before resuspending in RPMI medium with 0.5% FCS. Cell numbers were then determined by FACS, cells centrifuged again for 5 minutes at 1,200 rpm and the supernatant was removed. As per the manufacturer's instructions, cells were resuspended in Hypo-osmolar Electroporation buffer (Eppendorf) at a concentration of 2.5 x 10^6 cells/mL. siRNA (to a final concentration of 25-50nM) was added and 800µL of the cell suspension was transferred into an electroporation cuvette. The electroporator parameters were set as follows:

Mode	Eukaryotes
Voltage	760-1100 V
Time constant	60-100 µs
No of pulses	1

After the pulse, the cell suspension was allowed to stand in the cuvette for 5-10 minutes at room temperature before transferring to 3-5mL RPMI/10% FCS medium in a 35mm dish. Cells were harvested for immunoblotting after 48-72 hours.

2.13 Nucleofection

Transfection efficiency of RIVA and HBL-1 cells was established 24 hours post-transfection using the Amaxa™ 4D-Nucleofector™ (Lonza) optimization protocol: cells were transfected with 0.4µg of pmaxGFP™ vector in 20µl Nucleovette™ strips, and after 24 hours, cells were analyzed by flow cytometry using the green fluorescence channel. Following this, RIVA and HBL-1 cells were co-transfected with siRNA and pmaxGFP™ vector in 100µL single Nucleocuvettes, using nucleofection buffer SF and programmes P137 and P138, respectively. siRNA was used at a final concentration of 25-50nM, and non-targeting NT2 siRNA (Dharmacon), at the same concentration, was used as the negative control.

2.14 Lentiviral transduction

MyD88 shRNA knockdown cells were created in RIVA cells using MyD88 shRNA lentiviral particles (Santa Cruz, Biotechnology, Inc.) and following the manufacturer's protocol: 62,500, 125,000 or 250,000 cells were plated in a 6-well dish and grown for 24 hours. Following this, cells were pelleted and re-suspended in 1mL of medium containing polybrene (Santa Cruz, sc-134220) at a final concentration of 5µg/mL, before cells were then infected with lentiviral particles. Several amounts of lentiviral stock (20µL, 10µL, 5µL) were used in order to optimize conditions. One well containing cells infected with control shRNA particles (Santa Cruz, sc-108080) was included for each condition. After three days, cells were split 1:2 and transferred to a T25 flask, and selection for stable shRNA clones with puromycin dihydrochloride (MP Biomedicals) at a concentration of 2µg/mL was begun. Stable polyclonal cell lines were maintained in medium containing puromycin, and lysates for Western Blotting were prepared as described above (Section 2.4).

2.15 Patient samples

Individual formalin-fixed paraffin-embedded (FFPE) patient tissue biopsy samples or disease-specific tumour microarrays (TMAs) were obtained from the Oxford Biobank (Approval number: 09/H0606/5+5.). All sections were anonymized. Tissue sections obtained were annotated for being malignant (versus non-malignant), type of malignancy and tissue of origin (e.g. bone marrow, lymph node etc).

Peripheral blood mononuclear cells (PBMCs) for the evaluation of histone acetylation were obtained from patients undergoing treatment with CXD101 on a clinical trial (NCT01977638). Peripheral blood samples were processed by the Oxford GCP laboratory as described elsewhere (Steele), and the PBMC cell pellet was used for histone extraction.

2.16 Immunohistochemistry and pathology examination

A previously published protocol (Khan*, et al* 2010) from Professor La Thangue's group was obtained and optimized with the help of a consultant histopathologist, Dr Elizabeth Soilleux (Oxford University Hospitals NHS Trust), for manual MyD88 staining, and, for automation of HR23B staining, a GCP laboratory expert in immunohistochemistry, Leticia Campo (Department of Oncology, University of Oxford).

For manual staining, tissue biopsy samples were de-paraffinized by treating with Histoclear (National Diagnostics) and an ethanol (Fisher Chemical) gradient. Antigen retrieval was carried out with sodium citrate pH=6 in a waterbath at 99^{o}C for 20 minutes. Slides were then treated with 6% H_2O_2 (Merck)/methanol (Fisher Chemical) for 15 minutes and blocked with diluted normal blocking serum (Vectastain ABC kit, Vector Laboratories) for 20 minutes. Primary antibody, diluted in PBS, was applied to the slides and left overnight at 4^{o}C. The following day, slides were washed and incubated with the appropriate biotinylated secondary antibody (Vectastain ABC kit, Vector Laboratories) at room temperature for 30 minutes, followed by ABC reagent (Vectastain ABC kit, Vector Laboratories) for 30 minutes and finally DAB substrate (Vector Laboratories) for 10 minutes. After counter-staining with haematoxylin (Sigma), slides were air-dried and mounted with Aquatex (Merck) before being analyzed by standard light microscopy (Leica DM 2000).

A 1/2000 cut-off for the dilution of the MyD88 antibody was established with Dr Soilleux using a dilution curve assessing dilutions of 1/100-1/12,000.

HR23B staining was automated on a Leica Bond-max™ immunostainer (with Leticia Campo) using a multi-tumour microarray (TMA) which was built by the in-house GCP laboratory with matched normal tissue blocks (ProteoGenex Inc), and a mini-TMA of three tumour tissue cores chosen for high-, medium, or low HR23B expression built by The Oxford Centre for Histopathology Research (OCHRe).

2.17 CADOR array

Based on the known MyD88 protein acetylation site (K132) as determined by mass spectrometry (New*, et al* 2016), four peptides of 17 amino acid-length were designed to be either mono-acetylated (at residues K128 and K132, respectively), di-acetylated (at residues K128 and K132) or non-acetylated. The peptides were synthesized by LifeTein (LifeTein LLC), and contain a flexible linker (Ahx) between the peptide sequence and the N-terminal biotin tag.

Peptide name	Peptide sequence
MyD88 non-acetylated	Biotin-Ahx-EDCQKYILKQQQEEAEK
MyD88 mono-acetylated at K 132	Biotin-Ahx-EDCQKYIL-(K-Ac)-QQQEEAEK
MyD88 mono-acetylated at K 128	Biotin-Ahx-EDCQ-(K-Ac)-YILKQQQEEAEK
MyD88 di-acetylated	Biotin-Ahx-EDCQ-(K-Ac)-YIL-(K-Ac)-QQQEEAEK

The peptides were then used in a CADOR (chromatin-associated domain) array carried out by the Bedford Laboratory (MD Anderson Cancer Centre, Austin, Texas). The generation of protein microarrays has been described (Kim*, et al* 2006a), and a list of the protein domains on the array has been published (Yang*, et al* 2010). Biotinylated peptides were labeled as described (Kim*, et al* 2006a).

2.18 Immunoprecipitation of His-tagged proteins

Cells were lysed in RIPA buffer (200-500µL, depending on size of pellet) (Section 2.4), incubated on ice for 30 minutes and centrifuged at 13,000 rpm for 10 minutes at 4^{o}C. 2% of the lysate was kept aside to use as the input for immunoblotting. For the IP, cell lysates were mixed with three volumes of IP wash buffer (50mM Tris pH=7.5, 150mM NaCl, 0.1mM EDTA, 10mM imidazole, 5% glycerol, 0.5% triton-100) and incubated with 1µg His-tagged bromodomain protein and 30µL Ni-agarose beads (Qiagen) for 2 hours at 4^{o}C on a rotating wheel. The IP was then washed 4-5 times with 1mL wash buffer, and protein complexes were

eluted with SDS-loading dye and boiled at 95^{o}C for 5 minutes. Lysates were run on an SDS-PAGE gel and immunoblotted as described above (Section 2.4).

CHAPTER 3. MYD88 EXPRESSION AND RESPONSE TO HDI TREATMENT

3.1 Introduction

As outlined in Chapter 1 (Section 1.5.1), MyD88 acts as an essential cytosolic adapter protein that mediates downstream signalling through the TLR- and IL-1- receptor pathways, leads to activation of the NF-kB pathway and influences the levels of pro-inflammatory extra-cellular cytokines (Ngo*, et al* 2011, Wang*, et al* 2014). MyD88 is expressed at high levels in haematological malignancy and the presence of the MyD88 L265P mutation is thought to act as a gain-of-function driver mutation (Ngo*, et al* 2011, Treon*, et al* 2012).

MyD88 can be detected on immunohistochemistry (IHC) in tissue samples obtained from cancer patients (Choi*, et al* 2013b); most commercially available antibodies suitable for investigating the immunohistochemical expression of MyD88 have been raised against the entire, or a large part, of its amino acid sequence. At the time the experiments described below were carried out, no antibody specific for the detection of the mutated form, MyD88 L265P, was available. Therefore, it is assumed that both mutated and unmutated forms of MyD88 will be detected on IHC with the available MyD88 antibodies used here.

Previous work in Professor La Thangue's research group identified MyD88 as a potential predictive biomarker to determine cancer cell sensitivity to HDAC inhibition, and HDIs have been shown to be particularly effective in the treatment of relapsed haematological malignancies, especially those of lymphoid origin (Chapter 1, Section 1.6.7).

One of the outcomes of HDI treatment of cancer cells is cell death by apoptosis (Chapter 1, Section 1.6.6). The level of apoptosis in cells treated with an HDI can be measured by demonstrating cleavage of poly-ADP ribose polymerase (PARP) and caspase 3 on immunoblot. PARP cleavage usually occurs during the early stages of apoptosis and is mediated by caspases, in particular caspase 3, in response to extensive DNA damage. PARP cleavage typically results in fragments of 89 and 24 kD. Caspase 3 is one of the key executioners of apoptosis, and its

activation requires proteolytic processing of its inactive zymogen into activated p17 and p12 fragments (Herceg and Wang 1999, Soldani and Scovassi 2002). Another way of assessing apoptosis in cells treated with an HDI is to measure the percentage of cells in sub-G1 cell cycle phase on FACS analysis (Riccardi and Nicoletti 2006). Following propidium iodide (PI) staining, apoptotic cells will stain less intensely and can be quantitated by measuring the peak below the G1 peak. This sub-G1 peak is therefore thought to correlate with the fraction of apoptotic cells present.

Finally, MTT assays (Riss*, et al* 2004) are a useful method of determining cell viability after treatment with potentially cytotoxic compounds. Taken together, the results from immunoblotting, FACS and MTT experiments should therefore allow a comprehensive evaluation of the influence of an HDI on apoptosis in cancer cells.

The aim of the experiments described in this chapter was to demonstrate MyD88 protein expression by IHC in tissue biopsies taken from patients with lymphoid malignancies, including LPL and DLBCL, and to compare this to MyD88 expression in patients with solid malignancies. After showing MyD88 expression at a tissue level, I then planned to determine MyD88 expression in a number of lymphoid cancer cell lines and assess the sensitivity of these cell lines to the pan-HDAC inhibitor SAHA and the HDAC6-specific HDI tubastatin. I would then analyze the role of MyD88 as a sensitivity determinant for HDI treatment in lymphoma cells by testing the hypothesis that depletion of MyD88 levels leads to a decrease in apoptosis markers and that MyD88 levels therefore may allow us to predict susceptibility of malignant cells to treatment with an HDI. In addition, the description of MyD88 L265P as a frequent gain-of-function mutation in lymphoma (Ngo*, et al* 2011) led to the reasoning that the presence of the mutant protein may impact on MyD88 being a sensitizer for HDI treatment.

3.2 MyD88 expression in clinical disease

MyD88 is thought to be constitutively expressed in most tissues, but levels of protein expression may vary (www.proteinatlas.org). This can be a reflection of the actual expression of the protein at tissue level, but when interpreting IHC results, one also has to take into consideration that the result could reflect the experimental design, age and fixation method of the tissue biopsy, the immunohistochemical staining method employed, as well as the antibody and its corresponding epitope. As MyD88 has been previously reported to be highly expressed in haematopoietic tissue (Choi*, et al* 2013b, Ngo*, et al* 2011), I obtained tissue biopsies from patients with a range of lymphoid malignancies and, for comparison, tissue biopsies from patients with a range of (relatively common) solid malignancies, via the Oxford Biobank. The lymphoid malignancies included high-grade (DLBCL) and low-grade (LPL) lymphomas; the solid tumours included colorectal, prostate and breast cancer, and melanoma. All tumour samples were from patients at first diagnosis, and had not been taken during or after treatment.

In addition, I obtained sections of "normal" (i.e. non-cancerous and not otherwise pathological) tonsil and bone marrow to use as control tissue. After establishing a dilution curve with a commercially available MyD88 antibody and discussion with a consultant histopathologist (Chapter 2, Section 2.16), MyD88 protein expression in haematopoietic tissue was shown to be prominent, and high levels of MyD88 were detected in biopsy samples, both lymph node and bone marrow, from patients with haematological malignancies (Figure 3.1a). This was in contrast to biopsy samples obtained from patients with solid malignancies where MyD88 expression levels were very low (Figure 3.1b). In order to expand on this finding and look at a range of different tumours in each subgroup, I obtained tissue microarrays (TMAs) from patients with DLBCL, prostate and colorectal cancer: a range of MyD88 expression could be observed in DLBCL but expression was uniformly high, whereas MyD88 expression in colorectal and prostate cancer showed much lower levels of expression across the range of

tumours present (Figure 3.1c). MyD88 was predominantly expressed in the cytoplasm, as would be expected in its role as a cytosolic adapter protein, although the possibility of a nuclear or peri-nuclear expression pattern will be explored in Chapter 5 (Section 5.5).

Stained individual patient biopsies as well as TMAs were reviewed by a consultant histopathologist (Dr Soilleux) to confirm optimization of the IHC protocol and specificity of the antibody. However, no statistical analysis was carried out at this point, and information on patient outcome was also sparse. Moreover, it appears that none of the patients whose biopsies were stained in the above experiments received an HDI as part of their treatment. Therefore, it is difficult to draw any definite conclusions from this preliminary analysis, and as the primary aim of these initial IHC experiments was to determine MyD88 expression in lymphoma tissue and ascertain that there is variable expression across tumour types, a more quantitative approach with the biopsies was not pursued at this point.

However, as there was clearly a variation in MyD88 expression across individual tumour samples and tumour types, a logical next step for a more accurate comparison would be to further validate the antibody and devise an immunohistochemical scoring system based on staining intensity and tumour area stained. This process is illustrated in Figure 3.2 using the previously identified candidate biomarker, HR23B (Chapter 1, Sections 1.8.2 and 1.9.1), as an example. Specifically, in a collection of CTCL biopsies taken from a phase II trial, HR23B expression levels were related to clinical response to the HDI SAHA, with a positive predictive value of 71.7% (Khan*, et al* 2010). I then carried out validation of the HR23B antibody for IHC using a Leica Bond-max™ autostainer together with a histopathologist, Dr Soilleux, and the Oxford Cancer Centre GCP laboratory (Leticia Campo) for use in a clinical trial setting: staining protocols are programmed and carried out from start to finish by the machine using quality controlled, ready-to-use reagents, meaning slide-to-slide and run-to-run variation is minimized in order to improve quality, consistency and throughput. A multi-tumour TMA containing multiple tumour and matched normal tissue blocks was used to identify high-, medium-, and

low-staining tumour tissue cores that were then chosen to construct a mini-TMA that could be cut onto slides together with patient tumour samples from a clinical trial evaluating the novel HDAC inhibitor CXD101 (NCT01977638). Dr Soilleux reviewed the stained TMAs and devised a tumour staining score (TSS) based on staining intensity and frequency, and for the trial, patient tissue samples were scored independently by two histopathologists (Khan*, et al* 2010); (Eyre et al, submitted).

Figure 3.1

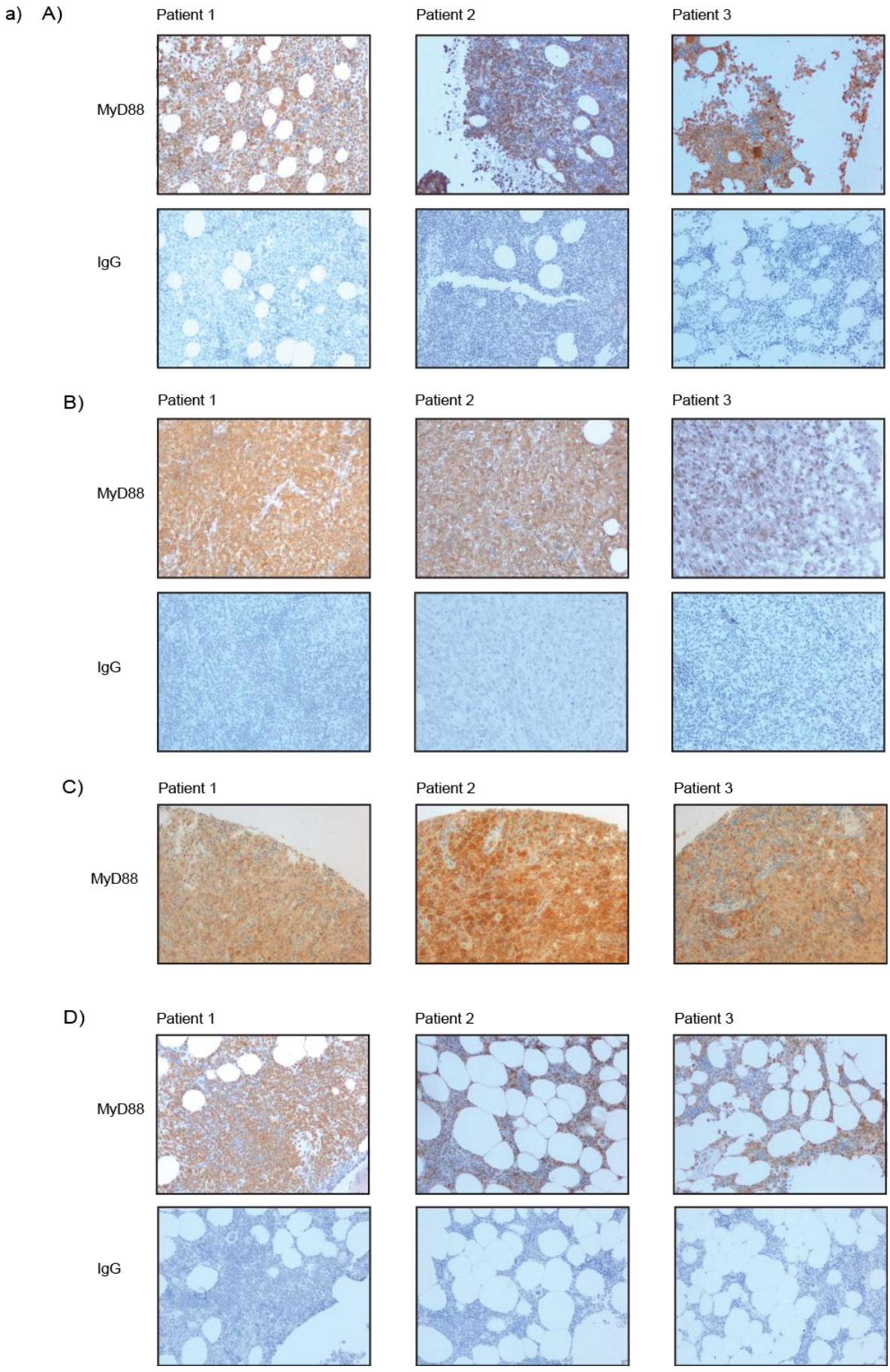

a) A)
Patient 1
Patient 2
Patient 3
MyD88
IgG
B)
Patient 1
Patient 2
Patient 3
MyD88
IgG
C)
Patient 1
Patient 2
Patient 3
MyD88
D)
Patient 1
Patient 2
Patient 3
MyD88
IgG

Figure 3.1 continued

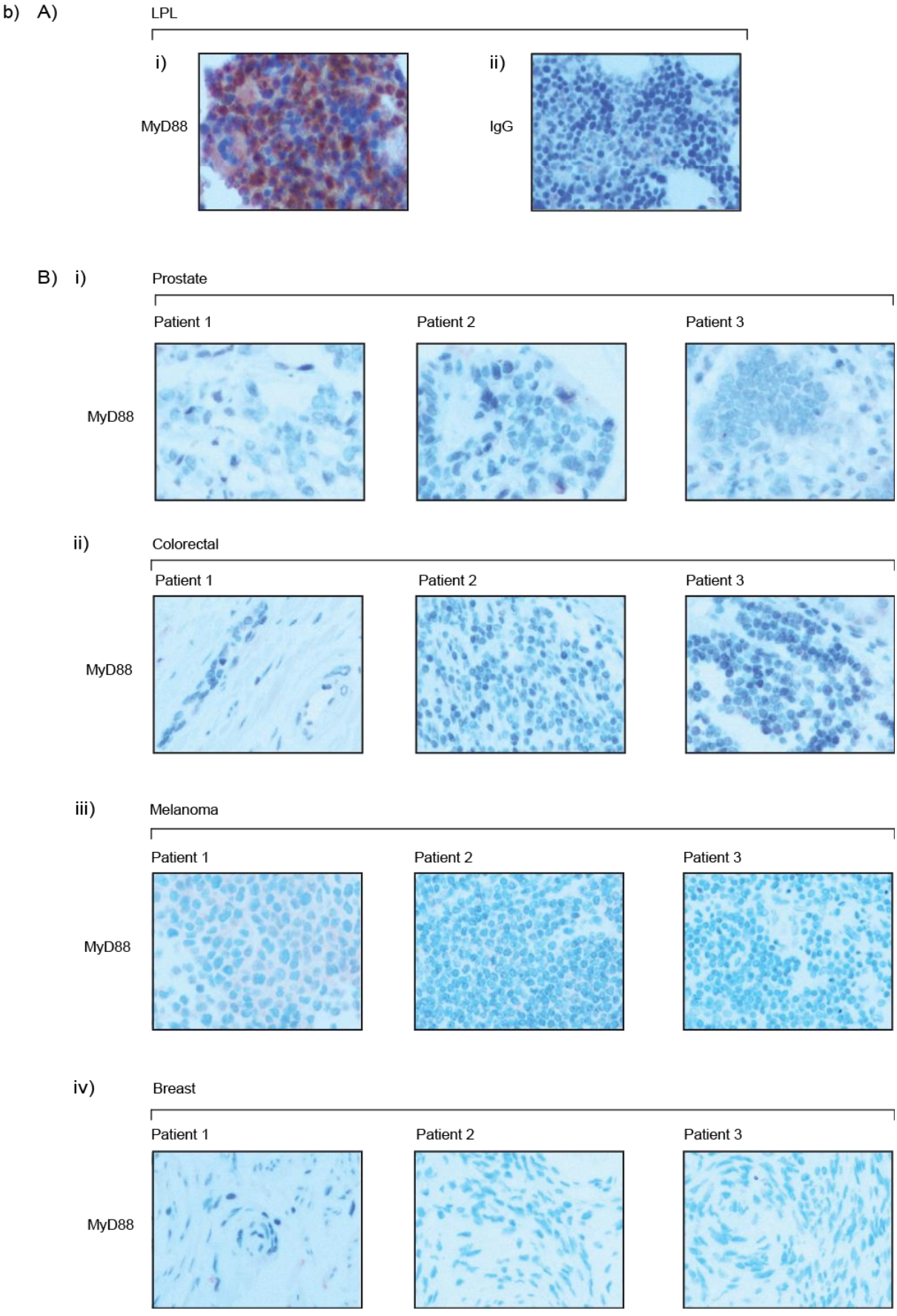


Figure 3.1 continued

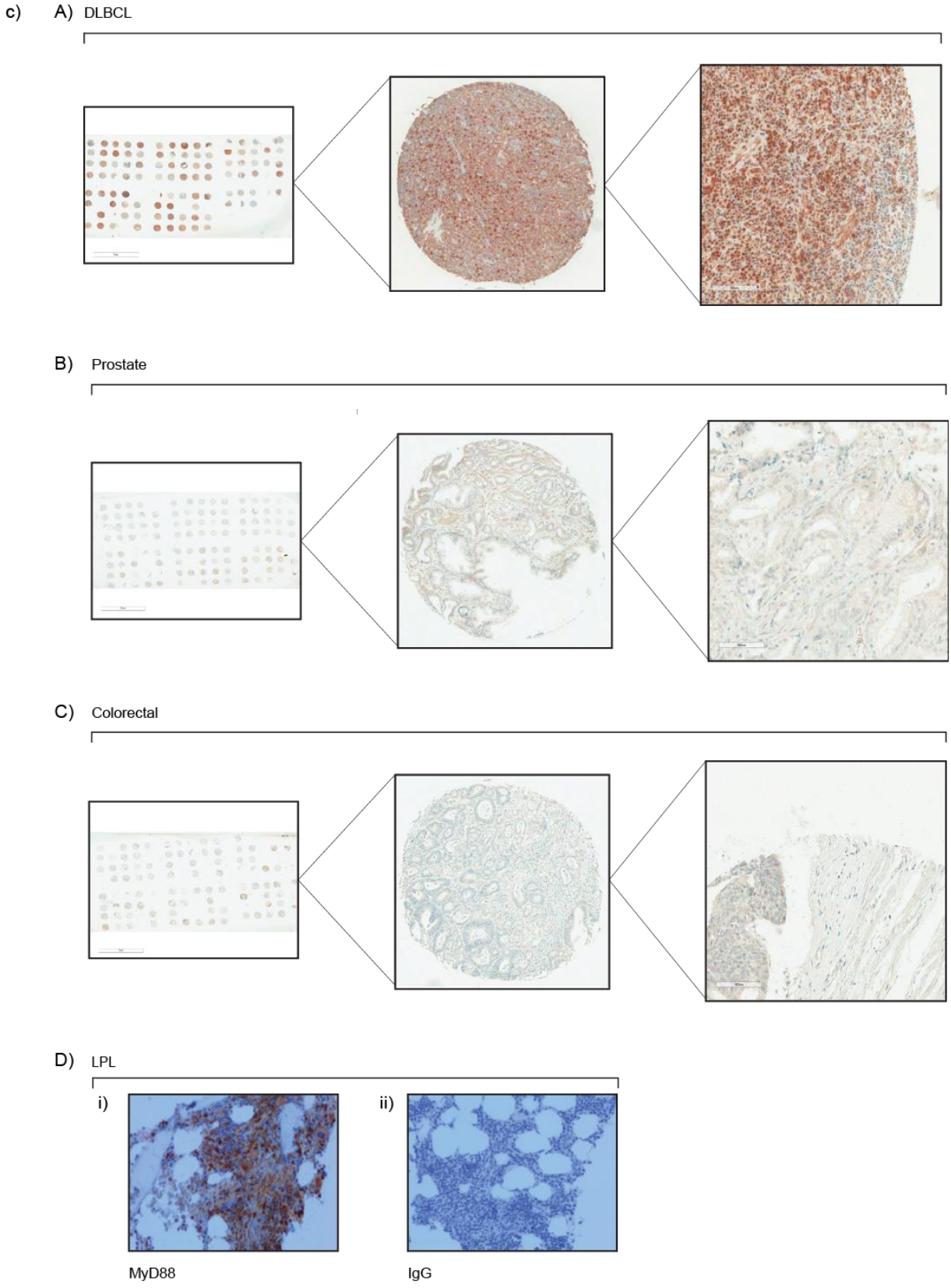


Figure 3.1 MyD88 expression in clinical disease.

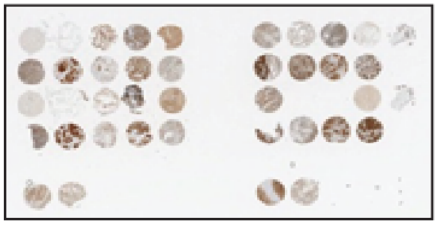
a. Immunohistochemical staining for MyD88, or IgG (as the negative control) was performed on formalin fixed paraffin embedded (FFPE) tissue sections of cancerous and non-cancerous lymphoid tissue. Three representative sections (i.e. from three different patients) are shown per example. Bone marrow sections from patients with LPL are shown (A, i-iii), and compared to lymph node sections from patients with DLBCL (B, i-iii). Non-cancerous tonsillar tissue from three different lymph node biopsies is shown (C, i-iii) and compared to non-cancerous bone marrow sections (D, i-iii). All sections were stained under the same conditions, within the same experiment, except the lymph node sections which were stained alongside the TMA samples (see below). Magnification is x20.

b. Immunohistochemistry was performed on sections from patients with solid cancers. Sections from patients with LPL (A, i) stained for MyD88 and (ii) IgG were used as a comparative "positive" and negative control, respectively. Shown are representative tissue sections each from three different patients with prostate cancer (B, i-iii), colorectal cancer (C, i-iii), melanoma (D, i-iii), or breast cancer (E, i-iii), respectively, which were stained for MyD88. All were stained under the same conditions, within the same experiment. Magnification is x40.

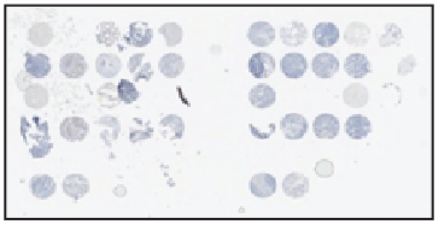
c. Tissue microarrays (TMAs) from patients with DLBCL (A), prostate (B) and colorectal (C) cancer were stained for MyD88 expression. LPL sections stained for MyD88 (D, i) and IgG (D, ii) served as the comparative “positive” and negative controls, respectively. All represented sections were stained under the same conditions, within the same experiment. Magnification is x5, x10 and x20, respectively, for the TMAs, and x20 for the control samples.

Figure 3.2

a) i) HR23B



ii) IgG negative control



iii)

Cerebral Cortex	Skin	Prostate	Pancreas	Liver
Glio-blastoma	Prostate Tm	Pancreas Tm	Liver Tm	Renal Tm
Cerebral Cortex	Skin	Prostate	Pancreas	Liver
Glio-blastoma	Prostate Tm	Prostate	Liver Tm	Renal Tm

Melanoma	Placenta

Kidney	Lung	Ovary	Colon	Breast
Lung Tm	Ovarian Tm	Colon Tm	Breast Tm	Tonsil
Kidney	Lung	Ovary	Colon	Breast
Lung Tm	Ovarian Tm	Colon Tm	Breast Tm	Tonsil

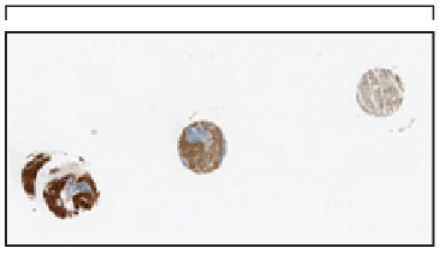
Melanoma	Placenta

b)

Staining Intensity	Description
0	Negative
1	Weak
2	Moderate
3	High

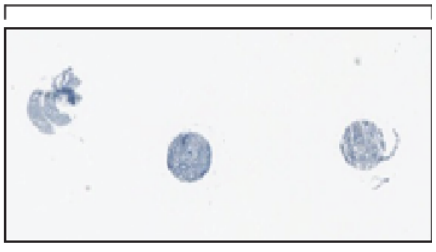
Staining extent/frequency	Tumour area stained
0	0- <25%
1	25-50%
2	>50-75%
3	>75%

c) i) HR23B



high medium low

ii) IgG negative control



high medium low

Figure 3.2 Validation of HR23B antibody and tissue staining score (TSS)

a. A multi-TMA (described in Section 3.2) was stained for HR23B (i). IgG was used as the negative control (ii). The layout for the TMA is shown in (iii).

b. A TSS was derived by analyzing HR23B expression intensity and frequency across different tissue types as shown in a(i). A combined score of greater than or equal to 4 was considered to be strong HR23B staining and therefore represented the threshold for differentiating between positive and negative immunostaining in the CXD101 trial (Eyre et al, submitted).

c. A mini-TMA built from three tissue cores chosen for their (from left to right) high, medium, and low expression of HR23B (i), shown with the negative IgG control (ii). Patient tissue blocks from the CXD101 trial were cut onto slides together with the mini-TMA in order to improve consistency of staining and minimize variability between samples. The TMA and mini-TMA were contructed, and images taken and provided by Leticia Campo.

3.3 MyD88 expression in a panel of cell lines

In order to examine MyD88 expression in the context of HDI treatment, I assessed MyD88 expression in a range of cell lines as shown in Figure 3.3: RIVA, HBL-1, U2932, HL-60 and U937 are suspension cell lines of haematological origin; RIVA and HBL-1 are DLBCL cell lines of the ABC subtype, whereas U2932 is a DLBCL cell line of the GCB subtype. U2OS and MCF7 are both adherent solid cancer cell lines; U2OS is an osteosarcoma cell line, whereas MCF7 is a breast cancer cell line. All cell lines were shown to express MyD88 (Figures 3.3a and b), and in the myeloid cell lines HL-60 and U937, higher MyD88 levels were demonstrated after 72 hours of DMSO treatment to induce monocytic differentiation (Figure 3.3b) which is consistent with the published literature (Baek*, et al* 2009).

The two ABC DLBCL cell lines, RIVA and HBL-1, were chosen to evaluate whether the presence of the MyD88 L265P mutation may affect the propensity of lymphoma cells to undergo apoptosis after HDI treatment. The HBL-1 cell line has previously been described to carry a heterozygous MyD88 L265P mutation (Ngo*, et al* 2011). This was confirmed by direct sequencing (Figure 3.3c), whereas RIVA cells were found to express MyD88 wild-type (not shown). As immunoblotting is a semi-quantitative measure for evaluating MyD88 expression, qPCR was performed in RIVA and HBL-1 cells (Figure 3.3d). Levels of MyD88 mRNA were shown to be higher in HBL-1 cells. This is in contrast to the results obtained on immunoblotting (Figure 3.3a) where protein levels of MyD88 in RIVA cells were increased relative to HBL-1 cells. The discrepancy between mRNA and protein levels of MyD88 in the two cell lines could have several different explanations: firstly, the higher MyD88 transcript levels in HBL-1 cells may lead to translation of a MyD88 protein that is more unstable and therefore targeted for degradation and turned over more rapidly in these cells. This question was addressed by treating RIVA and HBL-1 cells with cycloheximide which shuts down protein translation and allows evaluation of MyD88 protein expression (Figure 3.3e): immunoblotting revealed that after 24 hours, the mutated form MyD88 L265P was expressed at a lower level than

unmutated MyD88, suggesting that the mutant may indeed be more unstable. This is in keeping with what has previously been reported in the literature, although the investigators in this study used a higher dose of cycloheximide and earlier time points (MyD88 expression was monitored until 6 hours only) (Nagao*, et al* 2015). Secondly, it is also not known what the proportion of transcripts for mutated MyD88 (i.e. carrying the L265P mutation) versus unmutated MyD88 is, and whether this could have a significant effect on protein translation.

Thirdly, in its role as an adaptor protein in IL-1-R- and TLR-signalling, the mutated form of the MyD88 protein may be sequestered in the Myddosome signalling platform to a greater extent than the unmutated form, thus leading to an increase in downstream signalling and NF-kB activation (Ngo*, et al* 2011, Treon*, et al* 2012). On a technical level this may mean that the aggregated mutant MyD88 L265P protein is more difficult to extract when cell lysates are prepared using conventional buffers such as RIPA or TNN, as used in the above experiments. Another method that could be considered for the extraction of proteins that aggregate and form complexes of high molecular mass is to use either 8M urea or guanidine:HCl protein extraction buffer (Palmer and Wingfield 2012, Peach*, et al* 2012).

Figure 3.3

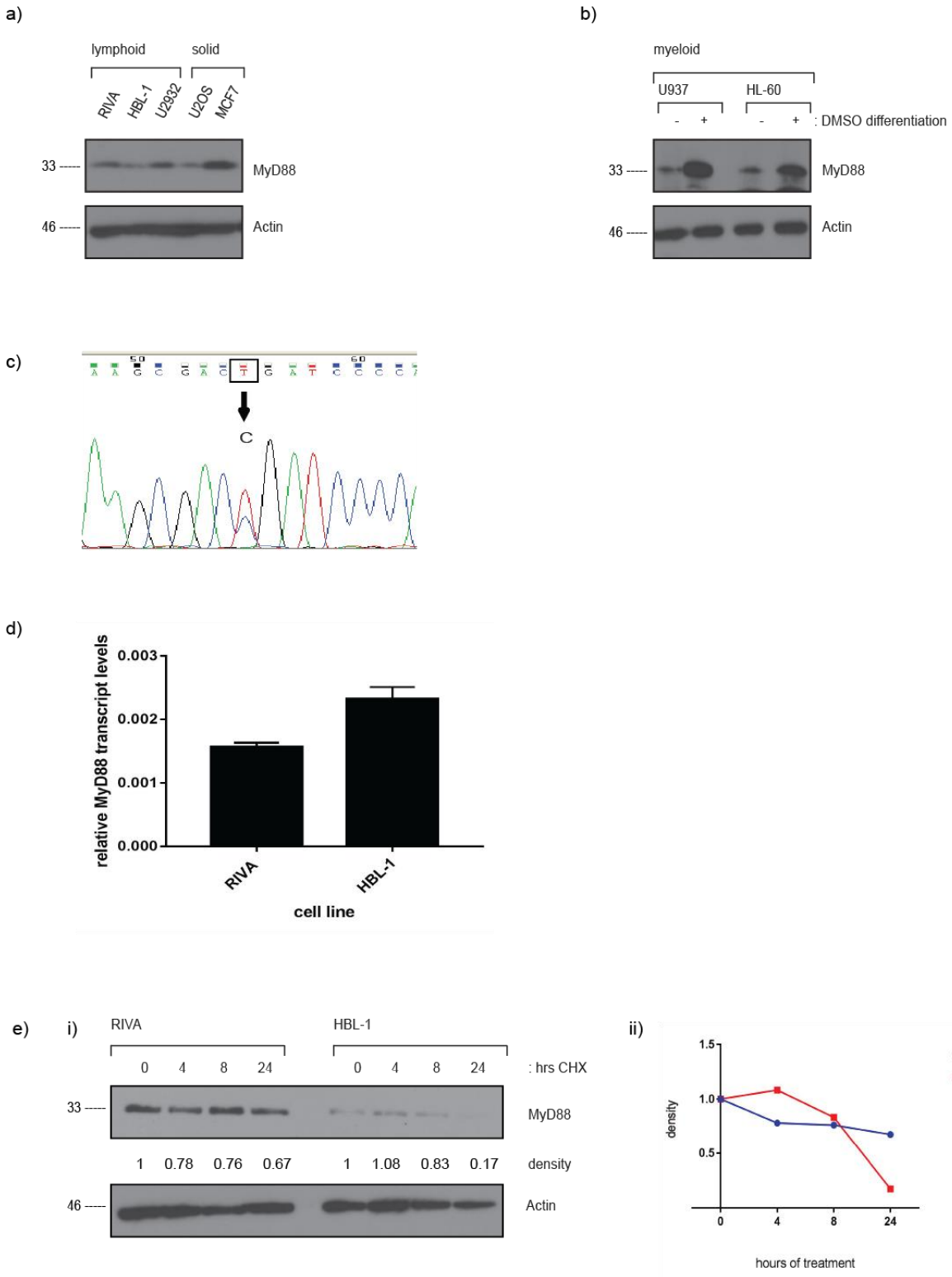

a)
lymphoid
solid
RIVA
HBL-1
U2932
U2OS
MCF7
33
MyD88
46
Actin
b)
myeloid
U937
HL-60
- + - + : DMSO differentiation
33
MyD88
46
Actin
c)
C
d)
relative MyD88 transcript levels
0.003
0.002
0.001
0.000
RIVA
HBL-1
cell line
e)
i)
RIVA
HBL-1
0 4 8 24 0 4 8 24 : hrs CHX
33
MyD88
1 0.78 0.76 0.67 1 1.08 0.83 0.17 density
46
Actin
ii)
density
1.5
1.0
0.5
0 4 8 24
hours of treatment
RIVA
HBL-1

Figure 3.3 MyD88 expression in different haematological and solid cancer cell lines.

a. Lysates of untreated haematological and solid cancer cell line pellets were run on the same SDS-PAGE gel and immunoblotted with anti-MyD88 to show baseline MyD88 expression; actin was the loading control. RIVA, HBL-1 and U2932 represent lymphoid cell lines, whereas U2OS and MCF7 represent solid cancer cell lines. Protein markers are indicated.

b. Myeloid cell lines HL-60 and U937 were grown for 72 hours, and either not treated, or treated with 1% DMSO (which was added at time point 0 hours) in order to augment MyD88 expression. Cells were harvested and pellets lysed before immunoblotting for MyD88; actin served as the loading control.

c. Direct DNA sequencing of the HBL-1 cell line shows a heterozygous mutation of the MyD88 gene on chromosome 3 (wild-type C**T**G (leucine) codon to C**C**G (proline) codon) confirming its MyD88 L265P status. Sequencing was also carried out in the RIVA cell line but this is not shown here.

d. Differences in MyD88 mRNA expression were assessed by qPCR in extracts from RIVA and HBL-1 cells. MyD88 transcript levels are shown as normalized to actin expression in each cell line.

e. RIVA and HBL-1 cells were treated with 100mg/mL of cycloheximide (CHX) for the indicated times, before harvesting. Cell lysates were run on the same SDS-PAGE gel and analyzed for MyD88 expression (i). Actin served as the loading control. MyD88 levels were normalized to actin, and the relative expression of MyD88 in CHX-treated as compared to control cells (timepoint 0 hrs) was determined by densitometric analysis (using ImageJ software) and indicated numerically below each lane (i), and in a graph (ii).

3.4 Lymphoid cell lines show sensitivity to HDI treatment

Both ABC DLBCL cell lines, RIVA and HBL-1, displayed sensitivity to treatment with SAHA, a pan-HDAC inhibitor, in a dose- and time-dependent manner (Figures 3.4a and b). Apoptosis was measured by immunoblotting for cleaved caspase 3 and cleaved PARP (Figure 3.4a(i) and (ii)). HBL-1 cells appeared to be more sensitive to SAHA, with more cleaved caspase 3 apparent at lower SAHA concentrations (e.g. 2.5μM), and higher levels of both cleaved caspase 3 and cleaved PARP being observed in cell lysates from HBL-1 cells on immunoblotting after treatment of both cell lines with 5μM SAHA for 24 hours (Figure 3.4a(ii)). SUDHL-4 (Figure 3.4a(ii)) represents a DLBCL cell line of the GCB subtype which does not carry a MyD88 mutation and was used as a comparator. Levels of acetylated histone H3 (Ac-H3) were measured as a control (Figure 3.4a(iii)), and increased as predicted in cells treated with SAHA, reflecting its role as inhibitor of nuclear HDAC enzymes that are responsible for deacetylating histone H3 (Drogaris*, et al* 2012). Increased levels of Ac-H3 could not be demonstrated in peripheral blood monoculear cells (PBMCs) from patients treated with the novel HDI CXD101 (Appendix A(a), p 202).

Comparing levels of cleaved caspase 3 or cleaved PARP between cell lines on immunoblot is, however, at best a semi-quantitative measure, and comparisons between different blots is not recommended due to varying assay conditions (despite standardized protocols), and therefore small changes, for example in temperature, composition of running or blotting buffers, or the length of x-ray film exposure may affect the signal intensity of the bands. Therefore, FACS analysis with measurement of sub-G1 and MTT assays of cellular viability were performed in order to obtain a more quantitative assessment of cell viability after HDI treatment.

Again, HBL-1 cells were shown to be more sensitive to SAHA treatment (5μM) when sub-G1 percentage was assessed by PI staining on FACS (Figure 3.4c), and by MTT assay (Figures 3.4b and d), where a SAHA concentration of 10μM led to a more rapid decrease in cell viability in HBL-1 cells. A comparison of the increase in sub-G1 on FACS analysis between different

lymphoid cell lines demonstrated differential sensitivity to treatment with SAHA at a dose of 5μM (Figure 3.4e): the GCB DLBCL cell lines CRL and U2932 displayed higher levels of sub-G1 on SAHA treatment, whereas the ABC DLBCL cell lines RIVA and HBL-1 were shown to be comparatively less sensitive to SAHA treatment, but HBL-1, which carries the MyD88 L265P mutation, was shown to be more sensitive to SAHA treatment than the MyD88-unmutated DLBCL cell lines RIVA and RCK8. In addition, 24 hours of SAHA treatment had less of an effect on the sub-G1 fraction in the Hodgkin lymphoma cell line L428. Although SAHA has been previously shown to induce apoptosis in Hodgkin lymphoma cell lines (Martin-Sanchez*, et al* 2011) this has been described to be preceded by cell cycle G2/M or G1 arrest, and appears to be most prominent after 48-72 hours of treatment, often with SAHA concentrations ranging from 1-10μM. These time points were not assessed in the respective Hodgkin lymphoma cell line.

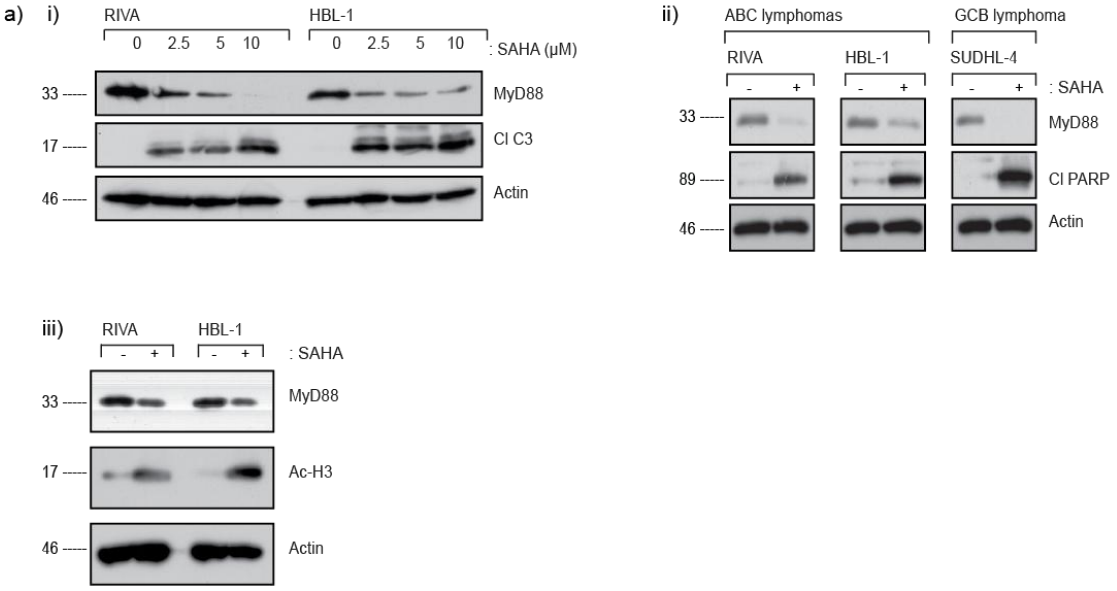
As MyD88 is thought to be a predominantly cytoplasmic protein and previous work carried out in our group suggested that MyD88 may itself be a target for HDAC inhibition (New*, et al* 2016), and in particular by HDAC6, I evaluated the effect of an HDAC6-specific inhibitor, tubastatin, on RIVA and HBL-1 cells. Both cell lines express HDAC6 (Figure 3.4g(iv)). FACS analysis demonstrated a greater sub-G1 percentage in HBL-1 cells after treatment with 10μM tubastatin (Figure 3.4f), and cell viability in HBL-1 cells reduced more rapidly in HBL-1 cells on MTT assay (Figure 3.4g), suggesting that HBL-1 cells are more sensitive to tubastatin than RIVA cells.

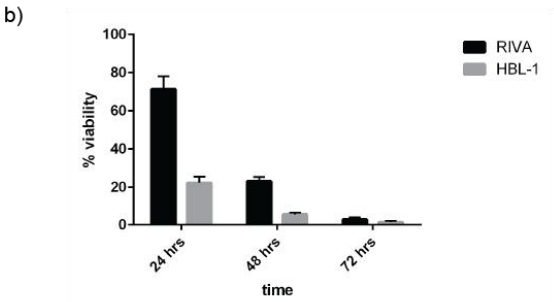
Finally, the effect of a commonly used chemotherapy agent, doxorubicin, at a concentration of 2μM, on the fraction of sub-G1 cells in RIVA and HBL-1 cells is shown in Figure 3.4h and compared to the effect of HDAC inhibition. Doxorubicin is used in the treatment of DLBCL, as part of the R-CHOP regimen, and although specific MTT IC_{50} data for dosing in RIVA and HBL-1 cells was not established by myself for this particular drug, IC_{50} data available for a panel of DLBCL cell lines from a large database (http://www.cancerrxgene.org/translation/Drug/133)

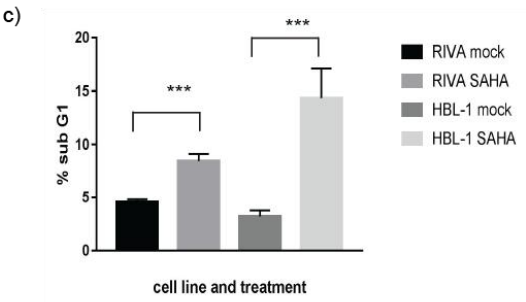
suggests that cytotoxicity may be achieved at this dose. The results of this comparison suggest that in the setting of ABC DLBCL, HDAC inhibition may induce apoptosis more effectively than agents that are more conventionally used in the clinical setting. However, to explore this assumption further and to be able to draw a more definitive conclusion, it would be preferable to test a number of different, preferably class-selective, HDIs on a panel of DLBCL cell lines (of both the ABC and GCB subtypes) and compare this with a range of mechanistically unrelated agents. Finally, it is important to note the concentration of SAHA established in RIVA and HBL-1 cell lines and used in the above experiments is comparable to doses described in clinical studies in the literature, where reported serum concentrations vary between 1.1µM and 10µM (Fujiwara*, et al* 2009, Ramalingam*, et al* 2010, Ramalingam*, et al* 2007, Richardson*, et al* 2013).

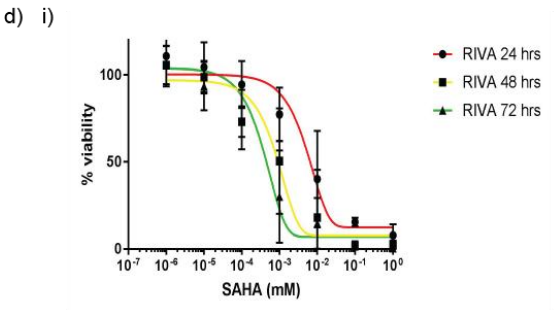
Another observation that was made in this context was the decrease in MyD88 protein levels on SAHA treatment (Figure 3.4a). This decrease was observed across DLBCL subtypes and irrespective of MyD88 mutation status, and may be a finding that is in keeping with the level of cytotoxicity demonstrated after SAHA treatment or the presence of caspase cleavage sites in the MyD88 protein (Kumar*, et al* 2014). MyD88 mRNA transcript levels in RIVA cells were shown to decrease after SAHA treatment, but perhaps rather surprisingly, in HBL-1 cells, MyD88 transcript levels increased after 24 hours (Figure 3.4h). This is in contrast to a recent investigation of CUDC-907, a dual HDAC and PI3K inhibitor (Mondello*, et al* 2017) where a uniform decrease in MyD88 protein and transcript levels after 24 hours of drug treatment in MyD88-mutated and -unmutated cell lines was described. The unexpected increase in MyD88 transcript levels in HBL-1 cells observed here could be related to the fact that continued signalling through the MyD88-NF-kB pathway is thought to take place in cells that carry the MyD88 L265P mutation, and therefore continued sequestration of the mutated form of MyD88 in the Myddosome may drive a feedback loop to maintain its own transcription. This may link in with the earlier hypothesis that mutated MyD88 transcripts may undergo more rapid turnover in cells (Section 3.3).

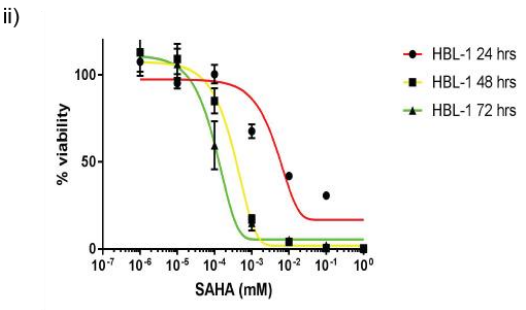
Figure 3.4









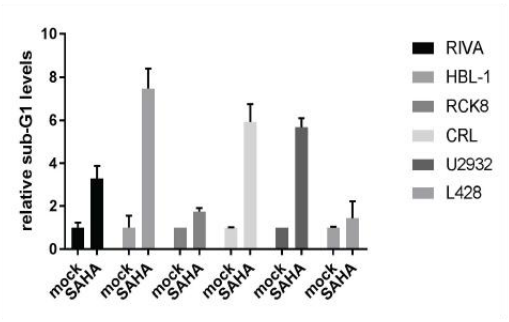


iii)

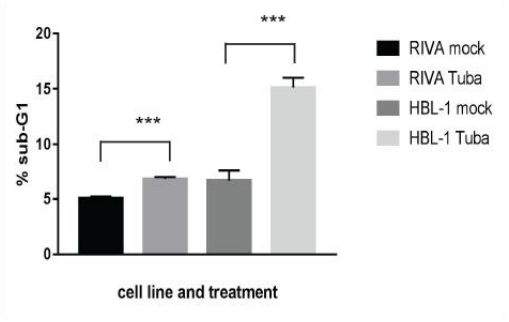
SAHA IC50 (μM)	24 hrs	48 hrs	72 hrs
RIVA	4.01	1.79	0.35
HBL-1	3.37	0.37	0.12

Figure 3.4 continued

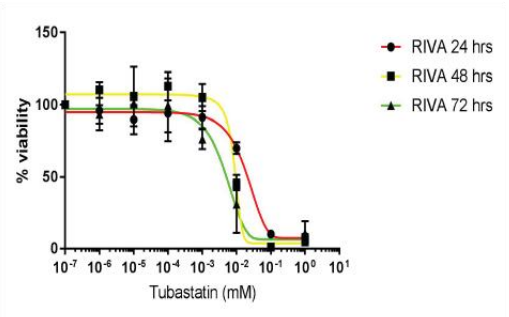
e)



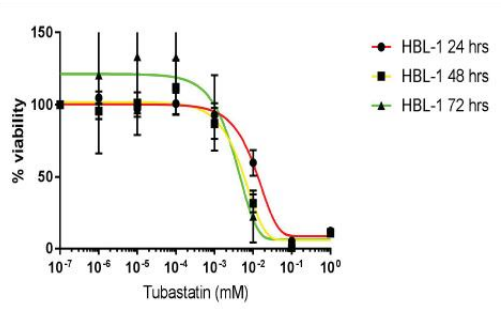
f)



g) i)



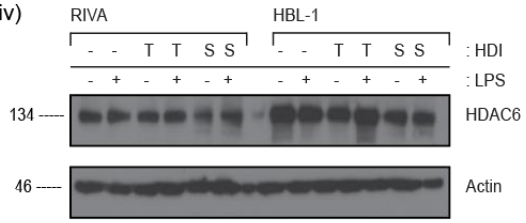
ii)



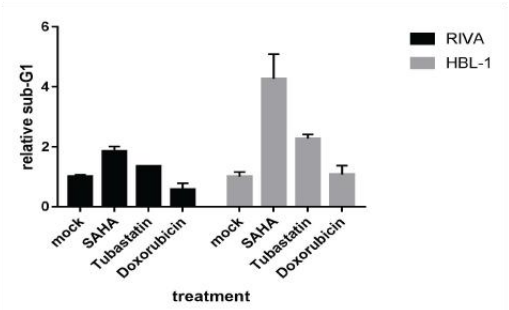
iii)

Tubastatin IC50 (μM)	24 hrs	48 hrs	72 hrs
RIVA	10.78	3.26	1.93
HBL-1	5.99	2.24	0.79

iv)



h)



j)

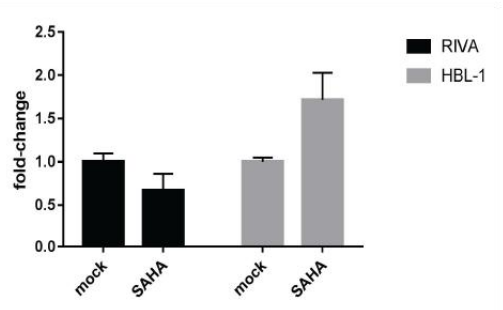


Figure 3.4 Lymphoid cell lines and their response to HDI treatment.

a. (i) RIVA and HBL-1 cells were treated with increasing concentrations of the pan-HDAC inhibitor SAHA (2.5, 5 and 10μM) for 24 hours, and lysates were immunoblotted with anti-MyD88 and anti-cleaved caspase 3 (Cl C3) antibodies; actin served as the loading control. Protein markers are indicated.

(ii) RIVA, HBL-1 and SUDHL-4 cells were treated with 5μM SAHA for 24 hours, and lysates were immunoblotted with anti-MyD88 and anti-cleaved PARP (Cl PARP) antibodies; actin served as the loading control.

(iii) RIVA and HBL-1 cells were treated with 5μM SAHA for 24 hours as above (ii), and lysates were immunoblotted with anti-MyD88 and anti-acetylated Histone H3 (Ac-H3) antibodies; actin served as the loading control.

b. RIVA and HBL-1 cell lines were compared by MTT viability assay. Cells were plated in triplicate and then treated with SAHA at a concentration of 10μM for 24, 48, or 72 hours before adding MTT and assessing viability. Percentage of viable cells (compared to the mock-treated control which is set at 100%) at the indicated time points is shown.

c. RIVA and HBL-1 cells, in triplicate, were treated with SAHA (5μM for 24 hours), harvested and analyzed by PI staining on flow cytometry. Percentage of cells in sub-G1 are shown. (*** denotes $p<0.0001$). Full cell cycle profiles are shown in Appendix A(b), p 202.

d. RIVA (i) and HBL-1 (ii) cells, in triplicate, were further compared by MTT viability assay over 24, 48 and 72 hours of SAHA treatment, and the IC_{50} calculated (iii). Represented are the results from three biological replicates.

e. Six different lymphoid cell lines, in triplicate, were treated with SAHA (5μM) for 24 hours, harvested and analyzed by flow cytometry. Relative sub-G1 levels are shown as normalized to sub-G1 in the DMSO (mock)-treated control samples. RIVA, HBL-1, CRL and U2932 cells represent DLBCL, L428 is a Hodgkin lymphoma cell line and RCK8 is a transformed DLBCL cell line. MyD88 mutation status in RIVA and HBL-1 cells was confirmed by direct sequencing (see Figure 3.3c), whereas MyD88 mutation status in the other cell lines was confirmed by database and literature searches (Chapter 2, Section 2.2).

f. RIVA and HBL-1 cells, in triplicate, were treated with the HDAC6-specific inhibitor tubastatin (10μM for 24 hours), harvested and analyzed by flow cytometry. Percentage of cells in sub-G1 are shown. (*** denotes $p<0.0001$).

g. RIVA (i) and HBL-1 (ii) cells, in triplicate, were further compared by MTT viability assay over 24, 48 and 72 hours of tubastatin treatment, and the IC_{50} calculated (iii). Represented are the results from two biological replicates.

(iv) RIVA and HBL-1 cells were treated with tubastatin (T) or SAHA (S), and HDI treatment was either preceded by treatment with LPS (100ng/mL) (+), or not (-). Lysates were immunoblotted with anti-HDAC6 antibody; actin was the loading control.

h. RIVA and HBL-1 cells were plated in triplicate, and treated with SAHA (5μM), tubastatin (10μM), or the anthracycline doxorubicin (2μM) for 24 hours, and then harvested and analyzed by flow cytometry. Relative sub-G1 levels are shown as compared to DMSO-only (mock) treated controls.

j. Quantitative PCR was used to assess fold-change in MyD88 transcript expression (compared to cells pre-treatment) in RIVA and HBL-1 cells treated with SAHA (5μM for 24 hours). MyD88 transcript levels were normalized to actin expression in each cell line.

3.5 Strategies for depleting MyD88 in non-adherent cells: transient transfection, electroporation, nucleofection and generation of shRNA cell lines

To further investigate the role of MyD88 in influencing treatment outcome with an HDI, depletion of MyD88 by knockdown in lymphoma cell lines was attempted. Previous work in Professor La Thangue's research group carried out by Maria New showed that short-term silencing of MyD88 in the adherent U2OS osteosarcoma cell line reduced sensitivity of these cells to SAHA, whereas, conversely, over-expression of ectopic MyD88 enhanced sensitivity to SAHA treatment (New*, et al* 2016). Over-expression experiments however need to be interpreted with caution as the levels of protein expression achieved may far surpass what is normally found in the cell and thus could lead to off-target and/or spurious effects. In addition, ectopically expressed MyD88 protein has an additional Flag-tag and so one must consider that the tag may alter normal protein function and/or location within the cell (Sheikh*, et al* 2016). Therefore, in the first instance, short-term knockdown of MyD88 was prioritized in the DLBCL cells.

As shown in Figure 3.5a(i), transient transfection with MyD88 short interfering RNA (siRNA) led to knockdown of MyD88 in U2OS cells using a standard liposomal technique (see Chapter 2, Section 2.11). Attempts at optimizing this protocol (as per the manufacturer's recommendations) for the use of MyD88 siRNA in non-adherent lymphoma cells, however, proved unsuccessful, and no decrease in MyD88 protein level was seen (Figure 3.5a(ii)). Other approaches, such as altering the transfection reagent (i.e. using lipofectamine® 2000 or RNAiMax instead of oligofectamine), and using different MyD88 siRNA (Chapter 2, Section 2.11) also did not achieve efficient knockdown of MyD88 in the DLBCL cell lines.

Electroporation (Chapter 2, Section 2.12) has previously been used to successfully transfect non-adherent mammalian cells such as lymphocytes (Chicaybam*, et al* 2016, Shigekawa and Dower 1988, Wong and Neumann 1982). Although the mechanism of nucleic acid transfer is not fully understood, it is thought that the application of electrical pulses to the cells

destabilize the cell membrane temporarily to form pores which allow the nucleic acid material to pass into cells. When the electric field is turned off, the pores in the membrane reseal, retaining the transfected material. This technique does require a greater starting number of cells since toxicity is relatively high compared to other methods. This effect can be seen in Figure 3.5b. Although initially MyD88 appears to be successfully knocked down in RIVA cells, transfected cells could not be grown successfully beyond 72 hours and showed high attrition rates within the first 24 hours after transfection (see effect on HBL-1 cells, and actin levels in both RIVA and HBL-1 cells, on the same Western Blot).

More recently, nucleofection (Chapter 2, Section 2.13) has emerged as a promising method to transfer genetic material into cells considered difficult to transfect (Aluigi*, et al* 2006, Leclere*, et al* 2005, Maasho*, et al* 2004). Nucleofection is based on the principles of electroporation but uses a combination of electrical parameters and cell-type specific reagents that allow a more direct delivery of transfected genetic material into the nucleus. Using the Lonza 4D nucleoporator system, RIVA and HBL-1 cells could be shown to express transfected GFP during the optimization process (Figure 3.5c(i)), but transfection of MyD88 siRNA at different concentrations was unable to produce any significant knockdown and reduction in MyD88 protein levels (Figure 3.5c(ii)).

Subsequently, lentiviral transduction of lymphoma cells with MyD88 small hairpin (sh) RNA was explored (Chapter 2, Section 2.14). The principle of this technique is based on integration of the plasmid vector into genomic DNA allowing for longer-term or stable gene expression and thus longer-lasting knockdown of the target mRNA (Brummelkamp*, et al* 2002, Paddison*, et al* 2002). Both RIVA and HBL-1 cell lines were transduced and subsequent puromycin selection was attempted. After 5-7 days in culture, RIVA cells were evaluated for MyD88 knockdown but this was not found to be present in cells transduced with the recommended amount of lentiviral particles (10-20µL) (Figure 3.5d). In those RIVA cells transduced with a lower amount of virus (5µL), MyD88 protein expression on immunoblotting appeared absent

at first but subsequent single-cell selection and continued growth in puromycin proved not to be possible owing to rapid cell death (presumably of those cells with MyD88 knockdown), or outgrowth of clones that did not demonstrate stable shRNA expression and therefore MyD88 knockdown, as evidenced by recurrent MyD88 protein expression. HBL-1 cells did not grow in puromycin-selection medium beyond a period of 5-7 days, and in the viable cells that were harvested for immunoblotting, no MyD88 knockdown could be shown. For both cell lines, the growth of untreated control cells rapidly declined (within 48-72 hours) after the addition of puromycin, whereas cells transduced with control shRNA grew freely.

Interestingly, lentiviral transduction in HBL-1 cells has been described before (Ngo*, et al* 2011) but the resulting knockdown was not complete, and MyD88 shRNA-transduced cells remained viable only after being rescued by ectopically co-expressed mutant MyD88. The possible conclusions from these combined observations, therefore, are firstly, that MyD88 may play an important part in maintaining cell growth in RIVA and HBL-1 cells, and that cell viability declines rapidly in these cells when they lose MyD88 expression. Secondly, it may also be possible that MyD88 shRNA cannot be expressed effectively in the transduced cells, and therefore MyD88 knockdown could not be demonstrated in my experiments.

Figure 3.5

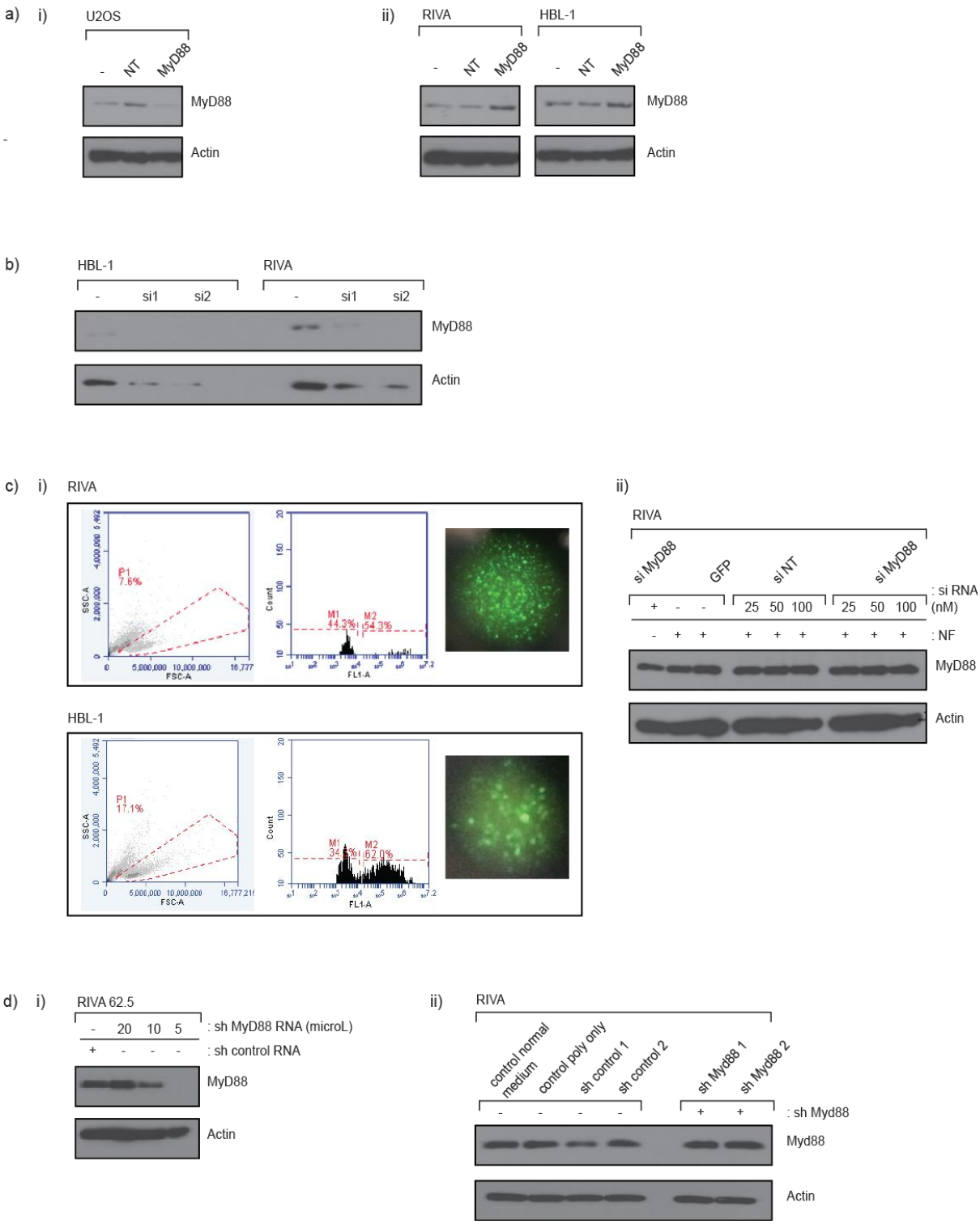

a) i)
U2OS
- NT MyD88
MyD88
Actin
ii)
RIVA
HBL-1
- NT MyD88
- NT MyD88
MyD88
Actin
b)
HBL-1
RIVA
- si1 si2
- si1 si2
MyD88
Actin
c) i)
RIVA
P1
7.8%
SSC-A
FSC-A
Count
FL1-A
M1
44.3%
M2
54.3%
HBL-1
P1
17.1%
M1
34.8%
M2
62.0%
ii)
RIVA
si MyD88
GFP
si NT
si MyD88
: si RNA (nM)
+ - - 25 50 100 25 50 100
- + + + + + + + + : NF
MyD88
Actin
d) i)
RIVA 62.5
- 20 10 5 : sh MyD88 RNA (microL)
+ - - - : sh control RNA
MyD88
Actin
ii)
RIVA
control normal medium
control poly only
sh control 1
sh control 2
sh Myd88 1
sh Myd88 2
- - - - + + : sh Myd88
Myd88
Actin

Figure 3.5 MyD88 knockdown in lymphoma cell lines.

a. (i) MyD88 was knocked down in U2OS osteosarcoma cells using short-term siRNA transfection with a chemical method (oligofectamine). Cells were harvested after 72 hours and immunoblotted for MyD88; actin served as the loading control. "NT" denotes the non-targeting siRNA control; "-" the negative control.

(ii) MyD88 knockdown was attempted in RIVA and HBL-1 cells as outlined in (i). Cell lysates were immunoblotted for MyD88; actin was the loading control.

b. MyD88 knockdown was attempted in HBL-1 and RIVA cells using electroporation. "si1" and "si2" represent two different concentrations of MyD88 siRNA (si1=25nM; si2=50nM). "-" represents the untreated (negative) control cells. Actin was the loading control.

c. (i) RIVA and HBL-1 cells were transfected with GFP (1μM) in order to optimize the Lonza 4D optimization protocol (Chapter 2, Section 2.13). After 24 hours, cells were analyzed for GFP expression by fluorescence microscopy (right-hand panel) and FACS analysis, after gating on the viable cells and using the green fluorescence channel (left-hand and middle panels, respectively).

(ii) RIVA cells treated with MyD88 siRNA at the indicated concentrations were transfected by nucleofection (NF) using the optimized Lonza 4D protocol as described above (i). The controls used (the first three lanes, on the far left-hand side of the Western Blot) were as follows: MyD88 siRNA only (+) but not subjected to nucleofection (-); no MyD88 siRNA (-) but subjected to nucleofection (+); and treated only with GFP but no MyD88 siRNA (-) and subjected to nucleofection (+). Lysates were immunoblotted for MyD88; actin was the loading control.

d. (i) RIVA cells (plated at a density of 62,500 cells per well in a 6 well plate, hence denoted as "62.5"), were treated with 0 (-), 20, 10, or 5μL of MyD88 shRNA, or 20μL of control shRNA, as per lentiviral transduction protocol (Chapter 2, Section 2.14). Five days after transduction, cell lysates were run on an SDS-PAGE gel and immunoblotted for MyD88; actin was the loading control.

(ii) RIVA cells underwent lentiviral transduction as described above (i). Ten days after lentiviral transduction, and five days after commencing puromycin selection, cells were harvested and lysates were immunoblotted for MyD88. The Western Blot shown is representative of two biological replicates ("sh cont 1" and "sh cont 2" represent the cells transduced with control shRNA; "sh MyD1" and "shMyD2" represent those cells transduced with MyD88 shRNA); "control normal medium" are control cells that were non-transduced but grown for the same amount of time, under the same conditions, and "control poly only" are similarly non-transduced cells, exposed to polybrene only, that were grown in normal medium (without puromycin); actin represented the loading control.

3.6 Chemical inhibition of MyD88

As knockdown of MyD88 through transfection or lentiviral transduction proved challenging, an alternative, chemical biology approach using the small-molecule MyD88 dimerization inhibitor T6167923 (Olson*, et al* 2015) was considered. A crucial first step in innate immune signalling following TLR engagement and pathogen recognition is thought to be the recruitment of MyD88 which functions as an adaptor, or anchor, protein to allow the assembly of a complex signalling platform (Chapter 1, Section 1.5). MyD88 dimerizes through its TIR domains, and MyD88 homodimerization then leads to downstream activation of IRAK kinases and NF-kB signalling (Motshwene*, et al* 2009). The MyD88 TIR-TIR interaction can be targeted with small inhibitor peptides that contain a sequence from the MyD88 TIR domain and are able to bind to the MyD88 monomer, thus blocking MyD88 dimerization. T6167932 was identified through a computational screen and shown to abrogate pro-inflammatory cytokine production in human primary cells; in addition, mice treated with lethal doses of *Staphylococcal* enterotoxin B (SEB) were protected from developing toxic shock after treatment with T6167932 (Olson*, et al* 2015). Therefore, the effect of T6167932 on MyD88 silencing was found to be comparable to a MyD88 $^{-/-}$ mouse model where mice have been shown to be protected from the lethal effects of SEB-induced toxic shock (Kissner*, et al* 2011a).

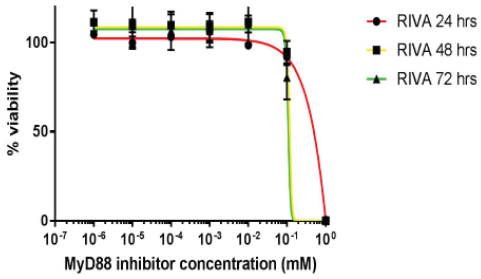
In order to test the effects of T6167932 on the DLBCL cell lines, I established the IC_{50} of T6167932 in RIVA and HBL-1 cells (Figure 3.6a). T6167932 appeared to be cytotoxic at high micromolar concentrations only. The anti-inflammatory effects of T6167932 in cell-based studies were shown using concentrations of 100-500µM (Olson*, et al* 2015). Using this as a guide, I titrated the dose of MyD88 inhibitor up from 10µM to 100µM, adding the compound after stimulation with a fixed amount of LPS to initiate MyD88 aggregation via TLR engagement. Similarly, a fixed amount of SAHA (5µM) was used in order to evaluate the effect of MyD88 inhibition on sensitivity to an HDI.

In RIVA cells, a dose of 100µM of the MyD88 inhibitor T6167932 added after LPS stimulation showed a reduction in SAHA-induced apoptosis (Figure 3.6b(i)) which was seen do be dose-dependent (Figure 3.6b(ii)). By comparison, T6167932 did not appear to mediate a similar effect on HBL-1 cells after SAHA treatment, as the levels of cleaved caspase 3 were not appreciably different (Figure 3.6c). MyD88 protein levels did not seem to be directly affected by the addition of T6167932 on its own (no LPS), and MyD88 mRNA levels did not change significantly in RIVA or HBL-1 cells after exposure to T6167932 for 2 hours (Figure 3.6d).

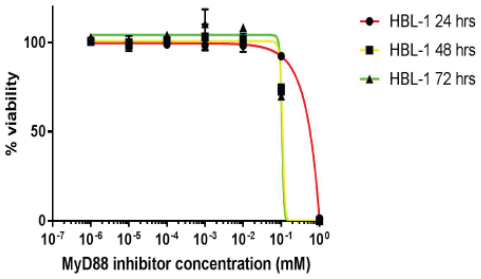
Taken together, these results suggest that chemical MyD88 inhibition may alter the effect of HDI treatment on RIVA (MyD88 wild-type) but not HBL-1 (MyD88 L265P-mutated) cells. Therefore, T6167932 may be effective at disrupting MyD88 homodimerization when MyD88 is not mutated. As the L265P mutation occurs in the TIR domain of the MyD88 protein, it is therefore possible to speculate that the inhibitor was allosterically hindered or unable to bind to the TIR domain of the mutated form of MyD88 in HBL-1 cells, or that dis-aggregation of the Myddosome occurs much more slowly in these cells. In order to check that the MyD88 inhibitor is indeed active, Myd88 aggregation could be assessed by means of immunofluorescence or a readout of pro-inflammatory cytokines could be performed; the latter option was explored (Chapter 4, Figure 4.3f).

Figure 3.6

a) i)



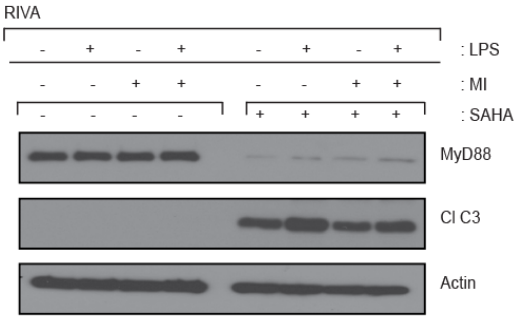
ii)



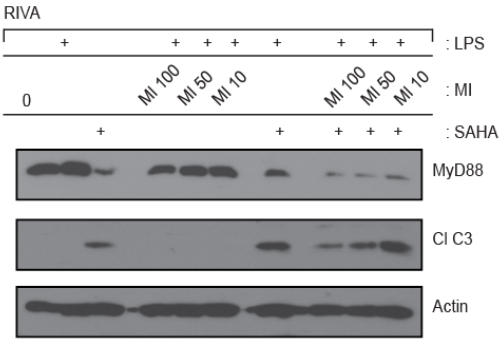
iii)

T6167932 IC50 (mM)	24 hrs	48 hrs	72 hrs
RIVA	0.599	0.645	0.2339
HBL-1	0.950	0.309	0.194

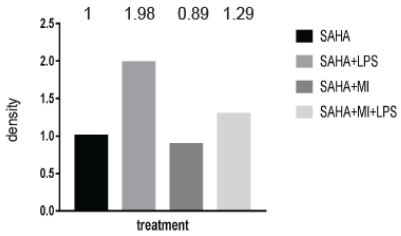
b) i)



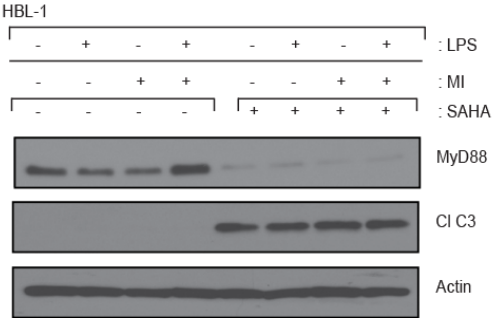
iii)



ii)



c)



d)

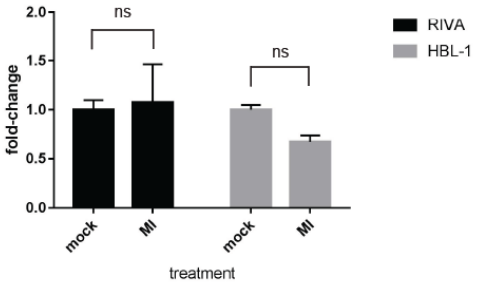


Figure 3.6 Chemical inhibition of MyD88 aggregation with the small-molecule inhibitor T6167932.

a. RIVA (i) and HBL-1 (ii) cells, in triplicate, were compared by MTT viability assay over 24, 48 and 72 hours of treatment with the MyD88 inhibitor (MI) T6167932, and the IC_{50} calculated (iii).

b. (i) RIVA cells were treated with LPS (100ng/mL), T6167932 (100μM), and SAHA (5μM), either alone or in combination. For combination treatments, LPS was added 2 hours prior to further treatments in order to stimulate TLR signalling. T6167932 was added subsequently for two hours before SAHA was added as the final agent for 24 hours. Cell lysates were immunoblotted for MyD88 and cleaved caspase 3 (Cl C3); actin served as the loading control. *MI*, Myd88 inhibitor.

(ii) The relative levels of cleaved caspase 3 in LPS/T6167932/SAHA-treated as compared to SAHA-only-, LPS/SAHA-, or T6167932/SAHA-treated cells were determined by densitometric analysis and are indicated numerically, and in a graph, as shown below the Western Blot.

(iii) RIVA cells were treated as above (i), using standard concentrations of LPS (100ng/mL) and SAHA (5μM), and three different concentrations of T6167932 (MI 10, 50 or 100μM). Cell lysates were immunoblotted for MyD88 and cleaved caspase 3 (Cl C3); actin served as the loading control.

c. HBL-1 cells were treated with LPS (100ng/mL), T6167932 (100μM), and SAHA (5μM), either alone or in combination, as described above (b(i)). Cell lysates were immunoblotted for MyD88 and cleaved caspase 3 (Cl C3); actin served as the loading control.

d. Quantitative PCR was used to assess fold-change in MyD88 transcript expression (compared to cells pre-treatment) for RIVA and HBL-1 cells treated with T6167932 (100μM for 2 hours). MyD88 transcript levels were normalized to actin expression in each cell line.

3.7 Conclusions

Previous work in transfected U2OS cells has shown that MyD88 affects sensitization of cells to treatment with HDIs: over-expression of MyD88 led to increased sensitivity to an HDI, whereas low MyD88 expression resulted in reduced sensitivity. In addition, the presence of the MyD88 L265P mutation conferred an enhanced effect on apoptosis in U2OS cells after HDI treatment (New*, et al* 2016).

The aim of the experiments presented above was to establish the importance of these effects in relevant DLBCL cell lines: both ABC cell lines, RIVA and HBL-1, displayed sensitivity to treatment with the pan-HDAC inhibitor SAHA. HBL-1 cells, which carry a heterozygous MyD88 L265P mutation, were shown to be more sensitive to apoptosis. Although manipulating MyD88 in these suspension cells proved to be technically very challenging, chemical inhibition of MyD88 with T6167932, a small-molecule inhibitor of MyD88 aggregation, could be shown to negatively affect HDI sensitivity in RIVA cells.

At a tissue level, MyD88 protein could be seen to be highly expressed in haematopoietic tissue, and in particular in lymphoid malignancies, whereas MyD88 expression in other tumour types, such as colorectal and prostate cancer appeared to be low. Although no general conclusions with regards to patient treatment and outcome could be drawn from the analysis of these limited samples, taken together with the results from the cell-based studies, the level of MyD88 and its mutation status may play an important role in mediating the response of lymphoid malignancies to HDI- based therapies.

As a next step, in order to investigate some of the differences that might underlie the differential sensitivity to HDAC inhibition that was observed in the two ABC DLBCL cell lines, the role of the NF-kB pathway in mediating pro-inflammatory cytokine secretion was examined.

CHAPTER 4. CYTOKINE EXPRESSION IN LYMPHOMA CELL LINES AND EFFECT OF CYTOKINE SIGNALLING PATHWAYS ON HDI SENSITIVITY

4.1 Introduction

Toll-like receptors (TLRs) are pattern recognition receptors that identify highly preserved pathogen associated molecular patterns (PAMPs) during the early phase of the immune response (Takeda and Akira 2004, Wang*, et al* 2014). TLR expression has been shown to be driven in part by the exposure of cells to pathogens, the extracellular cytokine milieu and various environmental factors (Akira*, et al* 2006).

As outlined in Chapter 1 (Section 1.5.2) TLRs are capable of recognizing a vast number of different pathogens, but their downstream signalling pathways are strikingly similar and are activated through highly conserved intracytoplasmic TIR domains. Downstream events of TLR-mediated signalling result in the expression of genes that are necessary for mediating the evolving immune response, and usually lead to the release of pro-inflammatory cytokines and the maturation of antigen-presenting cells (Lee and Iwasaki 2007, Lu*, et al* 2008).

The sequence similarity of *MyD88* with the intracytoplasmic TIR domains of the IL-1 and TLR-receptors was recognized in Drosophila (Hultmark 1994). This finding suggested its role as a signal transducer and central player in immune signalling through these pathways (Akira*, et al* 2006, Wang*, et al* 2014) (Chapter 1, Section 1.5.2).

Activation of the MyD88-dependent pathway upon TLR stimulation leads to the expression of pro-inflammatory cytokines such as IL-6, which has been shown to promote the growth and survival of tumour cells. For example, in a murine hepatocellular cancer cell model, MyD88 was shown to be necessary for IL-6 production, and the reduction of circulating IL-6 levels led to relative protection from hepatocarcinogenesis (Naugler*, et al* 2007). Moreover, high levels of IL-6 in patients with endometrial cancer have been linked to poor prognostic outcome (Bellone*, et al* 2005). Dysregulation of STAT3 signalling has also been implicated in IL-6-mediated tumour progression (Chang*, et al* 2014, Grivennikov and Karin 2011, Libermann and

Baltimore 1990). For example, inappropriate activation of the TLR pathway through the MyD88 L265P mutation has been shown to result in constitutive NF-κB signalling, leading to increased JAK-STAT3 activity and pro-inflammatory cytokine production (Ngo*, et al* 2011).

For the next part of my thesis, therefore, I set out to investigate the levels of pro-inflammatory cytokine production in RIVA and HBL-1 cells, and how the respective cytokine expression profiles and signalling pathways may impact on response to SAHA treatment in these cells.

4.2 Cytokine expression profiles of RIVA and HBL-1 cell lines

MyD88-dependent TLR signalling leads to the activation of NF-κB -dependent transcription of cytokine genes (Takeda and Akira 2004, Wang*, et al* 2014). In a mouse model of toxic shock syndrome, mouse spleen cells treated with Staphylococcal enterotoxin B (SEB) were shown to produce increased levels of the pro-inflammatory cytokines TNF-α, IFN-γ, IL-1α/β, and IL-6, a process which was regulated by MyD88: elevated levels of MyD88 protein were observed in spleen cells of mice treated with SEB, whereas abrogation of MyD88 signalling in the spleen cells of MyD88$^{-/-}$mice resulted in the impaired release of pro-inflammatory cytokines (Kissner*, et al* 2011b). Similarly, previous work carried out in Professor La Thangue's research group was able to show that the expression of ectopic MyD88 in U2OS cells leads to the activation of NF-κB, and results in a significant increase in the levels of IL-6 and IL-8 (New*, et al* 2016). Moreover, ABC DLBCL has been described to be driven in part by constitutive MyD88 signalling and NF-κB activation (Ngo*, et al* 2011). In order to investigate some of the differences that might underlie the differential sensitivity to HDAC inhibition that was observed in the two ABC DLBCL cell lines RIVA and HBL-1 as described in Chapter 3, the cytokine profiles of these cells were studied.

Using the BD™ Cytometric Bead Array (CBA; Chapter 2, Section 2.10), the levels of six pro-inflammatory human cytokines, IL-12p, TNF-α, IL-10, IL-6, IL-1β and IL-8 were measured in the supernatant of four lymphoid cell lines (Figure 4.1a). The fluorescent signal that is generated by the reaction of the capture bead and its respective analyte in the CBA is measured by flow cytometry, and is proportional to the amount of bound cytokine. The relative levels of cytokines compared to baseline levels (in cell culture medium, set at 1) were plotted.

Comparison of cytokine expression in untreated cells showed that RIVA cells secreted more TNF-α than the other cell lines, whereas supernatant from HBL-1 cells had elevated levels of both IL-10 and IL-6. The ABC DLBCL cell line RCK8 was shown to release relatively more IL-6, and the GCB DLBCL cell line Mieu had cytokine levels that were close to baseline, at the time

point examined (24 hours after plating cells). The cytokine profiles of RIVA, RCK8 and Mieu cells have, to the best of my knowledge and at the time of writing (May 2017), not been published in the literature.

Previous research in ABC DLBCL has shown that the HBL-1 cell line secretes high levels of IL-6 and IL-10 which could be significantly diminished by MyD88 knockdown (Ngo*, et al* 2011). Interestingly, in this context, the ability of wild-type and mutant MyD88 isoforms to activate NF-κB was investigated by expressing these as GFP-tagged fusion proteins in GCB cell lines. Whereas wild-type MyD88 could only cause modest activation of an NF-κB -dependent reporter, L265P had strong activity (Ngo*, et al* 2011). Cytokine release was not measured in this experiment but the implication is that the presence of the MyD88 L265P mutation may lead to higher levels of IL-6 and IL-10 in ABC DLBCL cell lines.

The relative cytokine levels in the supernatant of RIVA and HBL-1 cells were investigated in more detail before and after treatment with SAHA (Figures 4.1b and c). In a comparison between untreated RIVA and HBL-1 cells, RIVA cells can be seen to express significantly higher amounts of TNF-α, whereas HBL-1 cells produce significantly more IL-10 and IL-6 (Figure 4.1b (i)-(iii)). The differences in IL12p, IL-1β and IL-8 levels were found to be not significant (Figure 4.1b(iv)-(vi)) so these were not pursued further in the investigation.

Furthermore, when RIVA and HBL-1 cells were treated with either DMSO (as the control/"mock") or SAHA, TNF-α levels could be shown to reduce to 61% compared to baseline in RIVA cells (vs 75% in HBL-1 cells), and IL-6 levels decreased to 54.9% in HBL-1 cells (but did not change significantly in RIVA cells). Levels of IL-1β dropped to 68.4% in HBL-1 cells (versus no significant change in RIVA cells), but the differences measured between pre-and post-treatment levels for the other three cytokines (IL-10, IL-12p and IL-8) were not statistically significant (Figure 4.1c). These results are consistent with the published literature (Dinarello 2010); for example, in a mouse model, high levels of circulating IL-6 and TNF-α after LPS-

stimulation were reduced following the administration of a single dose of SAHA. By contrast, SAHA did not affect LPS-induced synthesis of the IL-1β precursor, or IL-8 (Leoni*, et al* 2002). The differences in IL-1β were not further investigated in the experiments presented below.

Of note, using DMSO as a mock control for treatment did not seem to influence the level of pro-inflammatory cytokine secretion, and the differences observed between cell lines were consistent, whether DMSO was used, or whether cells were grown in untreated (i.e. no DMSO added) medium only. This is important, as DMSO has previously been reported to reduce the levels of pro-inflammatory cytokines, including IL-6, IL-10 and TNF-α in human monocytes (Elisia*, et al* 2016). These effects were dependent on the amount of DMSO added to cultures, with a DMSO concentration of 0.5% having a suppressive effect on cytokine release, whereas a DMSO concentration of 2% could almost completely abrogate cytokine production and affected cell viability in vitro (Elisia*, et al* 2016). By contrast, the concentration of DMSO used in the experiments investigating cytokine release that are described here, was 0.05%.

Figure 4.1

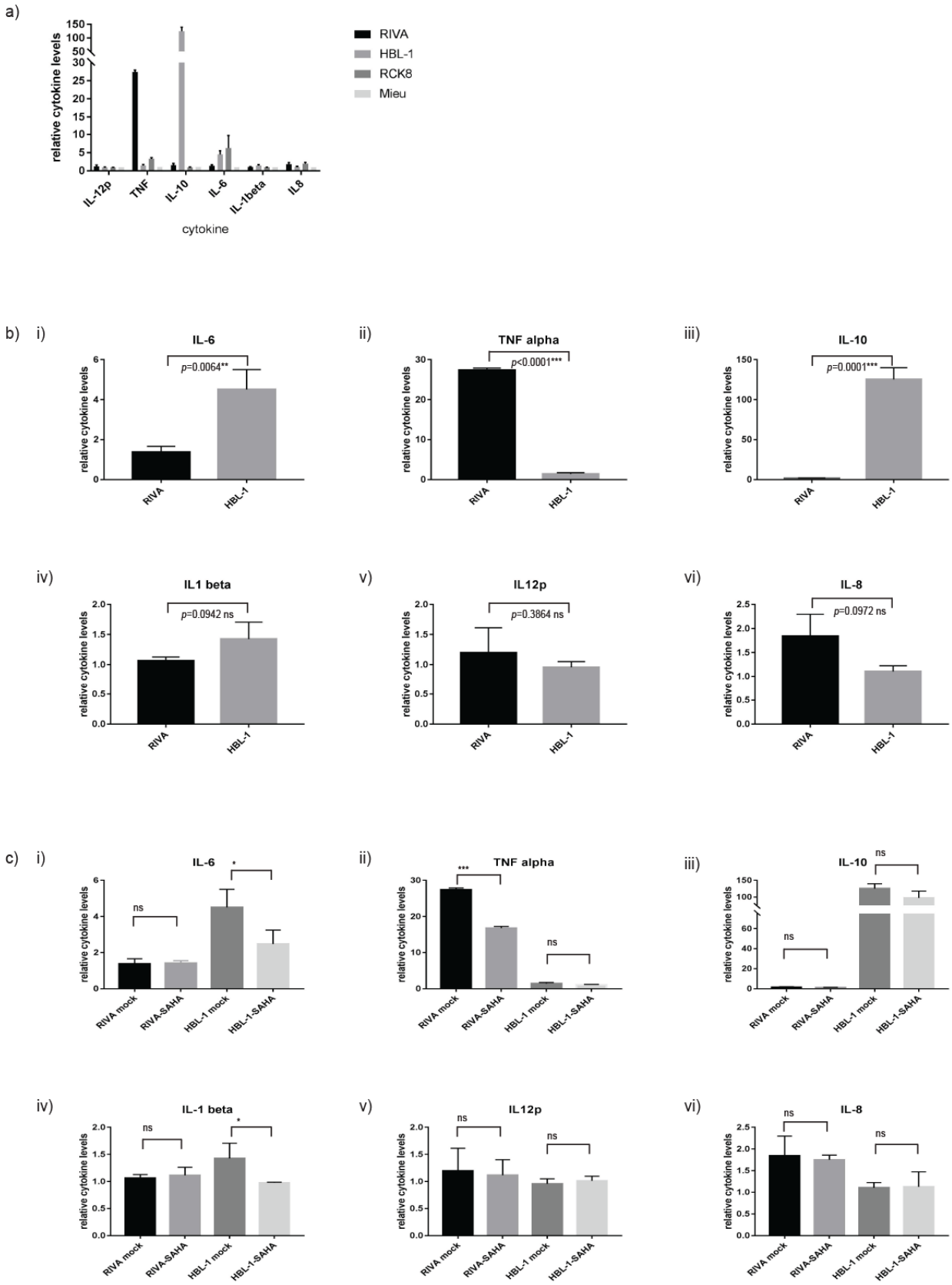

a)
relative cytokine levels
150
100
50
30
25
20
15
10
5
0
IL-12p
TNF
IL-10
IL-6
IL-1beta
IL8
cytokine
RIVA
HBL-1
RCK8
Mieu
b) i)
IL-6
p=0.0064**
ii)
TNF alpha
p<0.0001***
iii)
IL-10
p=0.0001***
iv)
IL1 beta
p=0.0942 ns
v)
IL12p
p=0.3864 ns
vi)
IL-8
p=0.0972 ns
c) i)
IL-6
ns
*
ii)
TNF alpha
***
ns
iii)
IL-10
ns
ns
iv)
IL-1 beta
ns
*
v)
IL12p
ns
ns
vi)
IL-8
ns
ns
RIVA mock
RIVA-SAHA
HBL-1 mock
HBL-1-SAHA

Figure 4.1 Pro-inflammatory cytokine expression in lymphoma cell lines.

a. Baseline levels of six human pro-inflammatory cytokines, IL-12p, TNF-α, IL-10, IL-6, IL-1β, and IL-8, present in the cell supernatant of four different lymphoma cell lines, RIVA, HBL-1, RCK8 and Mieu are shown. Cell-free RPMI culture medium served as the negative control; cytokine levels are expressed relative to the negative control (set at 1). Cells were not drug-or DMSO-treated for this experiment. The values represented are the mean from three biological replicates.

b. (i-vi) Breakdown of individual cytokine levels of the six human pro-inflammatory cytokines, IL-12p, TNF-α, IL-10, IL-6, IL-1β, and IL-8, as described above, expressed by untreated RIVA and HBL-1 cells in cell culture supernatant are shown. For this experiment, equal numbers of cells were plated and grown in RPMI medium for 24 hours before harvesting the cell supernatant and analyzing cytokine levels. RPMI medium served as the negative control; cytokine levels are expressed relative to the negative control (set at 1). The experiment was performed in triplicate. **, *** denote significant *p* values; ns, non-significant *p* values.

c. (i-vi) Individual cytokine levels in the cell supernatant of RIVA and HBL-1 cells after mock (DMSO)- or SAHA (5μM) -treatment for 24 hours. RPMI medium was the negative control, as above. Values are representative of *n*=3 biological replicates. *, *** denote significant *p* values; ns, non-significant *p* values. The table below summarizes *p* values for differences in cytokine levels between mock-treated and SAHA-treated cells for each cell line, as follows:

Cytokine	**RIVA (treated versus mock-treated)**	**HBL-1 (treated versus mock-treated)**
IL-12p	*p*=0.8005	*p*=0.4833
TNF-α	*p*<0.0001***	*p*=0.1491
IL-10	*p*=0.5593	*p*=0.1239
IL-6	*p*=0.8234	*p*=0.0498*
IL-1β	*p*=0.6092	*p*=0.0496*
IL-8	*p*=0.7484	*p*=0.9259

IL-10 has been recognized as a cytokine with pleiotropic effects in inflammation and immuno-regulation (Saraiva and O'Garra 2010). Although initially it was thought that IL-10 had mainly immunosuppressive effects via inhibition of Th1-type cytokines including TNF-α, IL-12, IL-1β and IFN-γ, downregulation of MHC class II, and antigen presentation, it has also emerged that in B cells IL-10 is involved in cell proliferation and differentiation (de Waal Malefyt*, et al* 1991, Fiorentino*, et al* 1991). Cell lines generated from non-Hodgkin lymphoma patients, for example, have been shown to express high levels of IL-10 which is thought to serve as an autocrine growth factor (Cortes and Kurzrock 1997, Rousset*, et al* 1992). More recently, IL-10 and IL-10 polymorphisms have been implicated in skewing the Th1/Th2 immune response and the risk of lymphoma although the mechanism for this is not exactly clear (Kim et al G&I).

TNF-α is a central player in mediating inflammatory responses and has a well-defined role in activating multiple pathways important for inflammation, including signalling through NF-κB (Wajant*, et al* 2003). Consequent upregulation of pro-inflammatory cytokines and anti-apoptotic molecules is thought to contribute to lymphomagenesis, and elevated levels of circulating TNF-α in patients with non-Hodgkin lymphoma have been associated with poor treatment outcome (Lech-Maranda*, et al* 2010, Salles*, et al* 1996).

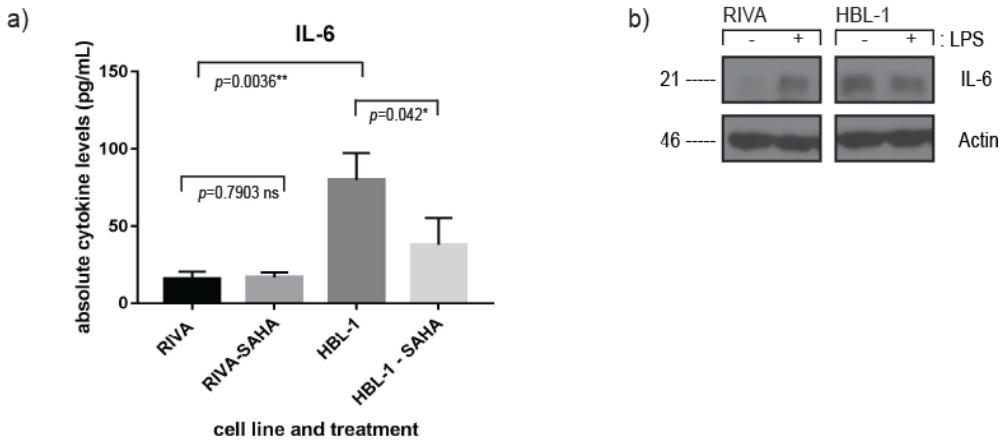
Although it is clear from the above that IL-10 and TNF-α are important contributors to the pathogenesis of lymphoma, my subsequent line of investigation focused on the role of IL-6 in mediating susceptibility of lymphoma cells to HDI treatment. This was based on previous work carried out in Professor La Thangue's laboratory (by Maria New) which showed that over-expression of MyD88 or the MyD88 L265P mutant in the osteosarcoma cell line U2OS led to an increase in the extra-cellular level of IL-6, but did not affect the levels of either TNF-α or IL-10 (New*, et al* 2016).

Therefore, the absolute concentration of IL-6 in the cell supernatant of HDI-treated and mock-treated RIVA and HBL-1 cells was determined (Figure 4.2a) by using a standard curve of known

cytokine concentrations (Chapter 2, Section 2.10). The differences in IL-6 levels between RIVA and HBL-1 cells remained significant, and IL-6 levels reduced, as before, after SAHA treatment. Levels of IL-6 were also shown to be higher and present at baseline in mock-treated HBL-1 cells on immunoblot; in RIVA cells IL-6 levels were very low at baseline but increased following treatment with LPS (Figure 4.2b; and see also Section 4.4 below). Finally, IL-6 mRNA levels were measured in untreated RIVA and HBL-1 cells and could be shown to be approximately ten-fold increased in HBL-1 cells relative to RIVA cells (Appendix B(a), p 203).

Having established differences in IL-6 expression between RIVA and HBL-1 cells, the next step was to test whether extracellular IL-6 levels could impact on the outcome of HDI treatment.

Figure 4.2



IL-6 levels in RIVA and HBL-1 cells.

a. Absolute cytokine levels in the tissue culture medium of mock (DMSO)- and SAHA-treated RIVA and HBL-1 cells were determined from a standard curve (Chapter 2, Section 2.10). *, ** denote significant *p* values; ns, non-significant. The experiment was performed in triplicate. The mean absolute cytokine levels are shown in the table below.

IL-6 (pg/mL)	**RIVA supernatant**	**HBL-1 supernatant**
mock-treated	13.1 (13.0-21.3)	79.9 (59.9-91.8)
SAHA-treated	16.8 (13.2-19.7)	37.98 (19.0-53.0)

b. RIVA and HBL-1 cells were harvested after 24 hours, either having been mock-treated (-), or after having been treated with LPS (100ng/mL,+) for 24 hours in order to stimulate the TLR pathway. Lysates were immunoblotted with anti-MyD88 and anti-IL-6 antibody; actin was used as the loading control. All lysates were run on the same gel and the same exposures for RIVA and HBL-1 blots are shown.

4.3 Effect of IL-6 inhibition on HDI sensitivity

In order to address whether the increased levels of extracellular IL-6 influence the sensitivity of lymphoma cells to HDAC inhibition, I obtained an IL-6-neutralizing antibody that has previously been shown in the literature (Hubackova*, et al* 2012) and by Professor La Thangue's group (New*, et al* 2016) to effectively neutralize IL-6 in cell culture.

Pre-incubation with the IL-6 neutralizing antibody prior to SAHA treatment reduced the level of cells in sub-G1 phase in the HBL-1 cells on FACS analysis compared with SAHA treatment on its own (Figure 4.3a(i)). HBL-1 cells were also shown to display reduced markers of apoptosis (cleaved PARP and cleaved caspase 3) on immunoblot after co-treatment with anti-IL-6 antibody and SAHA compared to RIVA cells (Figure 4.3a(ii)). These results suggest that IL-6 may be an important effector in mediating cell sensitivity to HDAC inhibition. The reduced effect of anti-IL-6 in RIVA cells compared to HBL-1 cells most likely reflects the lower levels of IL-6 secreted by RIVA compared to HBL1 cells (Figure 4.1).

As a comparison, IL-6 neutralization was carried out in other lymphoid cell lines: U2932 (Figure 4.3b(i)) and RCK8 (Figure 4.3c(i)) are both ABC DLBCL cell lines, whilst SUDHL4 (Figure 4.3d) represents a GCB DLBCL cell line. Both U2932 and SUDHL4 cells have been described in the literature as having very low levels of baseline IL-6 secretion compared to HBL-1 (Hailfinger*, et al* 2009, Nagel*, et al* 2012). No decrease in sub-G1 was observed in either cell line following SAHA treatment after IL-6 neutralization. The RCK8 cell line showed high levels of extracellular IL-6 (Figure 4.1a) but carries no MyD88 mutation (Chapter 2, Section 2.2) and represents a transformed ABC DLBCL cell line. Treatment of RCK8 cells with the anti-IL-6 antibody and, subsequently SAHA, did not lead to a decrease in sub-G1 percentage on FACS analysis, possibly reflecting a difference in disease biology and pathways important for SAHA-induced apoptosis between ABC DLBCL subtypes (Figure 4.3c(i)).

As can be seen from the cell cycle phases of the different (non-synchronized) cell lines as analyzed by FACS (Figure 4.3a(iii) and (iv), 4.3b(ii), 4.3c(ii) and 4.3d(ii)), no clear effect of anti-IL-6 could be observed other than relevant changes in sub-G1 as outlined above.

In order to assess whether neutralization of IL-6 had indeed taken place after treating cells with the neutralizing anti-IL-6 antibody, cytokine release was measured when cells were harvested 24 hours after mock or anti-IL-6 treatment. A reduction in extracellular IL-6 levels could be observed in RIVA, HBL-1 and RCK8 cells (Figure 4.3e). A useful confirmatory experiment in this context that may have permitted linking MyD88 mutation status to IL-6 secretion in the different cell lines would have been to knock down MyD88 in the respective DLBCL subtypes and measure the production of pro-inflammatory cytokines, IL-6 in particular, pre- and post-knockdown. Due to the difficulties with transfection of non-adherent cells described in Chapter 3 (Section 3.5), however, this was not possible.

It is also important to note that IL-6 receptor (IL-6 R) expression has been described in Burkitt lymphoma and lymphoblastoid cell lines (Klein et al, 1995), but, to the best of my knowledge, previous publications on RIVA and HBL-1 cells have not specifically investigated IL-6 R cell surface or mRNA expression. IL-6 R mRNA levels could be seen to be increased in HBL-1 cells compared to RIVA cells, and following LPS stimulation, IL-6 R levels could be seen to increase substantially in RIVA cells (but not HBL-1 cells) (Appendix B(b), p 203). Cell surface expression of the IL-6 R by FACS was, however, not assessed in these experiments. It is therefore only assumed that both cell lines express the IL-6 R on their cell surface, which would allow cells to react to changes in IL-6 levels in the cellular microenvironment.

The MyD88 inhibitor T6167932 (Chapter 3, Section 3.6) was previously shown to suppress the production of the pro-inflammatory cytokines, IL-6, TNF-α, IL-1β and IFN-γ (IL-10 not measured), by human peripheral blood mononuclear cells in primary culture (Olson*, et al* 2015). In HBL-1 lymphoma cells, the administration of T6167932 led to a small decrease of IL-6

and IL-10 (Figure 4.3f(ii)), and the effect of MyD88 inhibition with T6167932 on SAHA-treated HBL-1 cells was previously not found to be remarkable with respect to the degree of apoptosis (Chapter 3, Figure 3.6c). This finding may have several explanations, including the choice of time point for sampling (in this case, 2 hours after adding T6167932), the concentration of T6167932, or the ability of T6167932 to target the mutated isoform of the MyD88 protein.

Using other DLBCL cell lines that are known to express the MyD88 L265P mutation and measuring cytokine release in these (in particular levels of IL-6 and IL-10) would have complemented the results presented here. In the published literature, ABC DLBCL cell lines other than HBL-1 which also carry a heterozygous MyD88 L265P mutation are TMD8 (Mondello*, et al* 2017, Ngo*, et al* 2011) and Oci-Ly10 (Lam*, et al* 2008); one ABC DLBCL cell line, Oci-Ly3, has been reported to be homozygous for the MyD88 L265P mutation (Ngo*, et al* 2011). All of these four cell lines have been demonstrated to have raised extra-cellular levels of IL-6, but at the time of writing (May 2017), no experiments testing IL-6 neutralization and SAHA treatment have been performed with these cells. Interestingly, however, inhibition of downstream MyD88 signalling by targeting IRAK4 has been shown to decrease IL-6 levels in TMD8 cells, and shRNA knockdown of MyD88 in HBL-1 cells also led to reduced extracellular IL-6, implicating the importance of an intact MyD88 pathway in mediating IL-6 release (Ngo*, et al* 2011).

Finally, being able to neutralize IL-10 both separately, and then co-neutralizing it together with IL-6, before SAHA treatment, would have given additional information on the contribution of IL-10 to SAHA sensitivity of lymphoma cells. For example, MyD88 knockdown in HBL-1 cells was also shown to reduce levels of IL-10 (Ngo*, et al* 2011). However, in the original transfection experiments carried out in Professor La Thangue's research group (New*, et al* 2016), IL-10 was not found to be significantly elevated, either after MyD88 expression was induced in U2OS cells, or after transfection of U2OS cells with wild-type Myd88 or the L265P Myd88 mutant; therefore the role of IL-10 was not further investigated in this context.

The next question that I wanted to address was whether the presence of a pro-inflammatory cytokine milieu in itself, regardless of MyD88 mutation status, can sensitize lymphoma cells to HDI-induced apoptosis, and whether this could be achieved through the stimulation of increased endogenous cytokine production by exposing cells to LPS, or the addition of exogenous, i.e. recombinant, IL-6.

Figure 4.3

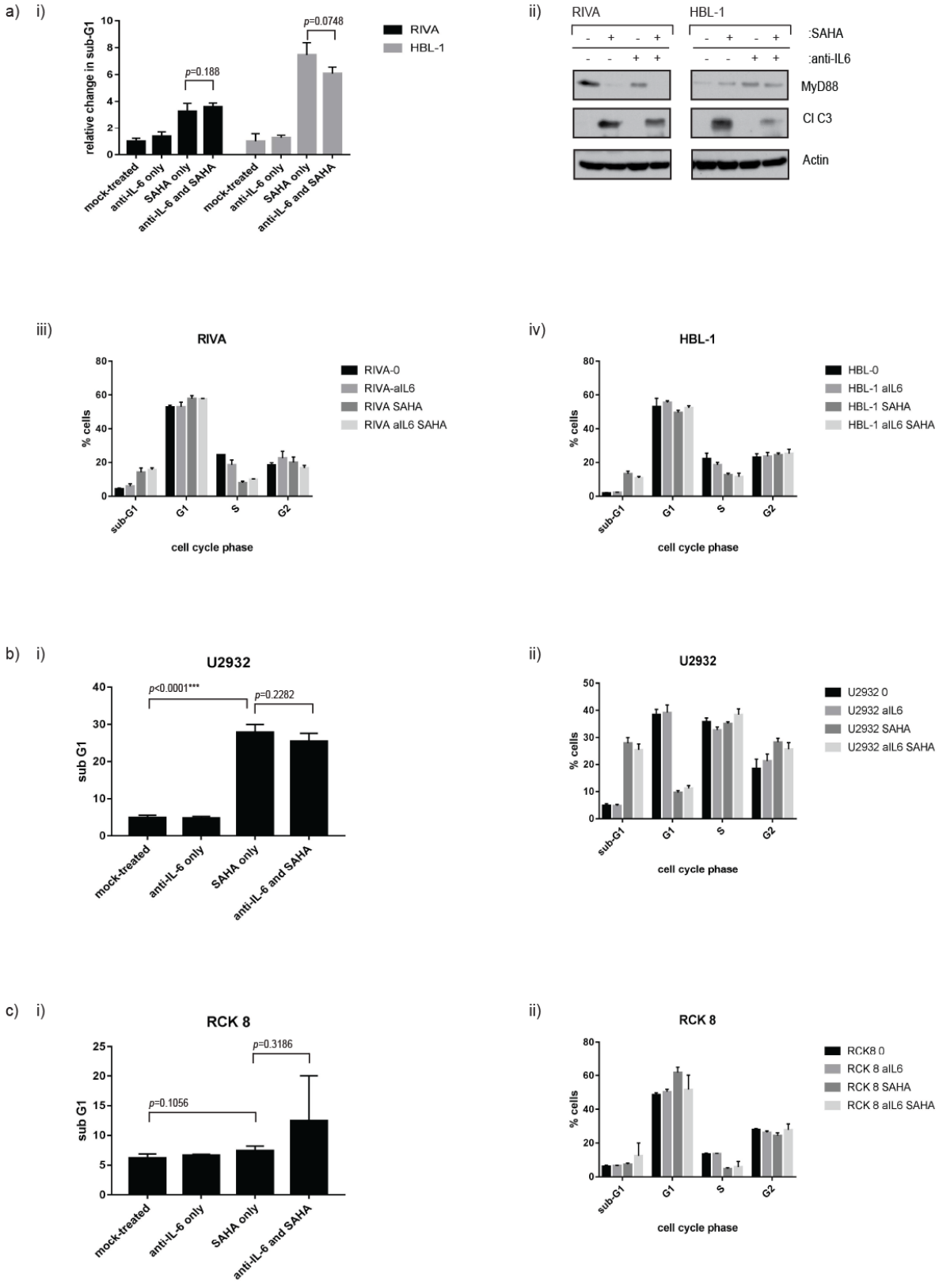

a) i)
relative change in sub-G1
p=0.188
p=0.0748
RIVA
HBL-1
mock-treated
anti-IL-6 only
SAHA only
anti-IL-6 and SAHA
ii)
RIVA
HBL-1
:SAHA
:anti-IL6
MyD88
Cl C3
Actin
iii)
RIVA
% cells
RIVA-0
RIVA-aIL6
RIVA SAHA
RIVA aIL6 SAHA
sub-G1
G1
S
G2
cell cycle phase
iv)
HBL-1
HBL-0
HBL-1 aIL6
HBL-1 SAHA
HBL-1 aIL6 SAHA
b) i)
U2932
sub G1
p<0.0001***
p=0.2282
ii)
U2932
U2932 0
U2932 aIL6
U2932 SAHA
U2932 aIL6 SAHA
c) i)
RCK 8
p=0.3186
p=0.1056
ii)
RCK 8
RCK8 0
RCK 8 aIL6
RCK 8 SAHA
RCK 8 aIL6 SAHA

Figure 4.3 continued

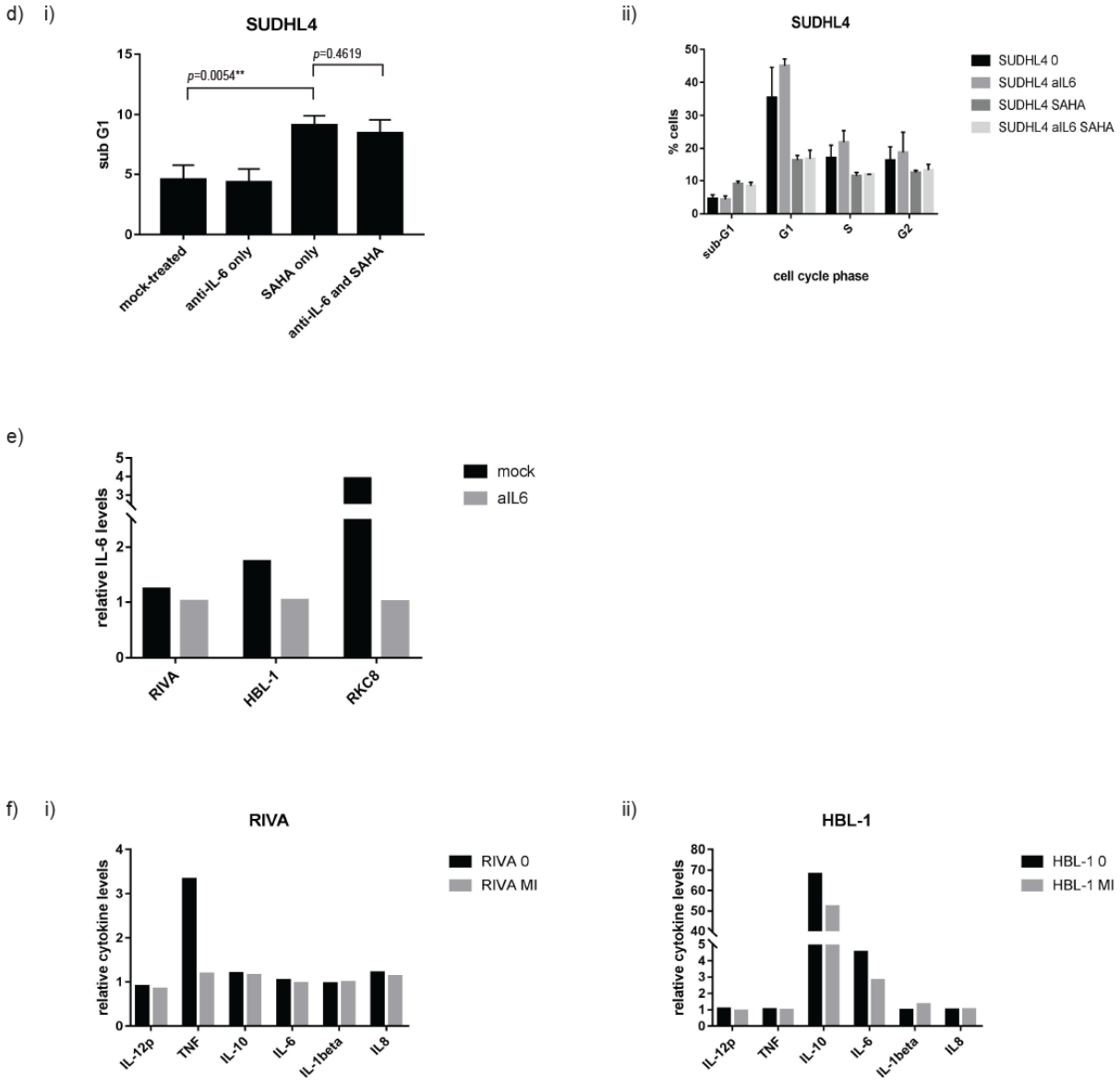


Figure 4.3 Effect of IL-6 neutralization on HDI sensitivity of lymphoma cells.

a. (i) RIVA and HBL-1 cells, in triplicate, were either treated with DMSO (mock), or an IL-6 neutralizing antibody (aIL-6), and/or SAHA (5μM) for 24 hours, harvested and the sub-G1 fraction was analyzed by PI staining and flow cytometry. Relative levels of cells in sub-G1 are shown. *p* values are indicated.

(ii) RIVA and HBL-1 cells were treated as above (i), and cell lysates were immunoblotted with anti-MyD88 and anti-cleaved caspase 3 antibodies; actin served as the loading control.

(iii) and (iv) RIVA and HBL-1cells, in triplicate, were treated as above (i), and cell cycle phases were analyzed by PI staining and flow cytometry.

b. (i) U2932 cells, in triplicate, were either treated with DMSO (mock), or an IL-6 neutralizing antibody (aIL-6), and/or SAHA (5μM) for 24 hours, harvested and the sub-G1 fraction was analyzed by PI staining and flow cytometry. Relative levels of cells in sub-G1 are shown. *p* values are indicated. ***denotes significance.

(ii) U2932 cells, in triplicate, were treated as above (i), and cell cycle phases were analyzed by PI staining and flow cytometry.

c. (i) RCK8 cells, in triplicate, were either treated with DMSO (mock), or an IL-6 neutralizing antibody (aIL-6), and/or SAHA (5μM) for 24 hours, harvested and the sub-G1 fraction was analyzed by PI staining and flow cytometry. Relative levels of cells in sub-G1 are shown. *p* values are indicated.

(ii) RCK8 cells, in triplicate, were treated as above (i), and cell cycle phases were analyzed by PI staining and flow cytometry.

d. (i) SUDHL4 cells, in triplicate, were either treated with DMSO (mock), or an IL-6 neutralizing antibody (aIL-6), and/or SAHA (5μM) for 24 hours, harvested and the sub-G1 fraction was analyzed by PI staining and flow cytometry. Relative levels of cells in sub-G1 are shown. *p* values are indicated. **denotes significance.

(ii) SUDHL4 cells, in triplicate, were treated as above (i), and cell cycle phases were analyzed by PI staining and flow cytometry.

e. RIVA, HBL-1 and RCK8 cells were either DMSO (mock)-treated or treated with a neutralizing anti-IL-6 antibody for 24 hours. Cell supernatants were harvested and IL-6 cytokine levels were measured. Relative cytokine levels are shown. The experiment is representative of *n*=2 biological replicates.

f. RIVA (i) and HBL-1 (ii) cells were treated with the small molecule MyD88 inhibitor T6167932 (100μM) for 24 hours. Cell supernatants were analyzed for the levels of the six pro-inflammatory cytokines, IL-12p, TNF-α, IL-10, IL-6, IL-1β, and IL-8. The experiment is representative of *n*=2 biological replicates.

4.4 Effect of LPS and recombinant IL-6 on lymphoid cell lines and HDI sensitivity

In order to characterize the impact of IL-6 on SAHA-induced apoptosis in lymphoma cells further, I attempted to augment extracellular levels of pro-inflammatory cytokines by stimulating cells with LPS. TLR4 is recognized as the main signalling receptor for LPS, and the formation of a TLR4-LPS receptor complex leads to downstream MyD88-dependent signalling and NF-κB activation (Palsson-McDermott and O'Neill 2004, Wang*, et al* 2014).

When LPS was added to the culture medium of RIVA and HBL-1 cells for 2 hours before SAHA treatment, an increase in apoptosis markers was observed in both cell lines (Figure 4.4a and b (i)); a dose-dependent increase could be shown in HBL-1 cells (Figure 4.4b(ii)). On FACS analysis, an increase in the percentage of cells in sub-G1 could also be demonstrated in RIVA and HBL-1 cells after 24 hours of treatment with SAHA and LPS.

When the levels of pro-inflammatory cytokines after 2 hours of LPS stimulation were assessed in the cell supernatants, RIVA cells were found to have significantly increased levels of TNF-α (Figure 4.4c(i)), whereas HBL-1 cells displayed a modest increase in IL-6 levels and also an increase in IL-6 mRNA (Figure 4.4c(ii)). These findings suggest that the increase in LPS-mediated HDI sensitivity is likely driven by IL-6 in HBL-1 cells but that this may not entirely be the case in RIVA cells. Of note, when RIVA cells were treated with LPS for 24 hours, an increase in IL-6 could be shown on immunoblot (Figure 4.2b).

Pre-formed cytokines may be released as quickly as within 30 minutes of LPS exposure, whereas mRNA levels and subsequent secretion of newly synthesized cytokines may take between 3-18 hours to become detectable (Kranzer*, et al* 2004). Therefore, the time point at which the cytokine release assay took place in the above experiments may have missed an early peak in IL-6 secretion, or it was performed too early (before more IL-6 was synthesized in the cell); moreover, no time course was carried out to assess the kinetics of cytokine secretion following induction with LPS. However, the IL-6 mRNA result in HBL-1 cells suggests that more

IL-6 is indeed produced on LPS stimulation. Measuring the mRNA levels of all the implicated pro-inflammatory cytokines after LPS stimulation may have been useful in this context in order to correlate these with the levels found in the cell supernatants to give a more complete picture.

LPS and TLR4 stimulation in these experiments were chosen because TLRs have been shown to play a central role in controlling the secretion of different subsets of cytokines that are produced by activated B cells during an immune response. Thus, in B cells isolated from mice, LPS was shown to upregulate the level of IL-6, whereas levels of IL-10 and IFN-γ did not increase significantly. By contrast, a combination of TLR agonists that stimulated cells through TLR2 and TLR9 (which also signal through MyD88), as well as TLR4, showed much larger increases in IL-10 and IFN-γ (Barr*, et al* 2007). Similarly, the dose of the activating stimulus can significantly influence the cytokines that are secreted: in one study, for instance, B cells co-cultured with LPS doses ranging from 0.1ng/mL to 10µg/mL showed dose-dependent increases in IL-10 but no consistent increases in TNF-α or IL-6 production (Xu*, et al* 2008).

In summary, the addition of LPS to lymphoma cells increased HDI-mediated apoptosis but the pathways involved in this response may be diverse and dose-dependent. One additional interesting observation is that on immunoblotting, Myd88 protein levels could often be seen to increase on LPS exposure in RIVA and HBL-1 cells (Figure 4. 4a and b(i)), and in RIVA cells a 3.5-fold increase in MyD88 transcript levels in LPS-treated cells was shown (Figure 4.4d). This is consistent with the published literature, where LPS stimulation of B cells has previously been shown to lead to an increase in MyD88 mRNA levels (Barr*, et al* 2007). The relative decrease in MyD88 transcript levels in HBL-1 cells, on the other hand, is counter-intuitive and difficult to explain. It is possible that due to the constitutive activation of the MyD88 pathway on account of the presence of the L265P isoform, the process of signalling through TLR4 induced by LPS is different than in MyD88 wild-type cells and therefore may lead to differences in MyD88 transcription.

In order to assess whether IL-6 may directly impact SAHA-mediated apoptosis in lymphoma cells, exogenous (recombinant) IL-6 was added to RIVA and HBL-1 cells in culture for 3 hours prior to treating cells with SAHA. RIVA cells were sensitized to HDI treatment in this way, as shown by increased levels of cleaved PARP (Figure 4.4e); a similar effect was not observed in HBL-1 cells, quite possibly due to the fact that HBL-1 cells already secrete higher levels of IL-6. Therefore, it is plausible that IL-6 may act in an autocrine or paracrine manner, sensitizing lymphoma cells to HDI treatment. FACS analysis of cell cycle phases during treatment with recombinant IL-6 would have been a useful follow-on experiment in order to examine how cell cycle progression in lymphoma cells is affected by the addition of exogenous IL-6. Previous experiments where MyD88 was over-expressed in U2OS cells have suggested that IL-6 neutralization leads to an increased proportion of cells stalled in G2 phase (New*, et al* 2016). Conversely, this could mean that the presence of increased levels of IL-6 cells may allow for a more rapid cell cycle progression which could make cells more vulnerable to treatment with an HDI such as SAHA.

Figure 4.4

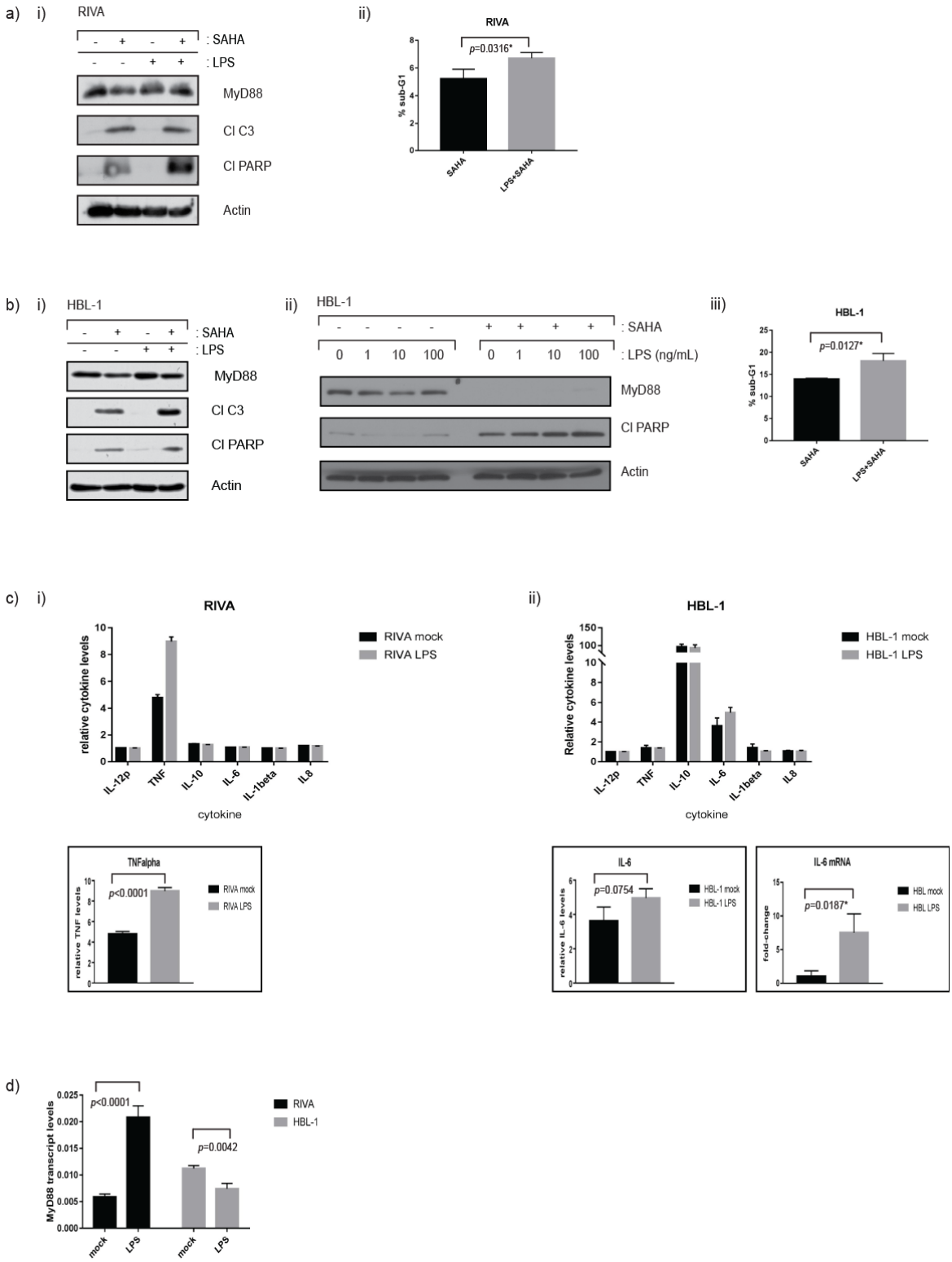
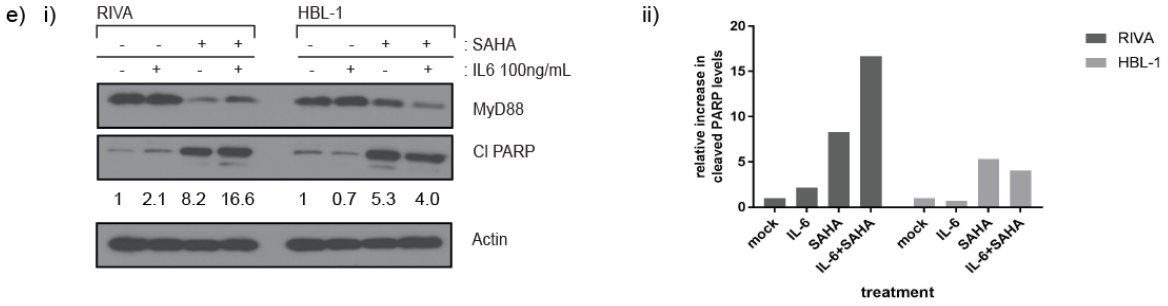

a) i)
RIVA
: SAHA
: LPS
MyD88
Cl C3
Cl PARP
Actin
ii)
RIVA
p=0.0316*
% sub-G1
SAHA
LPS+SAHA
b) i)
HBL-1
: SAHA
: LPS
MyD88
Cl C3
Cl PARP
Actin
ii)
HBL-1
: SAHA
0 1 10 100 0 1 10 100
: LPS (ng/mL)
MyD88
Cl PARP
Actin
iii)
HBL-1
p=0.0127*
% sub-G1
SAHA
LPS+SAHA
c) i)
RIVA
RIVA mock
RIVA LPS
relative cytokine levels
IL-12p
TNF
IL-10
IL-6
IL-1beta
IL8
cytokine
TNFalpha
p<0.0001
relative TNF levels
RIVA mock
RIVA LPS
ii)
HBL-1
HBL-1 mock
HBL-1 LPS
Relative cytokine levels
cytokine
IL-6
p=0.0754
relative IL-6 levels
HBL-1 mock
HBL-1 LPS
IL-6 mRNA
p=0.0187*
fold-change
HBL mock
HBL LPS
d)
p<0.0001
p=0.0042
MyD88 transcript levels
RIVA
HBL-1
mock
LPS
mock
LPS

Figure 4.4 continued



Influence of lipopolysaccharide (LPS) or recombinant IL-6 on HDI sensitivity and cytokine expression in RIVA and HBL-1 cells.

a. (i) RIVA cells were treated with either DMSO (mock; -), SAHA (5μM; +), LPS (100ng/mL; +), or LPS (100ng/mL) for 3 hours, followed by SAHA treatment (LPS+SAHA; +/+). After harvesting, lysates were immunoblotted with anti-MyD88, anti-cleaved caspase 3 and anti-cleaved PARP antibody; actin served as the loading control.

(ii) RIVA cells, in triplicate, were treated with SAHA (5μM), or co-treated with LPS (100ng/mL) and SAHA (5μM). Cells were harvested after 24 hours and analyzed for sub-G1 by flow cytometry. *p* values are indicated. * denotes significance. The example shown is representative of *n*=2 biological replicates.

b. (i) HBL-1 cells were treated as above (a), and lysates were immunoblotted with anti-MyD88, anti-cleaved caspase 3 and anti-cleaved PARP antibody; actin served as the loading control.

(ii) HBL-1 cells were treated as above (a), with increasing concentrations of LPS (1, 10 and 100ng/mL), and lysates were immunoblotted with anti-MyD88 and anti-cleaved PARP antibody; actin served as the loading control.

(iii) HBL-1 cells, in triplicate, were treated with SAHA (5μM), or co-treated with LPS (100ng/mL) and SAHA (5μM). Cells were harvested after 24 hours and analyzed for sub-G1 by flow cytometry. *p* values are indicated. * denotes significance.

c. RIVA (i) and HBL-1 (ii) cells were either treated with DMSO (mock) or LPS (100ng/mL) for 16 hours before cell supernatants were harvested and levels of pro-inflammatory cytokines analyzed. The inset panels show TNF-α cytokine levels in response to LPS stimulation in RIVA cells (i), and IL-6 cytokine and mRNA levels in response to LPS stimulation (100ng/mL) in HBL-1 cells (ii). The examples shown are representative of *n*=2 biological replicates.

d. Differences in MyD88 transcript expression are shown as assessed by qPCR in extracts from cell pellets from RIVA and HBL-1 cells before and after stimulation with LPS (100ng/mL). MyD88 transcript levels are shown as normalized to actin expression in each cell line.

Figure 4.4 continued

e. (i) RIVA and HBL-1 cells were treated with either DMSO (mock;-), SAHA (5μM; +), recombinant IL-6 (100ng/mL; +), or both. Lysates were immunoblotted with anti-MyD88 and anti-cleaved PARP antibody; actin served as the loading control. Cleaved PARP levels were normalized to actin, and relative cleaved PARP levels in treated, as compared to mock-treated cells, were determined by densitometric analysis and indicated numerically below each lane (i), and in a graph (ii).

4.5 Intersection of IL-6 signalling and the JAK-STAT pathway

As described in Chapter 1 (Section 1.2) constitutive NF-κB activation is thought to be crucial for the survival of ABC DLBCL cell lines (Lam*, et al* 2008, Ngo*, et al* 2011). IL-6 is a key downstream target gene of NF-κB signalling in ABC DLBCL (Lam*, et al* 2008). Autocrine or paracrine secretion of IL-6 has been described in some lymphoid malignancies, in particular myeloma and LPL, as contributing to the growth and survival of malignant cells (Kawano*, et al* 1988, Uchiyama*, et al* 1993, Yang*, et al* 2016). Binding to its cell surface receptor, IL-6 can activate JAK family kinases leading to further downstream signalling events such as the phosphorylation of STAT3 (Ding*, et al* 2008, Lam*, et al* 2008), and a signature of JAK kinase signalling in ABC DLBCL overlapped with the MyD88 signature (Ngo*, et al* 2011). Immunoblotting for STAT3 in lymphoma cell lines showed that this protein, and in particular its phosphorylated form (pSTAT3), is upregulated in HBL-1 cells compared to RIVA cells (Figure 4.5a). Furthermore, co-culturing RIVA cells with the cell culture supernatant from HBL-1 cells (which was previously shown to contain IL-6) or recombinant IL-6, was shown to lead to increased levels of STAT3 protein expression (Figure 4.5b). Although pSTAT3 was not measured in this experiment, it is possible that augmented JAK-STAT signalling after the addition of exogenous IL-6 leads to an increase in total STAT3 levels, as *STAT3* itself has been described to be a target of pSTAT3 (Lam*, et al* 2008, Yang*, et al* 2007).

Constitutive STAT3 activation has been observed in a subset of ABC DLBCL with high IL-6 expression (Lam*, et al* 2008, Yang*, et al* 2007), suggesting functional cross-talk between the JAK-STAT and NF-κB pathways. The increased production of IL-6 observed in MyD88 L265P-mutated lymphoma cells may act in a positive feedback loop, increasing intracellular levels of both STAT3 and pSTAT3 which, in turn, can potentiate both NF-κB pathway activity and, of its own accord, promote further IL-6 secretion (Figure 4.5c). Interestingly, the presence of the MyD88 L265P mutation has previously been shown to support the survival of LPL cells, with the most likely mechanism being the formation of complexes between the mutated MyD88

protein and phosphorylated Bruton tyrosine kinase, resulting in prolonged signalling through the NF-κB pathway (Yang*, et al* 2013). It would therefore be possible to hypothesize that mutated MyD88 could also bind to pSTAT3, thereby slowing down its degradation through the ubiquitin-proteasome system, and thus leading to increased NF-κB activity. This line of investigation was briefly explored but attempts to co-immunoprecipitate pSTAT3 and MyD88 were not successful (data not shown). In addition, the fact that there was no commercially available antibody that allowed specific detection of the MyD88 L265P mutant in cells or in tissue at the time made it even more difficult to distinguish between the effects of wild-type and mutant forms of MyD88. Nevertheless, the interaction between the JAK-STAT and NF-κB pathways as described above could also be therapeutically exploited in cells harbouring the MyD88 L265P mutation, and a combination of a JAK-inhibitor with an HDI may be used to synergistically increase cell killing. To this effect, I established the IC_{50} of the JAK 1/2 inhibitor ruxolitinib in RIVA and HBL-1 cell lines (Appendix C(a), p 204). Ruxolitinib on its own showed no, or only a very small, increase in cleaved caspase 3 levels in the ABC DLBCL cell lines, but rates of apoptosis were increased when it was used together with SAHA in HBL-1 but not RIVA cells at higher concentrations (Appendix C(b), p 204). These findings were not pursued further but are an example of how potentially effective drug combinations that target multiple pathways in cancer cells may be explored.

One of the caveats of interpreting Figure 4.5a of course is the fact that MyD88 expression could not be definitively linked to STAT3 expression, e.g. by knockdown studies, and the influence of IL-10 levels, observed to be elevated in MyD88 L265P-mutated HBL-1 cells (but not MyD88 L265P-transfected U2OS cells) was not evaluated. STAT3 expression in itself has been recognized as a cancer dependency in a wide range of solid and haematological cancers, and the main mechanism driving abnormal STAT3 activity appears to be abnormal cytokine signalling (Xiang, Mizowaki). IL-6 has been established as a critical survival factor in acute myeloid leukaemia and multiple myeloma, and inhibition of STAT3 has been shown to

downregulate IL-6 signalling. Interestingly, however, a subset of non-GCB central nervous system DLBCL tumours have also been found to express high levels of IL-10 which was correlated with increased levels of pSTAT3: those patients with elevated IL-10 levels in their cerebrospinal fluid (CSF) also had a high pSTAT3 IHC staining score on tissue biopsy, whereas IL-6 CSF levels could not be associated with pSTAT3 staining score (Mizowaki). Therefore, the contribution of IL-10 to the JAK-STAT pathway would be an interesting subject for further exploration (Chapter 6, Section 6.2.4).

Figure 4.5

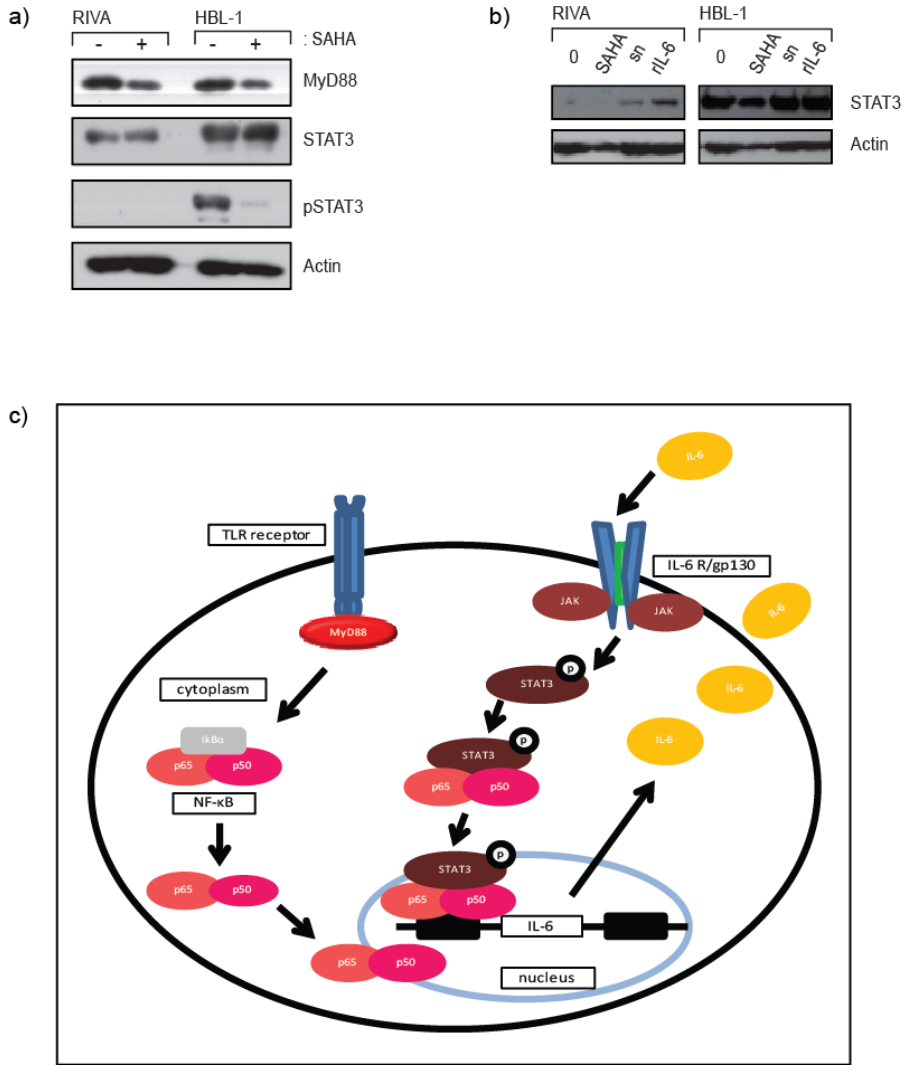


Figure 4.5 STAT3 expression in RIVA and HBL-1 cells.

a. RIVA and HBL-1 cells were treated with SAHA (5µM) for 24 hours and then harvested. Lysates were immunoblotted with anti-MyD88, anti-STAT3 and anti-pSTAT3 antibodies; actin was used as the loading control.

b. RIVA and HBL-1 cells were treated with SAHA (5µM), recombinant IL-6 (100ng/mL), or re-suspended in cell-free HBL-1 supernatant (sn) for 24 hours. Lysates were immunoblotted with anti-STAT3 antibody; actin was the loading control. All lysates were run on the same gel and the same exposures for RIVA and HBL-1 blots are shown.

c. Schematic model depicting the potential molecular cross-talk between the JAK-STAT3 and TLR-MyD88 pathways. See Section 4.5 for details.

4.6 TLR4 receptor blockade affects HDI sensitivity in RIVA but not HBL-1 cells

The presence of mutated MyD88 in lymphoma cells is thought to lead to constitutive downstream NF-κB activation and increased pro-inflammatory cytokine signalling due to the fact that the MyD88 L265P isoform is able to augment its own oligomerization via its TIR domains, both with the mutated and unmutated forms of the protein, leading to the spontaneous assembly of cytosolic Myddosome aggregates (Avbelj*, et al* 2014, Ngo*, et al* 2011, Yang*, et al* 2016, Yang*, et al* 2013).

To test whether an intact upstream TLR-signalling pathway is required for the differences in HDI sensitivity described above, RIVA and HBL-1 cells in culture were blocked with a functional anti-TLR-4 antibody before treatment with SAHA.

RIVA and HBL-1 cell lines were shown to both express TLR4 at baseline (Figure 4.6a). On co-treatment, RIVA cells showed a decrease in PARP cleavage on immunoblot and a significant decrease in sub-G1 percentage on FACS analysis (Figure 4.6b(i) and (ii)) compared to SAHA treatment alone, suggesting that HDI-mediated apoptosis may require an intact TLR4 signalling pathway in cells that are MyD88 wild-type. HBL-1 cells under these conditions by contrast displayed no decrease in sub-G1 levels on FACS, or PARP cleavage on immunoblotting (Figure 4.6c(i) and (ii)). Taken together with the results of TLR stimulation (Section 4.4), it appears that an intact TLR signalling pathway is present in HBL-1 cells which express one wild-type MyD88 allele, as IL-6 levels could be shown to be augmented by LPS stimulation and enhanced apoptosis occurred after HDI treatment when cells were co-cultured with LPS. However, it remains unclear from my experiments whether the mutated MyD88 L265P isoform is able to transmit TLR signals. Blocking TLR4 may only have had a moderate effect on MyD88-associated TLR-dependent signalling as a whole, and the already inherent increase in NF-κB activation in HBL-1 cells may have mitigated any effects of TLR4 blockade. It would have been useful to carry out additional cytokine measurements after treatment of cells with the TLR4 antibody to check for a decrease in cytokine levels; similarly, evaluating levels of the NF-κB subunit p65 on

immunoblot may have been helpful to assess NF-κB pathway activity. I considered using a small-molecule combined TLR2-and TLR4-inhibitor (OxPAPC, Invivogen) but these experiments could not be pursued further.

TLR signalling in B cells under physiological conditions provides a mechanism for innate immune signals to regulate the adaptive immune response. Depending on the context, TLR signalling has been shown to play a variety of roles in B cell development and activation, such as B lineage determination, cell differentiation and negative selection. Subsets of peripheral B cells appear to express TLRs differentially, with naive B cells expressing low leves of TLR1, TLR7 and TLR9, whilst memory B cells have been shown to express high levels of TLR6, TLR7, TLR9 and TLR 10 (Hua and Hou 2013, Isaza-Correra, *et al* 2014). On the other hand, the contribution of TLR signalling to B cell lymphomagenesis is only starting to be elucidated and may be implicated in cellular transformation, lymphoma progression and immune evasion. Similarly, the pattern of TLR expression in B cell malignancies appears to differ compared to normal B cells and has not been fully characterized; malignant B cells in CLL have been described to express higher levels of TLR1, TLR2, TLR6, TLR7, TLR7 and TLR9, whereas in multiple myeloma, TLR1, TLR4, TLR7 and TLR9 are expressed more commonly. In DLBCL, higher levels of TLR2 and TLR8 have been found at both the protein and mRNA levels, whereas in PTCL and some of the more indolent B cell lymphomas such as mucosa associated lymphoid tissue (MALT) lymphoma and mantle cell lymphoma TLR4 in particular was reported to be upregulated at mRNA level (Adam, *et al* 2008, Isaza-Correra, *et al* 2014, Smith *et al* 2010, Wang, *et al* 2013b). TLR antagonism, or blockade, therefore may be a novel therapeutic mechanism for treating B cell malignancies, but the potential for targeting TLR signalling in lymphoma is not completely understood. For example, in ABC DLBCL cell lines, the MyD88 L265P oncoprotein was shown to bind constitutively to TLR7 and TLR9, and knockdown of either TLR7 or TLR9 abrogated NF-kB activity and promoted apoptosis (Kian-Huat Lim 2013). Subsequently, treatment of a mouse xenograft model with IMO-8400, a selective antagonist of TLR7, TLR8 and TLR9 led to a

reduction in tumour size, and this agent has now been advanced into Phase I/II trials in patients with WM (Bhagat 2014, Wang 2014). Similarly, the finding that TLR9 deficiency and defects in TLR7-and TLR9-dependent signalling inhibited MyD88 L265P-induced proliferation of CLL cells in culture, led to an experimental approach of TLR9 knockdown. Paradoxically, TLR9 deficiency only suppressed B cell growth in vitro, whereas in vivo, an accumulation of B cells with the MyD88 L265P mutation was observed (Wang*, et al* 2016).

At the time of writing (May 2017), no reports of TLR4 blockade in lymphoma and the role of MyD88 L265P in this context had been published. The TLR4 receptor was chosen for my experiments as both RIVA and HBL-1 cell lines were shown to both express TLR4 at baseline and the receptor is expressed on the cell surface (Chapter 1, Table 1.2). The stimulation of TLR4 by LPS leads to early MyD88 aggregation, NF-kB activation and release of pro-inflammatory cytokines and has been widely studied, and is a readily available reagent which is easy to use in cell culture (Into, *et al* 2010, Lu, *et al* 2008, Olson, *et al* 2015).

Figure 4.6

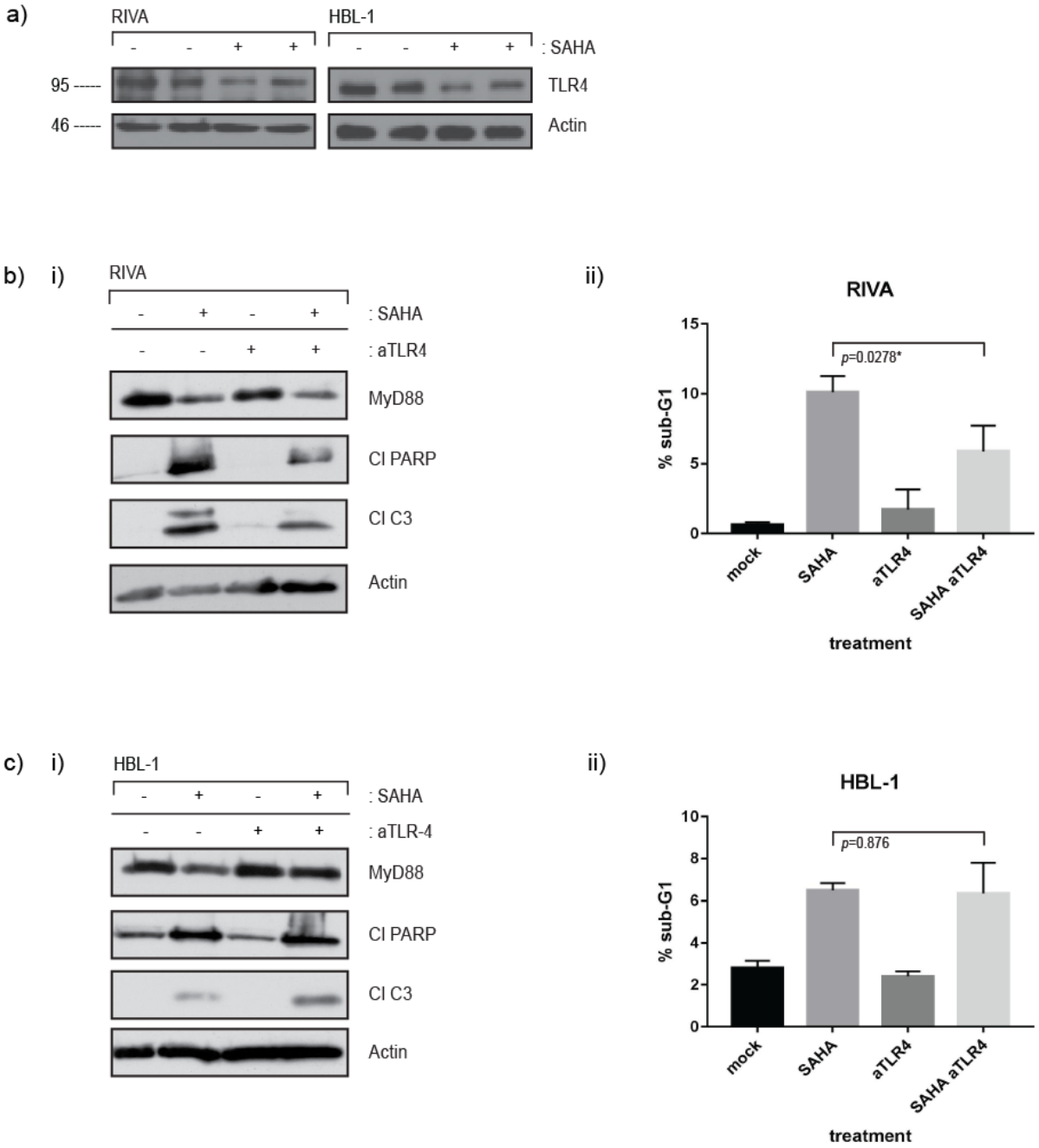

a)
RIVA
HBL-1
- - + + - - + + : SAHA
95 -----
46 -----
TLR4
Actin
b) i)
RIVA
- + - + : SAHA
- - + + : aTLR4
MyD88
Cl PARP
Cl C3
Actin
ii)
RIVA
p=0.0278*
% sub-G1
15
10
5
0
mock
SAHA
aTLR4
SAHA aTLR4
treatment
c) i)
HBL-1
- + - + : SAHA
- - + + : aTLR-4
MyD88
Cl PARP
Cl C3
Actin
ii)
HBL-1
p=0.876
% sub-G1
10
8
6
4
2
0
mock
SAHA
aTLR4
SAHA aTLR4
treatment

Figure 4.6 TLR4 receptor blockade in RIVA and HBL-1 cells and HDI sensitivity.

a. RIVA and HBL-1 lysates were immunoblotted with anti-TLR4 antibody to assess cells for TLR4 expression, and actin was the loading control. Cells were either untreated (lane 1 of each blot), or treated with SAHA (lanes 3 and 4 of each blot). Lanes 2 and 3 were also treated (or co-treated) with ruxolitinib (not relevant for the purpose of this figure). Protein markers are indicated.

b. (i) RIVA cells were treated with SAHA (5μM), a functional anti-TLR4 antibody (2μM), or both, for 24 hours before cells were harvested. Lysates were immunoblotted for MyD88, cleaved PARP and cleaved caspase 3; actin served as the loading control.

(ii) RIVA cells were treated as above (i), and cells were harvested and analyzed for sub-G1 by flow cytometry. *p* values are indicated. * denotes significance.

c. (i) HBL-1 cells were treated with SAHA (5μM), a functional anti-TLR4 antibody (2μM), or both, for 24 hours before cells were harvested. Lysates were immunoblotted for MyD88, cleaved PARP and cleaved caspase 3; actin served as the loading control.

ii) HBL-1 cells were treated as above (i), and cells were harvested and analyzed for sub-G1 by flow cytometry. *p* values are indicated.

4.7 Conclusion

In this chapter I focused on the consequences of the cytokine profiles expressed by lymphoma cells, in mediating HDI sensitivity in the context of increased NF-κB activation and MyD88 mutation status (New*, et al* 2016, Ngo*, et al* 2011): HBL-1 cells were shown to produce increased amounts of IL-6 compared to the RIVA cell line which is also of the ABC DLBCL subtype but does not carry the MyD88 L265P mutation. Neutralization of IL-6 with an anti-IL-6 antibody negatively affected the sensitivity of HBL-1 cells to treatment with an HDI but did not appear to have a significant impact on the other, MyD88 wild-type, lymphoma cell lines, RIVA, U2932, RCK8 or SUDHL4.

HBL-1 cells were also found to have higher expression of total STAT3 and pSTAT3 at the protein level, suggesting a constitutively active JAK-STAT signalling pathway in these cells. IL-6 may therefore act in an autocrine or paracrine fashion, driving STAT3 expression through a positive feedback loop. Interestingly, the addition of LPS or recombinant IL-6 to RIVA cells in order to increase extracellular cytokine levels seemed to augment sensitivity to an HDI in these cells, and an increased total STAT3 protein level was observed after treatment with recombinant IL-6.

IL-6 has been implicated as an important factor in driving the proliferation and survival of B cells in lymphoproliferative disorders (Burger 2013). Why, therefore, IL-6 should sensitize lymphoma cells to treatment with an HDI is not entirely clear. One explanation, as discussed above, could be that HDAC inhibitors preferentially target actively proliferating cells and that ongoing proliferation and cell cycle progression is important for HDI-mediated sensitivity. No consistent effects of HDI and/or anti-IL-6 treatment on the cell cycle could be demonstrated in the experiments presented here and synchronization experiments to compare the different cell lines were not carried out. The effects of HDAC inhibition on immune cells in particular are only incompletely understood (Kroesen*, et al* 2014), and treatment of B cell neoplasms with an

HDI may impact on multiple pathways at once, with the outcome being related to the functional cross-talk between immune-related and oncogenic pathways.

To understand whether HDAC inhibition may impact directly on MyD88 in lymphoma cells, I next set out to investigate whether endogenous MyD88 could be shown to be acetylated and whether any bromodomain readers could be identified in this context.

CHAPTER 5. MYD88 ACETYLATION AND RESPONSE OF CANCER CELL LINES TO BROMODOMAIN INHIBITION

5.1 Introduction

Taken together, the results presented in Chapters 3 and 4, along with results from experiments carried out in MyD88-transfected U2OS cells by other members of Professor La Thangue's research group (Dr Maria New, Dr Heidi Olzscha, Mina Bekheet; Chapter 1, Section 1.9), suggest that MyD88 plays a role in mediating cell sensitivity to HDAC inhibition, and also that IL-6 release, activated through the TLR-MyD88-NF-κB signalling pathway, may be involved in this process through an autocrine, or paracrine, feedback loop. Mechanistically, however, it remains unclear how HDAC inhibition relates to these events. HDAC inhibition in general is thought to influence transcription by increasing acetylation of histone proteins, thereby disrupting nucleosomal structure and allowing improved access of transcription factors to areas of unfolded DNA, thus effecting changes in gene expression (Mitsiades*, et al* 2003). Importantly, SAHA has been shown to induce lysine acetylation not only of chromatin-associated proteins such as histones, but also a number of non-histone proteins that can be found both in the nucleus and the cytoplasm (Chaudhary*, et al* 2012, Kim*, et al* 2006b, Zhou*, et al* 2010); a SILAC-based proteomics approach in human breast cancer cell lines, for example, identified transcriptional factors and regulators, chaperones and cell structure proteins as targets of SAHA-mediated acetylation. Moreover, SAHA enhanced lysine acetylation in a time-dependent manner which was distinct for different sets of proteins, indicating that SAHA may mediate its anti-tumour effects over a period of time (Zhou*, et al* 2010).

Based on these findings, therefore, the possibility was considered that MyD88 itself may be a target for acetylation. Using a mass spectrometric approach, a single acetylation site on MyD88 (at residue K132) was identified, and acetylation of the ectopically expressed MyD88 protein could be shown by immunoprecipitation experiments (New*, et al* 2016).

The histone deacetylase HDAC6 was investigated as a key regulator of MyD88 acetylation: HDAC6 is predominantly located in the cytoplasm, and has been shown to reversibly deacetylate non-histone proteins such as HSP90, thereby modulating its chaperone activity (Lee*, et al* 2013). Together with sequestosome 1 (SQSTM1), HDAC6 is thought to be necessary for MyD88 aggregation and MyD88-dependent signal transduction (Into*, et al* 2010). Work in Professor La Thangue's research group also showed that inhibition of HDAC6 with the HDAC6-specific HDI tubastatin causes apoptosis in cancer cell lines ((New*, et al* 2016); Chapter 3, Section 3.4).

By recognizing and binding to acetylated lysine residues on both histone- and non-histone proteins, bromodomains (BRDs) may be instrumental mediators of protein-protein interactions (Brand*, et al* 2015, Filippakopoulos*, et al* 2012). Small-molecule BRD inhibitors can selectively disrupt these BRD-acetyl-lysine-mediated protein interactions, displaying significant activity in cancer cell lines and pre-clinical cancer models ((Abedin*, et al* 2016); Chapter 1, Section 1.7)).

To investigate MyD88 acetylation and its potential implications for HDI treatment in lymphoma cells, I endeavoured to address three overlapping questions: firstly, was it possible to show that MyD88 is acetylated in lymphoma cells; secondly, if MyD88 is indeed acetylated, could its BRD reader be identified; and finally, would BRD inhibition affect the response to HDI treatment in lymphoma cells. To this effect, a CADOR (chromatin-associated domain) array was carried out; in addition, the effect of BRD inhibitors on cancer cell lines was observed.

5.2 Acetylation of MyD88 in lymphoma cells

As treatment with an HDI leads to increased global acetylation in cells (Figure 5.1a), some work carried out in Professor La Thangue's research group (by Maria New) focused on the acetylation status of MyD88 itself. Immunoprecipitation experiments in U2OS cells over-expressing transfected Flag-MyD88 found an acetylation band at 33kD on immunoblotting, and mass spectrometry identified a single lysine residue at position 132 (K132) to be acetylated (Maria New, data not shown).

In order to investigate whether endogenous MyD88 in lymphoma cells could be shown to be acetylated, I performed immunoprecipitation experiments in RIVA and HBL-1 cells. MyD88 pull-down was found to be variable, depending on the lysis buffer and/or the antibody used for immunoprecipitation; however, adjustment of the antibody and change of lysis buffer (from RIPA to TNN; Chapter 2, Section 2.4) allowed pull-down of endogenous MyD88. Membranes were first probed for acetylated lysine before stripping and re-probing for MyD88, and then checking for overlapping bands at 33kD. This way, it would be more likely that an acetylation band would correspond to a band considered to be the immunoprecipitated MyD88 protein. Alternatively, of course, it could always be possible that the acetylated lysine antibody could identify another acetylated protein with the molecular weight of 33kDa, completely unrelated to MyD88, that happened to be present in the lysate. Therefore, a simultaneously run IgG fraction, treated with a non-specific IgG antibody of the same species as the MyD88 antibody, was used as a control.

Treatment of cells with low concentrations of SAHA or tubastatin (2.5µM) before carrying out immunoprecipitation was initially thought to be useful to augment and stabilize the acetylation of proteins in the eventual lysate, but was found to negatively affect endogenous MyD88 pull-down, and therefore was not used in further experiments.

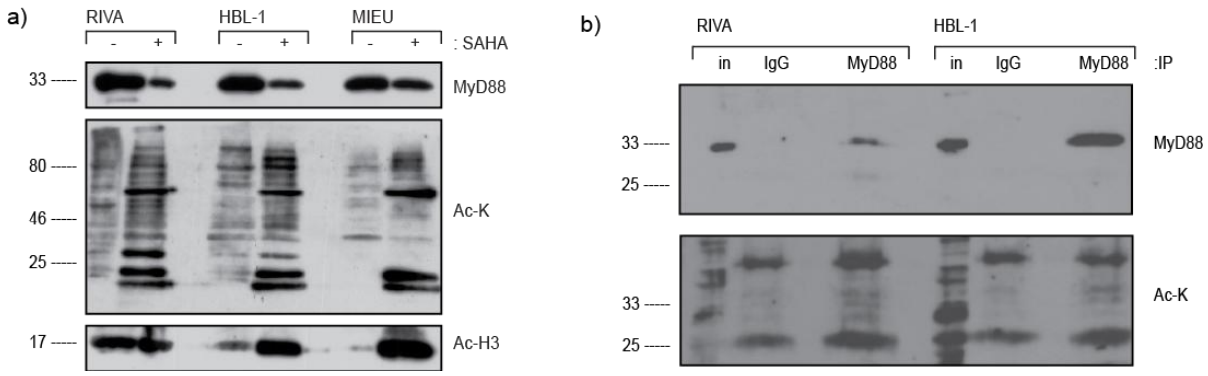
Finally, carrying out the "reverse" immunoprecipitation experiment, where proteins in the lysate would be pulled down with the acetylated lysine antibody before probing for MyD88 on immunoblot, remained unsuccessful.

As can be seen in Figure 5.1b, MyD88 could be immunoprecipitated in RIVA and HBL-1 cells and a faint acetylation band could be detected for both cell lines at 33kD, although this was more prominent in RIVA cells as compared to HBL-1 cells.

Immunoprecipitation of endogenous proteins is an important technique because it allows the evaluation of native proteins and their modifications. However, several factors may impact on successful immunoprecipitation. For example, in the case of endogenous immunoprecipitation of MyD88, commercially available antibodies could not detect the L265P-mutated form of MyD88, and antibodies for detecting acetylation status vary in quality. The amount of the endogenous protein itself can vary depending on cell type, and membrane-bound proteins may be more difficult to extract using standard protocols (although, interestingly, in Figure 5.1c, MyD88 pull-down appeared more successful in HBL-1 cells). Alternatively, pre-immobilized specific antibodies could be used, but free, non-bound antibody, as used in the experiments presented here, is considered to be more beneficial if the target protein is present at low concentrations, or the antigen-antibody interaction has weak affinity or slow kinetics (Harlow and Lane 1999).

Similarly, detecting protein-protein interactions by immunoprecipitation can be challenging if the interaction is transient or weak, and the efficiency of the antibodies used can be a limiting factor as described above. Hence, in order to identify likely bromodomain-containing proteins that may interact with MyD88 in its acetylated form I collaborated with the Bedford Lab at the MD Anderson to carry out a CADOR array. The experimental rationale was to determine potential interacting proteins and then proceed to further immunoprecipitation experiments to validate those interactions both in vitro and in vivo in cell culture.

Figure 5.1



Acetylation of MyD88.

a. Three DLBCL cell lines (RIVA and HBL-1 are representative of the ABC subtype; Mieu is representative of the GCB subtype) were treated with SAHA (5μM for 24 hours). Lysates were immunoblotted for MyD88, acetylated lysine (Ac-K) and acetylated histone H3 (Ac-H3).

b. Extracts from RIVA and HBL-1 cells were immunoprecipitated with IgG (negative control) or MyD88 antibody, and immunoblotted with anti-MyD88 or anti-acetyl-lysine (Ac-K) antibody. Input (2% of total lysate) level of MyD88 is shown.

5.3 CADOR array and potential bromodomain readers of MyD88

The CADOR array is a chip that has been constructed by the Bedford lab, and contains every BRD characterized to date (Figure 5.2a). So far, 61 BRDs have been identified in the human proteome, present in 46 diverse proteins (Filippakopoulos*, et al* 2012). The CADOR chip can be analyzed with a library of different peptides that vary in their position and degree of acetylation and are based on the sequence of the region of MyD88 that previously has been found to be acetylated by mass spectrometry. The goal is to identify which of the immobilized BRDs preferentially bind to the acetylated peptides (Mark Bedford and Cari Sagum, personal communication).

MyD88 contains 15 lysine residues which could potentially be acetylated (www.uniprot.org/uniprot/Q99836). Of those, only one, at position K132, was found to be acetylated by mass spectrometry (Section 5.2). Interestingly, close to the K132 residue there is another lysine residue, K128, which was considered another potential target for acetylation. Based on this finding, I therefore designed four individual peptides of varying acetylation state, each 16-amino acids long (Figure 5.2b). To distinguish between acetylated lysine-dependent and –independent binding, a corresponding non-modified (i.e. non-acetylated) peptide was included in the screen. The reason for also including di-acetylated peptides is based on the finding that single BRDs can cooperatively bind two acetylation marks (Moriniere*, et al* 2009), and that a number of BRDs have been shown to have an acetyl-lysine binding site architecture that is thought to be compatible with binding di-acetylated peptides (Filippakopoulos*, et al* 2012).

The two main findings from the CADOR array were rather unexpected: firstly, the strongest BRD interactions are seen with the peptide acetylated at K128 and the di-acetylated peptide, and not the peptide acetylated at K132 as would have been anticipated from the mass spectrometry data. Secondly, of the eight BRDs identified as interacting with the acetylated peptides, the majority (six) are thought to be located in the nucleus and involved in

transcription regulation. A summary table with details of their known functions and locations is shown in Figure 5.2c.

Before any conclusions can be drawn from the data gathered through the CADOR array, it is important to bear in mind several caveats and limitations of the experimental set-up. This includes the technique of mass spectrometry, the peptides used for the CADOR array, and the interactions elicited in the CADOR array itself.

One of the most frequently used methods for identifying post-translational modifications of proteins is tandem mass spectrometry combined with searching a protein sequence database (Savitski and Savitski 2010). However, this analysis can be difficult for various reasons, including the mass shift in the peptide molecular weight, the overall abundance of the modified peptide, the stability of the modification during mass spectrometry, and the effect of the modification on the peptide's ionization efficiency (and therefore the sensitivity) (Parker*, et al* 2010). Locating the exact site of a modification in addition requires detection, and in most cases MS/MS sequencing of the specific modified peptide. As not all peptides are equally detected, this can be difficult. Furthermore, extracting the protein of interest by in-solution digest may lead to incomplete sequence coverage of the protein. It is therefore possible that MyD88 could be acetylated at the two different lysine residues identified (i.e. K128 and K132), or may indeed exist in either a singly or di-acetylated form.

It is possible to argue that using small peptides with additional attached tags and linker sequences for the CADOR array may not be able to correctly identify the protein-protein interactions that occur in cells in vivo. Due to its short sequences, peptides do not have the conformation and three-dimensional structure of the native protein which may be required for specific protein interactions to take place. Steric constraints, therefore, could be a reason for the lack of detection of a strong interaction between BRDs and K132-monoacetylated peptides. The inclusion of a non-acetylated peptide essentially served as a negative control,

and no strong interactions between BRDs and the unmodified peptide were observed that would indicate a high degree of non-specific interactions, thereby suggesting that the interactions observed are indeed a result of target-specific binding.

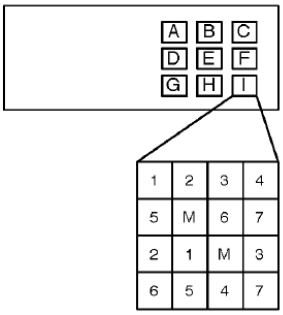
As a logical next step, therefore, it was necessary to independently validate these potential domain-peptide interactions. An important question that remained (and that is addressed in Section 5.6) is whether MyD88, given its documented cytoplasmic location, will be able to interact with any of the predominantly nuclear BRDs identified in the screen. To exclude the possibility and check that the peptides chosen for the CADOR array could also be representative of a MyD88-unrelated protein which happens to be located in the nucleus, the peptide sequences were run through the Uniprot protein sequence database using the BLAST tool (www.uniprot.org/blast/). MyD88 was the predominant protein that came up in the search, suggesting that the BRDs identified could indeed and most likely be binding to a peptide sequence of the MyD88 protein.

Figure 5.2

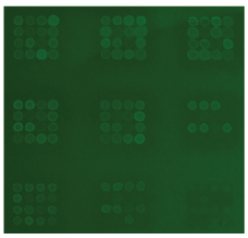
a)

Acetyl Domain Readers Array

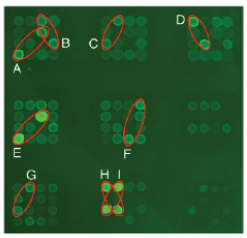
BROMO A1) ASH1L(short) [Q9NR48] A2) ATAD2A [NP_054828.2] A3) ATAD2B [Q9ULI0] A4) BAZ1A [Q9NRL2] A5) BAZ2A/BMZF-2 [Q9UIF9] A6) BAZ2B [Q9UIF8] A7) CECR2 [Q9BXF3]	**BROMO** B 1) BRD1(1) [O95696] B 2) BRD2(1) [P25440] B 3) BRD2(2) [P25440] B 4) BRD3(1) [Q15059] B 5) BRD3(2) [Q15059] B 6) BRD4(1) [O60885] B 7) BRD4(2) [O60885]	**BROMO** C1) BRD7 [Q9NPI1] C2) BRD8(1) [Q9H0E9] C3) BRD9 [Q9H8M2] C4) BRDT(1) [Q58F21] C5) BRDT(2) [Q58F21] C6) BRPF1/Peregrin [P55201] C7) BRPF3 [Q9ULD4]
BROMO D1) BRWD1/WDR9(2) [Q9NSI6] D2) BRWD3(2) [Q6RI45] D3) SMARCA2 [P51531] D4) SMARCA4 [P51532] D5) TAF1(1) [P21675] D6) TAF1(2) [P21675] D7) MLL1 [Q03164]	**BROMO** E1) PBRM1/PB1(1) [Q86U86] E2) PBRM1/PB1(2) [Q86U86] E3) PBRM1/PB1(3) [Q86U86] E4) PBRM1/PB1(4) [Q86U86] E5) PBRM1/PB1(5) [Q86U86] E6) PBRM1/PB1(6) [Q86U86] E7) PHIP(2) [Q8WWQ0]	**BROMO** F1) KIAA2026 [Q5HYC2] F2) GCN5/KAT2A [Q92830] F3) PCAF/KAT2B [Q92831]
BROMO/PHD G1) CBP/CREBBP [Q92793] G2) FALZ/BPTF [Q12830] G3) p300/EP300 [Q09472] G4) TRIM24 [O15164] G5) TRIM33/TIF1G [Q9UPN9] G6) TRIM66 [O15016] **BROMO/PHD/PWWP** G7) ZMYND11 [Q15326]	**BROMO(2)** H1) TAF1(1+2) [P21675] H2) TAF1L(1+2) [Q8IZX4] **PHD(2)** H3) DPF3 [Q92784] **BROMO/PHD/BAH** H4) ASH1L(long) [Q9NR48]	**YEATS** I1) YEATS4/GAS41 [NP_006521.1] I2) ENL/MLLT1 [NP_005925] I3) AF9/MLLT3 [NP_004520.2] I4) YEATS2 [NP_060493]



b)

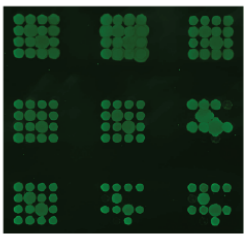


Myd88 unmodified - 100 µg
Biotin-Ahx-EDCQKYILKQQQEEAEK



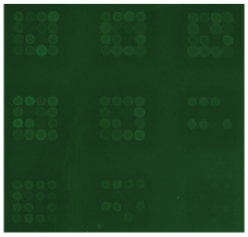
Myd88 ac128 - 100 µg
Biotin-Ahx-EDCQ[acK]YILKQQQEEAEK

A. BAZ2B Bromo
B. ATAD2B Bromo
C. BRD2(1) Bromo
D. BRD7 Bromo
E. TAF1(2) Bromo
F. PBRM1/PB1(4) Bromo
G. FALZ/BPTF Bromo+PHD
H. TAF1(1+2) Bromo
I. TAF1L(1+2) Bromo



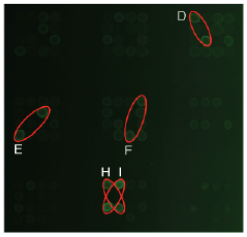
αGST

Acetyl Domain Readers Array
Full Range Intensity
PMT Gain: 300
Power: 5



Myd88 ac132 - 100 µg
Biotin-Ahx-EDCQKYIL[acK]QQQEEAEK

Acetyl Domain Readers Array
Preserved Middle Intensity
PMT Gain: 340
Power: 14



Myd88 di-ac - 100 µg
Biotin-Ahx-EDCQ[acK]YIL[acK]QQQEEAEK

D. BRD7 Bromo
E. TAF1(2) Bromo
F. PBRM1/PB1(4) Bromo
H. TAF1(1+2) Bromo
I. TAF1L(1+2) Bromo

Figure 5.2 continued

c)

BRD-containing protein	Name	Other abbreviations	Protein function	Subcellular localisation	Number of BRDs
BAZ2B	Bromodomain adjacent to zinc finger domain, 2B	WALp4	Unknown	N, C	1
ATAD2	Two AAA domain containing protein	ANCCA	Transcriptional regulator, co-activator	N	1
BRD2	Bromodomain-containing protein 2	FSH, RING3	Transcriptional regulator	N	2
BRD7	Bromodomain-containing protein 7	BP75, NAG4, CELTIX1	Transcriptional regulator/repressor	N	1
TAF1	TAF1 RNA polymerase II, TATA box-binding protein (TBP)-associated factor	TAFII250	Transcription initiation	N	2
PBRM1/PB1	Polybromo 1	BAF 180	Chromatin remodelling factor	N,C	6
FALZ/BPTF	Fetal Alzheimer antigen	FAC 1	Transcription factor, chromatin remodelling	N	1
TAF1L	TAF1-like RNA polymerase II, TATA box-binding protein (TBP)-associated factor	TAF(II)210	Transcription initiation	N	2

Figure 5.2 Acetylated peptides bind to bromodomains on the CADOR chip.

a. Forty-eight bromodomain (GST) fusion proteins were arrayed on a nitrocellulose slide. The layout of the array is shown. The middle position (M) contains GST alone as a background indicator.

b. The array was first probed with an anti-GST antibody, and this subsequently detected with a fluorescein isothiocyanate-conjugated secondary antibody to establish roughly equal loading (right-hand panel). The array was subsequently probed with MyD88-derived peptides, including mono-acetylated, di-acetylated and non-acetylated forms (Chapter 2, Section 2.17). Acetyl-dependent interactions are marked with red ovals.

c. Table detailing cellular locations and known functions of bromodomain-containing proteins identified as having acetyl-dependent interactions with MyD88-derived peptides as shown in (b).
Sources: (Barbieri*, et al* 2013, Filippakopoulos*, et al* 2012, Muller*, et al* 2011)

5.4 Recognition of MyD88 acetylation by bromodomain readers

Three approaches were considered to corroborate the peptide-BRD interactions detected with the CADOR chip: firstly, by expressing the recombinant BRDs used for the array and performing in vitro peptide pull-downs with the variously acetylated MyD88 peptides; secondly, by using the recombinant BRDs together with cell lysates from RIVA and HBL-1 cells to investigate potential binding interactions with native MyD88 (in this context, as MyD88 levels in cell lysates may be too low to detect a meaningful interaction, transfection of U2OS cells with Flag-tagged MyD88 before proceeding to peptide-pulldown was considered as an option); finally, immunoprecipitation of MyD88 and probing for associated BRDs could be used to validate the endogenous protein-protein interactions, although this approach would be subject to similar limitations as described in Section 5.2.

Plasmids for the eight implicated BRDs were obtained (through collaboration with the Bedford lab). Unfortunately, however, repeated attempts at optimizing the recommended protocol for the expression of the GST-tagged BRDs failed. Therefore, this approach at validation had to be abandoned.

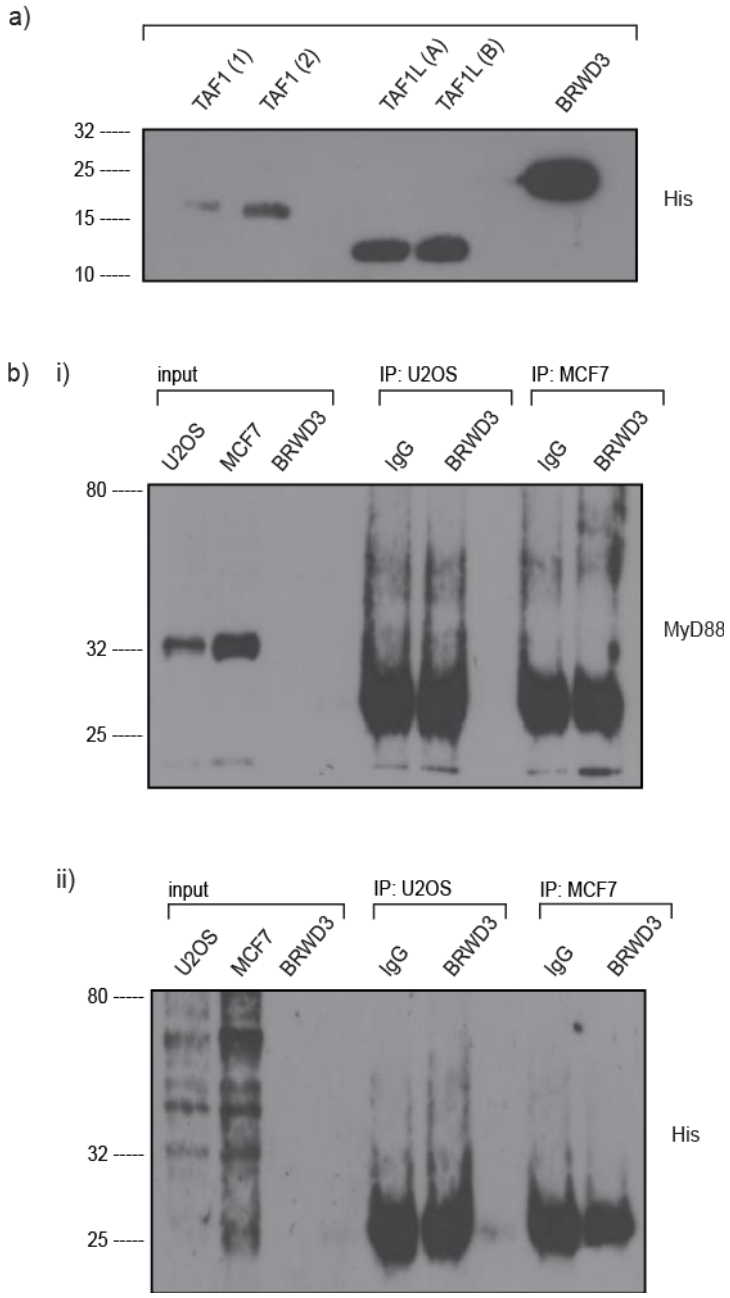
An alternative approach that I then explored was to use His-tagged recombinant BRD peptides (kind gift from Panagis Filippakopoulos from the Structural Genomics Consortium, University of Oxford) and incubate those BRDs of interest with lysates from cancer cell lines, prior to pull-down with either anti-MyD88 or anti-His-antibody. Several BRDs of interest were run on an SDS-PAGE gel and found to be detectable on immunoblotting (Figure 5.3a). Two BRDs were chosen to carry out exploratory sets of experiments, TAF-1 and BRWD3. The rationale for this was that TAF1 had been detected by CADOR array to bind to both the mono-acetylated and di-acetylated forms of the MyD88 peptide. TAF1, however, is thought to be an exclusively nuclear protein. BRWD3, by contrast, is thought to be located in the cytoplasm, and despite not being detected on CADOR array, had previously been shown to immunoprecipitate Flag-tagged MyD88 (Maria New, personal communication).

Repeated attempts at detecting BRDW3 in immunoprecipitation experiments with endogenous MyD88 (Appendix E, p 206), and pull-down with TAF-1 or BRWD3 in cancer cell lysates, however, proved unsuccessful as evidenced by the absence of a detectable His-tag (Figure 5.3b). This may be due to a variety of reasons: firstly, the interaction may not exist, especially if one accepts that MyD88 is exclusively cytoplasmic and associated with the cell membrane as part of the Myddosome cell signalling complex, whereas TAF-1 is exclusively nuclear. Secondly, the interaction may be too weak or too transient to be demonstrable on immunoprecipitation. Similarly, the amounts of the proteins involved in the interaction may be too low in the cell lysates to be detectable. Finally, technical problems were also encountered; for example, the His-tag on the BRD peptides proved to be unstable and subsequently undetectable after several freeze-thawing cycles (Figure 5.3b).

Further optimization of the immunoprecipitation protocol and attempts at pull-down with all eight BRDs identified on CADOR array would have been desirable. However, given time constraints on the project and technical issues as detailed above, this path of investigation was not pursued further.

Instead, it was of interest to consider whether MyD88 may be able to traffic to the cell nucleus and this formed the basis for some additional and subsequent experiments.

Figure 5.3



Immunoprecipitation pull-down approach to detect MyD88-interacting BRDs.

a. His-tagged BRDs of interest were run on an SDS-PAGE gel (1µg loaded for each) and detected using an anti- His-antibody.

b. Example of attempted pull-down approach with His-tagged BRWD3 is shown in lysates of U2OS and MCF7 cells. Cell lysates were immunoprecipitated with either IgG (negative control) or His-tagged BRWD3, and the whole membrane was immunoblotted with anti-MyD88 (i) or anti-His (ii; His) antibody. Input (2% of total lysate) level of MyD88 is shown.

5.5 Investigation of potential nuclear localization of MyD88

The current literature on MyD88 has predominantly concentrated on its role in TLR signalling and its presence in aggregated structures in the cytosol, and therefore MyD88 is mainly described as a cytoplasmic protein (www.proteinatlas.org; www.uniprot.org); (Into*, et al* 2010, Takeda and Akira 2004).However, nuclear localization of MyD88 has previously been reported: using ultrastructural immunohistochemistry it was shown that Flag-tagged MyD88 could be found in the nucleus of transiently transfected HeLa cells, but only those cells with no detectable morphological signs of apoptosis (Jaunin*, et al* 1998); similarly, GFP-tagged MyD88 and its TIR-domain derivative, $MyD88_{TIR}$, could be detected both in the cytoplasm and the nucleus of HEK-293 cells, whereas the isolated DD-domain form was excluded from the nucleus (Aguirre and Hermoso 2005, Chaudhary*, et al* 2012). Moreover, mammalian MyD88 was found to have canonical nuclear localization and export motives which are thought to play a crucial role in nuclear-cytoplasmic transit when TLR2 is activated, and may be implicated in cell death (Aguirre and Hermoso 2005, Arancibia*, et al* 2007). More recently it was also observed that the co-expression of trout ST2 (also known as IL-1RL1 receptor, which is thought to regulate TLR signalling by sequestering MyD88 (Brint*, et al* 2004)), and trout MyD88, allowed the translocation of MyD88 into the nucleus in human HEK-293 cells (Rebl*, et al* 2017).

Nuclear localization signals (NLS) are amino acid sequences that tag proteins for transport into the cell nucleus. Using an online NLS mapper (http://nls-mapper.iab.keio.ac.jp/), putative NLS specific to the importin αβ pathway can be predicted from a given protein sequence and assigned a score (Kosugi*, et al* 2009). Higher scores indicate stronger NLS activities. Thus, scores of 8-10 suggest exclusive localization of a protein to the nucleus, whereas proteins with scores of 1 or 2 are thought to be only found in the cytoplasm. Proteins with scores of 3,4, or 5 therefore can be localized both in the nucleus and the cytoplasm.

When the MyD88 sequence was run through the NLS mapper, five potential bipartite NLS were identified (Figure 5.4a). No additional NLS were detected when the MyD88 sequence was

changed to represent the mutant L265P. This finding is in itself probably not surprising as only one change was introduced in the amino acid sequence, and classical NLS are usually considered to preferentially contain arginine or lysine residues (Kalderon*, et al* 1984). The scores of the MyD88 NLS that were generated ranged between 3.1 and 3.6, and although these scores are overall low (see scoring system above), they give an indication that MyD88 may indeed be found in the nucleus and not just the cytoplasm.

IHC for MyD88 had previously been carried out on biopsy specimens from patients with DLBCL and LPL (Chapter 3, Section 3.2). A nuclear staining pattern could be observed in individual cells in some samples (Figure 5.4b). However, it could not be determined whether the cells displaying this particular staining pattern were always part of the lymphoproliferative infiltrate, or rather constituted cells that were present as part of the normal microenvironment within the respective lymph node or bone marrow. Double staining, for instance with an anti-CD20 antibody may have been useful to distinguish these possibilities in this context, but was not carried out. It is also important to remember that all the biopsies examined for this project were taken at diagnosis, and therefore are pre-treatment (and none of the patients whose biopsies were stained for MyD88 received HDI treatment).

To examine whether MyD88 can be found in the nucleus of lymphoma cells, I next performed nuclear extractions on untreated RIVA and HBL-1 cells (Figure 5.4c). After the nuclear and cytoplasmic fractions were separated, immunoblotting revealed that MyD88 (albeit in smaller amounts) could be detected in the nucleus in each cell line. Further experiments after HDI-treatment of lymphoma cells would have been useful to assess whether MyD88 disappears from the nucleus as cells start to undergo apoptosis, as described previously (Jaunin*, et al* 1998). Moreover, using increasing concentrations of an HDI and tracking the cellular sub-localization of MyD88 in different phases of cell cycle arrest could give more information on what MyD88 does in, or around, the nucleus. One of the problems with nuclear extraction however is that in particular the nuclear fraction can easily become contaminated with

cytoplasmic proteins, and that Western Blots are at best semi-quantitative. Another technique that could help to corroborate the above results would be immunofluorescence. Again, due to time constraints on the project, optimization of this technique could not be achieved.

Although it was not possible to conclusively determine whether MyD88 transits to the nucleus during HDI treatment and what role, if any, this process may play in a nuclear or peri-nuclear setting, there is a growing interest in using BRD inhibitors in lymphoma (Abedin*, et al* 2016, Barbieri*, et al* 2013, Chapuy*, et al* 2013). Therefore, as a next step of my investigation I treated RIVA and HBL-1 cell lines with a BRD inhibitor, an HDI, or both, in order to explore the cellular outcomes with a combination of treatments using these agents.

Figure 5.4

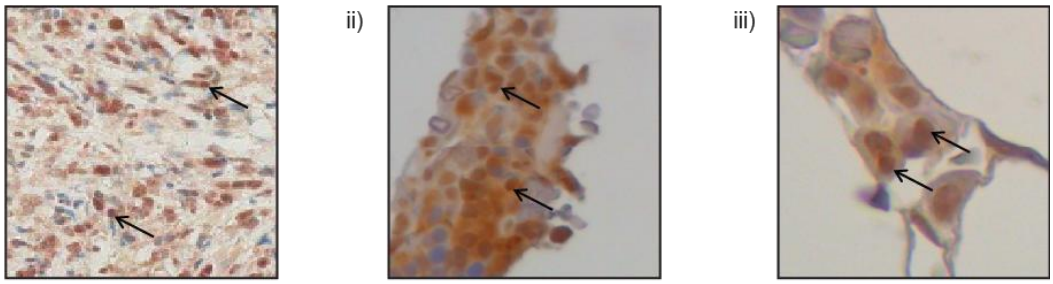
a) i)

Predicted bipartite NLS		
Position		**Score**
88	RLLELLTKLGRDDVLLELGPSIEEDCQKYIL	**3.1**
88	RLLELLTKLGRDDVLLELGPSIEEDCQKYILKQ	**3.6**
234	DFQTKFALSLSPGAHQKRLIPIKYKAMKKE	**3.5**
249	QKRLIPIKYKAMKKEFPSILRFITVCDYT	**3.3**
267	ILRFITVCDYTNPCTKSWFWTRLAKALSLP	**3.3**

ii)

Predicted NLSs in query sequence (MyD88 Q99836 www.uniprot.org)	
MAAGGPGAGSAAPVSSTSSLPLAALNMRVRRRLSLFLNVRTQVAADWTAL	50
AEEMDFEYLEIRQLETQADPTGRLLDAWQGRPGASVGRLLELLTKLGRDD	100
VLLELGPSIEEDCQKYILKQQQEEAEKPLQVAAVDSSVPRTAELAGITTL	150
DDPLGHMPERFDAFICYCPSDIQFVQEMIRQLEQTNYRLKLCVSDRDVLP	200
GTCVWSIASELIEKRCRRMVVVVSDDYLQSKECDFQTKFALSLSPGAHQK	250
RLIPIKYKAMKKEFPSILRFITVCDYTNPCTKSWFWTRLAKALSLP	296

b) i) ii) iii)



c)

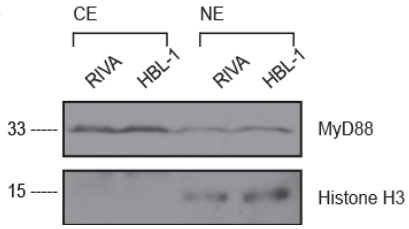


Figure 5.4 Nuclear localization of MyD88.

a. The MyD88 amino acid sequence (Uni Prot no 99836) was run through an NLS mapper programme (http://nls-mapper.iab.keio.ac.jp/cgi-bin/NLS_Mapper_form.cgi), and a cut-off score of 3.0 or higher was selected.
(i) The five predicted bipartite NLS sequences and their scores are shown.
(ii) The position of the identified NLS sequences in the MyD88 sequence are shown (in red type): the first two sequences locate to the MyD88 DD domain, whereas the other NLS locate to the MyD88 TIR domain.

b. Biopsy sections from lymphoma patients were stained for MyD88 expression, and arrows depict nuclear localization of MyD88.
(i) Lymph node from a patient with DLBCL. Magnification is x20.
(ii) Bone marrow from a patient with LPL. Magnification is x40.
(iii) Bone marrow from a patient with LPL (different from the one shown in (ii)). Magnification is x63.

c. Nuclear extracts of untreated RIVA and HBL-1 cells are shown. The same number of cells was plated for 24 hours before harvesting, and nuclear extraction was performed. Cytoplasmic and nuclear fractions were run on the same SDS-PAGE gel and probed for MyD88 and histone H3. CE denotes "cytoplasmic extract"; NE, "nuclear extract".

5.6 Effect of bromodomain inhibition on HDI response in lymphoid cell lines

Given the previously described difficulties with transfecting suspension cells (Chapter 3, Section 3.6), I anticipated that individual knockdown of implicated BRD-containing proteins or the generation of individual BRD mutant controls would likely be technically challenging and exceed the time limitations of this project. However, I reasoned that BRD inhibitors, which are small-molecule compounds, could be used as tools for probing the interaction between BRD-containing proteins and their targets, in this case acetylated MyD88. If acetylation was required for MyD88 to sensitize lymphoma cells to HDI treatment, using a broad-spectrum BRD inhibitor such as bromosporine might negatively impact on this process. Bromosporine binds to a deep, largely hydrophobic acetyl-lysine binding site within the conserved BRD fold of BRD-containing proteins and acts as a competitive inhibitor of the acetylated target proteins which would normally be bound. It has been described as a pan-bromodomain ligand, with at least low micromolar activity documented against 25 BRDs, including BRD2, BRD3, BRD4, BRDT, TAF1, PB, ATAD2, BRD9 and CBP (Brand*, et al* 2015, Hewings*, et al* 2011, Picaud*, et al* 2016); (www.thesgc.org/chemical-probes/bromosporine). In HeLa cells, bromosporine has been documented to have moderate cytotoxicity at 18µM (Brand*, et al* 2015) but in haematological cell lines bromosporine has been reported to have an IC_{50} in the low micro-to nanomolar range (Picaud*, et al* 2016).

When used at a concentration of 1µM, bromosporine was shown to induce a low amount of cleaved caspase 3 after 24 hours of treatment in both RIVA and HBL-1 cells (Figure 5.5). In RIVA cells, the amount of cleaved caspase 3 increased when cells were co-treated with bromosporine and SAHA (Figure 5.5a(i)), whereas in HBL-1 cells, the amount of cleaved caspase 3 decreased (Figure 5.5b). In RIVA cells, the combination of bromosporine and tubastatin could also be shown to lead to an increased amount of cleaved PARP on co-treatment, especially as increasing concentrations of tubastatin were used (Figure 5.5a(ii)). FACS analysis of PI-stained cells after treatment with 1µM bromosporine alone for 24 hours

only showed very small increases in sub-G1 percentage in RIVA and HBL-1 cells when compared with mock (DMSO)-treated control cells (Figure 5.5c(i) and (ii)). Taken together, if one assumes that bromosporine inhibits a bromodomain reader that acts on acetylated MyD88, these results suggest that HBL-1 cells but not RIVA cells seem to be affected in their propensity to undergo effective apoptosis after co-treatment with SAHA. It could be argued that the presence of the MyD88 L265P mutation in HBL-1 cells which has been associated with constitutive NF-kB activation requires a functional BRD for docking or assembly of multi-protein complexes that facilitate signalling through the Myddosome structure. The effect of bromosporine on HBL-1 cells showed a decrease in S phase on cell cycle analysis. Interestingly, a similar effect was observed in IL-6 neutralization experiments (New*, et al* 2016): when MyD88 was over-expressed in U2OS cells, treatment with anti-IL-6 antibody could be seen to lead to a decrease in S phase and a concomitant increase in the size of the G2 population. In fact, whilst some BRD inhibitors have been documented to directly affect IL-6 regulation in cancer cell lines (Boi*, et al* 2015, Brand*, et al* 2015, Ceribelli*, et al* 2014), this has not been observed as a dominant effect after treatment of leukaemia cells with bromosporine (Picaud*, et al* 2016). Rather, bromosporine is thought to predominantly affect the cell cycle, with sensitive cells showing a distinct G1 arrest with reduced S-phase populations (Picaud*, et al* 2016). However, these cell cycle changes were not clearly observed in either RIVA or HBL-1 cells at the drug concentrations used, and because of the broad-spectrum activity of bromosporine on BRDs, its effects on cells may be complex and non-specific, with perhaps little or no direct connection to MyD88 and MyD88 mutation status.

In contrast to bromosporine, JQ1 is a small-molecule BRD inhibitor with specific activity in the nanomolar range against BRD4, a scaffolding factor that associates with acetylated chromatin and facilitates active transcription (Trabucco*, et al* 2015). JQ1 has been shown to have promising activity in pre-clinical models of haematological malignancies including multiple myeloma, acute myeloid leukaemia and DLBCL, with its therapeutic effect thought to be

mediated mainly by a downregulation of *MYC* (Barbieri*, et al* 2013, Bhadury*, et al* 2014). Preferential localization of BRD4 at super-enhancers in DLBCL cells has been observed, and thereby establishes a rationale for evaluating JQ1 inhibition in DLBCL. In the next set of exploratory experiments, therefore, I wanted to investigate whether JQ1 would synergize with an HDI when DLBCL cells were co-treated, and whether JQ1 treatment would have a different effect to bromosporine treatment in HBL-1 cells. Etoposide, a mechanistically unrelated agent, was included as a control in these experiments.

As can be seen in Figure 5.5d, JQ1 co-treatment with SAHA in RIVA and HBL-1 cells led to an increase in cleaved caspase 3 in both RIVA and HBL-1 cells on Western Blot. Interestingly, JQ1 treatment on its own has previously been shown to induce G1 cell cycle arrest followed by either apoptosis or senescence in a panel of DLBCL cells, regardless of DLBCL subtype (Trabucco*, et al* 2015). When investigated by FACS analysis after PI staining, however, 100nM JQ1 did not affect the sub-G1 percentage of RIVA and HBL-1 cells after 24 hours of treatment. Similarly, there was no evidence of a G1 cell cycle arrest, although in both cell lines a reduction in S phase was observed (Appendix D, p 205).

Therefore, additional Western Blot and FACS data documenting the time- and dose-dependent changes in both lymphoma cell lines after JQ1 treatment would have been useful in this case. Similarly, MYC protein and mRNA levels could have been assessed to document the anticipated effect of JQ1 on *MYC* expression and helped to establish whether different pathways may come into play when cells are treated with either bromosporine or JQ1.

Figure 5.5

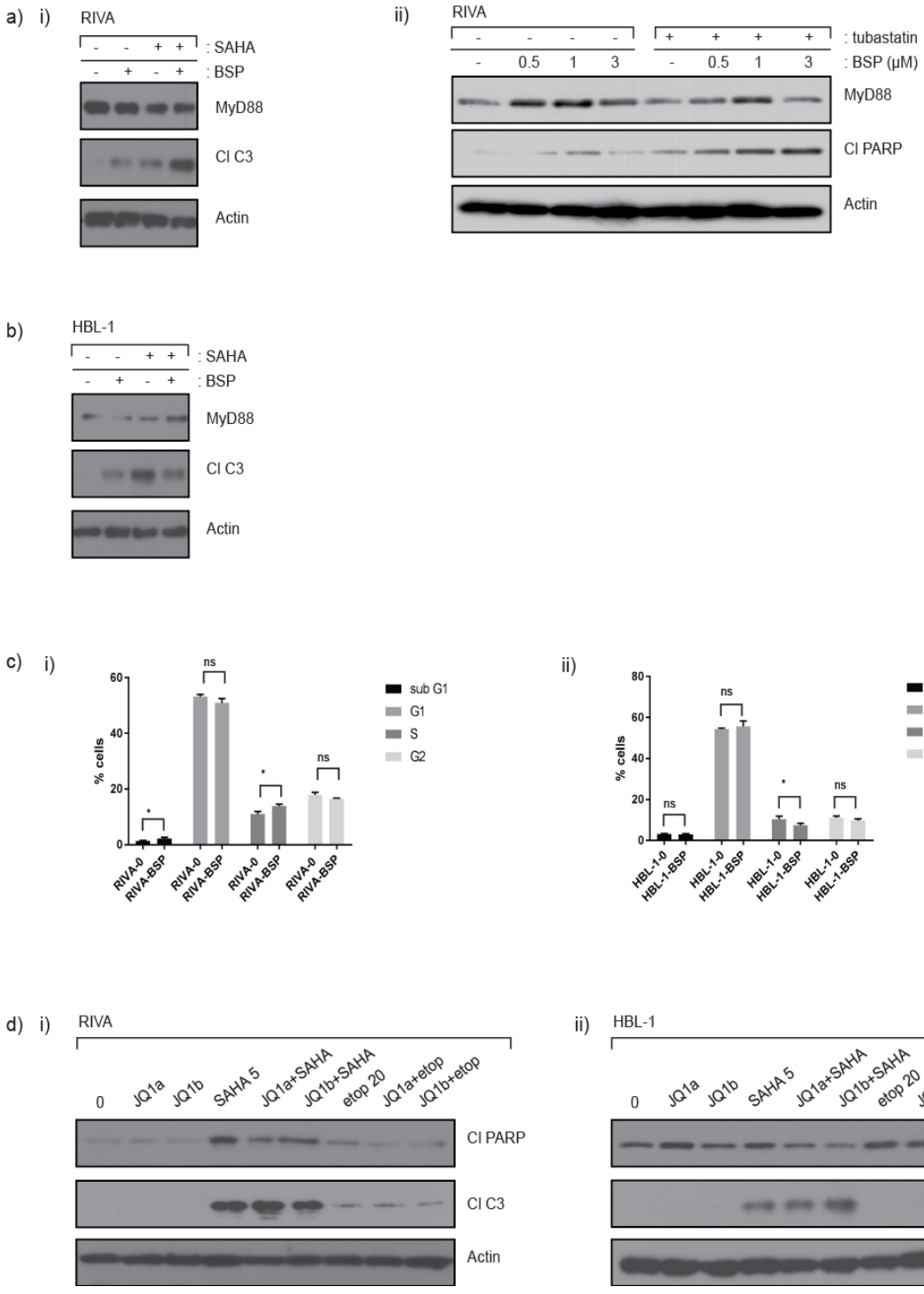

a) i)
RIVA
- - + + : SAHA
- + - + : BSP
MyD88
Cl C3
Actin
ii)
RIVA
- - - - + + + + : tubastatin
- 0.5 1 3 - 0.5 1 3 : BSP (μM)
MyD88
Cl PARP
Actin
b)
HBL-1
- - + + : SAHA
- + - + : BSP
MyD88
Cl C3
Actin
c) i)
% cells
sub G1
G1
S
G2
ns
*
RIVA-0
RIVA-BSP
ii)
HBL-1-0
HBL-1-BSP
d) i)
RIVA
0 JQ1a JQ1b SAHA 5 JQ1a+SAHA JQ1b+SAHA etop 20 JQ1a+etop JQ1b+etop
Cl PARP
Cl C3
Actin
ii)
HBL-1
MyD88

Figure 5.5 Bromodomain inhibition in lymphoma cells.

a. (i) RIVA cells were treated with bromosporine (BSP; 1μM) and SAHA (5μM), or both concomitantly. Cell lysates were immunoblotted with anti-MyD88 and anti-cleaved caspase 3 antibody; actin served as the loading control.

(ii) RIVA cells were treated with bromosporine at escalating concentrations (0.5, 1 and 3μM), with or without tubastatin (10μM). Cell lysates were immunoblotted with anti-MyD88 and anti-cleaved PARP antibody; actin was the leading control.

b. HBL-1 cells were treated as in a(i) and lysates immunoblotted as above. Both RIVA and HBL-1 cell lysates shown in a(i) and b(i) were in fact run on the same blot and the same exposures are shown for each condition.

c. RIVA (i) and HBL-1 cells (ii) were treated with bromosporine (1μM) for 24 hours before harvesting and analyzing by FACS with PI staining. Differences in cell cycle phases between mock (DMSO)-treated and bromosporine-treated cells are shown. The experiment was performed in triplicate and reflects the trend of *n*=2 biological replicates. *p* values were calculated as follows; * denotes significance; ns, non-significant.

RIVA Cell cycle phase	***p* value**
sub-G1	0.0366 *
G1	0.0867 ns
S	0.0136 *
G2	0.0529 ns

HBL-1 Cell cycle phase	***p* value**
sub-G1	0.4983 ns
G1	0.4614 ns
S	0.0418 *
G2	0.1174 ns

c. RIVA (i) and HBL-1 (ii) cells were treated with JQ1b (the active form of JQ1) at 1μM, JQ1a (the inactive enantiomer, used as an internal negative control) at 1μM, SAHA at 5μM, etoposide at 20μM, or a combination of the above compounds (as indicated), for 24 hours. Cell lysates were immunoblotted with anti-MyD88, anti-cleaved PARP, and/or anti-cleaved caspase 3 antibody; actin was used as the loading control.

5.7 Conclusion

In this final chapter of investigation, I aimed to explore the link between MyD88 acetylation, HDAC inhibition and BRD recognition. MyD88 was shown to be acetylated on one lysine residue (K132) in previous experiments carried out in Professor La Thangue's research group (New*, et al* 2016), and immunoprecipitation experiments were used to demonstrate acetylation of the endogenous protein in lymphoma cells. A CADOR array identified potential interacting BRDs that could bind to acetylated peptides derived from the MyD88 protein sequence and centered around the presumed acetylation site. Rather surprisingly, the implicated BRDs are all thought to be localized in the nucleus, a finding which prompted an evaluation of whether MyD88 can indeed be found in the nucleus of cells. Evidence from nuclear extracts in lymphoma cell lines and IHC on patient biopsies with lymphoma seems to suggest that this is indeed possible, although the mechanism and biological function of Myd88 localizing to the nucleus is not immediately apparent but may merit further investigation. Finally, targeting BRDs with a pan-specific (bromosporine) and a highly specific (JQ1) BRD inhibitor in lymphoma cells led to differential outcomes in cell fate in HBL-1 cells. These results suggest that the combination of BRD and HDAC inhibition may be useful in some subtypes of DLBCL. In fact there is additional evidence from the literature that some BRD inhibitors can induce similar sets of genes to HDI and may synergize with HDI in MYC-driven murine lymphoma (Bhadury*, et al* 2014), and combination treatments of BRD inhibitors and HDAC inhibitors are being trialled in Phase 1 trials in haematological malignancies (Berthon*, et al* 2016).

CHAPTER 6. DISCUSSION

6.1 Outcomes of project and conclusions

As stated in the Introduction (Chapter 1, Section 1.10), the aims of this research project were firstly, to try and gain a mechanistic understanding of the role of MyD88 in lymphoma cells, and secondly, to evaluate its usefulness as a biomarker in predicting the response of patients to an HDI. The central hypothesis of my thesis was based around the fact that MyD88 had been shown to score highly in a genome-wide loss-of-function screen investigating markers indicating HDI sensitivity (Fotheringham*, et al* 2009), and that previous work in adherent cancer cell lines had shown that MyD88 expression can drive IL-6 production and thereby sensitization of cells to HDI treatment (New*, et al* 2016).

6.1.1 MyD88 is highly expressed in tissue samples from patients with lymphoma

Tissue samples from patients with lymphoma were found to express MyD88 at high levels compared to tissue biopsies from patients with some commonly occurring solid tumours (Chapter 3). High levels of MyD88 expression have previously been reported predominantly in haematopoietic tissues (www.proteinatlas.org); (Choi*, et al* 2013b, Lord*, et al* 1990). Although MyD88 has also been demonstrated in solid tumours at both the protein and RNA level (www.proteinatlas.org), only a few reports have provided a comparative analysis. Strikingly, MyD88 mRNA downregulation has been found in paired cancerous and para-cancerous tissue biopsies from patients with colorectal cancer (Li*, et al* 2014), whereas, by contrast, protein levels of MyD88 were found to be upregulated in gastric cancer cells compared to surrounding normal gastric tissue (Je*, et al* 2012).

The biopsy samples analyzed as part of this project included tissue from patients with melanoma, and colorectal, prostate and breast cancers, but not gastric cancer. The very low expression levels of MyD88 in these biopsy samples may seem surprising but samples represented in Figures 3.1b and 3.1c were stained on different occasions and together with known positive controls. Clearly, the use of paired tumour/non-tumour samples and a robust

immunohistochemical analysis (with a scoring system and statistical analysis) would have allowed to quantify these findings more systematically, and therefore only limited conclusions can be drawn from the data presented here.

As expected, MyD88 was highly expressed in haematopoietic tissues (both lymph node and bone marrow). However, although there was variation between cases, no clear differences were observed between tissue samples from patients with lymphoma, and those tissue samples used as "negative" controls (i.e. non-cancerous lymph node and bone marrow samples) (Figure 3.1a): MyD88 could be seen to be expressed predominantly in the cytoplasm of cells, and in cells of both myeloid and lymphoid origin. A more detailed immunohistochemical analysis and double-labeling of cells (e.g. with anti-CD20 in order to identify the lymphomatous infiltrate that expresses MyD88) could have perhaps allowed the identification of more subtle differences in the staining pattern.

However, it is also important to highlight in this context that these non-cancerous samples do not represent a true "negative" control. The lymph node and bone marrow samples used here were all samples taken not from healthy volunteers but from patients in whom a haematological diagnosis was originally suspected but, after histopathological evaluation, not found to be present. This would have included patients with infectious conditions and inflammatory disorders where MyD88 could reasonably also be expected to be highly expressed due to the presence of a pro-inflammatory environment (Serezani*, et al* 2011, Takeuchi and Akira 2002). Therefore, cell pellets of lymphoma cells where MyD88 has been successfully knocked down would represent a "true" negative control. Given the previously reported problems with achieving knockdown in suspension cells (Chapter 3, Section 3.5 and Discussion 6.2.1 below), however, this strategy could not be pursued.

A more practical approach to comparing expression patterns in tissue samples could incorporate a scoring system as outlined in Figure 3.2 (Chapter 3) which was used to assess

HR23B expression in a recent clinical trial (Eyre et al, submitted): identifying tissue samples with known high and low MyD88 expression, for example, would provide a reliable standard to compare patient samples against, and could be incorporated prospectively into clinical trials.

An alternative approach that has been taken to assess MyD88 expression in tissues has relied on measuring MyD88 mRNA levels (Li*, et al* 2014). The implicit assumption of this approach is that changes in mRNA levels correspond to changes in protein levels but this is not always found to be true (Koussounadis*, et al* 2015, Maier*, et al* 2009): reasons for this discrepancy include differential mRNA expression, alternative splicing and post-translational modifications that may impact on protein translation or degradation. Of note, a collaboration with Professor Reuben Tooze from the Leeds Institute of Cancer and Pathology, found that MyD88 at gene expression level was not a very variable gene in DLBCL datasets, and no direct correlation between MyD88 mRNA levels and DLBCL cell of origin could be established across the 10 available DLBCL datasets (comprising 2030 DLBCL cases in total) (Professor Reuben Tooze, personal communication). If MyD88 expression at a protein level, however, can indeed be affected by its mutational status or post-translational modification, such as acetylation, IHC of patient biopsies would give a more accurate picture of inter-patient variability.

6.1.2 The MyD88-mutated cell line HBL-1 secretes IL-6, and neutralization of IL-6 can reduce the sensitivity of HBL-1 cells to HDI treatment

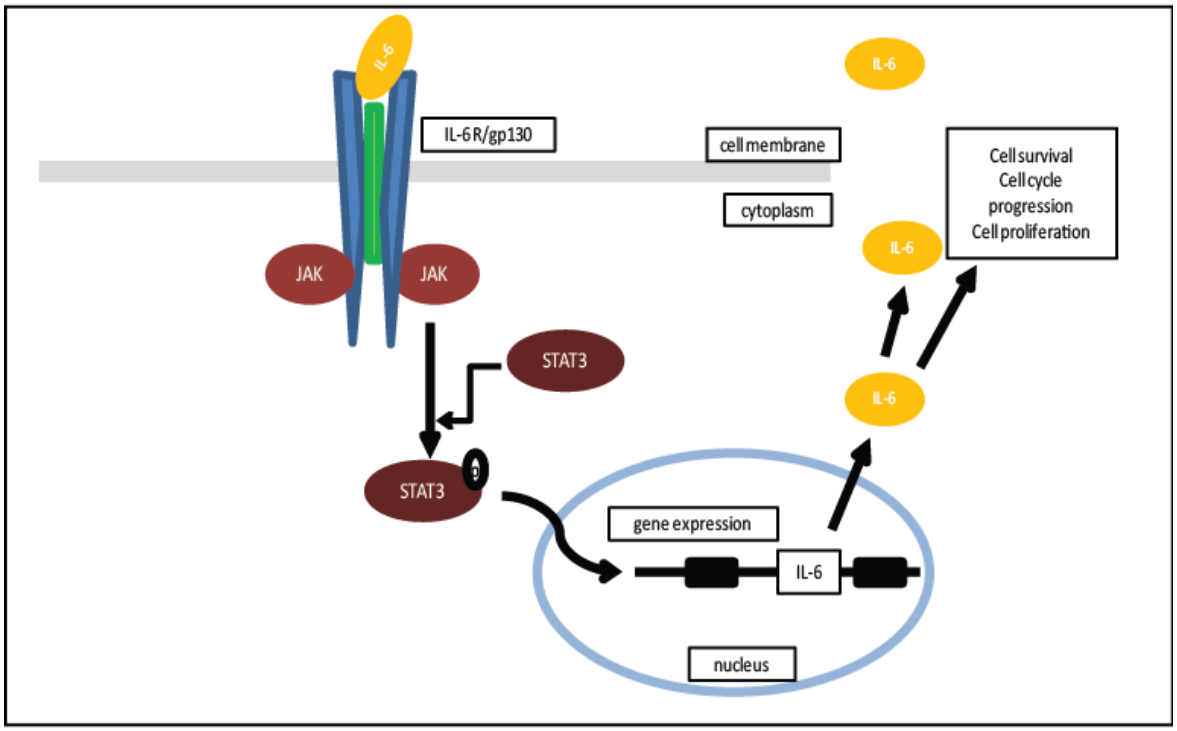
MyD88 is a known mediator of inflammatory cytokine secretion, and therefore the role of cytokines in HDI-mediated cell death was investigated. The heterozygously MyD88-mutated ABC DLBCL cell line, HBL-1, was found to express higher levels of IL-6 and display features of constitutive activation of both the NF-κB and STAT3 pathways compared to the MyD88 wild-type ABC DLBCL cell line RIVA. Moreover, the HBL-1 cell line was shown to be more sensitive to apoptosis after HDI treatment, a process that appears to be partially reversed by neutralizing

extracellular IL-6. This suggests that IL-6 may act via an autocrine loop, sensitizing cells to the effects of HDAC inhibition.

IL-6 mediates gp130/JAK-STAT3 signalling (Figure 6.1), and is thought to promote cell proliferation, tumour growth and metastasis: exogenous administration of IL-6 in a mouse model of colorectal cancer, for example, led to an increase in tumour burden (Grivennikov*, et al* 2009). Persistent STAT3 activation has also been described in many cancers, and may in part be driven by autocrine or paracrine production of IL-6 which leads to STAT3 phosphorylation. As a transcription factor, STAT3 is involved in regulating gene expression, and STAT3 target genes include BCL-X_L, c-MYC, survivin, HSP70 and cyclin D1 (Bollrath*, et al* 2009, Grivennikov*, et al* 2009). The therapeutic potential of IL-6 R blockade was explored in a mouse model of breast cancer, and shown to interfere with tumour-supportive stromal functions, such as angiogenesis, fibroblast infiltration, and myeloid suppressor cell recruitment (Chang*, et al* 2013, Chang*, et al* 2014).

In lymphoid malignancies, the role of IL-6 is well documented but complex: in myeloma and low-grade lymphomas, IL-6 is thought to create a pro-inflammatory microenvironment that favours tumour progression. Recently, in chronic lymphocytic leukaemia (CLL), IL-6 secreted by co-cultured stromal cells has also been shown to facilitate STAT3 expression, but surprisingly this led to inhibition of TLR signaling via TLR7 by activating transcription of microRNAs that prevented the translation of TNF-α and TLR7 mRNA (Li*, et al* 2015). Furthermore, IL-6 could also be shown to modulate apoptosis genes in the pre-B lymphoma cell line 1A9-M: within 24 hours of co-culture with IL-6, 1A9-M cells were found to down-regulate BCL2 gene expression, and these cells were then shown to undergo apoptosis within 48 hours (Oritani*, et al* 1999). Therefore, IL-6 may have context-dependent effects, and its role in the tumour microenvironment may also depend on the cell type it is produced by.

Figure 6.1



The classic IL-6 signalling pathway.

When IL-6 binds to its receptor (IL-6R) on target cells, the gp130 signalling chain (shown in green) is recruited. The signalling-competent IL-6R complex is a hexamer of two molecules of IL-6, IL-6R and gp130 (not shown as a hexamer here). gp130 dimerization leads to activation of associated janus kinases (JAKs), and subsequent phosphorylation of tyrosine residues on gp130, which then allows docking of adapter proteins and transcription factors such as STAT3 (depicted). Depending on the cell type and the pathways induced, different target genes are expressed. STAT3, for example, can drive the expression of further IL-6, as is illustrated here. *p*, phosphorylated.

Sources: (Burger 2013, Chang, *et al* 2014)

The interaction of IL-6 and STAT3 in DLBCL has been recognized but is not well understood. A panel of ABC DLBCL cell lines was previously shown to have higher levels of IL-6 and STAT3 expression and activation compared to GCB DLBCL (Ding*, et al* 2008). However, within ABC DLBCL tissue, others have identified a molecular signature based on STAT3-high or STAT3-low subsets. In this context, high STAT3 expression was linked to higher NF-κB activity, increased IL-6 and IL-10 secretion, proliferation and glycolysis, suggesting functional cross-talk between the JAK-STAT and NF-κB pathways (Lam*, et al* 2008).

STAT3 inhibition by either expressing a dominant negative form of STAT3, using small interfering RNA, a small-molecule STAT3 inhibitor or a JAK-STAT inhibitor, have all been described to inhibit proliferation and to trigger apoptosis in lymphoma cells in culture (Ding*, et al* 2008, Lam*, et al* 2008, Oritani*, et al* 1999).

As outlined in Chapter 4, constitutive NF-κB activity could explain the increased production of IL-6 in MyD88-mutated lymphoma cells. This may act in a positive feedback loop, increasing intracellular levels of STAT3 and pSTAT3 which, in turn, can potentiate both NF-κB pathway activity and, of its own accord, promote further IL-6 secretion (Chapter 4, Figure 4.5c). The microarray data of DLBCL datasets analyzed by the Leeds group also showed a correlation between IL-6 expression and NF-κB activation but STAT3 expression was not investigated in this context, and MyD88 expression again could not be linked to IL-6/NF-κB due to its invariant status in some of the datasets (Professor Reuben Tooze, personal communication).

IL-6 neutralization, as described in Chapter 4 (Section 4.3), may therefore have several different effects on lymphoma cells: firstly, if HDIs predominantly target actively proliferating cells (Reichert*, et al* 2012), decreasing the levels of paracrine IL-6 could lead to a delay in cell cycle progression (New*, et al* 2016) and thereby affect the influence of HDIs on intracellular events such as DNA repair or protein quality control (Chapter 1, Section 1.6.6). Secondly, lowering the levels of IL-6 through neutralization could also alter the expression and balance of

pro-and anti-apoptotic proteins, thereby blunting the effect of an HDI. Although a differential effect of IL-6 neutralization on different lymphoma cell lines could be demonstrated by FACS analysis and on immunoblot, the mechanism through which these changes operate remains unclear. My experiments did not measure BCL2 protein expression or inhibit IL-6 by alternative means such as for example IL-6R blockade. Moreover, a comparison of the proliferation index of the different cell lines before and after neutralization of IL-6 would have been useful but also difficult to interpret due to the confounding effects of cell density and passage number on the result, and cells were not synchronized for these experiments which may explain why no clear effect on cell cycle progression could be demonstrated.

The MyD88 L265P mutation has been implicated as a driver of pro-inflammatory cytokine production, and therefore MyD88 mutation status in DLBCL may be an important hallmark of pathways that can be targeted with small-molecule inhibitors. Importantly, as demonstrated by increased levels of IL-6 in the RCK8 DLBCL cell line, however, measuring IL-6 alone may not be sufficient to predict for a response to HDAC inhibition (Chapter 4, Section 4.2).

It would be interesting to investigate a possible correlation between MyD88 mutation status and IL-6 expression using microarray data, and this could be an area of future investigation.

6.1.3 MyD88 may be acetylated and several potential interacting bromodomain readers can be identified using a CADOR array

There is increasing evidence that HDACs have a role in mediating the acetylation status of non-histone proteins (Chapter 1, Section 1.6.3). Previous work in U2OS cells identified a lysine residue on MyD88 which could be acetylated, and a direct interaction between HDAC6 and MyD88 was demonstrated in immunoprecipitation experiments (New*, et al* 2016). Therefore, determining whether acetylated MyD88 can interact with a specific bromodomain reader was of particular interest, not least because there has been a growing recognition that targeting

the protein-protein interaction modules of bromodomain readers with small-molecule inhibitors has been shown to be a viable therapeutic approach in molecular medicine (Filippakopoulos*, et al* 2010, Muller*, et al* 2011). A CADOR array with acetylated MyD88 peptide-derivatives identified several potential interacting BRD-containing proteins (Chapter 5, Section 5.3) but unfortunately due to technical difficulties and lack of time I was unable to establish their relative significance in lymphoma cells.

Acetylation can influence proteins in different ways, for example by affecting protein stability and turnover, protein localization or protein-protein interactions. Acetylation has been shown to increase the stability of WRN (Werner Syndrome ATP-dependent helicase), a protein involved in DNA damage repair, by reducing its ubiquitination (Li*, et al* 2010); similarly, deacetylation of the tumour suppressor protein MST1 (mammalian STE20-like kinase 1) by HDAC6 induced its premature degradation and promoted the growth of breast cancer cells (Li*, et al* 2015).

Demonstrating the acetylation status of endogenous MyD88 in lymphoma cells proved difficult and several factors may have contributed to this: for example, due to its involvement in the Myddosome (Chapter 1, Section 1.5.2), MyD88 may be present in an aggregated state and therefore more difficult to precipitate, and in addition, MyD88 protein may not be present in large amounts within the cell which would make it more difficult to extract. MyD88 in the heterozygously mutated HBL-1 cell line appeared to be less stable than MyD88 in RIVA cells (Chapter 3, Figure 3.3e), a finding that could be due to either a new steric property conferred by the mutation itself, or a change in the post-translational modification of the protein. In the case of lysine acetylation, this would be an indirect effect of the L265P mutation, as the lysine residues of interest identified by mass spectrometry and used in the CADOR array are at amino acid positions 132 and 128, respectively. Maria New from Professor La Thangue's group was able to show that the K132R mutant isoform of MyD88, which due to the substitution of the lysine residue cannot be acetylated, had a longer half-life than wild-type MyD88. Under

conditions of hyperacetylation, caused by HDAC inhibition or depletion of HDAC6, for example, MyD88 protein stability therefore would be expected to be low, resulting in higher turnover. Of note, there are also several ubiquitination sites in the TIR domain (Table 6.1), and it is possible that the turnover of the MyD88 protein is regulated by a balance between several post-translational modifications. Ascertaining differences in the acetylation status of the endogenous MyD88 protein in the HBL-1 cell line which is heterozygous for MyD88 L265P, could not be shown by immunoprecipitation in my experiments, and thus, a mass spectrometric approach would have been more useful. It is also likely that changes in MyD88 protein acetylation are dynamic and dosage-dependent (i.e. the presence of the L265P mutation could confer changes in the stability of the acetylated MyD88 protein and affect the interaction or equilibrium with the acetylated wild-type MyD88 protein) which could account for the changes in HDI sensitivity observed between the two ABC DLBCL cell lines. A possible mechanism of how MyD88 levels and acetylation status affect HDI sensitivity is outlined in Figure 6.2. In an analysis of DLBCL patient datasets by the Leeds group, MyD88 expression in ABC DLBCL correlated with a subgroup-specific cluster of genes which exhibited distinct ontological relationships compared to GCB DLBCL: GO cluster analysis revealed a high representation of genes encoding lysine acetylation targets, suggesting a potential wider role for lysine acetylation mechanisms in ABC DLBCL (New*, et al* 2016). Moreover, several other proteins involved in the TLR4 signalling pathway, such as NF-κB and IRF3, have been found to be targets of acetylation, and therefore these, together with MyD88, may represent a group of proteins that are subject to acetylation control and under normal conditions serve to fine-tune cytokine production as part of the innate immune response (Hu*, et al* 2013). In the future, more specific acetyl-lysine antibodies and more sensitive mass spectrometric screening techniques should allow a more comprehensive characterization of protein acetylation sites.

Table 6.1 Reported post-translational modification sites in the Myd88 protein, phosphorylation sites are represented in blue, ubiquitination sites in red.

Residue	Modification
K95	ubiquitination
K190	ubiquitination
K231	ubiquitination
S244	phosphorylation
K250	ubiquitination
Y257	phosphorylation
Y276	phosphorylation
K291	ubiquitination

Source: www.phosphosite.org

Figure 6.2

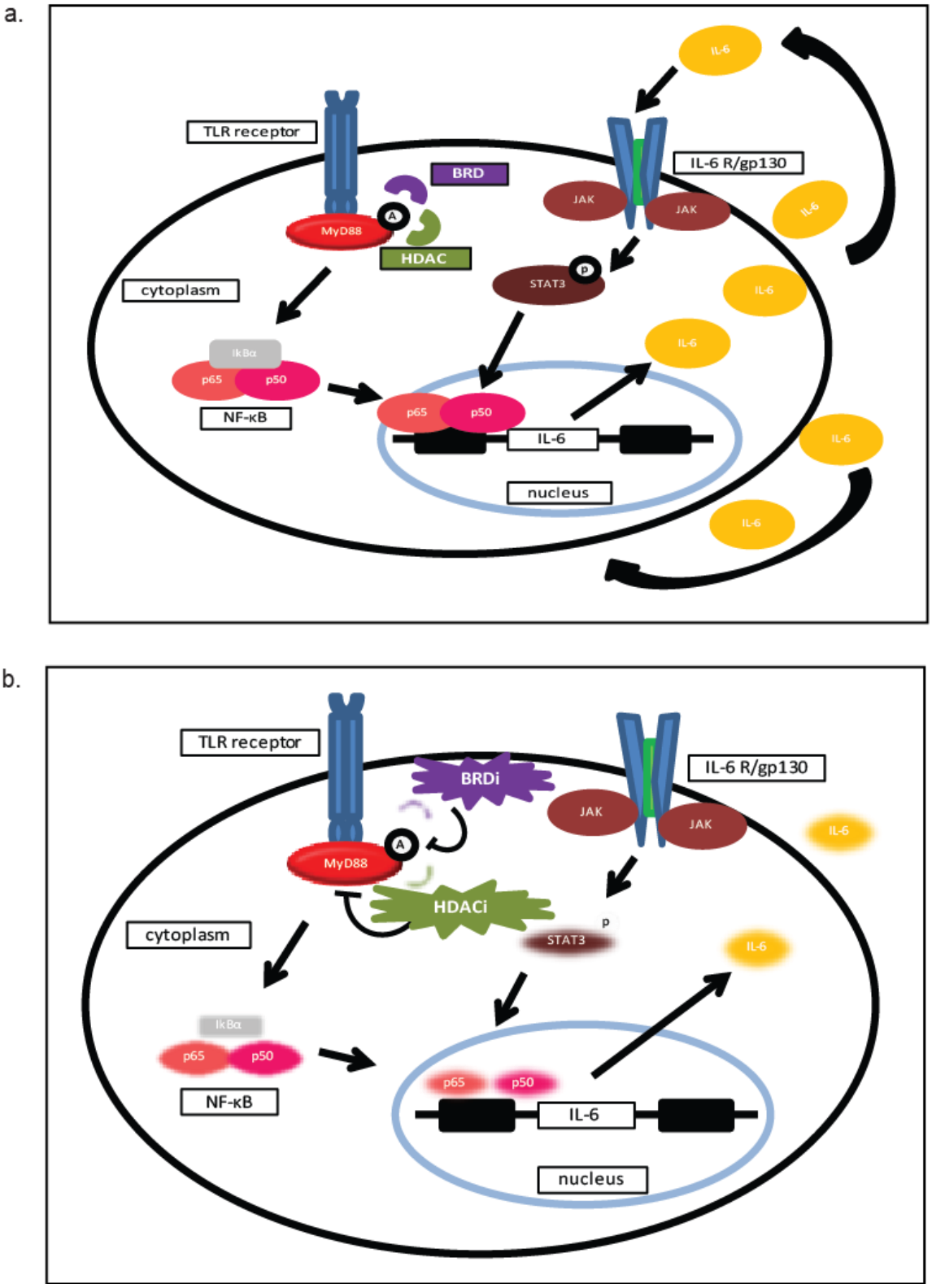

a.
TLR receptor
BRD
MyD88
A
HDAC
cytoplasm
IkBα
p65
p50
NF-κB
JAK
JAK
IL-6 R/gp130
STAT3
p
IL-6
IL-6
IL-6
IL-6
IL-6
p65
p50
IL-6
nucleus
b.
TLR receptor
BRDi
MyD88
A
HDACi
cytoplasm
IkBα
p65
p50
NF-κB
JAK
JAK
IL-6 R/gp130
STAT3
p
IL-6
p65
p50
IL-6
nucleus

Figure 6.2 Model depicting the putative roles of MyD88, STAT3 and IL-6.

In this model, TLR-signalling through MyD88 (and especially its mutated form, MyD88 L265P) augments NF-κB activity and leads to expression of target genes such as IL-6. Secreted IL-6 acts through an autocrine mechanism by binding to the cell-surface IL-6 receptor, activating JAKs which in turn can phosphorylate STAT3 and activate STAT3 signalling, thus promoting further IL-6 production and cell proliferation (Panel a). MyD88 can be de-acetylated by HDACs, such as HDAC6, which serve as a target for HDAC inhibition. Bromodomain-containing proteins (BRDs) may also be involved in modulating the acetylation status of MyD88 and therefore may be targeted by BRD inhibitors (BRDi).

Through inhibition of HDACs or BRDs (faded symbols in Panel b), it is envisaged that NF-κB activity decreases and less IL-6 is produced, resulting in an anti-proliferative effect on lymphoma cells. Simultaneous blocking of the NF-κB and JAK-STAT pathways by adding a JAK inhibitor such as ruxolitinib could potentially augment this effect (see text for details, Section 6.3.3).

6.2 Project limitations

6.2.1 Manipulation of MyD88 levels in suspension cells

One of the major limitations of this project was the inability to develop an approach that could consistently knock down MyD88 in lymphoma cells. As outlined in Chapter 3, multiple techniques were used, including transient chemical knockdown, electroporation, nucleofection, and lentiviral transduction. In the literature, most success in transfecting lymphoma cells in suspension appears to have been achieved using chemical transfection or lentiviral transduction (Avbelj*, et al* 2014, Into*, et al* 2010, Ngo*, et al* 2011), but in my hands, despite following the recommended optimization steps, this was unfortunately not achieved. It would have been instructive to try several of these approaches in suspension cell lines other than RIVA and HBL-1, a strategy which may have provided better insights into how best to optimize a given protocol.

Precise genome editing using the CRISPR-Cas9 system is now also a possibility (Ran*, et al* 2013), and in the future, this may prove a valuable tool in mediating MyD88 knockdown but also enable specific mutations such as L265P to be engineered into wild-type cells. However, introducing the expression plasmid into the cells also requires transfection which may be a rate-limiting step affecting the success of the procedure.

Instead of transfection or transduction, a small-molecule inhibitor (T6167923) was used to achieve a chemical form of "knockdown". Ultimately, both chemical and biological approaches would have ideally complemented each other.

6.2.2 HDAC and BRD specificities

HDAC6 was identified as the likely HDAC interacting with MyD88 (New*, et al* 2016), and inhibition of HDAC6 with tubastatin caused apoptosis in lymphoma cells. Whilst HDAC6 has been described as the only cytoplasmic HDAC, other HDACs are able to shuttle between the nucleus and the cytoplasm (Chapter 1, Section 1.6.4), and could potentially therefore also have

a role in acetylating MyD88. Moreover, the potential interacting BRDs identified in the CADOR array are mainly nuclear, and there is some evidence that MyD88 may localize to the nucleus in some circumstances (Chapter 5, Section 5.5). In order to investigate which HDACs and BRDs truly interact with MyD88, therefore, one approach would be to systematically knock down individual HDACs or BRDs and document MyD88 interactions and the effect of HDI treatment under those conditions, thereby establishing individual MyD88-HDAC/BRD functional dependencies. In addition, using knock-down studies in conjunction with chemical inhibition (as outlined above) would be an approach that could help to identify potential targeted agents.

6.2.3 Cell fate measurements

HDIs have many potential therapeutic outcomes, as outlined in Chapter 1 (Section 1.6.6). In my experiments I measured apoptosis and cell viability in response to HDAC inhibition. MTT assays are useful for assessing the effect of a drug (or several drugs) on cell metabolism but require accurate plating of cell numbers and precise drug dispensing. These assays can be done at scale but would perhaps give the best and most consistent results in an automated setting.

Apoptosis was assessed by demonstrating cleaved PARP and/or cleaved caspase 3 on immunoblot, a semi-quantitative approach, and measuring sub-G1 percentage by FACS. Annexin V staining could be used to better distinguish viable from apoptotic and necrotic cells. Currently, no good biomarkers are available to measure necrosis, which is most commonly associated with injury and trauma, and not usually recognized as an outcome of HDI treatment. Annexin V staining would therefore be able to provide more information on how cells die under HDI treatment.

Autophagy, a catabolic process during which cytosolic components and organelles are degraded in order to recycle key cellular materials, has been increasingly recognized as an important mechanism in the initiation and progression of cancer (Choi*, et al* 2013a), and HDI

treatment can induce autophagy in human cancer cell lines (Rikiishi 2011). This could be assessed either by electron microscopy, which is a specialized and time-intensive technique, or, more commonly, by measuring autophagocytic markers such as LC3 and LC3-II. Importantly, SAHA has been found to activate autophagy in cancer cells, and this is thought to act as a pro-survival mechanism (Gammoh*, et al* 2012). Quantifying the proportion of cells undergoing autophagy on HDI treatment could also help to optimize the therapeutic effects of an HDI by targeting autophagy as part of the treatment strategy.

6.2.4 Cell lines

Most of the experiments detailed above were only carried out in two lymphoma cell lines: RIVA and HBL-1. MyD88 mutation status was ascertained for these two cell lines, and the HBL-1 cell line in particular is frequently referenced in the literature as an example of a MyD88 L265P-mutated ABC DLBCL cell line (Mondello*, et al* 2017, Ngo*, et al* 2011). As described in Chapter 4 (Section 4.3), there is only a limited number of available DLBCL cell lines that carry the MyD88 L265P mutation, and most of these are heterozygously mutated. A limitation of the experiments carried out, therefore, is the small number of cell lines that were used.

The original loss-of-function screen which identified MyD88 as a potential biomarker was carried out in the U2OS osteosarcoma cell line, and subsequent experiments that determined the role of MyD88 as HDI-sensitivity determinant continued to use this cell line because it is a well-established cancer cell line model and Professor La Thangue's laboratory has great experience of using this cell system. An extrapolation of the results presented here to, ideally, a panel of both ABC and GCB cell lines, as well as other lymphoid cell lines (e.g. LPL cell lines), would therefore have been desirable in order to make more conclusive statements about the HDI sensitivity of DLBCL cell lines in general. Similarly, investigation of the contribution of other cytokines which were detected to be elevated in some of the cell lines used, for instance TNF-α (in RIVA cells) and IL-10 (in HBL-1 cells), instead of focusing solely on IL-6, would have helped

with dissecting the functional contributions (if any) of these different cytokines to HDI sensitivity.

Finally, the conclusions that can be drawn from cell line models about the behaviour of tumours in vivo are generally also limited by the fact that there are clear genomic differences between cancer cell lines and tumour samples, with cell lines lacking the complexity and heterogeneity of a tumour as well as the influence of the microenvironment on the evolution and progression of a tumour (Domcke*, et al* 2013, van Staveren*, et al* 2009).

6.2.5 Use of small-molecular agents

Small-molecule agents including HDIs, BRD inhibitors and a MyD88 inhibitor (T6167923) were used in these experiments, both to assess cytotoxicity, and also to chemically inhibit specific components of the TLR signalling pathway. The main limitations of this approach are twofold: firstly, HDIs and BRD inhibitors may be specific for more than one particular HDAC (or BRD) isoform, and secondly, all these compounds could potentially have off-target effects.

SAHA is known to be a pan-HDAC inhibitor, whereas tubastatin is an HDAC6-specific HDI, albeit with some selectivity for other HDAC isoforms (e.g. HDAC8) at higher concentrations (Gryder*, et al* 2012). Similarly, bromosporine is a pan-BRD inhibitor, but JQ1 predominantly inhibits the BET family of BRDs, with increased selectivity for BRD4 (Brand*, et al* 2015). Comparisons between pan-inhibitors and more selective agents may, however, still be beneficial in order to dissect their effects on different biological pathways. Therefore, selective agents can be informative with regards to targeting individual components of a particular biologic pathway, if potential drug effects on other isoforms are taken into account.

Off-target effects are another important consideration when using small-molecular agents: for example, in the clinical setting, many HDIs have been shown to have a degree of cardiac toxicity (Gryder*, et al* 2012), which suggests that other cellular pathways than those under investigation can be affected which is not always immediately apparent.

Taken together, these considerations show that a complementary approach of small interfering RNA knockdown and use of a selective chemical inhibitor may be a more robust way of investigating specific cellular targets.

Another important point in this context is how drug combinations and their respective concentrations can be determined. In the experiments described above, drug concentrations were chosen based on the existing literature and established IC_{50} values. However, the rationale of many drug combinations is to achieve synergy and lower individual drug concentrations, and therefore using a combination of screening technology and computational methods such as for example the high-throughput platform described by Matthews Griner et al, allows exploring multiple drug combinations at a wide range of dosages (Mathews Griner*, et al* 2014).

6.2.6 IHC staining consistency

In order to be able to make meaningful comparisons between IHC samples, it is important to have a reliable antibody that gives reproducible results. In the initial stages of the project, I was able to optimize a staining protocol for a MyD88 antibody with the help of Dr Soilleux, consultant histopathologist at OUH (described in Chapters 2 and 3). As expected, MyD88 was found predominantly in the cytoplasm of cells and showed strong expression in haematopoietic tissue. However, subsequent aliquots of the same antibody (but different Lot numbers) were found to be highly variable in detecting MyD88 expression (including in tissue samples that had been validated as expressing high levels of MyD88 previously). Both manual and automated staining techniques were used to try and optimize these new antibodies but with negative results. This technical issue therefore limited the use of IHC staining for the evaluation of MyD88 expression in a cohort of patients treated on a trial with the novel HDI CXD101 (Eyre et al, submitted).

6.3 Future work

6.3.1 MyD88 acetylation status, and implicated bromodomains (readers) and histone acetyltransferases (writers)

Transfected Flag-tagged MyD88 could be shown to be acetylated on lysine K132 (New*, et al* 2016). Immunoprecipitated endogenous MyD88 gave a faint acetylation band on immunoblot, as shown in Chapter 5 (Section 5.2), and acetylated MyD88-derived peptides were found to have a number of potential bromodomain interactors on CADOR array (Chapter 5, Section 5.3). Similarly, other proteins involved in the TLR signalling pathway have been shown to be acetylated (Hu*, et al* 2013), suggesting that acetylation of non-histone proteins may play an important part in TLR signalling, perhaps allowing the integration of different cellular inputs and thereby fine-tuning the downstream response and conferring a degree of plasticity.

Acetylation may influence protein stability, either directly or indirectly by affecting other post-translational modifications such as for example ubiquitination which can target proteins for degradation. Therefore, extracting MyD88 from lymphoma cells and identifying acetylation and ubiquitination sites by mass spectrometry under conditions of hyperacetylation (e.g. after HDI treatment) and deacetylation (e.g. HDAC over-expression) could help to ascertain whether there are multiple sites that can be modified on the wild-type protein. Several ubiquitination sites on MyD88 have already been described (Table 6.1). This approach could then be extended to cells that are known to carry MyD88 mutations to allow a comparison of whether mutated isoforms of MyD88 behave differently under the same biological conditions.

Due to time constraints, it was not possible to further characterize the interactions between MyD88 and its potential BRD interactors. Initially, as outlined in Chapter 5 (Section 5.4), the implicated interactions would have to be validated in vitro, before investigating these further within cells. Measuring the interactions between endogenous proteins can be limited by several factors, such as the amount of protein in the cell, the strength of the interactions and

the fact that some BRDs may have multiple cellular substrates, but techniques such as immunoprecipitation and immunofluorescence could be considered. Finally, to further confirm these interactions, chemical inhibition or knockdown of the implicated BRDs and observation on the effects of HDAC inhibition in lymphoma cells could then be used.

Another important aspect not addressed in this project is the role of the histone acetyltransferase (HAT) that may be responsible for acetylating MyD88. Frequent inactivating structural alterations in the two ubiquitous HATs, CBP and p300, have recently been described in lymphoma: in an analysis of 134 cases of DLBCL, CBP mutations, which were usually mono-allelic, were identified in 32% of GCB DLBCL (21/65) and 13% of ABC DLBCL (9/69). Moreover, mutant CBP/p300 proteins were found to be deficient in acetylating p53 and BCL6, consequently deregulating the DNA damage response within the cell (Pasqualucci*, et al* 2011a). Given the fact that CBP/p300 fulfill many roles in transcriptional activation and gene regulation, it is difficult to predict which other cellular pathways may be affected by a reduction in HAT dosage. Interestingly, CBP/p300 also contain BRD domains (Filippakopoulos*, et al* 2012) and are predominantly nuclear in their localization, and as MyD88 is thought of as predominantly cytoplasmic, and no interactions between MyD88-derived peptides and CBP/p300 were observed in the CADOR array (Chapter 5, Sections 5.3), other HATs may be implicated in acetylating MyD88. Therefore, a screen with specific small-molecule inhibitors of different HATs (or systematic HAT knockdown) could be carried out to observe the effects of HAT inhibition on MyD88 acetylation in lymphoma cells. Several different DLBCL cell lines with differential CBP/p300 mutation status are known (Andersen*, et al* 2012) and could be used in a comparative screen of this type. Prospective incorporation of HAT mutation screening in clinical trials evaluating the effects of HDIs could therefore also help to elucidate the reasons behind the heterogeneous clinical responses that have been observed in response to HDI treatment in DLBCL.

From a clinical point of view, it would be very useful to collect information on the mutational status and expression (ideally both at the mRNA and protein level) of HDACs, HATs and BRDs systematically in tissue samples from patients with DLBCL. As modern DNA sequencing technologies continue to advance and become more widely available to allow large-scale characterization of tumour genomes, a clearer picture of the acetylation network within cells will emerge and allow more meaningful conclusions on the impact of HDIs to be drawn. One promising approach in this context has been the combined use of whole exome and RNA sequencing to analyze 1000 DLBCL genomes and associate the spectrum of genetic mutations with clinical outcome (Zhang*, et al* 2016).

6.3.2 Introducing targeted mutations in MyD88 with the CRISPR-Cas9 system

CRISPR-Cas9 has recently emerged as a new powerful tool for gene manipulation (Ran*, et al* 2013). In terms of advantages over siRNA, CRISPR-Cas9 can induce an irreversible absolute null phenotype or can be used to introduce precise mutations into genes as it targets DNA directly. Whilst siRNA techniques have well-described off-target effects, the potential for off-target effects of the CRISPR-Cas9 system still needs to be fully characterized (Unniyampurath*, et al* 2016). As mentioned above, plasmid delivery for the CRISPR-Cas9 system in suspension cells would require the optimization of transfection techniques (Section 6.2.1), as would be necessary for siRNA. However, applying CRISPR-Cas9 to lymphoma cells in order to either knock out MyD88 or introduce precise MyD88 mutations such as L265P may greatly improve our understanding of how MyD88 influences TLR signalling. Thus, it would be possible to ascertain how MyD88 knockout in ABC DLBCL cells affects NF-kB activation and cytokine signalling; introducing the MyD88 L265P mutation into wild-type MyD88 ABC DLBCL cells and comparing these to ABC DLBCL cells that are already (naturally) MyD88 L265P-mutated could give important insights into cross-talk between different biological pathways.

6.3.3 Identifying potential drug combinations

As shown here (Chapter 4, Section 4.5) HBL-1 cells were observed to have activated NF-kB and STAT3 pathways. Further work to determine whether a combination of a JAK inhibitor with an HDI may synergistically improve cell killing was commenced but not completed. Identifying targetable mutations or pathways in DLBCL is a promising approach that would allow the delivery of specifically tailored combination therapy with the additional aim of minimizing toxicity. In order to determine the dose of each drug, MTT cell viability assays could be carried out for each drug individually, and then increasing concentrations of each drug could be tested together, and isobolograms could be used to determine additive, synergistic or antagonistic interactions between the drugs under investigation (Tallarida 2006).

Interestingly, the cytoplasmic BRD, BRWD3, has been implicated in JAK-STAT signalling (Muller*, et al* 2005). Therefore, if BRWD3 was implicated in recognizing MyD88 acetylation, the effect of BRD inhibition at the intersection of NF-kB and JAK-STAT signalling pathways could be explored. Mechanistically, this could be carried out using a range of different approaches such as either specifically targeted small-molecule inhibitors, siRNA knockdown, or inducible cell lines.

In this context it is also worth noting that bortezomib, a proteasome inhibitor, has been shown to have synergistic activity with HDIs in preclinical models of multiple myeloma. The basis of this synergistic activity is likely to be multifactorial in origin and is thought to include disruption of protein degradation and effects on the tumour microenvironment (Hideshima*, et al* 2011). Acetylation of MyD88 in lymphoma cells could affect its stability and therefore impact on its degradation via the proteasome pathway. This hypothesis could be investigated in the first instance by using proteasome inhibition (e.g. with the well-established proteasome inhibitors velcade or MG-132) and monitoring MyD88 expression, stability and acetylation status.

This project has come up with some potential leads for drug combinations, based on the analysis of different cellular signalling pathways. In conjunction with growing knowledge of targetable mutations in DLBCL, it is likely that in the near future high-throughput combination screening of a rationally selected drug versus a library of, potentially hundreds, approved and investigational drugs will be used to identify promising combination treatment strategies.

6.3.4 Correlating MyD88 protein expression and MyD88 mutation status with patient outcome

One of the initial aims of this project was to optimize an IHC staining protocol that would allow quantification of MyD88 expression in patient tissue samples from a Phase I trial evaluating the novel HDI CXD101 in patients with advanced malignancy. This aim was only partially achieved due to the variation observed in MyD88 staining depending on the antibody Lot number. In addition, no antibody that could specifically detect the MyD88 L265P mutation was commercially available (although there is one antibody available now (July 2017): https://www.civicbio.com/product/anti-myd88-l265p-rabbit-monoclonal-antibody-clone-rm5/). Once better antibodies become available, though, it would be worthwhile to assess MyD88 protein expression in patient samples and correlate this with outcome after HDI therapy. Furthermore, it would be useful to determine whether particular elements of the tumour express MyD88 more highly than others (e.g. expression of MyD88 in the microenvironment versus in the lymphoma infiltrate). Finally, determination of MyD88 mutation status, either by IHC or by sequencing would provide important information in conjunction with patient outcome data.

6.3.5 Measuring circulating free DNA from patients with DLBCL

Further development of MyD88 L265P as a blood-based biomarker (liquid biopsy) would help to provide important information on DLBCL at diagnosis and relapse as well as during treatment. The concept of measuring disease-related mutations in free circulating DNA is relatively new and has not entered routine clinical practice. It offers several advantages

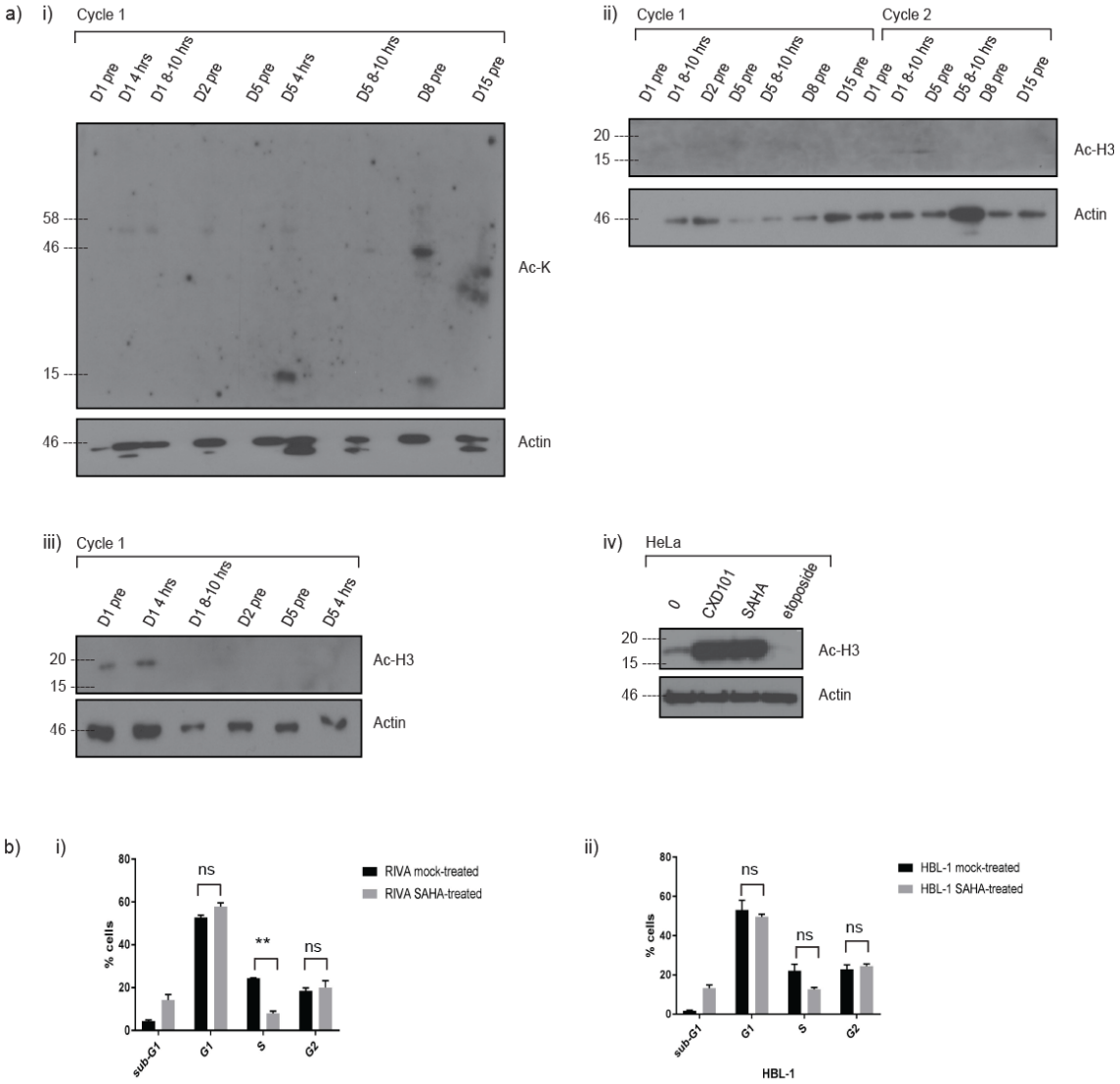
compared to tumour biopsies, such as ease of collection (through a simple blood test), and the availability of samples at any time during the disease course, allowing real-time detection and monitoring of biomarker dynamics (Camus*, et al* 2016, Cree 2015). Digital PCR assays for the detection of MyD88 L265P and two other recurrent mutations in DLBCL, exportin-1 (XPO1) E571K and EZH2 Y641N, were recently developed in a proof-of-concept study: the authors were able to show that they could detect mutations in plasma circulating cell free DNA (cfDNA) with a sensitivity of 0.05% (Camus*, et al* 2016). The ability to detect MyD88 L265P and track minimal residual disease through analysis of cfDNA, therefore, would be a useful companion test for targeted therapies that could be incorporated into clinical trials.

6.4 Project Summary

Table 6.2 Aims and main findings of this project.

Aim 1: Develop a mechanistic understanding of MyD88 in lymphoma cells	
Main findings	
Differences between MyD88 L265P-mutated and non-mutated DLBCL cell lines HBL-1 and RIVA influence HDI sensitivity	• HBL-1 cells are more sensitive to HDAC inhibition compared to RIVA cells • Chemical inhibition of MyD88 aggregation with a small-molecule inhibitor partially reverses HDI sensitivity in RIVA cells • HBL-1 cells express more IL-6 than RIVA cells • Neutralization of IL-6 in HBL-1 cells partially reverses HDI sensitivity • HBL-1 cells display higher protein levels of STAT3 and pSTAT3, which can also be induced by exogenous addition of recombinant IL-6
Acetylation status of endogenous MyD88 in lymphoma cells, identification of potential bromodomain readers and response to bromodomain inhibition	• MyD88 in lymphoma cells appears to be acetylated • Using a CADOR array, several BRD-containing proteins are identified that can potentially interact with MyD88-derived acetylated peptides • Both RIVA and HBL-1 DLBCL cell lines display sensitivity to combined bromodomain and HDAC inhibition
Aim 2: Explore the potential of using MyD88 as a biomarker for lymphoma that may respond to HDAC inhibition	
Main findings	
MyD88 is differentially expressed in tumour tissues	• MyD88 is highly expressed in tissue samples from patients with lymphoma (LPL and DLBCL) • Lower levels of MyD88 protein expression occurs in some solid tumours (including colorectal, prostate and breast cancer) • Haematopoietic tissue in general (lymph node and bone marrow not involved by lymphoma) may also express high levels of MyD88

APPENDIX A



Outcome of HDI treatment in patient PBMCs and lymphoid cell lines.

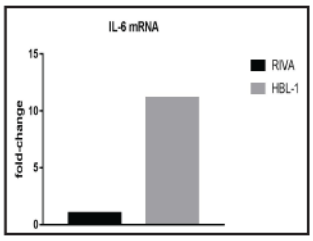
a. (i-iii) PBMC lysates from patients treated with the HDI CXD101 were immunoblotted with either anti-acetyl-lysine (Ac-K) or and anti-acetylated Histone H3 (Ac-H3) antibodies to determine histone acetylation; actin served as the loading control. *D*, day of treatment cycle; *pre*, blood taken pre-taking of the drug; number of hours after taking CXD101 is indicated.

(iv) HeLa cells were either mock-treated (0), or treated with CXD101 (10µM), SAHA (5µM), or etoposide (20µM), for 24 hours, harvested and lysates immunoblotted with anti-acetylated Histone H3 (Ac-H3) antibody; actin served as the loading control.

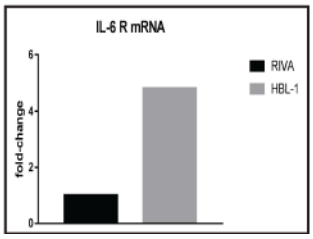
b. RIVA (i) and HBL-1 (ii) cells, in triplicate, were treated with SAHA (5µM for 24 hours), harvested and analyzed by PI staining on flow cytometry. Cell cycle profiles are shown (**denotes significant *p* values; *ns*, non-significant).

APPENDIX B

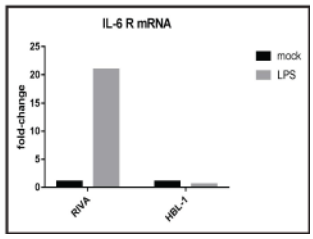
a)



b) i)



ii)



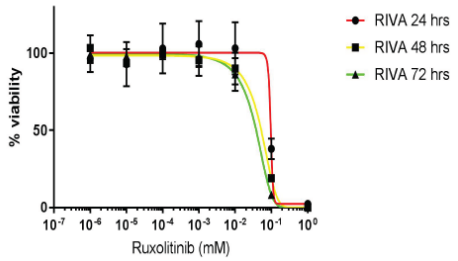
IL-6 and IL-6 R transcript levels in RIVA and HBL-1 cells.

a. Differences in IL-6 transcript expression are shown in RNA extracts from cell pellets from RIVA and HBL-1 cells. IL-6 transcript levels were normalized to actin expression in each cell line but are represented as fold-change increase to expression in RIVA cells. The example shown is representative of the trend observed in biological duplicates.

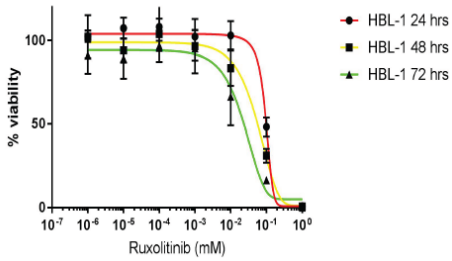
b. Differences in IL-6 receptor (IL-6R) transcript expression are shown in RNA extracts from cell pellets from RIVA and HBL-1 cells before (i) and after (ii) stimulation with LPS (100ng/mL). IL-6R transcript levels were normalized to actin expression in each cell line but are represented as fold-change increase to baseline expression in mock-treated RIVA and HBL-1 cells, respectively. The example shown is representative of the trend observed in biological duplicates.

APPENDIX C

a) i)



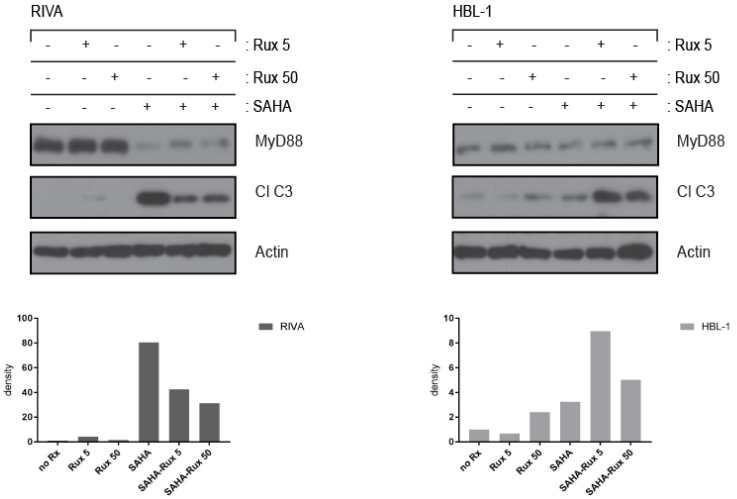
ii)



iii)

Ruxolitinib IC50 (μM)	24 hrs	48 hrs	72 hrs
RIVA	57.57	15.44	14.29
HBL-1	64.23	21.12	11.02

b) i)

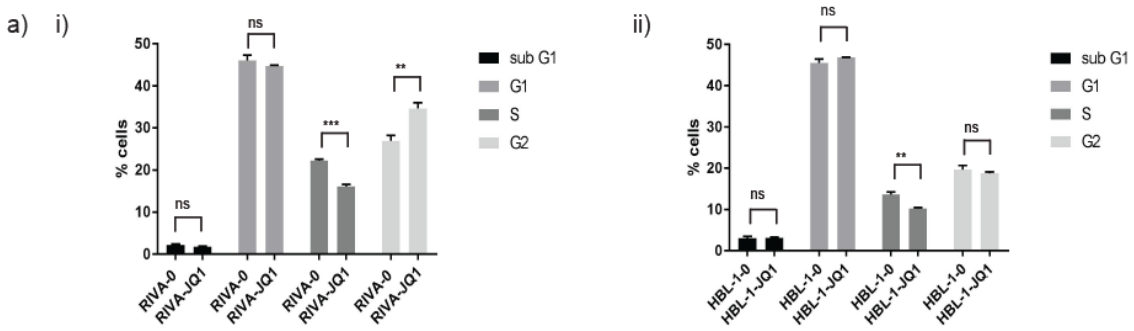


Response of RIVA and HBL-1 cell lines to ruxolitinib and SAHA treatment.

a. RIVA (i) and HBL-1 (ii) cells, in triplicate, were compared by MTT viability assay over 24, 48 and 72 hours of treatment with ruxolitinib, and the IC_{50} calculated (iii).

b. RIVA (i) and HBL-1 (ii) cells were treated ruxolitinib (at 5μM or 50μM), and SAHA (5μM), either alone or in combination. Cell lysates were immunoblotted for MyD88 and cleaved caspase 3 (Cl C3); actin served as the loading control. The relative levels of cleaved caspase 3 were determined by densitometric analysis and are represented in a graph, as shown below each Western Blot. *Rux,* ruxolitinib.

APPENDIX D



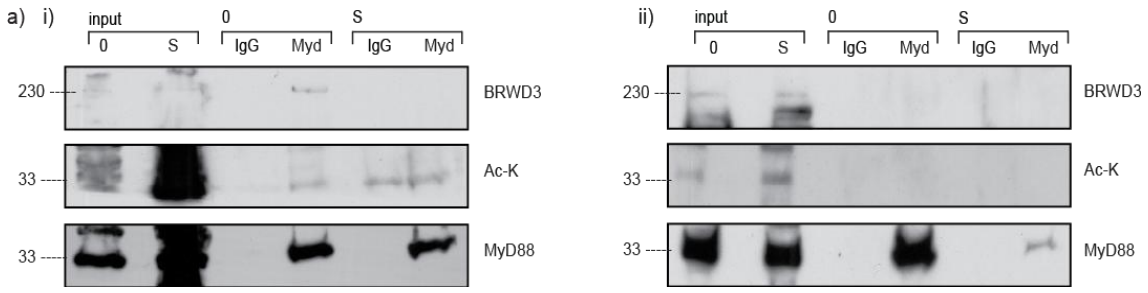
JQ1b inhibition in lymphoma cells.

RIVA and HBL-1 cells were treated with JQ1b (100nM) or with DMSO (mock, 0) as the control. Cell cycle phases were analyzed by FACS after PI staining. The experiment was performed in triplicate and reflects the trend of *n*=2 biological replicates. *p* values were calculated as follows; * denotes significance; ns, non-significant.

RIVA JQ1b **Cell cycle phase**	***p* value**
sub-G1	0.0505 ns
G1	0.1507 ns
S	<0.0001 ***
G2	0.0020 **

HBL-1 JQ1b **Cell cycle phase**	***p* value**
sub-G1	0.8292 ns
G1	0.0669 ns
S	0.0008 **
G2	0.2407 ns

APPENDIX E



Immunoprecipitation approach to determine MyD88 acetylation and potential interaction with BRWD3.

a. Extracts from RIVA (i) and HBL-1 (ii) cells were immunoprecipitated with IgG (negative control) or MyD88 antibody, before (0) or after (S) treatment with SAHA (2.5μM; for at least 6 hours), and immunoblotted with anti-BRWD3, anti-MyD88 or anti-acetyl-lysine (Ac-K) antibody. Input (2% of total lysate) level of MyD88 is shown.

REFERENCES

Abedin, S.M., Boddy, C.S. & Munshi, H.G. (2016) BET inhibitors in the treatment of hematologic malignancies: current insights and future prospects. *Onco Targets Ther,* **9,** 5943-5953.

Abramson, J.S., Blum, K.A., Flinn, I., Gutierrez, M., Goy, A., Maris, M., Cooper, M., O'Meara, M., Borger, D., Mertz, J., Sims, R., Jeffrey, S. & Younes, A. (2015) BET Inhibitor CPI-0610 Is Well Tolerated and Induces Responses in Diffuse Large B-Cell Lymphoma and Follicular Lymphoma: Preliminary Analysis of an Ongoing Phase 1 Study. p. 1491.

Adachi, O., Kawai, T., Takeda, K., Matsumoto, M., Tsutsui, H., Sakagami, M., Nakanishi, K. & Akira, S. (1998) Targeted disruption of the MyD88 gene results in loss of IL-1- and IL-18-mediated function. *Immunity,* **9,** 143-150.

Aguirre, I. & Hermoso, M. (2005) Nuclear localization of MyD88 and its role in Apoptosis. In: *VII Latin American Congress of Immunology*, Cordoba, Argentina

Akira, S., Uematsu, S. & Takeuchi, O. (2006) Pathogen recognition and innate immunity. *Cell,* **124,** 783-801.

Alizadeh, A.A., Eisen, M.B., Davis, R.E., Ma, C., Lossos, I.S., Rosenwald, A., Boldrick, J.C., Sabet, H., Tran, T., Yu, X., Powell, J.I., Yang, L., Marti, G.E., Moore, T., Hudson, J., Jr., Lu, L., Lewis, D.B., Tibshirani, R., Sherlock, G., Chan, W.C., Greiner, T.C., Weisenburger, D.D., Armitage, J.O., Warnke, R., Levy, R., Wilson, W., Grever, M.R., Byrd, J.C., Botstein, D., Brown, P.O. & Staudt, L.M. (2000) Distinct types of diffuse large B-cell lymphoma identified by gene expression profiling. *Nature,* **403,** 503-511.

Aluigi, M., Fogli, M., Curti, A., Isidori, A., Gruppioni, E., Chiodoni, C., Colombo, M.P., Versura, P., D'Errico-Grigioni, A., Ferri, E., Baccarani, M. & Lemoli, R.M. (2006) Nucleofection is an efficient nonviral transfection technique for human bone marrow-derived mesenchymal stem cells. *Stem Cells,* **24,** 454-461.

Amini, R.M., Berglund, M., Rosenquist, R., Von Heideman, A., Lagercrantz, S., Thunberg, U., Bergh, J., Sundstrom, C., Glimelius, B. & Enblad, G. (2002) A novel B-cell line (U-2932) established from a patient with diffuse large B-cell lymphoma following Hodgkin lymphoma. *Leuk Lymphoma,* **43,** 2179-2189.

Amorim, S., Stathis, A., Gleeson, M., Iyengar, S., Magarotto, V., Leleu, X., Morschhauser, F., Karlin, L., Broussais, F., Rezai, K., Herait, P., Kahatt, C., Lokiec, F., Salles, G., Facon, T., Palumbo, A., Cunningham, D., Zucca, E. & Thieblemont, C. (2016) Bromodomain inhibitor OTX015 in patients with lymphoma or multiple myeloma: a dose-escalation, open-label, pharmacokinetic, phase 1 study. *Lancet Haematol,* **3,** e196-204.

Andersen, C.L., Asmar, F., Klausen, T., Hasselbalch, H. & Gronbaek, K. (2012) Somatic mutations of the CREBBP and EP300 genes affect response to histone deacetylase inhibition in malignant DLBCL clones. *Leuk Res Rep,* **2,** 1-3.

Angelika Ihle, M., Merkelbach-Bruse, S., Hartmann, W., Bauer, S., Ratner, N., Sonobe, H., Nishio, J., Larsson, O., Aman, P., Pedeutour, F., Taguchi, T., Wardelmann, E., Buettner, R. & Schildhaus, H.U. (2016) HR23b expression is a potential predictive biomarker for HDAC inhibitor treatment in mesenchymal tumours and is associated with response to vorinostat. *J Pathol Clin Res,* **2,** 59-71.

Arancibia, S.A., Beltran, C.J., Aguirre, I.M., Silva, P., Peralta, A.L., Malinarich, F. & Hermoso, M.A. (2007) Toll-like receptors are key participants in innate immune responses. *Biol Res,* **40,** 97-112.

Ashkenazi, A. (2002) Targeting death and decoy receptors of the tumour-necrosis factor superfamily. *Nat Rev Cancer,* **2,** 420-430.

Avbelj, M., Wolz, O.O., Fekonja, O., Bencina, M., Repic, M., Mavri, J., Kruger, J., Scharfe, C., Delmiro Garcia, M., Panter, G., Kohlbacher, O., Weber, A.N. & Jerala, R. (2014) Activation of lymphoma-associated MyD88 mutations via allostery-induced TIR-domain oligomerization. *Blood,* **124,** 3896-3904.

Baek, Y.S., Haas, S., Hackstein, H., Bein, G., Hernandez-Santana, M., Lehrach, H., Sauer, S. & Seitz, H. (2009) Identification of novel transcriptional regulators involved in macrophage differentiation and activation in U937 cells. *BMC Immunol,* **10,** 18.

Bali, P., Pranpat, M., Bradner, J., Balasis, M., Fiskus, W., Guo, F., Rocha, K., Kumaraswamy, S., Boyapalle, S., Atadja, P., Seto, E. & Bhalla, K. (2005) Inhibition of histone deacetylase 6 acetylates and disrupts the chaperone function of heat shock protein 90: a novel basis for antileukemia activity of histone deacetylase inhibitors. *J Biol Chem,* **280,** 26729-26734.

Bannister, A.J. & Kouzarides, T. (2011) Regulation of chromatin by histone modifications. *Cell Res,* **21,** 381-395.

Barbieri, I., Cannizzaro, E. & Dawson, M.A. (2013) Bromodomains as therapeutic targets in cancer. *Brief Funct Genomics,* **12,** 219-230.

Barr, T.A., Brown, S., Ryan, G., Zhao, J. & Gray, D. (2007) TLR-mediated stimulation of APC: Distinct cytokine responses of B cells and dendritic cells. *Eur J Immunol,* **37,** 3040-3053.

Bates, S.E., Eisch, R., Ling, A., Rosing, D., Turner, M., Pittaluga, S., Prince, H.M., Kirschbaum, M.H., Allen, S.L., Zain, J., Geskin, L.J., Joske, D., Popplewell, L., Cowen, E.W., Jaffe, E.S., Nichols, J., Kennedy, S., Steinberg, S.M., Liewehr, D.J., Showe, L.C., Steakley, C., Wright, J., Fojo, T., Litman, T. & Piekarz, R.L. (2015) Romidepsin in peripheral and cutaneous T-cell lymphoma: mechanistic implications from clinical and correlative data. *Br J Haematol,* **170,** 96-109.

Beguelin, W., Popovic, R., Teater, M., Jiang, Y., Bunting, K.L., Rosen, M., Shen, H., Yang, S.N., Wang, L., Ezponda, T., Martinez-Garcia, E., Zhang, H., Zheng, Y., Verma, S.K., McCabe, M.T., Ott, H.M., Van Aller, G.S., Kruger, R.G., Liu, Y., McHugh, C.F., Scott, D.W., Chung, Y.R., Kelleher, N., Shaknovich, R., Creasy, C.L., Gascoyne, R.D., Wong, K.K., Cerchietti, L., Levine, R.L., Abdel-Wahab, O., Licht, J.D., Elemento, O. & Melnick, A.M. (2013) EZH2 is required for germinal center formation and somatic EZH2 mutations promote lymphoid transformation. *Cancer Cell,* **23,** 677-692.

Bellone, S., Watts, K., Cane, S., Palmieri, M., Cannon, M.J., Burnett, A., Roman, J.J., Pecorelli, S. & Santin, A.D. (2005) High serum levels of interleukin-6 in endometrial carcinoma are associated with uterine serous papillary histology, a highly aggressive and chemotherapy-resistant variant of endometrial cancer. *Gynecol Oncol,* **98,** 92-98.

Berthon, C., Raffoux, E., Thomas, X., Vey, N., Gomez-Roca, C., Yee, K., Taussig, D.C., Rezai, K., Roumier, C., Herait, P., Kahatt, C., Quesnel, B., Michallet, M., Recher, C., Lokiec, F., Preudhomme, C. & Dombret, H. (2016) Bromodomain inhibitor OTX015 in patients with acute leukaemia: a dose-escalation, phase 1 study. *Lancet Haematol,* **3,** e186-195.

Bezecny, P. (2014) Histone deacetylase inhibitors in glioblastoma: pre-clinical and clinical experience. *Med Oncol,* **31,** 985.

Bhadury, J., Nilsson, L.M., Muralidharan, S.V., Green, L.C., Li, Z., Gesner, E.M., Hansen, H.C., Keller, U.B., McLure, K.G. & Nilsson, J.A. (2014) BET and HDAC inhibitors induce similar genes and biological effects and synergize to kill in Myc-induced murine lymphoma. *Proc Natl Acad Sci U S A,* **111,** E2721-2730.

Bohers, E., Mareschal, S., Bertrand, P., Viailly, P.J., Dubois, S., Maingonnat, C., Ruminy, P., Tilly, H. & Jardin, F. (2015) Activating somatic mutations in diffuse large B-cell lymphomas: lessons from next generation sequencing and key elements in the precision medicine era. *Leuk Lymphoma,* **56,** 1213-1222.

Bohers, E., Mareschal, S., Bouzelfen, A., Marchand, V., Ruminy, P., Maingonnat, C., Menard, A.L., Etancelin, P., Bertrand, P., Dubois, S., Alcantara, M., Bastard, C., Tilly, H. & Jardin, F. (2014) Targetable activating mutations are very frequent in GCB and ABC diffuse large B-cell lymphoma. *Genes Chromosomes Cancer,* **53,** 144-153.

Boi, M., Gaudio, E., Bonetti, P., Kwee, I., Bernasconi, E., Tarantelli, C., Rinaldi, A., Testoni, M., Cascione, L., Ponzoni, M., Mensah, A.A., Stathis, A., Stussi, G., Riveiro, M.E., Herait, P., Inghirami, G., Cvitkovic, E., Zucca, E. & Bertoni, F. (2015) The BET Bromodomain

Inhibitor OTX015 Affects Pathogenetic Pathways in Preclinical B-cell Tumor Models and Synergizes with Targeted Drugs. *Clin Cancer Res,* **21,** 1628-1638.
Bolden, J.E., Peart, M.J. & Johnstone, R.W. (2006) Anticancer activities of histone deacetylase inhibitors. *Nat Rev Drug Discov,* **5,** 769-784.
Bollrath, J., Phesse, T.J., von Burstin, V.A., Putoczki, T., Bennecke, M., Bateman, T., Nebelsiek, T., Lundgren-May, T., Canli, O., Schwitalla, S., Matthews, V., Schmid, R.M., Kirchner, T., Arkan, M.C., Ernst, M. & Greten, F.R. (2009) gp130-mediated Stat3 activation in enterocytes regulates cell survival and cell-cycle progression during colitis-associated tumorigenesis. *Cancer Cell,* **15,** 91-102.
Braggio, E., Van Wier, S., Ojha, J., McPhail, E., Asmann, Y.W., Egan, J., da Silva, J.A., Schiff, D., Lopes, M.B., Decker, P.A., Valdez, R., Tibes, R., Eckloff, B., Witzig, T.E., Stewart, A.K., Fonseca, R. & O'Neill, B.P. (2015) Genome-Wide Analysis Uncovers Novel Recurrent Alterations in Primary Central Nervous System Lymphomas. *Clin Cancer Res,* **21,** 3986-3994.
Brand, M., Measures, A.R., Wilson, B.G., Cortopassi, W.A., Alexander, R., Hoss, M., Hewings, D.S., Rooney, T.P., Paton, R.S. & Conway, S.J. (2015) Small molecule inhibitors of bromodomain-acetyl-lysine interactions. *ACS Chem Biol,* **10,** 22-39.
Brint, E.K., Xu, D., Liu, H., Dunne, A., McKenzie, A.N., O'Neill, L.A. & Liew, F.Y. (2004) ST2 is an inhibitor of interleukin 1 receptor and Toll-like receptor 4 signaling and maintains endotoxin tolerance. *Nat Immunol,* **5,** 373-379.
Brogdon, J.L., Xu, Y., Szabo, S.J., An, S., Buxton, F., Cohen, D. & Huang, Q. (2007) Histone deacetylase activities are required for innate immune cell control of Th1 but not Th2 effector cell function. *Blood,* **109,** 1123-1130.
Brown, P.J., Ashe, S.L., Leich, E., Burek, C., Barrans, S., Fenton, J.A., Jack, A.S., Pulford, K., Rosenwald, A. & Banham, A.H. (2008) Potentially oncogenic B-cell activation-induced smaller isoforms of FOXP1 are highly expressed in the activated B cell-like subtype of DLBCL. *Blood,* **111,** 2816-2824.
Brummelkamp, T.R., Bernards, R. & Agami, R. (2002) A system for stable expression of short interfering RNAs in mammalian cells. *Science,* **296,** 550-553.
Burger, R. (2013) Impact of interleukin-6 in hematological malignancies. *Transfus Med Hemother,* **40,** 336-343.
Burns, K., Janssens, S., Brissoni, B., Olivos, N., Beyaert, R. & Tschopp, J. (2003) Inhibition of interleukin 1 receptor/Toll-like receptor signaling through the alternatively spliced, short form of MyD88 is due to its failure to recruit IRAK-4. *J Exp Med,* **197,** 263-268.
Burz, C., Berindan-Neagoe, I., Balacescu, O. & Irimie, A. (2009) Apoptosis in cancer: key molecular signaling pathways and therapy targets. *Acta Oncol,* **48,** 811-821.
Butler, K.V., Kalin, J., Brochier, C., Vistoli, G., Langley, B. & Kozikowski, A.P. (2010) Rational design and simple chemistry yield a superior, neuroprotective HDAC6 inhibitor, tubastatin A. *J Am Chem Soc,* **132,** 10842-10846.
Butler, L.M., Zhou, X., Xu, W.S., Scher, H.I., Rifkind, R.A., Marks, P.A. & Richon, V.M. (2002) The histone deacetylase inhibitor SAHA arrests cancer cell growth, up-regulates thioredoxin-binding protein-2, and down-regulates thioredoxin. *Proc Natl Acad Sci U S A,* **99,** 11700-11705.
Cai, Y., Cui, W., Chen, W., Wei, P., Chi, Y., Zhang, P., Bi, R. & Zhou, X. (2013) The effects of a histone deacetylase inhibitor on biological behavior of diffuse large B-cell lymphoma cell lines and insights into the underlying mechanisms. *Cancer Cell Int,* **13,** 57.
Camus, V., Sarafan-Vasseur, N., Bohers, E., Dubois, S., Mareschal, S., Bertrand, P., Viailly, P.J., Ruminy, P., Maingonnat, C., Lemasle, E., Stamatoullas, A., Picquenot, J.M., Cornic, M., Beaussire, L., Bastard, C., Frebourg, T., Tilly, H. & Jardin, F. (2016) Digital PCR for quantification of recurrent and potentially actionable somatic mutations in circulating free DNA from patients with diffuse large B-cell lymphoma. *Leuk Lymphoma,* **57,** 2171-2179.

Cao, R., Wang, L., Wang, H., Xia, L., Erdjument-Bromage, H., Tempst, P., Jones, R.S. & Zhang, Y. (2002) Role of histone H3 lysine 27 methylation in Polycomb-group silencing. *Science,* **298,** 1039-1043.

Cao, Y., Zhu, T., Zhang, P., Xiao, M., Yi, S., Yang, Y., Li, Q., Ling, S., Wang, Y., Gao, L., Zhu, L., Wang, J., Wang, N., Huang, L., Zhang, P., Zhai, Q., Qiu, L. & Zhou, J. (2016) Mutations or copy number losses of CD58 and TP53 genes in diffuse large B cell lymphoma are independent unfavorable prognostic factors. *Oncotarget,* **7,** 83294-83307.

Carbone, A., Gloghini, A., Kwong, Y.L. & Younes, A. (2014) Diffuse large B cell lymphoma: using pathologic and molecular biomarkers to define subgroups for novel therapy. *Ann Hematol,* **93,** 1263-1277.

Caro, P., Kishan, A.U., Norberg, E., Stanley, I.A., Chapuy, B., Ficarro, S.B., Polak, K., Tondera, D., Gounarides, J., Yin, H., Zhou, F., Green, M.R., Chen, L., Monti, S., Marto, J.A., Shipp, M.A. & Danial, N.N. (2012) Metabolic signatures uncover distinct targets in molecular subsets of diffuse large B cell lymphoma. *Cancer Cell,* **22,** 547-560.

Ceribelli, M., Kelly, P.N., Shaffer, A.L., Wright, G.W., Xiao, W., Yang, Y., Mathews Griner, L.A., Guha, R., Shinn, P., Keller, J.M., Liu, D., Patel, P.R., Ferrer, M., Joshi, S., Nerle, S., Sandy, P., Normant, E., Thomas, C.J. & Staudt, L.M. (2014) Blockade of oncogenic IkappaB kinase activity in diffuse large B-cell lymphoma by bromodomain and extraterminal domain protein inhibitors. *Proc Natl Acad Sci U S A,* **111,** 11365-11370.

Chaidos, A., Caputo, V. & Karadimitris, A. (2015) Inhibition of bromodomain and extra-terminal proteins (BET) as a potential therapeutic approach in haematological malignancies: emerging preclinical and clinical evidence. *Ther Adv Hematol,* **6,** 128-141.

Chang, Q., Bournazou, E., Sansone, P., Berishaj, M., Gao, S.P., Daly, L., Wels, J., Theilen, T., Granitto, S., Zhang, X., Cotari, J., Alpaugh, M.L., de Stanchina, E., Manova, K., Li, M., Bonafe, M., Ceccarelli, C., Taffurelli, M., Santini, D., Altan-Bonnet, G., Kaplan, R., Norton, L., Nishimoto, N., Huszar, D., Lyden, D. & Bromberg, J. (2013) The IL-6/JAK/Stat3 feed-forward loop drives tumorigenesis and metastasis. *Neoplasia,* **15,** 848-862.

Chang, Q., Daly, L. & Bromberg, J. (2014) The IL-6 feed-forward loop: a driver of tumorigenesis. *Semin Immunol,* **26,** 48-53.

Chapuy, B., Cheng, H., Watahiki, A., Ducar, M.D., Tan, Y., Chen, L., Roemer, M.G., Ouyang, J., Christie, A.L., Zhang, L., Gusenleitner, D., Abo, R.P., Farinha, P., von Bonin, F., Thorner, A.R., Sun, H.H., Gascoyne, R.D., Pinkus, G.S., van Hummelen, P., Wulf, G.G., Aster, J.C., Weinstock, D.M., Monti, S., Rodig, S.J., Wang, Y. & Shipp, M.A. (2016) Diffuse large B-cell lymphoma patient-derived xenograft models capture the molecular and biological heterogeneity of the disease. *Blood,* **127,** 2203-2213.

Chapuy, B., McKeown, M.R., Lin, C.Y., Monti, S., Roemer, M.G., Qi, J., Rahl, P.B., Sun, H.H., Yeda, K.T., Doench, J.G., Reichert, E., Kung, A.L., Rodig, S.J., Young, R.A., Shipp, M.A. & Bradner, J.E. (2013) Discovery and characterization of super-enhancer-associated dependencies in diffuse large B cell lymphoma. *Cancer Cell,* **24,** 777-790.

Chaudhary, A., Ganguly, K., Cabantous, S., Waldo, G.S., Micheva-Viteva, S.N., Nag, K., Hlavacek, W.S. & Tung, C.S. (2012) The Brucella TIR-like protein TcpB interacts with the death domain of MyD88. *Biochem Biophys Res Commun,* **417,** 299-304.

Chen, J.D., Umesono, K. & Evans, R.M. (1996) SMRT isoforms mediate repression and anti-repression of nuclear receptor heterodimers. *Proc Natl Acad Sci U S A,* **93,** 7567-7571.

Chen, L., Monti, S., Juszczynski, P., Ouyang, J., Chapuy, B., Neuberg, D., Doench, J.G., Bogusz, A.M., Habermann, T.M., Dogan, A., Witzig, T.E., Kutok, J.L., Rodig, S.J., Golub, T. & Shipp, M.A. (2013) SYK inhibition modulates distinct PI3K/AKT- dependent survival pathways and cholesterol biosynthesis in diffuse large B cell lymphomas. *Cancer Cell,* **23,** 826-838.

Chicaybam, L., Barcelos, C., Peixoto, B., Carneiro, M., Limia, C.G., Redondo, P., Lira, C., Paraguassu-Braga, F., Vasconcelos, Z.F., Barros, L. & Bonamino, M.H. (2016) An

Efficient Electroporation Protocol for the Genetic Modification of Mammalian Cells. *Front Bioeng Biotechnol,* **4,** 99.

Choi, A.M., Ryter, S.W. & Levine, B. (2013a) Autophagy in human health and disease. *N Engl J Med,* **368,** 1845-1846.

Choi, J.W., Kim, Y., Lee, J.H. & Kim, Y.S. (2013b) MYD88 expression and L265P mutation in diffuse large B-cell lymphoma. *Hum Pathol,* **44,** 1375-1381.

Choi, S.W., Gatza, E., Hou, G., Sun, Y., Whitfield, J., Song, Y., Oravecz-Wilson, K., Tawara, I., Dinarello, C.A. & Reddy, P. (2015) Histone deacetylase inhibition regulates inflammation and enhances Tregs after allogeneic hematopoietic cell transplantation in humans. *Blood,* **125,** 815-819.

Choudhary, C., Kumar, C., Gnad, F., Nielsen, M.L., Rehman, M., Walther, T.C., Olsen, J.V. & Mann, M. (2009) Lysine acetylation targets protein complexes and co-regulates major cellular functions. *Science,* **325,** 834-840.

Coiffier, B., Lepage, E., Briere, J., Herbrecht, R., Tilly, H., Bouabdallah, R., Morel, P., Van Den Neste, E., Salles, G., Gaulard, P., Reyes, F., Lederlin, P. & Gisselbrecht, C. (2002) CHOP chemotherapy plus rituximab compared with CHOP alone in elderly patients with diffuse large-B-cell lymphoma. *N Engl J Med,* **346,** 235-242.

Coiffier, B., Pro, B., Prince, H.M., Foss, F., Sokol, L., Greenwood, M., Caballero, D., Borchmann, P., Morschhauser, F., Wilhelm, M., Pinter-Brown, L., Padmanabhan, S., Shustov, A., Nichols, J., Carroll, S., Balser, J., Balser, B. & Horwitz, S. (2012) Results from a pivotal, open-label, phase II study of romidepsin in relapsed or refractory peripheral T-cell lymphoma after prior systemic therapy. *J Clin Oncol,* **30,** 631-636.

Coiffier, B., Thieblemont, C., Van Den Neste, E., Lepeu, G., Plantier, I., Castaigne, S., Lefort, S., Marit, G., Macro, M., Sebban, C., Belhadj, K., Bordessoule, D., Ferme, C. & Tilly, H. (2010) Long-term outcome of patients in the LNH-98.5 trial, the first randomized study comparing rituximab-CHOP to standard CHOP chemotherapy in DLBCL patients: a study by the Groupe d'Etudes des Lymphomes de l'Adulte. *Blood,* **116,** 2040-2045.

Cortes, J. & Kurzrock, R. (1997) Interleukin-10 in non-Hodgkin's lymphoma. *Leuk Lymphoma,* **26,** 251-259.

Coste, I., Le Corf, K., Kfoury, A., Hmitou, I., Druillennec, S., Hainaut, P., Eychene, A., Lebecque, S. & Renno, T. (2010) Dual function of MyD88 in RAS signaling and inflammation, leading to mouse and human cell transformation. *J Clin Invest,* **120,** 3663-3667.

Cree, I. (2015) Liquid biopsy for cancer patients: Principles and practice. In: *Pathogenesis*, Vol. 2, pp. 1-4.

Crump, M., Coiffier, B., Jacobsen, E.D., Sun, L., Ricker, J.L., Xie, H., Frankel, S.R., Randolph, S.S. & Cheson, B.D. (2008) Phase II trial of oral vorinostat (suberoylanilide hydroxamic acid) in relapsed diffuse large-B-cell lymphoma. *Ann Oncol,* **19,** 964-969.

d'Ydewalle, C., Bogaert, E. & Van Den Bosch, L. (2012) HDAC6 at the Intersection of Neuroprotection and Neurodegeneration. *Traffic,* **13,** 771-779.

Dawson, M.A., Kouzarides, T. & Huntly, B.J. (2012) Targeting epigenetic readers in cancer. *N Engl J Med,* **367,** 647-657.

de Jong, D., Rosenwald, A., Chhanabhai, M., Gaulard, P., Klapper, W., Lee, A., Sander, B., Thorns, C., Campo, E., Molina, T., Norton, A., Hagenbeek, A., Horning, S., Lister, A., Raemaekers, J., Gascoyne, R.D., Salles, G., Weller, E. & Lunenburg Lymphoma Biomarker, C. (2007) Immunohistochemical prognostic markers in diffuse large B-cell lymphoma: validation of tissue microarray as a prerequisite for broad clinical applications--a study from the Lunenburg Lymphoma Biomarker Consortium. *J Clin Oncol,* **25,** 805-812.

de Waal Malefyt, R., Haanen, J., Spits, H., Roncarolo, M.G., te Velde, A., Figdor, C., Johnson, K., Kastelein, R., Yssel, H. & de Vries, J.E. (1991) Interleukin 10 (IL-10) and viral IL-10 strongly reduce antigen-specific human T cell proliferation by diminishing the antigen-

presenting capacity of monocytes via downregulation of class II major histocompatibility complex expression. *J Exp Med,* **174,** 915-924.
Deguine, J. & Barton, G.M. (2014) MyD88: a central player in innate immune signaling. *F1000Prime Rep,* **6,** 97.
Dhanak, D. & Jackson, P. (2014a) Development and classes of epigenetic drugs for cancer. *Biochem Biophys Res Commun,* **455,** 58-69.
Dhanak, D. & Jackson, P. (2014b) Development and classes of epigenetic drugs for cancer. *Biochem Biophys Res Commun*.
Dinarello, C.A. (2010) Anti-inflammatory Agents: Present and Future. *Cell,* **140,** 935-950.
Ding, B.B., Yu, J.J., Yu, R.Y., Mendez, L.M., Shaknovich, R., Zhang, Y., Cattoretti, G. & Ye, B.H. (2008) Constitutively activated STAT3 promotes cell proliferation and survival in the activated B-cell subtype of diffuse large B-cell lymphomas. *Blood,* **111,** 1515-1523.
Domcke, S., Sinha, R., Levine, D.A., Sander, C. & Schultz, N. (2013) Evaluating cell lines as tumour models by comparison of genomic profiles. *Nat Commun,* **4,** 2126.
Drogaris, P., Villeneuve, V., Pomies, C., Lee, E.H., Bourdeau, V., Bonneil, E., Ferbeyre, G., Verreault, A. & Thibault, P. (2012) Histone deacetylase inhibitors globally enhance h3/h4 tail acetylation without affecting h3 lysine 56 acetylation. *Sci Rep,* **2,** 220.
Dunleavy, K., Grant, C. & Wilson, W.H. (2013) Using biologic predictive factors to direct therapy of diffuse large B-cell lymphoma. *Ther Adv Hematol,* **4,** 43-57.
Duvic, M., Talpur, R., Ni, X., Zhang, C., Hazarika, P., Kelly, C., Chiao, J.H., Reilly, J.F., Ricker, J.L., Richon, V.M. & Frankel, S.R. (2007) Phase 2 trial of oral vorinostat (suberoylanilide hydroxamic acid, SAHA) for refractory cutaneous T-cell lymphoma (CTCL). *Blood,* **109,** 31-39.
Egunsola, A.T., Zawislak, C.L., Akuffo, A.A., Chalmers, S.A., Ewer, J.C., Vail, C.M., Lombardo, J.C., Perez, D.N. & Kurt, R.A. (2012) Growth, metastasis, and expression of CCL2 and CCL5 by murine mammary carcinomas are dependent upon Myd88. *Cell Immunol,* **272,** 220-229.
Elisia, I., Nakamura, H., Lam, V., Hofs, E., Cederberg, R., Cait, J., Hughes, M.R., Lee, L., Jia, W., Adomat, H.H., Guns, E.S., McNagny, K.M., Samudio, I. & Krystal, G. (2016) DMSO Represses Inflammatory Cytokine Production from Human Blood Cells and Reduces Autoimmune Arthritis. *PLoS One,* **11,** e0152538.
Ellis, L., Atadja, P.W. & Johnstone, R.W. (2009) Epigenetics in cancer: targeting chromatin modifications. *Mol Cancer Ther,* **8,** 1409-1420.
Ellis, L., Pan, Y., Smyth, G.K., George, D.J., McCormack, C., Williams-Truax, R., Mita, M., Beck, J., Burris, H., Ryan, G., Atadja, P., Butterfoss, D., Dugan, M., Culver, K., Johnstone, R.W. & Prince, H.M. (2008) Histone deacetylase inhibitor panobinostat induces clinical responses with associated alterations in gene expression profiles in cutaneous T-cell lymphoma. *Clin Cancer Res,* **14,** 4500-4510.
Esteller, M. (2008) Epigenetics in cancer. *N Engl J Med,* **358,** 1148-1159.
Ezell, S.A., Wang, S., Bihani, T., Lai, Z., Grosskurth, S.E., Tepsuporn, S., Davies, B.R., Huszar, D. & Byth, K.F. (2016) Differential regulation of mTOR signaling determines sensitivity to AKT inhibition in diffuse large B cell lymphoma. *Oncotarget,* **7,** 9163-9174.
Fernandez-Rodriguez, C., Bellosillo, B., Garcia-Garcia, M., Sanchez-Gonzalez, B., Gimeno, E., Vela, M.C., Serrano, S., Besses, C. & Salar, A. (2014) MYD88 (L265P) mutation is an independent prognostic factor for outcome in patients with diffuse large B-cell lymphoma. *Leukemia,* **28,** 2104-2106.
Feugier, P., Van Hoof, A., Sebban, C., Solal-Celigny, P., Bouabdallah, R., Ferme, C., Christian, B., Lepage, E., Tilly, H., Morschhauser, F., Gaulard, P., Salles, G., Bosly, A., Gisselbrecht, C., Reyes, F. & Coiffier, B. (2005) Long-term results of the R-CHOP study in the treatment of elderly patients with diffuse large B-cell lymphoma: a study by the Groupe d'Etude des Lymphomes de l'Adulte. *J Clin Oncol,* **23,** 4117-4126.

Filippakopoulos, P., Picaud, S., Mangos, M., Keates, T., Lambert, J.P., Barsyte-Lovejoy, D., Felletar, I., Volkmer, R., Muller, S., Pawson, T., Gingras, A.C., Arrowsmith, C.H. & Knapp, S. (2012) Histone recognition and large-scale structural analysis of the human bromodomain family. *Cell,* **149,** 214-231.

Filippakopoulos, P., Qi, J., Picaud, S., Shen, Y., Smith, W.B., Fedorov, O., Morse, E.M., Keates, T., Hickman, T.T., Felletar, I., Philpott, M., Munro, S., McKeown, M.R., Wang, Y., Christie, A.L., West, N., Cameron, M.J., Schwartz, B., Heightman, T.D., La Thangue, N., French, C.A., Wiest, O., Kung, A.L., Knapp, S. & Bradner, J.E. (2010) Selective inhibition of BET bromodomains. *Nature,* **468,** 1067-1073.

Fiorentino, D.F., Zlotnik, A., Vieira, P., Mosmann, T.R., Howard, M., Moore, K.W. & O'Garra, A. (1991) IL-10 acts on the antigen-presenting cell to inhibit cytokine production by Th1 cells. *J Immunol,* **146,** 3444-3451.

Fotheringham, S., Epping, M.T., Stimson, L., Khan, O., Wood, V., Pezzella, F., Bernards, R. & La Thangue, N.B. (2009) Genome-wide loss-of-function screen reveals an important role for the proteasome in HDAC inhibitor-induced apoptosis. *Cancer Cell,* **15,** 57-66.

French, C.A., Miyoshi, I., Aster, J.C., Kubonishi, I., Kroll, T.G., Dal Cin, P., Vargas, S.O., Perez-Atayde, A.R. & Fletcher, J.A. (2001) BRD4 bromodomain gene rearrangement in aggressive carcinoma with translocation t(15;19). *Am J Pathol,* **159,** 1987-1992.

French, C.A., Miyoshi, I., Kubonishi, I., Grier, H.E., Perez-Atayde, A.R. & Fletcher, J.A. (2003) BRD4-NUT fusion oncogene: a novel mechanism in aggressive carcinoma. *Cancer Res,* **63,** 304-307.

French, C.A., Ramirez, C.L., Kolmakova, J., Hickman, T.T., Cameron, M.J., Thyne, M.E., Kutok, J.L., Toretsky, J.A., Tadavarthy, A.K., Kees, U.R., Fletcher, J.A. & Aster, J.C. (2008) BRD-NUT oncoproteins: a family of closely related nuclear proteins that block epithelial differentiation and maintain the growth of carcinoma cells. *Oncogene,* **27,** 2237-2242.

Fujiwara, Y., Yamamoto, N., Yamada, Y., Yamada, K., Otsuki, T., Kanazu, S., Iwasa, T., Hardwick, J.S. & Tamura, T. (2009) Phase I and pharmacokinetic study of vorinostat (suberoylanilide hydroxamic acid) in Japanese patients with solid tumors. *Cancer Sci,* **100,** 1728-1734.

Gammoh, N., Lam, D., Puente, C., Ganley, I., Marks, P.A. & Jiang, X. (2012) Role of autophagy in histone deacetylase inhibitor-induced apoptotic and nonapoptotic cell death. *Proc Natl Acad Sci U S A,* **109,** 6561-6565.

Glaser, K.B., Staver, M.J., Waring, J.F., Stender, J., Ulrich, R.G. & Davidsen, S.K. (2003) Gene expression profiling of multiple histone deacetylase (HDAC) inhibitors: defining a common gene set produced by HDAC inhibition in T24 and MDA carcinoma cell lines. *Mol Cancer Ther,* **2,** 151-163.

Gloghini, A., Buglio, D., Khaskhely, N.M., Georgakis, G., Orlowski, R.Z., Neelapu, S.S., Carbone, A. & Younes, A. (2009) Expression of histone deacetylases in lymphoma: implication for the development of selective inhibitors. *Br J Haematol,* **147,** 515-525.

Glozak, M.A., Sengupta, N., Zhang, X. & Seto, E. (2005) Acetylation and deacetylation of non-histone proteins. *Gene,* **363,** 15-23.

Gonzalez-Aguilar, A., Idbaih, A., Boisselier, B., Habbita, N., Rossetto, M., Laurenge, A., Bruno, A., Jouvet, A., Polivka, M., Adam, C., Figarella-Branger, D., Miquel, C., Vital, A., Ghesquieres, H., Gressin, R., Delwail, V., Taillandier, L., Chinot, O., Soubeyran, P., Gyan, E., Choquet, S., Houillier, C., Soussain, C., Tanguy, M.L., Marie, Y., Mokhtari, K. & Hoang-Xuan, K. (2012) Recurrent mutations of MYD88 and TBL1XR1 in primary central nervous system lymphomas. *Clin Cancer Res,* **18,** 5203-5211.

Grivennikov, S., Karin, E., Terzic, J., Mucida, D., Yu, G.Y., Vallabhapurapu, S., Scheller, J., Rose-John, S., Cheroutre, H., Eckmann, L. & Karin, M. (2009) IL-6 and Stat3 are required for survival of intestinal epithelial cells and development of colitis-associated cancer. *Cancer Cell,* **15,** 103-113.

Grivennikov, S.I. & Karin, M. (2011) Inflammatory cytokines in cancer: tumour necrosis factor and interleukin 6 take the stage. *Ann Rheum Dis,* **70 Suppl 1,** i104-108.

Gryder, B.E., Sodji, Q.H. & Oyelere, A.K. (2012) Targeted cancer therapy: giving histone deacetylase inhibitors all they need to succeed. *Future Med Chem,* **4,** 505-524.

Guardiola, A.R. & Yao, T.P. (2002) Molecular cloning and characterization of a novel histone deacetylase HDAC10. *J Biol Chem,* **277,** 3350-3356.

Haberland, M., Montgomery, R.L. & Olson, E.N. (2009) The many roles of histone deacetylases in development and physiology: implications for disease and therapy. *Nat Rev Genet,* **10,** 32-42.

Habermann, T.M., Weller, E.A., Morrison, V.A., Gascoyne, R.D., Cassileth, P.A., Cohn, J.B., Dakhil, S.R., Woda, B., Fisher, R.I., Peterson, B.A. & Horning, S.J. (2006) Rituximab-CHOP versus CHOP alone or with maintenance rituximab in older patients with diffuse large B-cell lymphoma. *J Clin Oncol,* **24,** 3121-3127.

Hailfinger, S., Lenz, G., Ngo, V., Posvitz-Fejfar, A., Rebeaud, F., Guzzardi, M., Penas, E.M., Dierlamm, J., Chan, W.C., Staudt, L.M. & Thome, M. (2009) Essential role of MALT1 protease activity in activated B cell-like diffuse large B-cell lymphoma. *Proc Natl Acad Sci U S A,* **106,** 19946-19951.

Hanahan, D. & Weinberg, R.A. (2000) The hallmarks of cancer. *Cell,* **100,** 57-70.

Hans, C.P., Weisenburger, D.D., Greiner, T.C., Gascoyne, R.D., Delabie, J., Ott, G., Muller-Hermelink, H.K., Campo, E., Braziel, R.M., Jaffe, E.S., Pan, Z., Farinha, P., Smith, L.M., Falini, B., Banham, A.H., Rosenwald, A., Staudt, L.M., Connors, J.M., Armitage, J.O. & Chan, W.C. (2004) Confirmation of the molecular classification of diffuse large B-cell lymphoma by immunohistochemistry using a tissue microarray. *Blood,* **103,** 275-282.

Harlow, E. & Lane, D. (1999) *Using Antibodies.* Cold Spring Harbor, New York: Cold Spring Harbor Laboratory Press.

Hartl, F.U., Bracher, A. & Hayer-Hartl, M. (2011) Molecular chaperones in protein folding and proteostasis. *Nature,* **475,** 324-332.

Hatzimichael, E. & Crook, T. (2013) Cancer epigenetics: new therapies and new challenges. *J Drug Deliv,* **2013,** 529312.

Heerboth, S., Lapinska, K., Snyder, N., Leary, M., Rollinson, S. & Sarkar, S. (2014) Use of epigenetic drugs in disease: an overview. *Genet Epigenet,* **6,** 9-19.

Henderson, C., Mizzau, M., Paroni, G., Maestro, R., Schneider, C. & Brancolini, C. (2003) Role of caspases, Bid, and p53 in the apoptotic response triggered by histone deacetylase inhibitors trichostatin-A (TSA) and suberoylanilide hydroxamic acid (SAHA). *J Biol Chem,* **278,** 12579-12589.

Herceg, Z. & Wang, Z.Q. (1999) Failure of poly(ADP-ribose) polymerase cleavage by caspases leads to induction of necrosis and enhanced apoptosis. *Mol Cell Biol,* **19,** 5124-5133.

Hewings, D.S., Wang, M., Philpott, M., Fedorov, O., Uttarkar, S., Filippakopoulos, P., Picaud, S., Vuppusetty, C., Marsden, B., Knapp, S., Conway, S.J. & Heightman, T.D. (2011) 3,5-dimethylisoxazoles act as acetyl-lysine-mimetic bromodomain ligands. *J Med Chem,* **54,** 6761-6770.

Hideshima, T., Richardson, P.G. & Anderson, K.C. (2011) Mechanism of action of proteasome inhibitors and deacetylase inhibitors and the biological basis of synergy in multiple myeloma. *Mol Cancer Ther,* **10,** 2034-2042.

Horlein, A.J., Naar, A.M., Heinzel, T., Torchia, J., Gloss, B., Kurokawa, R., Ryan, A., Kamei, Y., Soderstrom, M., Glass, C.K. & et al. (1995) Ligand-independent repression by the thyroid hormone receptor mediated by a nuclear receptor co-repressor. *Nature,* **377,** 397-404.

Horng, T. & Medzhitov, R. (2001) Drosophila MyD88 is an adapter in the Toll signaling pathway. *Proc Natl Acad Sci U S A,* **98,** 12654-12658.

Hu, J. & Colburn, N.H. (2005) Histone deacetylase inhibition down-regulates cyclin D1 transcription by inhibiting nuclear factor-kappaB/p65 DNA binding. *Mol Cancer Res,* **3,** 100-109.

Hu, J., Jing, H. & Lin, H. (2014) Sirtuin inhibitors as anticancer agents. *Future Med Chem,* **6,** 945-966.

Hu, X., Yu, Y., Eugene Chin, Y. & Xia, Q. (2013) The role of acetylation in TLR4-mediated innate immune responses. *Immunol Cell Biol,* **91,** 611-614.

Huang, E.Y., Zhang, J., Miska, E.A., Guenther, M.G., Kouzarides, T. & Lazar, M.A. (2000) Nuclear receptor corepressors partner with class II histone deacetylases in a Sin3-independent repression pathway. *Genes Dev,* **14,** 45-54.

Hubackova, S., Krejcikova, K., Bartek, J. & Hodny, Z. (2012) Interleukin 6 signaling regulates promyelocytic leukemia protein gene expression in human normal and cancer cells. *J Biol Chem,* **287,** 26702-26714.

Hultmark, D. (1994) Macrophage differentiation marker MyD88 is a member of the Toll/IL-1 receptor family. *Biochem Biophys Res Commun,* **199,** 144-146.

Inche, A.G. & La Thangue, N.B. (2006) Chromatin control and cancer-drug discovery: realizing the promise. *Drug Discov Today,* **11,** 97-109.

Inoue, S., Riley, J., Gant, T.W., Dyer, M.J. & Cohen, G.M. (2007) Apoptosis induced by histone deacetylase inhibitors in leukemic cells is mediated by Bim and Noxa. *Leukemia,* **21,** 1773-1782.

Insinga, A., Monestiroli, S., Ronzoni, S., Gelmetti, V., Marchesi, F., Viale, A., Altucci, L., Nervi, C., Minucci, S. & Pelicci, P.G. (2005) Inhibitors of histone deacetylases induce tumor-selective apoptosis through activation of the death receptor pathway. *Nat Med,* **11,** 71-76.

Intlekofer, A.M. & Younes, A. (2014) Precision therapy for lymphoma--current state and future directions. *Nat Rev Clin Oncol,* **11,** 585-596.

Into, T., Inomata, M., Niida, S., Murakami, Y. & Shibata, K. (2010) Regulation of MyD88 aggregation and the MyD88-dependent signaling pathway by sequestosome 1 and histone deacetylase 6. *J Biol Chem,* **285,** 35759-35769.

Janssens, S., Burns, K., Vercammen, E., Tschopp, J. & Beyaert, R. (2003) MyD88S, a splice variant of MyD88, differentially modulates NF-kappaB- and AP-1-dependent gene expression. *FEBS Lett,* **548,** 103-107.

Jaunin, F., Burns, K., Tschopp, J., Martin, T.E. & Fakan, S. (1998) Ultrastructural distribution of the death-domain-containing MyD88 protein in HeLa cells. *Exp Cell Res,* **243,** 67-75.

Je, E.M., Kim, S.S., Yoo, N.J. & Lee, S.H. (2012) Mutational and expressional analyses of MYD88 gene in common solid cancers. *Tumori,* **98,** 663-669.

Jeong, J.W., Bae, M.K., Ahn, M.Y., Kim, S.H., Sohn, T.K., Bae, M.H., Yoo, M.A., Song, E.J., Lee, K.J. & Kim, K.W. (2002) Regulation and destabilization of HIF-1alpha by ARD1-mediated acetylation. *Cell,* **111,** 709-720.

Joos, S., Otano-Joos, M.I., Ziegler, S., Bruderlein, S., du Manoir, S., Bentz, M., Moller, P. & Lichter, P. (1996) Primary mediastinal (thymic) B-cell lymphoma is characterized by gains of chromosomal material including 9p and amplification of the REL gene. *Blood,* **87,** 1571-1578.

Juskevicius, D., Jucker, D., Klingbiel, D., Mamot, C., Dirnhofer, S. & Tzankov, A. (2017) Mutations of CREBBP and SOCS1 are independent prognostic factors in diffuse large B cell lymphoma: mutational analysis of the SAKK 38/07 prospective clinical trial cohort. *J Hematol Oncol,* **10,** 70.

Kalac, M., Scotto, L., Marchi, E., Amengual, J., Seshan, V.E., Bhagat, G., Ulahannan, N., Leshchenko, V.V., Temkin, A.M., Parekh, S., Tycko, B. & O'Connor, O.A. (2011) HDAC inhibitors and decitabine are highly synergistic and associated with unique gene-expression and epigenetic profiles in models of DLBCL. *Blood,* **118,** 5506-5516.

Kalderon, D., Roberts, B.L., Richardson, W.D. & Smith, A.E. (1984) A short amino acid sequence able to specify nuclear location. *Cell,* **39,** 499-509.
Katsumoto, T., Yoshida, N. & Kitabayashi, I. (2008) Roles of the histone acetyltransferase monocytic leukemia zinc finger protein in normal and malignant hematopoiesis. *Cancer Sci,* **99,** 1523-1527.
Kawaguchi, Y., Kovacs, J.J., McLaurin, A., Vance, J.M., Ito, A. & Yao, T.P. (2003) The deacetylase HDAC6 regulates aggresome formation and cell viability in response to misfolded protein stress. *Cell,* **115,** 727-738.
Kawai, T., Adachi, O., Ogawa, T., Takeda, K. & Akira, S. (1999) Unresponsiveness of MyD88-deficient mice to endotoxin. *Immunity,* **11,** 115-122.
Kawano, M., Hirano, T., Matsuda, T., Taga, T., Horii, Y., Iwato, K., Asaoku, H., Tang, B., Tanabe, O., Tanaka, H. & et al. (1988) Autocrine generation and requirement of BSF-2/IL-6 for human multiple myelomas. *Nature,* **332,** 83-85.
Kfoury, A., Virard, F., Renno, T. & Coste, I. (2014) Dual function of MyD88 in inflammation and oncogenesis: implications for therapeutic intervention. *Curr Opin Oncol,* **26,** 86-91.
Khan, J.A., Brint, E.K., O'Neill, L.A. & Tong, L. (2004) Crystal structure of the Toll/interleukin-1 receptor domain of human IL-1RAPL. *J Biol Chem,* **279,** 31664-31670.
Khan, O., Fotheringham, S., Wood, V., Stimson, L., Zhang, C., Pezzella, F., Duvic, M., Kerr, D.J. & La Thangue, N.B. (2010) HR23B is a biomarker for tumor sensitivity to HDAC inhibitor-based therapy. *Proc Natl Acad Sci U S A,* **107,** 6532-6537.
Khan, O. & La Thangue, N.B. (2008) Drug Insight: histone deacetylase inhibitor-based therapies for cutaneous T-cell lymphomas. *Nat Clin Pract Oncol,* **5,** 714-726.
Kim, J., Daniel, J., Espejo, A., Lake, A., Krishna, M., Xia, L., Zhang, Y. & Bedford, M.T. (2006a) Tudor, MBT and chromo domains gauge the degree of lysine methylation. *EMBO Rep,* **7,** 397-403.
Kim, S.C., Sprung, R., Chen, Y., Xu, Y., Ball, H., Pei, J., Cheng, T., Kho, Y., Xiao, H., Xiao, L., Grishin, N.V., White, M., Yang, X.J. & Zhao, Y. (2006b) Substrate and functional diversity of lysine acetylation revealed by a proteomics survey. *Mol Cell,* **23,** 607-618.
Kissner, T.L., Moisan, L., Mann, E., Alam, S., Ruthel, G., Ulrich, R.G., Rebek, M., Rebek, J., Jr. & Saikh, K.U. (2011a) A small molecule that mimics the BB-loop in the Toll interleukin-1 (IL-1) receptor domain of MyD88 attenuates staphylococcal enterotoxin B-induced pro-inflammatory cytokine production and toxicity in mice. *J Biol Chem,* **286,** 31385-31396.
Kissner, T.L., Ruthel, G., Cisney, E.D., Ulrich, R.G., Fernandez, S. & Saikh, K.U. (2011b) MyD88-dependent pro-inflammatory cytokine response contributes to lethal toxicity of staphylococcal enterotoxin B in mice. *Innate Immun,* **17,** 451-462.
Knittel, G., Liedgens, P., Korovkina, D., Pallasch, C.P. & Reinhardt, H.C. (2016) Rewired NFkappaB signaling as a potentially actionable feature of activated B-cell-like diffuse large B-cell lymphoma. *Eur J Haematol,* **97,** 499-510.
Kosugi, S., Hasebe, M., Tomita, M. & Yanagawa, H. (2009) Systematic identification of cell cycle-dependent yeast nucleocytoplasmic shuttling proteins by prediction of composite motifs. *Proc Natl Acad Sci U S A,* **106,** 10171-10176.
Koussounadis, A., Langdon, S.P., Um, I.H., Harrison, D.J. & Smith, V.A. (2015) Relationship between differentially expressed mRNA and mRNA-protein correlations in a xenograft model system. *Sci Rep,* **5,** 10775.
Kraan, W., Horlings, H.M., van Keimpema, M., Schilder-Tol, E.J., Oud, M.E., Scheepstra, C., Kluin, P.M., Kersten, M.J., Spaargaren, M. & Pals, S.T. (2013) High prevalence of oncogenic MYD88 and CD79B mutations in diffuse large B-cell lymphomas presenting at immune-privileged sites. *Blood Cancer J,* **3,** e139.
Kraan, W., van Keimpema, M., Horlings, H.M., Schilder-Tol, E.J., Oud, M.E., Noorduyn, L.A., Kluin, P.M., Kersten, M.J., Spaargaren, M. & Pals, S.T. (2014) High prevalence of

oncogenic MYD88 and CD79B mutations in primary testicular diffuse large B-cell lymphoma. *Leukemia,* **28,** 719-720.

Kranzer, K., Eckhardt, A., Aigner, M., Knoll, G., Deml, L., Speth, C., Lehn, N., Rehli, M. & Schneider-Brachert, W. (2004) Induction of maturation and cytokine release of human dendritic cells by Helicobacter pylori. *Infect Immun,* **72,** 4416-4423.

Kroesen, M., Gielen, P., Brok, I.C., Armandari, I., Hoogerbrugge, P.M. & Adema, G.J. (2014) HDAC inhibitors and immunotherapy; a double edged sword? *Oncotarget,* **5,** 6558-6572.

Kumar, S., van Raam, B.J., Salvesen, G.S. & Cieplak, P. (2014) Caspase cleavage sites in the human proteome: CaspDB, a database of predicted substrates. *PLoS One,* **9,** e110539.

La Thangue, N.B. & Kerr, D.J. (2011) Predictive biomarkers: a paradigm shift towards personalized cancer medicine. *Nat Rev Clin Oncol,* **8,** 587-596.

Lam, L.T., Wright, G., Davis, R.E., Lenz, G., Farinha, P., Dang, L., Chan, J.W., Rosenwald, A., Gascoyne, R.D. & Staudt, L.M. (2008) Cooperative signaling through the signal transducer and activator of transcription 3 and nuclear factor-{kappa}B pathways in subtypes of diffuse large B-cell lymphoma. *Blood,* **111,** 3701-3713.

Lech-Maranda, E., Bienvenu, J., Broussais-Guillaumot, F., Warzocha, K., Michallet, A.S., Robak, T., Coiffier, B. & Salles, G. (2010) Plasma TNF-alpha and IL-10 level-based prognostic model predicts outcome of patients with diffuse large B-Cell lymphoma in different risk groups defined by the International Prognostic Index. *Arch Immunol Ther Exp (Warsz),* **58,** 131-141.

Leclere, P.G., Panjwani, A., Docherty, R., Berry, M., Pizzey, J. & Tonge, D.A. (2005) Effective gene delivery to adult neurons by a modified form of electroporation. *J Neurosci Methods,* **142,** 137-143.

Lee, H.K. & Iwasaki, A. (2007) Innate control of adaptive immunity: dendritic cells and beyond. *Semin Immunol,* **19,** 48-55.

Lee, J.H., Mahendran, A., Yao, Y., Ngo, L., Venta-Perez, G., Choy, M.L., Kim, N., Ham, W.S., Breslow, R. & Marks, P.A. (2013) Development of a histone deacetylase 6 inhibitor and its biological effects. *Proc Natl Acad Sci U S A,* **110,** 15704-15709.

Lee, J.Y., Koga, H., Kawaguchi, Y., Tang, W., Wong, E., Gao, Y.S., Pandey, U.B., Kaushik, S., Tresse, E., Lu, J., Taylor, J.P., Cuervo, A.M. & Yao, T.P. (2010) HDAC6 controls autophagosome maturation essential for ubiquitin-selective quality-control autophagy. *EMBO J,* **29,** 969-980.

Lenz, G., Wright, G., Dave, S.S., Xiao, W., Powell, J., Zhao, H., Xu, W., Tan, B., Goldschmidt, N., Iqbal, J., Vose, J., Bast, M., Fu, K., Weisenburger, D.D., Greiner, T.C., Armitage, J.O., Kyle, A., May, L., Gascoyne, R.D., Connors, J.M., Troen, G., Holte, H., Kvaloy, S., Dierickx, D., Verhoef, G., Delabie, J., Smeland, E.B., Jares, P., Martinez, A., Lopez-Guillermo, A., Montserrat, E., Campo, E., Braziel, R.M., Miller, T.P., Rimsza, L.M., Cook, J.R., Pohlman, B., Sweetenham, J., Tubbs, R.R., Fisher, R.I., Hartmann, E., Rosenwald, A., Ott, G., Muller-Hermelink, H.K., Wrench, D., Lister, T.A., Jaffe, E.S., Wilson, W.H., Chan, W.C., Staudt, L.M. & Lymphoma/Leukemia Molecular Profiling, P. (2008a) Stromal gene signatures in large-B-cell lymphomas. *N Engl J Med,* **359,** 2313-2323.

Lenz, G., Wright, G.W., Emre, N.C., Kohlhammer, H., Dave, S.S., Davis, R.E., Carty, S., Lam, L.T., Shaffer, A.L., Xiao, W., Powell, J., Rosenwald, A., Ott, G., Muller-Hermelink, H.K., Gascoyne, R.D., Connors, J.M., Campo, E., Jaffe, E.S., Delabie, J., Smeland, E.B., Rimsza, L.M., Fisher, R.I., Weisenburger, D.D., Chan, W.C. & Staudt, L.M. (2008b) Molecular subtypes of diffuse large B-cell lymphoma arise by distinct genetic pathways. *Proc Natl Acad Sci U S A,* **105,** 13520-13525.

Leoni, F., Zaliani, A., Bertolini, G., Porro, G., Pagani, P., Pozzi, P., Dona, G., Fossati, G., Sozzani, S., Azam, T., Bufler, P., Fantuzzi, G., Goncharov, I., Kim, S.H., Pomerantz, B.J., Reznikov, L.L., Siegmund, B., Dinarello, C.A. & Mascagni, P. (2002) The antitumor histone

deacetylase inhibitor suberoylanilide hydroxamic acid exhibits antiinflammatory properties via suppression of cytokines. *Proc Natl Acad Sci U S A,* **99,** 2995-3000.
Li, K., Wang, R., Lozada, E., Fan, W., Orren, D.K. & Luo, J. (2010) Acetylation of WRN protein regulates its stability by inhibiting ubiquitination. *PLoS One,* **5,** e10341.
Li, W.L., Xiao, M.S., Zhang, D.F., Yu, D., Yang, R.X., Li, X.Y. & Yao, Y.G. (2014) Mutation and expression analysis of the IDH1, IDH2, DNMT3A, and MYD88 genes in colorectal cancer. *Gene,* **546,** 263-270.
Li, Y., Shi, Y., McCaw, L., Li, Y.J., Zhu, F., Gorczynski, R., Duncan, G.S., Yang, B., Ben-David, Y. & Spaner, D.E. (2015) Microenvironmental interleukin-6 suppresses toll-like receptor signaling in human leukemia cells through miR-17/19A. *Blood,* **126,** 766-778.
Li, Z.M., Rinaldi, A., Cavalli, A., Mensah, A.A., Ponzoni, M., Gascoyne, R.D., Bhagat, G., Zucca, E. & Bertoni, F. (2012) MYD88 somatic mutations in MALT lymphomas. *Br J Haematol,* **158,** 662-664.
Libermann, T.A. & Baltimore, D. (1990) Activation of interleukin-6 gene expression through the NF-kappa B transcription factor. *Mol Cell Biol,* **10,** 2327-2334.
Lin, S.C., Lo, Y.C. & Wu, H. (2010) Helical assembly in the MyD88-IRAK4-IRAK2 complex in TLR/IL-1R signalling. *Nature,* **465,** 885-890.
Lohr, J.G., Stojanov, P., Lawrence, M.S., Auclair, D., Chapuy, B., Sougnez, C., Cruz-Gordillo, P., Knoechel, B., Asmann, Y.W., Slager, S.L., Novak, A.J., Dogan, A., Ansell, S.M., Link, B.K., Zou, L., Gould, J., Saksena, G., Stransky, N., Rangel-Escareno, C., Fernandez-Lopez, J.C., Hidalgo-Miranda, A., Melendez-Zajgla, J., Hernandez-Lemus, E., Schwarz-Cruz y Celis, A., Imaz-Rosshandler, I., Ojesina, A.I., Jung, J., Pedamallu, C.S., Lander, E.S., Habermann, T.M., Cerhan, J.R., Shipp, M.A., Getz, G. & Golub, T.R. (2012) Discovery and prioritization of somatic mutations in diffuse large B-cell lymphoma (DLBCL) by whole-exome sequencing. *Proc Natl Acad Sci U S A,* **109,** 3879-3884.
Lord, K.A., Hoffman-Liebermann, B. & Liebermann, D.A. (1990) Nucleotide sequence and expression of a cDNA encoding MyD88, a novel myeloid differentiation primary response gene induced by IL6. *Oncogene,* **5,** 1095-1097.
Loven, J., Hoke, H.A., Lin, C.Y., Lau, A., Orlando, D.A., Vakoc, C.R., Bradner, J.E., Lee, T.I. & Young, R.A. (2013) Selective inhibition of tumor oncogenes by disruption of super-enhancers. *Cell,* **153,** 320-334.
Lu, Y.C., Yeh, W.C. & Ohashi, P.S. (2008) LPS/TLR4 signal transduction pathway. *Cytokine,* **42,** 145-151.
Luchenko, V.L., Litman, T., Chakraborty, A.R., Heffner, A., Devor, C., Wilkerson, J., Stein, W., Robey, R.W., Bangiolo, L., Levens, D. & Bates, S.E. (2014) Histone deacetylase inhibitor-mediated cell death is distinct from its global effect on chromatin. *Mol Oncol,* **8,** 1379-1392.
Maasho, K., Marusina, A., Reynolds, N.M., Coligan, J.E. & Borrego, F. (2004) Efficient gene transfer into the human natural killer cell line, NKL, using the Amaxa nucleofection system. *J Immunol Methods,* **284,** 133-140.
Mai, A. & Altucci, L. (2009) Epi-drugs to fight cancer: from chemistry to cancer treatment, the road ahead. *Int J Biochem Cell Biol,* **41,** 199-213.
Maier, T., Guell, M. & Serrano, L. (2009) Correlation of mRNA and protein in complex biological samples. *FEBS Lett,* **583,** 3966-3973.
Mareschal, S., Lanic, H., Ruminy, P., Bastard, C., Tilly, H. & Jardin, F. (2011) The proportion of activated B-cell like subtype among de novo diffuse large B-cell lymphoma increases with age. *Haematologica,* **96,** 1888-1890.
Marino-Ramirez, L., Jordan, I.K. & Landsman, D. (2006) Multiple independent evolutionary solutions to core histone gene regulation. *Genome Biol,* **7,** R122.
Marks, P.A. (2010) The clinical development of histone deacetylase inhibitors as targeted anticancer drugs. *Expert Opin Investig Drugs,* **19,** 1049-1066.

Marquard, L., Gjerdrum, L.M., Christensen, I.J., Jensen, P.B., Sehested, M. & Ralfkiaer, E. (2008) Prognostic significance of the therapeutic targets histone deacetylase 1, 2, 6 and acetylated histone H4 in cutaneous T-cell lymphoma. *Histopathology,* **53,** 267-277.

Martin-Sanchez, E., Sanchez-Beato, M., Rodriguez, M.E., Sanchez-Espiridion, B., Gomez-Abad, C., Bischoff, J.R., Piris, M.A., Garcia-Orad, A. & Garcia, J.F. (2011) HDAC inhibitors induce cell cycle arrest, activate the apoptotic extrinsic pathway and synergize with a novel PIM inhibitor in Hodgkin lymphoma-derived cell lines. *Br J Haematol,* **152,** 352-356.

Martinez-Lopez, A., Curiel-Olmo, S., Mollejo, M., Cereceda, L., Martinez, N., Montes-Moreno, S., Almaraz, C., Revert, J.B. & Piris, M.A. (2015) MYD88 (L265P) somatic mutation in marginal zone B-cell lymphoma. *Am J Surg Pathol,* **39,** 644-651.

Mathews Griner, L.A., Guha, R., Shinn, P., Young, R.M., Keller, J.M., Liu, D., Goldlust, I.S., Yasgar, A., McKnight, C., Boxer, M.B., Duveau, D.Y., Jiang, J.K., Michael, S., Mierzwa, T., Huang, W., Walsh, M.J., Mott, B.T., Patel, P., Leister, W., Maloney, D.J., Leclair, C.A., Rai, G., Jadhav, A., Peyser, B.D., Austin, C.P., Martin, S.E., Simeonov, A., Ferrer, M., Staudt, L.M. & Thomas, C.J. (2014) High-throughput combinatorial screening identifies drugs that cooperate with ibrutinib to kill activated B-cell-like diffuse large B-cell lymphoma cells. *Proc Natl Acad Sci U S A,* **111,** 2349-2354.

McDermott, J. & Jimeno, A. (2014) Belinostat for the treatment of peripheral T-cell lymphomas. *Drugs Today (Barc),* **50,** 337-345.

Medzhitov, R., Preston-Hurlburt, P., Kopp, E., Stadlen, A., Chen, C., Ghosh, S. & Janeway, C.A., Jr. (1998) MyD88 is an adaptor protein in the hToll/IL-1 receptor family signaling pathways. *Mol Cell,* **2,** 253-258.

Mitsiades, C.S., Mitsiades, N.S., McMullan, C.J., Poulaki, V., Shringarpure, R., Hideshima, T., Akiyama, M., Chauhan, D., Munshi, N., Gu, X., Bailey, C., Joseph, M., Libermann, T.A., Richon, V.M., Marks, P.A. & Anderson, K.C. (2004) Transcriptional signature of histone deacetylase inhibition in multiple myeloma: biological and clinical implications. *Proc Natl Acad Sci U S A,* **101,** 540-545.

Mitsiades, N., Mitsiades, C.S., Richardson, P.G., McMullan, C., Poulaki, V., Fanourakis, G., Schlossman, R., Chauhan, D., Munshi, N.C., Hideshima, T., Richon, V.M., Marks, P.A. & Anderson, K.C. (2003) Molecular sequelae of histone deacetylase inhibition in human malignant B cells. *Blood,* **101,** 4055-4062.

Mondello, P., Derenzini, E., Asgari, Z., Philip, J., Brea, E.J., Seshan, V., Hendrickson, R.C., de Stanchina, E., Scheinberg, D.A. & Younes, A. (2017) Dual inhibition of histone deacetylases and phosphoinositide 3-kinase enhances therapeutic activity against B cell lymphoma. *Oncotarget*.

Montesinos-Rongen, M., Godlewska, E., Brunn, A., Wiestler, O.D., Siebert, R. & Deckert, M. (2011) Activating L265P mutations of the MYD88 gene are common in primary central nervous system lymphoma. *Acta Neuropathol,* **122,** 791-792.

Monti, S., Savage, K.J., Kutok, J.L., Feuerhake, F., Kurtin, P., Mihm, M., Wu, B., Pasqualucci, L., Neuberg, D., Aguiar, R.C., Dal Cin, P., Ladd, C., Pinkus, G.S., Salles, G., Harris, N.L., Dalla-Favera, R., Habermann, T.M., Aster, J.C., Golub, T.R. & Shipp, M.A. (2005) Molecular profiling of diffuse large B-cell lymphoma identifies robust subtypes including one characterized by host inflammatory response. *Blood,* **105,** 1851-1861.

Mori, N., Ohwashi, M., Yoshinaga, K., Mitsuhashi, K., Tanaka, N., Teramura, M., Okada, M., Shiseki, M., Tanaka, J. & Motoji, T. (2013) L265P mutation of the MYD88 gene is frequent in Waldenstrom's macroglobulinemia and its absence in myeloma. *PLoS One,* **8,** e80088.

Morin, R.D., Mendez-Lago, M., Mungall, A.J., Goya, R., Mungall, K.L., Corbett, R.D., Johnson, N.A., Severson, T.M., Chiu, R., Field, M., Jackman, S., Krzywinski, M., Scott, D.W., Trinh, D.L., Tamura-Wells, J., Li, S., Firme, M.R., Rogic, S., Griffith, M., Chan, S., Yakovenko, O., Meyer, I.M., Zhao, E.Y., Smailus, D., Moksa, M., Chittaranjan, S., Rimsza, L., Brooks-

Wilson, A., Spinelli, J.J., Ben-Neriah, S., Meissner, B., Woolcock, B., Boyle, M., McDonald, H., Tam, A., Zhao, Y., Delaney, A., Zeng, T., Tse, K., Butterfield, Y., Birol, I., Holt, R., Schein, J., Horsman, D.E., Moore, R., Jones, S.J., Connors, J.M., Hirst, M., Gascoyne, R.D. & Marra, M.A. (2011) Frequent mutation of histone-modifying genes in non-Hodgkin lymphoma. *Nature,* **476,** 298-303.

Moriniere, J., Rousseaux, S., Steuerwald, U., Soler-Lopez, M., Curtet, S., Vitte, A.L., Govin, J., Gaucher, J., Sadoul, K., Hart, D.J., Krijgsveld, J., Khochbin, S., Muller, C.W. & Petosa, C. (2009) Cooperative binding of two acetylation marks on a histone tail by a single bromodomain. *Nature,* **461,** 664-668.

Motshwene, P.G., Moncrieffe, M.C., Grossmann, J.G., Kao, C., Ayaluru, M., Sandercock, A.M., Robinson, C.V., Latz, E. & Gay, N.J. (2009) An oligomeric signaling platform formed by the Toll-like receptor signal transducers MyD88 and IRAK-4. *J Biol Chem,* **284,** 25404-25411.

Muller, P., Kuttenkeuler, D., Gesellchen, V., Zeidler, M.P. & Boutros, M. (2005) Identification of JAK/STAT signalling components by genome-wide RNA interference. *Nature,* **436,** 871-875.

Muller, S., Filippakopoulos, P. & Knapp, S. (2011) Bromodomains as therapeutic targets. *Expert Rev Mol Med,* **13,** e29.

Mummaneni, P. & Shord, S.S. (2014) Epigenetics and oncology. *Pharmacotherapy,* **34,** 495-505.

Muzio, M., Scielzo, C., Bertilaccio, M.T., Frenquelli, M., Ghia, P. & Caligaris-Cappio, F. (2009) Expression and function of toll like receptors in chronic lymphocytic leukaemia cells. *Br J Haematol,* **144,** 507-516.

Nagao, T., Oshikawa, G., Ishida, S., Akiyama, H., Umezawa, Y., Nogami, A., Kurosu, T. & Miura, O. (2015) A novel MYD88 mutation, L265RPP, in Waldenstrom macroglobulinemia activates the NF-kappaB pathway to upregulate Bcl-xL expression and enhances cell survival. *Blood Cancer J,* **5,** e314.

Nagel, D., Spranger, S., Vincendeau, M., Grau, M., Raffegerst, S., Kloo, B., Hlahla, D., Neuenschwander, M., Peter von Kries, J., Hadian, K., Dorken, B., Lenz, P., Lenz, G., Schendel, D.J. & Krappmann, D. (2012) Pharmacologic inhibition of MALT1 protease by phenothiazines as a therapeutic approach for the treatment of aggressive ABC-DLBCL. *Cancer Cell,* **22,** 825-837.

Naugler, W.E., Sakurai, T., Kim, S., Maeda, S., Kim, K., Elsharkawy, A.M. & Karin, M. (2007) Gender disparity in liver cancer due to sex differences in MyD88-dependent IL-6 production. *Science,* **317,** 121-124.

Nebbioso, A., Carafa, V., Benedetti, R. & Altucci, L. (2012) Trials with 'epigenetic' drugs: an update. *Mol Oncol,* **6,** 657-682.

New, M., Olzscha, H. & La Thangue, N.B. (2012) HDAC inhibitor-based therapies: can we interpret the code? *Mol Oncol,* **6,** 637-656.

New, M., Olzscha, H., Liu, G., Khan, O., Stimson, L., McGouran, J., Kerr, D., Coutts, A., Kessler, B., Middleton, M. & La Thangue, N.B. (2013) A regulatory circuit that involves HR23B and HDAC6 governs the biological response to HDAC inhibitors. *Cell Death Differ,* **20,** 1306-1316.

New, M., Sheikh, S., Bekheet, M., Olzscha, H., Thezenas, M.L., Care, M.A., Fotheringham, S., Tooze, R.M., Kessler, B. & La Thangue, N.B. (2016) TLR Adaptor Protein MYD88 Mediates Sensitivity to HDAC Inhibitors via a Cytokine-Dependent Mechanism. *Cancer Res,* **76,** 6975-6987.

Ngo, V.N., Young, R.M., Schmitz, R., Jhavar, S., Xiao, W., Lim, K.H., Kohlhammer, H., Xu, W., Yang, Y., Zhao, H., Shaffer, A.L., Romesser, P., Wright, G., Powell, J., Rosenwald, A., Muller-Hermelink, H.K., Ott, G., Gascoyne, R.D., Connors, J.M., Rimsza, L.M., Campo, E., Jaffe, E.S., Delabie, J., Smeland, E.B., Fisher, R.I., Braziel, R.M., Tubbs, R.R., Cook, J.R., Weisenburger, D.D., Chan, W.C. & Staudt, L.M. (2011) Oncogenically active MYD88 mutations in human lymphoma. *Nature,* **470,** 115-119.

Nogai, H., Dorken, B. & Lenz, G. (2011) Pathogenesis of non-Hodgkin's lymphoma. *J Clin Oncol,* **29,** 1803-1811.
Nogai, H., Wenzel, S.S., Hailfinger, S., Grau, M., Kaergel, E., Seitz, V., Wollert-Wulf, B., Pfeifer, M., Wolf, A., Frick, M., Dietze, K., Madle, H., Tzankov, A., Hummel, M., Dorken, B., Scheidereit, C., Janz, M., Lenz, P., Thome, M. & Lenz, G. (2013) IkappaB-zeta controls the constitutive NF-kappaB target gene network and survival of ABC DLBCL. *Blood,* **122,** 2242-2250.
Nyman, H., Jerkeman, M., Karjalainen-Lindsberg, M.L., Banham, A.H. & Leppa, S. (2009) Prognostic impact of activated B-cell focused classification in diffuse large B-cell lymphoma patients treated with R-CHOP. *Mod Pathol,* **22,** 1094-1101.
Ohnishi, H., Tochio, H., Kato, Z., Orii, K.E., Li, A., Kimura, T., Hiroaki, H., Kondo, N. & Shirakawa, M. (2009) Structural basis for the multiple interactions of the MyD88 TIR domain in TLR4 signaling. *Proc Natl Acad Sci U S A,* **106,** 10260-10265.
Olsen, E.A., Kim, Y.H., Kuzel, T.M., Pacheco, T.R., Foss, F.M., Parker, S., Frankel, S.R., Chen, C., Ricker, J.L., Arduino, J.M. & Duvic, M. (2007) Phase IIb multicenter trial of vorinostat in patients with persistent, progressive, or treatment refractory cutaneous T-cell lymphoma. *J Clin Oncol,* **25,** 3109-3115.
Olson, M.A., Lee, M.S., Kissner, T.L., Alam, S., Waugh, D.S. & Saikh, K.U. (2015) Discovery of small molecule inhibitors of MyD88-dependent signaling pathways using a computational screen. *Sci Rep,* **5,** 14246.
Olzscha, H., Sheikh, S. & La Thangue, N.B. (2015) Deacetylation of chromatin and gene expression regulation: a new target for epigenetic therapy. *Crit Rev Oncog,* **20,** 1-17.
Oritani, K., Tomiyama, Y., Kincade, P.W., Aoyama, K., Yokota, T., Matsumura, I., Kanakura, Y., Nakajima, K., Hirano, T. & Matsuzawa, Y. (1999) Both Stat3-activation and Stat3-independent BCL2 downregulation are important for interleukin-6-induced apoptosis of 1A9-M cells. *Blood,* **93,** 1346-1354.
Ott, G., Ziepert, M., Klapper, W., Horn, H., Szczepanowski, M., Bernd, H.W., Thorns, C., Feller, A.C., Lenze, D., Hummel, M., Stein, H., Muller-Hermelink, H.K., Frank, M., Hansmann, M.L., Barth, T.F., Moller, P., Cogliatti, S., Pfreundschuh, M., Schmitz, N., Trumper, L., Loeffler, M. & Rosenwald, A. (2010) Immunoblastic morphology but not the immunohistochemical GCB/nonGCB classifier predicts outcome in diffuse large B-cell lymphoma in the RICOVER-60 trial of the DSHNHL. *Blood,* **116,** 4916-4925.
Paddison, P.J., Caudy, A.A., Bernstein, E., Hannon, G.J. & Conklin, D.S. (2002) Short hairpin RNAs (shRNAs) induce sequence-specific silencing in mammalian cells. *Genes Dev,* **16,** 948-958.
Palmer, I. & Wingfield, P.T. (2012) Preparation and extraction of insoluble (inclusion-body) proteins from Escherichia coli. *Curr Protoc Protein Sci,* **Chapter 6,** Unit6 3.
Palsson-McDermott, E.M. & O'Neill, L.A. (2004) Signal transduction by the lipopolysaccharide receptor, Toll-like receptor-4. *Immunology,* **113,** 153-162.
Parker, C., Mocanu, V., Mocanu, M., Dicheva, N. & Warren, M. (2010) Mass Spectrometry for Post-Translational Modifications. In: *Neuroproteomics*

(ed. by Alzate, O.). CRC Press/Taylor & Francis.
Pasqualucci, L., Dominguez-Sola, D., Chiarenza, A., Fabbri, G., Grunn, A., Trifonov, V., Kasper, L.H., Lerach, S., Tang, H., Ma, J., Rossi, D., Chadburn, A., Murty, V.V., Mullighan, C.G., Gaidano, G., Rabadan, R., Brindle, P.K. & Dalla-Favera, R. (2011a) Inactivating mutations of acetyltransferase genes in B-cell lymphoma. *Nature,* **471,** 189-195.
Pasqualucci, L., Trifonov, V., Fabbri, G., Ma, J., Rossi, D., Chiarenza, A., Wells, V.A., Grunn, A., Messina, M., Elliot, O., Chan, J., Bhagat, G., Chadburn, A., Gaidano, G., Mullighan, C.G., Rabadan, R. & Dalla-Favera, R. (2011b) Analysis of the coding genome of diffuse large B-cell lymphoma. *Nat Genet,* **43,** 830-837.
Patkar, N., Subramanian, P.G., Deshpande, P., Ghodke, K., Tembhare, P., Mascarenhas, R., Muranjan, A., Chaudhary, S., Bagal, B., Gujral, S., Sengar, M. & Menon, H. (2015)

MYD88 mutant lymphoplasmacytic lymphoma/Waldenstrom macroglobulinemia has distinct clinical and pathological features as compared to its mutation negative counterpart. *Leuk Lymphoma,* **56,** 420-425.

Peach, M., Marsh, N. & Macphee, D.J. (2012) Protein solubilization: attend to the choice of lysis buffer. *Methods Mol Biol,* **869,** 37-47.

Pfreundschuh, M., Trumper, L., Osterborg, A., Pettengell, R., Trneny, M., Imrie, K., Ma, D., Gill, D., Walewski, J., Zinzani, P.L., Stahel, R., Kvaloy, S., Shpilberg, O., Jaeger, U., Hansen, M., Lehtinen, T., Lopez-Guillermo, A., Corrado, C., Scheliga, A., Milpied, N., Mendila, M., Rashford, M., Kuhnt, E., Loeffler, M. & MabThera International Trial, G. (2006) CHOP-like chemotherapy plus rituximab versus CHOP-like chemotherapy alone in young patients with good-prognosis diffuse large-B-cell lymphoma: a randomised controlled trial by the MabThera International Trial (MInT) Group. *Lancet Oncol,* **7,** 379-391.

Pham-Ledard, A., Cappellen, D., Martinez, F., Vergier, B., Beylot-Barry, M. & Merlio, J.P. (2012) MYD88 somatic mutation is a genetic feature of primary cutaneous diffuse large B-cell lymphoma, leg type. *J Invest Dermatol,* **132,** 2118-2120.

Picaud, S., Leonards, K., Lambert, J.P., Dovey, O., Wells, C., Fedorov, O., Monteiro, O., Fujisawa, T., Wang, C.Y., Lingard, H., Tallant, C., Nikbin, N., Guetzoyan, L., Ingham, R., Ley, S.V., Brennan, P., Muller, S., Samsonova, A., Gingras, A.C., Schwaller, J., Vassiliou, G., Knapp, S. & Filippakopoulos, P. (2016) Promiscuous targeting of bromodomains by bromosporine identifies BET proteins as master regulators of primary transcription response in leukemia. *Sci Adv,* **2,** e1600760.

Piekarz, R.L., Frye, R., Turner, M., Wright, J.J., Allen, S.L., Kirschbaum, M.H., Zain, J., Prince, H.M., Leonard, J.P., Geskin, L.J., Reeder, C., Joske, D., Figg, W.D., Gardner, E.R., Steinberg, S.M., Jaffe, E.S., Stetler-Stevenson, M., Lade, S., Fojo, A.T. & Bates, S.E. (2009) Phase II multi-institutional trial of the histone deacetylase inhibitor romidepsin as monotherapy for patients with cutaneous T-cell lymphoma. *J Clin Oncol,* **27,** 5410-5417.

Plumb, J.A., Finn, P.W., Williams, R.J., Bandara, M.J., Romero, M.R., Watkins, C.J., La Thangue, N.B. & Brown, R. (2003) Pharmacodynamic response and inhibition of growth of human tumor xenografts by the novel histone deacetylase inhibitor PXD101. *Mol Cancer Ther,* **2,** 721-728.

Pon, J.R. & Marra, M.A. (2016) Clinical impact of molecular features in diffuse large B-cell lymphoma and follicular lymphoma. *Blood,* **127,** 181-186.

Poole, R.M. (2014) Belinostat: first global approval. *Drugs,* **74,** 1543-1554.

Poulain, S., Roumier, C., Decambron, A., Renneville, A., Herbaux, C., Bertrand, E., Tricot, S., Daudignon, A., Galiegue-Zouitina, S., Soenen, V., Theisen, O., Grardel, N., Nibourel, O., Roche-Lestienne, C., Quesnel, B., Duthilleul, P., Preudhomme, C. & Leleu, X. (2013) MYD88 L265P mutation in Waldenstrom macroglobulinemia. *Blood,* **121,** 4504-4511.

Prasad, V., Fojo, T. & Brada, M. (2016) Precision oncology: origins, optimism, and potential. *Lancet Oncol,* **17,** e81-86.

Puente, X.S., Pinyol, M., Quesada, V., Conde, L., Ordonez, G.R., Villamor, N., Escaramis, G., Jares, P., Bea, S., Gonzalez-Diaz, M., Bassaganyas, L., Baumann, T., Juan, M., Lopez-Guerra, M., Colomer, D., Tubio, J.M., Lopez, C., Navarro, A., Tornador, C., Aymerich, M., Rozman, M., Hernandez, J.M., Puente, D.A., Freije, J.M., Velasco, G., Gutierrez-Fernandez, A., Costa, D., Carrio, A., Guijarro, S., Enjuanes, A., Hernandez, L., Yague, J., Nicolas, P., Romeo-Casabona, C.M., Himmelbauer, H., Castillo, E., Dohm, J.C., de Sanjose, S., Piris, M.A., de Alava, E., San Miguel, J., Royo, R., Gelpi, J.L., Torrents, D., Orozco, M., Pisano, D.G., Valencia, A., Guigo, R., Bayes, M., Heath, S., Gut, M., Klatt, P., Marshall, J., Raine, K., Stebbings, L.A., Futreal, P.A., Stratton, M.R., Campbell, P.J., Gut, I., Lopez-Guillermo, A., Estivill, X., Montserrat, E., Lopez-Otin, C. & Campo, E. (2011)

Whole-genome sequencing identifies recurrent mutations in chronic lymphocytic leukaemia. *Nature,* **475,** 101-105.
Rakoff-Nahoum, S. & Medzhitov, R. (2007) Regulation of spontaneous intestinal tumorigenesis through the adaptor protein MyD88. *Science,* **317,** 124-127.
Ramalingam, S.S., Kummar, S., Sarantopoulos, J., Shibata, S., LoRusso, P., Yerk, M., Holleran, J., Lin, Y., Beumer, J.H., Harvey, R.D., Ivy, S.P., Belani, C.P. & Egorin, M.J. (2010) Phase I study of vorinostat in patients with advanced solid tumors and hepatic dysfunction: a National Cancer Institute Organ Dysfunction Working Group study. *J Clin Oncol,* **28,** 4507-4512.
Ramalingam, S.S., Parise, R.A., Ramanathan, R.K., Lagattuta, T.F., Musguire, L.A., Stoller, R.G., Potter, D.M., Argiris, A.E., Zwiebel, J.A., Egorin, M.J. & Belani, C.P. (2007) Phase I and pharmacokinetic study of vorinostat, a histone deacetylase inhibitor, in combination with carboplatin and paclitaxel for advanced solid malignancies. *Clin Cancer Res,* **13,** 3605-3610.
Ran, F.A., Hsu, P.D., Wright, J., Agarwala, V., Scott, D.A. & Zhang, F. (2013) Genome engineering using the CRISPR-Cas9 system. *Nat Protoc,* **8,** 2281-2308.
Rebl, A., Rebl, H., Kobis, J.M., Goldammer, T. & Seyfert, H.M. (2017) ST2 from rainbow trout quenches TLR signalling, localises at the nuclear membrane and allows the nuclear translocation of MYD88. *Dev Comp Immunol,* **67,** 139-152.
Ree, A.H., Saelen, M.G., Kalanxhi, E., Ostensen, I.H., Schee, K., Roe, K., Abrahamsen, T.W., Dueland, S. & Flatmark, K. (2014) Biomarkers of histone deacetylase inhibitor activity in a phase 1 combined-modality study with radiotherapy. *PLoS One,* **9,** e89750.
Reichert, N., Choukrallah, M.A. & Matthias, P. (2012) Multiple roles of class I HDACs in proliferation, differentiation, and development. *Cell Mol Life Sci,* **69,** 2173-2187.
Reynoird, N., Schwartz, B.E., Delvecchio, M., Sadoul, K., Meyers, D., Mukherjee, C., Caron, C., Kimura, H., Rousseaux, S., Cole, P.A., Panne, D., French, C.A. & Khochbin, S. (2010) Oncogenesis by sequestration of CBP/p300 in transcriptionally inactive hyperacetylated chromatin domains. *EMBO J,* **29,** 2943-2952.
Riccardi, C. & Nicoletti, I. (2006) Analysis of apoptosis by propidium iodide staining and flow cytometry. *Nat Protoc,* **1,** 1458-1461.
Richardson, P.G., Mitsiades, C.S., Laubach, J.P., Hajek, R., Spicka, I., Dimopoulos, M.A., Moreau, P., Siegel, D.S., Jagannath, S. & Anderson, K.C. (2013) Preclinical data and early clinical experience supporting the use of histone deacetylase inhibitors in multiple myeloma. *Leuk Res,* **37,** 829-837.
Richon, V.M., Sandhoff, T.W., Rifkind, R.A. & Marks, P.A. (2000) Histone deacetylase inhibitor selectively induces p21WAF1 expression and gene-associated histone acetylation. *Proc Natl Acad Sci U S A,* **97,** 10014-10019.
Rikiishi, H. (2011) Autophagic and apoptotic effects of HDAC inhibitors on cancer cells. *J Biomed Biotechnol,* **2011,** 830260.
Riss, T.L., Moravec, R.A., Niles, A.L., Duellman, S., Benink, H.A., Worzella, T.J. & Minor, L. (2004) Cell Viability Assays. In: *Assay Guidance Manual* (ed. by Sittampalam, G.S., Coussens, N.P., Brimacombe, K., Grossman, A., Arkin, M., Auld, D., Austin, C., Bejcek, B., Glicksman, M., Inglese, J., Iversen, P.W., Li, Z., McGee, J., McManus, O., Minor, L., Napper, A., Peltier, J.M., Riss, T., Trask, O.J., Jr. & Weidner, J.), Bethesda (MD).
Rosenwald, A., Wright, G., Chan, W.C., Connors, J.M., Campo, E., Fisher, R.I., Gascoyne, R.D., Muller-Hermelink, H.K., Smeland, E.B., Giltnane, J.M., Hurt, E.M., Zhao, H., Averett, L., Yang, L., Wilson, W.H., Jaffe, E.S., Simon, R., Klausner, R.D., Powell, J., Duffey, P.L., Longo, D.L., Greiner, T.C., Weisenburger, D.D., Sanger, W.G., Dave, B.J., Lynch, J.C., Vose, J., Armitage, J.O., Montserrat, E., Lopez-Guillermo, A., Grogan, T.M., Miller, T.P., LeBlanc, M., Ott, G., Kvaloy, S., Delabie, J., Holte, H., Krajci, P., Stokke, T., Staudt, L.M. & Lymphoma/Leukemia Molecular Profiling, P. (2002) The use of molecular profiling to

predict survival after chemotherapy for diffuse large-B-cell lymphoma. *N Engl J Med,* **346,** 1937-1947.

Rossi, D., Trifonov, V., Fangazio, M., Bruscaggin, A., Rasi, S., Spina, V., Monti, S., Vaisitti, T., Arruga, F., Fama, R., Ciardullo, C., Greco, M., Cresta, S., Piranda, D., Holmes, A., Fabbri, G., Messina, M., Rinaldi, A., Wang, J., Agostinelli, C., Piccaluga, P.P., Lucioni, M., Tabbo, F., Serra, R., Franceschetti, S., Deambrogi, C., Daniele, G., Gattei, V., Marasca, R., Facchetti, F., Arcaini, L., Inghirami, G., Bertoni, F., Pileri, S.A., Deaglio, S., Foa, R., Dalla-Favera, R., Pasqualucci, L., Rabadan, R. & Gaidano, G. (2012) The coding genome of splenic marginal zone lymphoma: activation of NOTCH2 and other pathways regulating marginal zone development. *J Exp Med,* **209,** 1537-1551.

Rousset, F., Garcia, E., Defrance, T., Peronne, C., Vezzio, N., Hsu, D.H., Kastelein, R., Moore, K.W. & Banchereau, J. (1992) Interleukin 10 is a potent growth and differentiation factor for activated human B lymphocytes. *Proc Natl Acad Sci U S A,* **89,** 1890-1893.

Ruefli, A.A., Bernhard, D., Tainton, K.M., Kofler, R., Smyth, M.J. & Johnstone, R.W. (2002) Suberoylanilide hydroxamic acid (SAHA) overcomes multidrug resistance and induces cell death in P-glycoprotein-expressing cells. *Int J Cancer,* **99,** 292-298.

Salles, G., Bienvenu, J., Bastion, Y., Barbier, Y., Doche, C., Warzocha, K., Gutowski, M.C., Rieux, C. & Coiffier, B. (1996) Elevated circulating levels of TNFalpha and its p55 soluble receptor are associated with an adverse prognosis in lymphoma patients. *Br J Haematol,* **93,** 352-359.

Saraiva, M. & O'Garra, A. (2010) The regulation of IL-10 production by immune cells. *Nat Rev Immunol,* **10,** 170-181.

Savitski, M.F. & Savitski, M.M. (2010) Unbiased detection of posttranslational modifications using mass spectrometry. *Methods Mol Biol,* **673,** 203-210.

Scanga, C.A., Aliberti, J., Jankovic, D., Tilloy, F., Bennouna, S., Denkers, E.Y., Medzhitov, R. & Sher, A. (2002) Cutting edge: MyD88 is required for resistance to Toxoplasma gondii infection and regulates parasite-induced IL-12 production by dendritic cells. *J Immunol,* **168,** 5997-6001.

Scott, D.W. (2015a) Cell-of-Origin in Diffuse Large B-Cell Lymphoma: Are the Assays Ready for the Clinic? *Am Soc Clin Oncol Educ Book,* **35,** e458-466.

Scott, D.W. (2015b) Cell-of-Origin in Diffuse Large B-Cell Lymphoma: Are the Assays Ready for the Clinic? *Am Soc Clin Oncol Educ Book***,** e458-466.

Sehn, L.H., Donaldson, J., Chhanabhai, M., Fitzgerald, C., Gill, K., Klasa, R., MacPherson, N., O'Reilly, S., Spinelli, J.J., Sutherland, J., Wilson, K.S., Gascoyne, R.D. & Connors, J.M. (2005) Introduction of combined CHOP plus rituximab therapy dramatically improved outcome of diffuse large B-cell lymphoma in British Columbia. *J Clin Oncol,* **23,** 5027-5033.

Sehn, L.H. & Gascoyne, R.D. (2015) Diffuse large B-cell lymphoma: optimizing outcome in the context of clinical and biologic heterogeneity. *Blood,* **125,** 22-32.

Serezani, C.H., Lewis, C., Jancar, S. & Peters-Golden, M. (2011) Leukotriene B4 amplifies NF-kappaB activation in mouse macrophages by reducing SOCS1 inhibition of MyD88 expression. *J Clin Invest,* **121,** 671-682.

Shaffer, A.L., 3rd, Young, R.M. & Staudt, L.M. (2012) Pathogenesis of human B cell lymphomas. *Annu Rev Immunol,* **30,** 565-610.

Shao, Y., Gao, Z., Marks, P.A. & Jiang, X. (2004) Apoptotic and autophagic cell death induced by histone deacetylase inhibitors. *Proc Natl Acad Sci U S A,* **101,** 18030-18035.

Sheikh, S., Bekheet, M., Olzscha, H. & La Thangue, N. (2015) Predicting and monitoring responses to epigenetic drugs. In: *Drug Discovery in Cancer Epigenetics* (ed. by Egger, G. & Arimondo, P.). Elsevier.

Sheikh, S., Coutts, A. & La Thangue, N. (2016) Transfection. In: *Basic Science Methdods for Clinical Researchers.* . Elsevier.

Shigekawa, K. & Dower, W.J. (1988) Electroporation of eukaryotes and prokaryotes: a general approach to the introduction of macromolecules into cells. *Biotechniques,* **6,** 742-751.
Slingerland, M., Guchelaar, H.J. & Gelderblom, H. (2014) Histone deacetylase inhibitors: an overview of the clinical studies in solid tumors. *Anticancer Drugs,* **25,** 140-149.
Soldani, C. & Scovassi, A.I. (2002) Poly(ADP-ribose) polymerase-1 cleavage during apoptosis: an update. *Apoptosis,* **7,** 321-328.
Solt, L.A. & May, M.J. (2008) The IkappaB kinase complex: master regulator of NF-kappaB signaling. *Immunol Res,* **42,** 3-18.
Strimbu, K. & Tavel, J.A. (2010) What are biomarkers? *Curr Opin HIV AIDS,* **5,** 463-466.
Swann, J.B., Vesely, M.D., Silva, A., Sharkey, J., Akira, S., Schreiber, R.D. & Smyth, M.J. (2008) Demonstration of inflammation-induced cancer and cancer immunoediting during primary tumorigenesis. *Proc Natl Acad Sci U S A,* **105,** 652-656.
Sykes, S.M., Mellert, H.S., Holbert, M.A., Li, K., Marmorstein, R., Lane, W.S. & McMahon, S.B. (2006) Acetylation of the p53 DNA-binding domain regulates apoptosis induction. *Mol Cell,* **24,** 841-851.
Takeda, K. & Akira, S. (2004) TLR signaling pathways. *Semin Immunol,* **16,** 3-9.
Takeuchi, O. & Akira, S. (2002) MyD88 as a bottle neck in Toll/IL-1 signaling. *Curr Top Microbiol Immunol,* **270,** 155-167.
Takeuchi, O., Hoshino, K. & Akira, S. (2000) Cutting edge: TLR2-deficient and MyD88-deficient mice are highly susceptible to Staphylococcus aureus infection. *J Immunol,* **165,** 5392-5396.
Tallarida, R.J. (2006) An overview of drug combination analysis with isobolograms. *J Pharmacol Exp Ther,* **319,** 1-7.
Testoni, M., Zucca, E., Young, K.H. & Bertoni, F. (2015) Genetic lesions in diffuse large B-cell lymphomas. *Ann Oncol,* **26,** 1069-1080.
Thompson, R.C., Vardinogiannis, I. & Gilmore, T.D. (2013) The sensitivity of diffuse large B-cell lymphoma cell lines to histone deacetylase inhibitor-induced apoptosis is modulated by BCL-2 family protein activity. *PLoS One,* **8,** e62822.
Tilly, H., Vitolo, U., Walewski, J., da Silva, M.G., Shpilberg, O., Andre, M., Pfreundschuh, M., Dreyling, M. & Group, E.G.W. (2012) Diffuse large B-cell lymphoma (DLBCL): ESMO Clinical Practice Guidelines for diagnosis, treatment and follow-up. *Ann Oncol,* **23 Suppl 7,** vii78-82.
Trabucco, S.E., Gerstein, R.M., Evens, A.M., Bradner, J.E., Shultz, L.D., Greiner, D.L. & Zhang, H. (2015) Inhibition of bromodomain proteins for the treatment of human diffuse large B-cell lymphoma. *Clin Cancer Res,* **21,** 113-122.
Treon, S.P., Cao, Y., Xu, L., Yang, G., Liu, X. & Hunter, Z.R. (2014) Somatic mutations in MYD88 and CXCR4 are determinants of clinical presentation and overall survival in Waldenstrom macroglobulinemia. *Blood,* **123,** 2791-2796.
Treon, S.P., Xu, L., Yang, G., Zhou, Y., Liu, X., Cao, Y., Sheehy, P., Manning, R.J., Patterson, C.J., Tripsas, C., Arcaini, L., Pinkus, G.S., Rodig, S.J., Sohani, A.R., Harris, N.L., Laramie, J.M., Skifter, D.A., Lincoln, S.E. & Hunter, Z.R. (2012) MYD88 L265P somatic mutation in Waldenstrom's macroglobulinemia. *N Engl J Med,* **367,** 826-833.
Uchiyama, H., Barut, B.A., Mohrbacher, A.F., Chauhan, D. & Anderson, K.C. (1993) Adhesion of human myeloma-derived cell lines to bone marrow stromal cells stimulates interleukin-6 secretion. *Blood,* **82,** 3712-3720.
Unniyampurath, U., Pilankatta, R. & Krishnan, M.N. (2016) RNA Interference in the Age of CRISPR: Will CRISPR Interfere with RNAi? *Int J Mol Sci,* **17,** 291.
van Staveren, W.C., Solis, D.Y., Hebrant, A., Detours, V., Dumont, J.E. & Maenhaut, C. (2009) Human cancer cell lines: Experimental models for cancer cells in situ? For cancer stem cells? *Biochim Biophys Acta,* **1795,** 92-103.
Varettoni, M., Arcaini, L., Zibellini, S., Boveri, E., Rattotti, S., Riboni, R., Corso, A., Orlandi, E., Bonfichi, M., Gotti, M., Pascutto, C., Mangiacavalli, S., Croci, G., Fiaccadori, V., Morello,

L., Guerrera, M.L., Paulli, M. & Cazzola, M. (2013) Prevalence and clinical significance of the MYD88 (L265P) somatic mutation in Waldenstrom's macroglobulinemia and related lymphoid neoplasms. *Blood,* **121,** 2522-2528.

von Bernuth, H., Picard, C., Jin, Z., Pankla, R., Xiao, H., Ku, C.L., Chrabieh, M., Mustapha, I.B., Ghandil, P., Camcioglu, Y., Vasconcelos, J., Sirvent, N., Guedes, M., Vitor, A.B., Herrero-Mata, M.J., Arostegui, J.I., Rodrigo, C., Alsina, L., Ruiz-Ortiz, E., Juan, M., Fortuny, C., Yague, J., Anton, J., Pascal, M., Chang, H.H., Janniere, L., Rose, Y., Garty, B.Z., Chapel, H., Issekutz, A., Marodi, L., Rodriguez-Gallego, C., Banchereau, J., Abel, L., Li, X., Chaussabel, D., Puel, A. & Casanova, J.L. (2008) Pyogenic bacterial infections in humans with MyD88 deficiency. *Science,* **321,** 691-696.

Wajant, H., Pfizenmaier, K. & Scheurich, P. (2003) Tumor necrosis factor signaling. *Cell Death Differ,* **10,** 45-65.

Wang, J., Jeelall, Y.S. & Horikawa, K. (2013) Emerging targets in human lymphoma: targeting the MYD88 mutation. *Blood and Lymphatic Cancer: Targets and Therapy,* **3,** 53—61

Wang, J.Q., Beutler, B., Goodnow, C.C. & Horikawa, K. (2016) Inhibiting TLR9 and other UNC93B1-dependent TLRs paradoxically increases accumulation of MYD88L265P plasmablasts in vivo. *Blood,* **128,** 1604-1608.

Wang, J.Q., Jeelall, Y.S., Ferguson, L.L. & Horikawa, K. (2014) Toll-Like Receptors and Cancer: MYD88 Mutation and Inflammation. *Front Immunol,* **5,** 367.

Wang JQ, J.Y.a.H.K. (2013) Emerging targets in human lymphoma: targeting the *MYD88* mutation. *Blood and Lymphatic Cancer: Targets and Therapy,* **3,** 53-61.

Wang, L., Lawrence, M.S., Wan, Y., Stojanov, P., Sougnez, C., Stevenson, K., Werner, L., Sivachenko, A., DeLuca, D.S., Zhang, L., Zhang, W., Vartanov, A.R., Fernandes, S.M., Goldstein, N.R., Folco, E.G., Cibulskis, K., Tesar, B., Sievers, Q.L., Shefler, E., Gabriel, S., Hacohen, N., Reed, R., Meyerson, M., Golub, T.R., Lander, E.S., Neuberg, D., Brown, J.R., Getz, G. & Wu, C.J. (2011) SF3B1 and other novel cancer genes in chronic lymphocytic leukemia. *N Engl J Med,* **365,** 2497-2506.

Weichert, W., Röske, A., Niesporek, S., Noske, A., Buckendahl, A.-C., Dietel, M., Gekeler, V., Boehm, M., Beckers, T. & Denkert, C. (2008) Class I histone deacetylase expression has independent prognostic impact in human colorectal cancer: specific role of class I histone deacetylases in vitro and in vivo. *Clinical cancer research : an official journal of the American Association for Cancer Research,* **14,** 1669-1677.

WHO (2014) Diffuse Large B cell lymphoma.

Wilson, A.J., Byun, D.S., Nasser, S., Murray, L.B., Ayyanar, K., Arango, D., Figueroa, M., Melnick, A., Kao, G.D., Augenlicht, L.H. & Mariadason, J.M. (2008) HDAC4 promotes growth of colon cancer cells via repression of p21. *Mol Biol Cell,* **19,** 4062-4075.

Wilson, A.J., Byun, D.S., Popova, N., Murray, L.B., L'Italien, K., Sowa, Y., Arango, D., Velcich, A., Augenlicht, L.H. & Mariadason, J.M. (2006) Histone deacetylase 3 (HDAC3) and other class I HDACs regulate colon cell maturation and p21 expression and are deregulated in human colon cancer. *J Biol Chem,* **281,** 13548-13558.

Wilson, W.H., Young, R.M., Schmitz, R., Yang, Y., Pittaluga, S., Wright, G., Lih, C.J., Williams, P.M., Shaffer, A.L., Gerecitano, J., de Vos, S., Goy, A., Kenkre, V.P., Barr, P.M., Blum, K.A., Shustov, A., Advani, R., Fowler, N.H., Vose, J.M., Elstrom, R.L., Habermann, T.M., Barrientos, J.C., McGreivy, J., Fardis, M., Chang, B.Y., Clow, F., Munneke, B., Moussa, D., Beaupre, D.M. & Staudt, L.M. (2015) Targeting B cell receptor signaling with ibrutinib in diffuse large B cell lymphoma. *Nat Med,* **21,** 922-926.

Wong, T.K. & Neumann, E. (1982) Electric field mediated gene transfer. *Biochem Biophys Res Commun,* **107,** 584-587.

Wright, G., Tan, B., Rosenwald, A., Hurt, E.H., Wiestner, A. & Staudt, L.M. (2003) A gene expression-based method to diagnose clinically distinct subgroups of diffuse large B cell lymphoma. *Proc Natl Acad Sci U S A,* **100,** 9991-9996.

Xu, H., Liew, L.N., Kuo, I.C., Huang, C.H., Goh, D.L. & Chua, K.Y. (2008) The modulatory effects of lipopolysaccharide-stimulated B cells on differential T-cell polarization. *Immunology,* **125,** 218-228.

Yamaguchi, T., Cubizolles, F., Zhang, Y., Reichert, N., Kohler, H., Seiser, C. & Matthias, P. (2010) Histone deacetylases 1 and 2 act in concert to promote the G1-to-S progression. *Genes Dev,* **24,** 455-469.

Yan, Q., Huang, Y., Watkins, A.J., Kocialkowski, S., Zeng, N., Hamoudi, R.A., Isaacson, P.G., de Leval, L., Wotherspoon, A. & Du, M.Q. (2012) BCR and TLR signaling pathways are recurrently targeted by genetic changes in splenic marginal zone lymphomas. *Haematologica,* **97,** 595-598.

Yang, G., Buhrlage, S.J., Tan, L., Liu, X., Chen, J., Xu, L., Tsakmaklis, N., Chen, J.G., Patterson, C.J., Brown, J.R., Castillo, J.J., Zhang, W., Zhang, X., Liu, S., Cohen, P., Hunter, Z.R., Gray, N. & Treon, S.P. (2016) HCK is a survival determinant transactivated by mutated MYD88, and a direct target of ibrutinib. *Blood,* **127,** 3237-3252.

Yang, G., Zhou, Y., Liu, X., Xu, L., Cao, Y., Manning, R.J., Patterson, C.J., Buhrlage, S.J., Gray, N., Tai, Y.T., Anderson, K.C., Hunter, Z.R. & Treon, S.P. (2013) A mutation in MYD88 (L265P) supports the survival of lymphoplasmacytic cells by activation of Bruton tyrosine kinase in Waldenstrom macroglobulinemia. *Blood,* **122,** 1222-1232.

Yang, J., Liao, X., Agarwal, M.K., Barnes, L., Auron, P.E. & Stark, G.R. (2007) Unphosphorylated STAT3 accumulates in response to IL-6 and activates transcription by binding to NFkappaB. *Genes Dev,* **21,** 1396-1408.

Yang, X.J. & Seto, E. (2008) The Rpd3/Hda1 family of lysine deacetylases: from bacteria and yeast to mice and men. *Nat Rev Mol Cell Biol,* **9,** 206-218.

Yang, Y., Lu, Y., Espejo, A., Wu, J., Xu, W., Liang, S. & Bedford, M.T. (2010) TDRD3 is an effector molecule for arginine-methylated histone marks. *Mol Cell,* **40,** 1016-1023.

Yee, A.J., Bensinger, W.I., Supko, J.G., Voorhees, P.M., Berdeja, J.G., Richardson, P.G., Libby, E.N., Wallace, E.E., Birrer, N.E., Burke, J.N., Tamang, D.L., Yang, M., Jones, S.S., Wheeler, C.A., Markelewicz, R.J. & Raje, N.S. (2016) Ricolinostat plus lenalidomide, and dexamethasone in relapsed or refractory multiple myeloma: a multicentre phase 1b trial. *Lancet Oncol,* **17,** 1569-1578.

Yeo, W., Chung, H.C., Chan, S.L., Wang, L.Z., Lim, R., Picus, J., Boyer, M., Mo, F.K., Koh, J., Rha, S.Y., Hui, E.P., Jeung, H.C., Roh, J.K., Yu, S.C., To, K.F., Tao, Q., Ma, B.B., Chan, A.W., Tong, J.H., Erlichman, C., Chan, A.T. & Goh, B.C. (2012) Epigenetic therapy using belinostat for patients with unresectable hepatocellular carcinoma: a multicenter phase I/II study with biomarker and pharmacokinetic analysis of tumors from patients in the Mayo Phase II Consortium and the Cancer Therapeutics Research Group. *J Clin Oncol,* **30,** 3361-3367.

Yu, H., Pardoll, D. & Jove, R. (2009) STATs in cancer inflammation and immunity: a leading role for STAT3. *Nat Rev Cancer,* **9,** 798-809.

Zain, J. & O'Connor, O.A. (2010) Targeting histone deacetyalses in the treatment of B- and T-cell malignancies. *Invest New Drugs,* **28 Suppl 1,** S58-78.

Zain, J., Rotter, A., Weiss, L., Forman, S. & Kirschbaum, M.H. (2007) Valproic acid monotherapy leads to CR in a patient with refractory diffuse large B cell lymphoma. *Leuk Lymphoma,* **48,** 1216-1218.

Zhang, J., Grubor, V., Love, C.L., Banerjee, A., Richards, K.L., Mieczkowski, P.A., Dunphy, C., Choi, W., Au, W.Y., Srivastava, G., Lugar, P.L., Rizzieri, D.A., Lagoo, A.S., Bernal-Mizrachi, L., Mann, K.P., Flowers, C., Naresh, K., Evens, A., Gordon, L.I., Czader, M., Gill, J.I., Hsi, E.D., Liu, Q., Fan, A., Walsh, K., Jima, D., Smith, L.L., Johnson, A.J., Byrd, J.C., Luftig, M.A., Ni, T., Zhu, J., Chadburn, A., Levy, S., Dunson, D. & Dave, S.S. (2013) Genetic heterogeneity of diffuse large B-cell lymphoma. *Proc Natl Acad Sci U S A,* **110,** 1398-1403.

Zhang, J., Reddy, A., Love, C.L., Moffit, A. & Rajagopalan, D. (2016) Integrative Genetic and Clinical Analysis through Whole Exome Sequencing in 1001 Diffuse Large B Cell Lymphoma (DLBCL) Patients Reveals Novel Disease Drivers and Risk Groups. In: *ASH*, Vol. 128, p. 1087. Blood.

Zhang, S.Q., Smith, S.M., Zhang, S.Y. & Lynn Wang, Y. (2015) Mechanisms of ibrutinib resistance in chronic lymphocytic leukaemia and non-Hodgkin lymphoma. *Br J Haematol,* **170,** 445-456.

Zhang, Y., Adachi, M., Kawamura, R. & Imai, K. (2006) Bmf is a possible mediator in histone deacetylase inhibitors FK228 and CBHA-induced apoptosis. *Cell Death Differ,* **13,** 129-140.

Zhang, Z., Zeng, B., Jiao, G., Li, Y., Liu, Y., Zhang, Y. & Yang, R. (2009) AA28-67 domain within MyD88 suppresses c-myc activity and expression to regulate differentiation and function of dendritic cells. *Clin Immunol,* **133,** 324-332.

Zhou, Q., Chaerkady, R., Shaw, P.G., Kensler, T.W., Pandey, A. & Davidson, N.E. (2010) Screening for therapeutic targets of vorinostat by SILAC-based proteomic analysis in human breast cancer cells. *Proteomics,* **10,** 1029-1039.